

Control of cleavage furrow formation by the RhoGEF Ect2

Kristýna Kotýnková

University College London

and

Cancer Research UK London Research Institute

PhD Supervisor: Mark Petronczki PhD

A thesis submitted for the degree of

Doctor of Philosophy

University College London

September 2015

Declaration

I Kristýna Kotýnková confirm that the work presented in this thesis is my own. Where information has been derived from other sources, I confirm that this has been indicated in the thesis.

Abstract

Cytokinesis is the final step of cell division that physically separates the cytoplasm of nascent daughter cells. The mitotic spindle plays a key role in positioning the cytokinetic furrow at the equator in animal cells but the exact mechanism is not yet understood. An important step during cleavage furrow formation is activation of small GTPase RhoA, which is brought about by the GEF factor Ect2. Our aim is to better understand the principles and regulation of cleavage furrow formation. Recent results in our lab have shown that the RhoGEF not only localizes to the spindle midzone after anaphase onset but also to the plasma membrane. Therefore we asked which lipids are involved in Ect2 membrane engagement and if the membrane translocation of Ect2 is an essential and rate-limiting step for cleavage furrow induction that confers spatial and temporal control of cytokinesis. Pharmacological interference with cellular lipids implicated PIP2 as an important anionic phospholipid for the association of Ect2 with the plasma membrane. We developed a chemical genetic system using hybrid proteins that allowed us to artificially target Ect2 to the plasma membrane. Our results demonstrate that the plasma membrane association of Ect2 is a prerequisite for cytokinesis in human cells. We also confirmed this finding by a complementary optogenetic approach of targeting Ect2 to the plasma membrane. Furthermore, light-induced membrane engagement of Ect2 highlighted the importance of local cortical Ect2 activity. Most current models for cytokinesis consider Ect2 recruitment to the spindle midzone as a key step in the furrow positioning in small animal cells. By replacing endogenous Ect2 with a mutated version that does not localize to the midzone, we have shown that this model cannot account for the placement and formation of the cleavage furrow at the cell equator. Unexpectedly, our results suggest that the midzone localization of Ect2 and the resulting equatorial gradient at the plasma membrane is dispensable for cytokinesis in mammalian cells. The equatorial concentration of Ect2 could still serve as a signal for furrow placement, but may be redundant with other not yet defined uncharacterized signals. In summary, our work firmly establishes plasma membrane engagement of Ect2 as a prerequisite for the execution of cytokinesis. It also reveals that prevailing models for how the cleavage furrow is placed in somatic cells are likely to be insufficient to explain the process.

Acknowledgement

At first, I would like to thank my supervisor Mark Petronczki for giving me the opportunity to work in his lab and offering me an exciting PhD project to work on. I am genuinely grateful for the time I could spend in the lab and for all the things I have learned under his supervision about designing experiments, data presentation and science in general. I am thankful to Mark for his continuous support and positive attitude. And last but not least, I also appreciate Mark's help with the thesis writing.

I am immensely indebted to Steve West for taking me under his wings after Mark left Clare Hall. Thanks to Steve for making me feel welcome in his lab and allowing me finish my PhD project. Last year was not a stress-free one, but Steve and all the people in the lab has made it much easier for me.

All the people that used to be part of Cell Division and Aneuploidy lab have made my life enjoyable even when the experiments did not go as planned. It was great to work with all of you, it took me some time to ask the right questions, but when I did, I always got a helpful answer. Firstly, I need to thank Kuan-Chung for starting the Ect2 project in the lab and making a lot of tools that I could use for my work. Thank you goes to Tohru for helpful advice with experiments. I am also grateful for the help from Sergey, especially with the lipid experiments. Big thank you goes to Laurent for always being happy to help with any issues and lighting the mood in the lab with his "serious face" jokes. Also big thank you to Lola for being a perfect big sister for me in the lab, answering all my questions, not just about science. I am grateful to Murielle for sharing the ups and downs of lab life with me. A big thank you goes to Ram who was always sharing his wisdom about life of PhD student at LRI and was especially helpful with weekend experiments. Special acknowledgment belongs to Ania, as she has been the perfect lab buddy and she is even better friend outside of the lab.

I am immensely grateful for the warm welcome from all members of Genetic Recombination lab and I am officially a proud Westie! It has been very helpful for

me to get comments and suggestions from you as an “outside” audience. And I even started to enjoy DNA repair after your great lab meetings. Warmest thank you goes to Maria Jose, as she is the best bay mate I could have asked for. Thanks for showing me around and for all the answered questions. I am also thankful for all the nice coffee breaks together with Marieke, Meghan and others. Our tennis sessions are great and they were really helping me to relax during writing, so thank you belongs to Gary, Raj and Michael. Thank you goes to Haley, my morning lab buddy and to Kasper for sharing the beauty of commuting to CH. I am grateful for the help of our great SOs Rajvee and Monica and I admire how they keep everything in the lab in order. Thanks everyone for tolerating my moaning during the thesis writing and for always being supportive.

I would like to thank my thesis committee namely John Diffley, Simon Boulton and for a short time Helle Ulrich, as they have made our meetings pleasant with lot of interesting discussions, and they have always been positive about my progress.

Big thank you to all the people working in Clare Hall for making the place so special. I am also grateful to all “bus and train” people for sharing the daily sagas about 398 service. Special thank you goes to Mark Johnson, Mary Nicolau, Kath Ames and everybody else who make our lives a lot easier. I would like to also thank Peter Jordan and Daniel Zicha for all the help with microscopes at LIF.

I am immensely grateful for the opportunity to work for a few weeks in the lab of Karen Oegema and Arshad Desai at Ludwig Cancer Research Institute in San Diego. It has been a great experience, even though it did not work as planned, and I really enjoyed working together with Franz and others.

Special acknowledgment belongs to Pavel, Ania and Maria Jose for reading my thesis chapters and commented on them. Thanks for your help!

Last but not least, I would like to thank my family and friends for their continuous support. And finally, I need to thank Pavel for being the best partner and critic at the same time, and for sharing the ups and downs of PhD and life in general.

Table of Contents

Abstract	3
Acknowledgement	4
Table of Contents	6
Table of figures	8
List of tables	11
Abbreviations	12
Chapter 1. Introduction	17
1.1 The cell cycle	17
1.1.1 Cell cycle stages and checkpoints	17
1.1.2 Cell cycle regulation	21
1.2 Mitosis	24
1.2.1 Stages of mitosis.....	24
1.2.2 Mechanisms of mitotic regulation.....	27
1.3 Cytokinesis	36
1.3.1 Central spindle assembly.....	37
1.3.2 Cleavage plane determination	40
1.3.3 Activation of RhoA	47
1.3.4 Contractile ring assembly and contraction	50
1.3.5 Membrane trafficking and cytokinesis	53
1.3.6 Lipids and cytokinesis	54
1.3.7 Abscission.....	55
1.4 Ect2	58
1.4.1 Ect2 protein domains and their function.....	59
1.4.2 Regulation of Ect2 activity.....	61
1.4.3 Other functions of Ect2	64
1.5 Goal of this research	66
Chapter 2. Materials & Methods	67
2.1 Plasmids and cell lines	67
2.2 siRNA transfection	72
2.3 Cell synchronization and drug treatments	72
2.4 Cell lysates preparation and western blotting (WB)	74
2.5 Immunofluorescence microscopy (IF)	75
2.6 Antibodies and dyes	75
2.7 Live-cell imaging	76
2.8 Image quantification	77
Chapter 3. Results 1 - Investigating the lipid requirements for the association of Ect2 with the plasma membrane	79
3.1 Ionomycin-Ca²⁺ treatment abrogates the localization of Ect2CT to the plasma membrane	79
3.2 PI3Ks inhibitor treatment does not prevent Ect2CT recruitment to the plasma membrane	81
3.3 Attempt to study Ect2 membrane localization using a chemically controlled lipid phosphatases	81
3.4 Conclusions - The lipid requirements for Ect2 plasma membrane association	83

Chapter 4. Results 2 - Using hybrid proteins and chemical genetic system to artificially target Ect2 to the plasma membrane	92
4.1 Construction of the system for Ect2 plasma membrane artificial targeting	92
4.2 Artificial plasma membrane targeting of Ect2 can bypass the requirement for the protein's PH domain and PBC	95
4.3 Artificial targeting of Ect2's GEF domain alone to the plasma membrane cannot support cytokinesis	97
4.3 Precocious artificial membrane targeting of Ect2.....	98
4.4 Conclusions - Chemical genetic system to artificially target Ect2 to the plasma membrane	99
Chapter 5. Results 3 - Optogenetic system to study the spatial requirements of Ect2 interaction with the plasma membrane during cytokinesis 117	
5.1 Developing an optogenetic system for spatially confined targeting of Ect2 to the plasma membrane	117
5.2 Optogenetic targeting of Ect2 to the plasma membrane causes cleavage furrow formation	119
5.3 One-sided Ect2 targeting causes formation of unilateral cleavage furrows	120
5.4 Polar activation of Cry2-mCh-Ect2 does not lead to local accumulation of the fusion protein at the plasma membrane	121
5.5 Conclusions - Optogenetic targeting of Ect2 to the plasma membrane	122
Chapter 6. Results 4 - Investigating the role of Ect2's recruitment to the spindle midzone for cleavage furrow formation	131
6.1 Localization of Ect2-BRCT^{TK} protein during cytokinesis	132
6.2 The effect of Ect2 BRCT1 domain mutations T153A and K195M on cytokinesis	135
6.3 Testing the role of astral microtubules and MgcRacGAP during cytokinesis in Ect2-BRCT^{TK} expressing cells.....	137
6.4 Conclusions - Role of Ect2 midzone recruitment in cleavage furrow formation	140
Chapter 7. Discussion.....	161
7.1 Polyanionic phosphoinositide lipids are implicated in recruiting Ect2 to the plasma membrane	161
7.2 Chemical genetics demonstrate that interaction of Ect2 with the plasma membrane is essential for cytokinesis	163
7.3 There is more to Ect2 than GEF activity and membrane engagement – a key function of the N-terminal region of Ect2?	165
7.4 What prevents a metaphase cell from forming a cleavage furrow?.....	166
7.5 Controlling cleavage furrow formation and cytokinesis using optogenetics	167
7.6 Enrichment of Ect2 at the equatorial membrane is not the main signal that places cleavage furrow in somatic cells	170
Reference List	177

Table of figures

Figure 1 The cell cycle.....	18
Figure 2 Cell cycle regulation by cyclins.....	23
Figure 3 Mitotic stages.....	26
Figure 4 Microtubule organization in a human anaphase cell	41
Figure 5 Rappaport “torus experiment”.....	42
Figure 6 Different models for cleavage furrow positioning.....	44
Figure 7 Molecular details of central spindle model of cleavage plane specification	46
Figure 8 How RhoA activation leads to contractile ring formation and furrow ingression	50
Figure 9 Ect2 domain structure.....	60
Figure 10 Ect2 localization during mitosis	66
Figure 11 Image quantification - mean intensity ratio cell periphery/cytoplasm	78
Figure 12 Ionomycin•Ca ²⁺ treatment releases PLCδ-PH and Ect2CT from the plasma membrane	86
Figure 13 Analysis of Ect2CT membrane localization after ionomycin•Ca ²⁺ treatment	87
Figure 14 PI3Ks inhibitors do not affect membrane localization of Ect2.....	88
Figure 15 Analysis of Ect2CT membrane localization after treatment with PI3Ks inhibitors	89
Figure 16 System of rapamycin-controlled hybrid phosphatases for specific depletion of phosphoinositides from the plasma membrane	90
Figure 17 Action of rapamycin-controlled hybrid PJ phosphatase displaces PLCδ- PH from the plasma membrane in HEK-293T but not HeLaK cells	91
Figure 18 C1B domain mutations	102
Figure 19 The mutation of Q27 abrogates TPA-induced membrane recruitment of the C1B domain.....	103
Figure 20 System for artificial membrane targeting of Ect2.....	104
Figure 21 Membrane translocation of Ect2 hybrid proteins after TPA addition in anaphase	105
Figure 22 TPA concentration optimization.....	106

Figure 23 Analysis of cellular phenotype after artificial membrane targeting of Ect2	107
Figure 24 Live-cell imaging analysis of cytokinesis after artificial membrane targeting of Ect2.....	108
Figure 25 Live-cell imaging analysis of cytokinetic phenotype after artificial membrane targeting of Ect2 - quantification	109
Figure 26 Live-cell imaging analysis of cytokinetic phenotype after artificial membrane targeting of Ect2 in anaphase.....	110
Figure 27 System for artificial membrane targeting of Ect2's GEF domain	111
Figure 28 Membrane translocation of Ect2's GEF domain after TPA treatment...	112
Figure 29 Analysis of cellular phenotype after artificial membrane targeting of GEF-C1B.....	113
Figure 30 Analysis of cellular phenotype after artificial membrane targeting of GEF-C1B – various TPA concentrations.....	114
Figure 31 Precocious targeting of Ect2 in metaphase cells – Anillin	115
Figure 32 Precocious targeting of Ect2 in metaphase cells – RhoA.....	116
Figure 33 Cry2 optogenetic system	125
Figure 34 Optogenetic membrane targeting of the adapted Cry2 system with swapped Cry2 and CIBN proteins	126
Figure 35 Optogenetic targeting of Cry2-mCh-Ect2 to the plasma membrane.....	127
Figure 36 Analysis of the cytokinetic phenotype upon optogenetic targeting of Ect2 to the plasma membrane	128
Figure 37 One-sided Ect2 targeting to the plasma membrane causes formation of unilateral cleavage furrow.....	129
Figure 38 Ect2 protein does not accumulate at the polar cell periphery after optogenetic targeting	130
Figure 39 Residues T153 and K195 are conserved in different BRCT domain-containing proteins and they directly coordinate the phosphate from the interacting protein	145
Figure 40 System to study Ect2-BRCT ^{TK} localization	146
Figure 41 BRCT mutations prevent spindle midzone localization of Ect2	147
Figure 42 Localization of Ect2-BRCT ^{TK} protein during mitosis	148
Figure 43 Analysis of peripheral Ect2 localization in anaphase cells	149
Figure 44 Localization of MyrPalm-GFP protein during mitosis.....	150

Figure 45 Analysis of the equatorial enrichment of Ect2 at the plasma membrane during mitosis.....	151
Figure 46 System to study the cytokinetic competency of the Ect2-BRCT ^{TK} protein	152
Figure 47 Analysis of the cytokinetic phenotype of Ect2-BRCT ^{TK} expressing cells	153
Figure 48 Live-cell imaging analysis of the cytokinetic phenotype of Ect2-BRCT ^{TK} expressing cells	154
Figure 49 Quantification of the cytokinetic phenotype of Ect2-BRCT ^{TK} expressing cells obtained by live-cell imaging	155
Figure 50 RhoA and Anillin localization in Ect2-BRCT ^{TK} expressing cells.....	156
Figure 51 Treatment with low concentration of nocodazole broadens the cortical zone of Anillin in anaphase cells.....	157
Figure 52 Treatment with low doses of nocodazole does not cause synergistic cytokinetic defects in Ect2-BRCT ^{TK} expressing cells.....	158
Figure 53 System of double cell lines expressing Ect2-BRCT ^{TK} and Mgc-ΔC1/K292L to test the role of MgcRacGAP's membrane interaction for furrowing.....	159
Figure 54 Co-depletion of Ect2 and MgcRacGAP causes minor enhancement of cytokinetic defects in Ect2-BRCT ^{TK} and Mgc-ΔC1/K292L expressing cells	160

List of tables

Table 1 List of plasmids used in this study	67
Table 2 List of stable cell lines used in this study	70

Abbreviations

aa	amino acid
ab	antibody
AcGFP	<i>Aequorea coerulea</i> green fluorescent protein
ADP	adenosine diphosphate
ALIX	ALG-2 interacting protein X
APC	anaphase promoting complex
Arf6	adenosine diphosphate -ribosylation factor 6
ARHGAP11A	Rho GTPase-activating protein 11A
ARPP19	cAMP-regulated phosphoprotein 19
Arp2/3	actin-related protein 2/3
Ark1	Aurora-related kinase 1
ATP	adenosine triphosphate
BACH1	BRCA1-associated C-terminal helicase 1
BF	bright field
BFA	brefeldin A
BRCT	BRCA-1 C-terminal
BSA	bovine serine albumin
BUB	budding uninhibited by benzimidazoles
BUBR1	BUB1-related kinase
CAK	Cdk-activating kinase
Cdc	cell division control
Cdh1	Cdc20 homologue 1
Cdk	cyclin-dependent kinase
CENP-E	centromere protein E
Cep55	centrosomal protein 55kDa
CHMP	charged multivesicular body protein
CIBN	N-terminal part of CIB1 protein
Cip	Cdk interacting protein
COS	CV-1 (simian) in origin, carrying the SV40 genetic material, cell line
CPC	chromosome passenger complex
Cry2	cryptochrome protein 2

CYK-4	cytokinesis defect 4
C1B	conserved region 1B
DAPI	4',6-diamidin-2-fenylindol
DAG	diacylglycerol
DbI	diffuse B-cell lymphoma
DH	DbI homology domain
DNA	deoxyribonucleic acid
DMEM	Dulbecco's modified eagle medium
DMSO	dimethyl sulfoxide
D-box	destruction box
ECL	electrogenerated chemiluminescence
Ect2	epithelial cell transforming sequence 2
EDTA	ethylenediaminetetraacetic acid
EGTA	ethylene glycol tetraacetic acid
Emi1	early mitotic inhibitor 1
ENSA	endosulphine alpha
ESCRT	endosomal sorting complex required for transport
FCS	foetal calf serum
FIP3	family interacting protein 3
FKBP	FK506 binding protein
FRB	FKBP-rapamycin binding
FRET	Förster resonance energy transfer
GAP	GTPase-activating protein
GDP	guanosine diphosphate
GEF	guanine nucleotide exchange factor
GEF-H1	guanine nucleotide exchange factor H1
GFP	green fluorescent protein
GM1	monosialotetrahexosylganglioside
GTP	guanosine triphosphate
Gwl	greatwall kinase
HEK-293T	human embryonic kidney 293 cells transformed by large T antigen
HRP	horseradish peroxidase
IF	immunofluorescence
INCENP	inner centromere protein

INNPP5E	inositol polyphosphate-5-phosphatase
Ipl1	increase in ploidy 1
IRES	internal ribosome entry site
ITC	isothermal titration calorimetry
Kip	kinase inhibitory protein
KIF	kinesin family member
LET-21	lethal gene 21
MAD2	mitotic arrest-deficient 2
MASTL	microtubule associated serine/threonine kinase-like
MCAK	mitotic centromere-associated kinesin
MCC	mitotic checkpoint complex
mCh	monomeric cherry tag
MEFs	mouse embryonic fibroblasts
MgcRacGAP	male germ cell Rac GTPase-activating protein
Mklp	mitotic kinesin-like protein
MPF	maturation promoting factor
MP-GAP	M phase GTPase-activating protein
MS	mass spectrometry
MTs	microtubules
MyoGEF	myosin-interacting guanine nucleotide exchange factor
MYPT1	myosin phosphatase target subunit 1
Myt1	membrane-associated tyrosine/threonine 1 kinase
MW	molecular weight
Nek2A	never in mitosis A related kinase 2
NLS	nuclear localization signal
NTC	non-targeting control
NuMA	nuclear mitotic apparatus protein
Par	partitioning defective
PBC	polybasic cluster
PBD	Polo-box domain
Pbl	pebble
PBS	phosphate-buffered saline
PBST	phosphate-buffered saline with Tween
PCM	pericentriolar material

PCR	polymerase chain reaction
PDB	protein data bank
PE	phosphatidylethanolamine
PFA	paraformaldehyde
PH	pleckstrin homology domain
PHR	photolyase homology region
PI	phosphatidylinositol
PIs	phosphoinositides
PIP2	phosphatidylinositol 4,5-bisphosphate
PI3K	phosphatidylinositol 4,5-bisphosphate 3-kinase
PI3P	phosphatidylinositol 3-phosphate
PI4K β	phosphatidylinositol 4-kinase β
PI4P	phosphatidylinositol 4-phosphate
PJ	pseudojanin
PLC	phospholipase C
Plk	Polo-like kinase
PK	protein kinase
PM	plasma membrane
PP	protein phosphatase
Prc1	protein regulator of cytokinesis 1
PVDF	polyvinylidene difluoride
Rab	ras-related protein
Rac1	ras-related C3 botulinum substrate 1
Ran	ras-related nuclear protein
Rb	retinoblastoma protein
RFP	red fluorescent protein
Rga	rho-type GTPase activating protein
Rho	ras homologous
rMLC	regulatory myosin light chain
RPE	retinal pigment epithelium cells
ROCK	rho-associated protein kinase
SAC	spindle assembly checkpoint
Ser	serine
Scc1	sister chromatid cohesion protein 1

SCF	skp, cullin, F-box containing complex
SD	standard deviation
SDS-PAGE	sodium dodecyl sulphate polyacrylamide gel electrophoresis
siRNA	small interfering RNA
SNARE	soluble <i>N</i> -ethylmaleimide-sensitive factor attachment protein receptor
SPR	surface plasmon resonance
TBST	Tris-buffered saline with Tween
TCA	trichloroacetic acid
Thr	threonine
TPA	12- <i>O</i> -Tetradecanoylphorbol-13-acetate
TPX2	targeting protein for Xklp2
Tsg10	tumour susceptibility gene 10
VPS34	vacuolar protein sorting-associated protein 34
WB	western blot
Wnt	wingless-related integration site
WT	wild type
XEct2	epithelial cell transforming sequence 2 from <i>X. laevis</i>

Chapter 1. Introduction

Life on Earth shows extreme diversity, but all living organisms share the simplest building unit, the cell. The original cell theory was postulated in the 19th century by Matthias Schleiden and Theodor Schwann and was completed by Rudolph Virchow in 1858 with his famous statement “*Omnis cellula e cellula*” (Tan and Brown, 2006). All cells arise from pre-existing cells and even the most complex organisms arise from single cells by the process of cell division. A repeating cycle of cell growth and duplication of genetic material, followed by the equal separation of cell content into new cells is the basic principle of life. Consequently, mistakes occurring during cell division can have detrimental effect for life of the cell and the organism, and are linked to various diseases. Therefore, the understanding of this fundamental process is crucial for the prevention and treatment of many of these diseases (Nurse, 2000) (Morgan, 2006).

1.1 The cell cycle

The cell cycle is a series of highly regulated steps that allow the cell to duplicate its content and to faithfully divide itself into two new daughter cells. The eukaryotic cell cycle is usually divided into four stages. Two main periods are S phase (Synthesis phase) and M phase (Mitotic phase), which are separated by two Gap stages namely G1 and G2 (Figure 1). Importantly, cell progression through different stages is tightly regulated to ensure unidirectional progression through the cell cycle. The two most important stages in cell cycle, namely the duplication of genetic content in S phase and the division of DNA and cytoplasm in M phase, are separated in time to strengthen the control of the cell cycle and to prevent deleterious mistakes (Morgan, 2006).

1.1.1 Cell cycle stages and checkpoints

G1, S and G2 phases of cell cycle are collectively called interphase, to emphasise their differences to M phase, which is characterized by dramatic changes in cell morphology. The whole period of interphase serves as a preparation for the process of mitotic cell division.

G1 is the first gap phase that occurs right after the previous mitosis has finished and it is usually the longest phase of the cell cycle. The cell needs to double its size during interphase, therefore both gap phases are periods of intense transcriptional and translational activity.

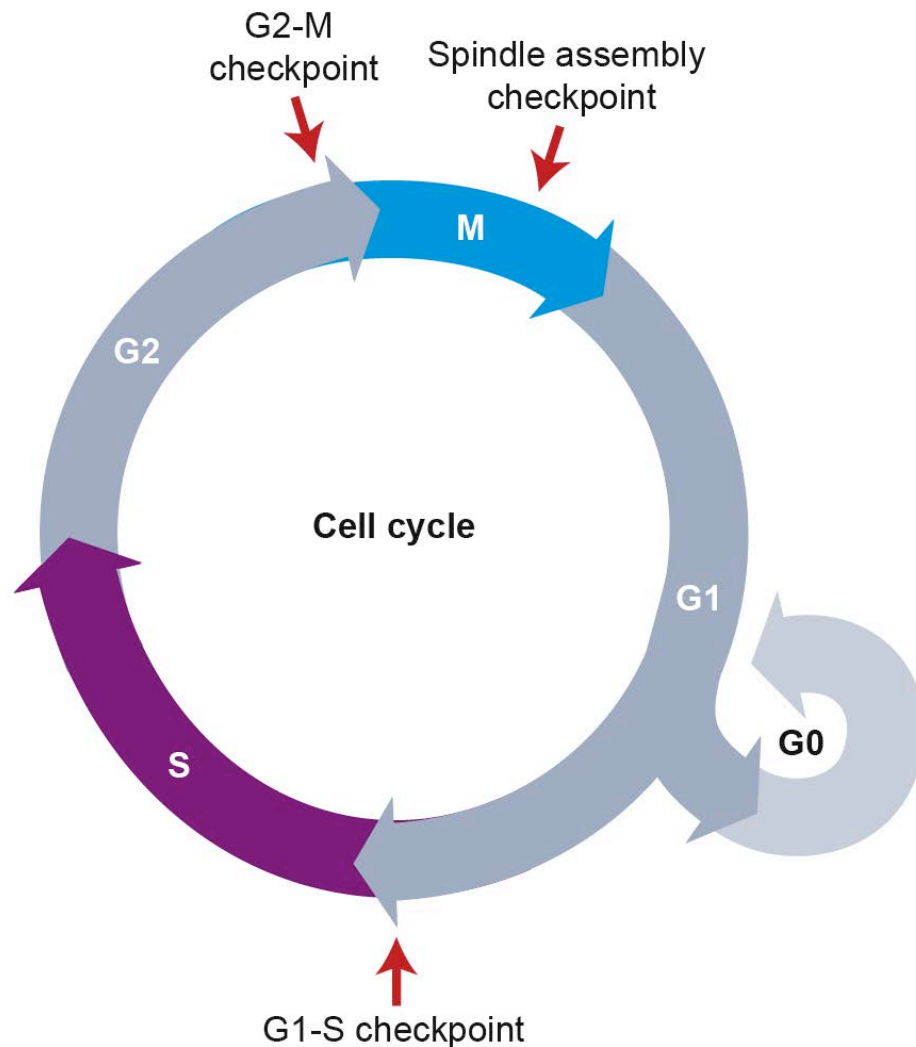


Figure 1 The cell cycle

Schematic representation of the eukaryotic cell cycle, a highly regulated step-wise process, which is divided into four distinct stages – G1, S, G2 and M phase. The first three stages of the cell cycle, collectively named interphase, prepare the cell to undergo mitosis and cytokinesis. DNA replication during S phase and cell division in M phase are separated by two gap phases that provide time for the cell to grow and synthesize all the necessary components for the next stage. Cells can also temporarily or permanently leave the cell cycle by entering G0 phase. Error-free progression through the cell cycle is ensured by a series of checkpoints that monitor if the cell is ready to proceed to the next phase. Adapted from (Morgan, 2006).

G1 is also the point from where cells can exit the cell cycle and enter a quiescent phase called G0. Cell cycle exit can be a reversible process, for example in cells waiting until favourable conditions for cell division occur, or irreversible in the case of terminally differentiated cells (Morgan, 2006). In late G1 phase the cell prepares for the onset of S phase and needs to pass the first G1-S checkpoint also known as the Start of the cell cycle. Here, the cell needs to assess if there are enough nutrients and enzymes available to progress to S phase. Additionally, an important DNA damage checkpoint halts progression through the cycle if necessary to give the cell time to repair its DNA. This is particularly important during G1-S transition, because during DNA replication unrepaired lesions can become fixed mutations that are passed on to the next generation (Li and Zou, 2005). After a cell enters S phase, DNA replication is initiated at multiple origins of replication. Replicative helicases unwind the DNA and create replication bubbles to allow bi-directional and semi-conservative replication of DNA (Masai et al., 2010). Once duplicated, the chromosomes (now called sister chromatids) are held together by a protein complex known as cohesin (Nasmyth and Haering, 2009). The genetic information stored in DNA needs to be replicated accurately, which is ensured by the S phase replication checkpoint, which shares many components with the DNA damage checkpoint. However, the S phase replication checkpoint also needs to coordinate the repair processes with the DNA synthesis (Gottifredi and Prives, 2005).

In addition to controlling the DNA synthesis, cells also have to tightly regulate the duplication of centrosomes, the main microtubule-organizing centres of animal cells (Nigg and Stearns, 2011). In cycling cells, there is normally only one centrosome that is duplicated in S phase and separated in mitosis. Other organelles and cytoplasmic components are synthesized gradually throughout the cell cycle and symmetrically distributed to two daughter cells randomly or through specific regulated mechanisms. Some organelles disassemble before mitosis like the Golgi apparatus, while others remain intact like peroxisomes (Menendez-Benito et al., 2013) (Jongsma et al., 2015).

S phase is followed by the second gap phase G2, during which the cell continues to grow and to synthesize RNAs and proteins in preparation for mitosis. Another

DNA damage checkpoint controls the state of the DNA before the transition to mitosis (Li and Zou, 2005).

M phase is distinguished from interphase because cells undergo a series of morphological changes in order to enable the faithful segregation and partitioning of chromosomes into two daughter cells. Firstly, the DNA condenses to form the structures known as chromosomes and the nuclear envelope breaks down. Chromosomes are then captured by microtubules, which attach to a large protein complex called the kinetochore, which is assembled in the centromeric region of the chromosome. Afterwards, sister chromatids are segregated by the mitotic spindle, a structure formed from microtubules nucleated by the centrosomes at opposite cell poles (Foley and Kapoor, 2013). The physical separation of the chromatids needs to be tightly controlled to prevent segregation errors and aneuploidy. A specific mitotic checkpoint, the spindle assembly checkpoint (SAC), plays a key role in ensuring the fidelity of chromosome segregation. The SAC acts prior to the metaphase-to-anaphase transition and ensures that all sister chromatids are correctly attached to kinetochore microtubules. Unattached kinetochores block anaphase onset until all chromosomes are correctly attached in a bioriented fashion, so that sister chromatids are connected to microtubules emanating from opposite spindle poles (Musacchio and Salmon, 2007).

After SAC is turned off, the anaphase promoting complex (APC) is activated, and chromosomes segregate to the opposite poles, which is a point of no return in mitosis (Sullivan and Morgan, 2007). Afterwards, cytokinesis physically divides the cell into two new daughter cells and cells exit mitosis, which completes the cell cycle (Green et al., 2012). Daughter cells formed by mitosis are diploid, i.e. they have two homologous copies of each chromosome. Haploid cells, important for the production of gametes and sexual reproduction, arise from meiosis. The meiotic program is a specialized form of nuclear division that involves two rounds of chromosome segregation without an intervening round of DNA replication (Morgan, 2006).

1.1.2 Cell cycle regulation

Control mechanisms ensure that all the complex steps of the cell cycle occur in the right order and without mistakes. Deregulation of the cell cycle can lead to aneuploidy and affects genome stability, consequently impairing the viability of the cell and in severe cases the health status of the whole organism. In particular, cell cycle defects have been linked to cancer (Kops et al., 2005) (Malumbres and Barbacid, 2009). Many control mechanisms function in all cells to prevent these deleterious consequences. The cell proceeds to the next cell cycle stage only if it has successfully completed the previous steps, thus it needs to pass series of checkpoints discussed in the previous section (Hartwell and Weinert, 1989).

In 1970, Rao and Johnson fused HeLa cells that were in different cell cycle stages to show that there are molecular factors regulating the cell cycle states and progression. For example, S-phase cell triggered DNA replication when fused to G1 cell and fusion to G1 cell prevented mitotic entry in G2 cell (Rao and Johnson, 1970). Soon thereafter the elusive factor was named maturation promoting factor (MPF) by Masui and Markert, when they found that injection of cytoplasm from dividing oocytes could drive meiotic entry in oocytes arrested in G2 phase (Masui and Markert, 1971). Following studies have shown oscillations in MPF activity during the cell cycle, and proposed that MPF is a protein whose activity is regulated by a post-translational modification (Masui, 1982) (Gerhart et al., 1984). At the same time, Tim Hunt and his colleagues discovered proteins that appeared and disappeared from sea urchin egg extracts in a similar fashion as the proposed activity of MPF, and they proposed to call them cyclins (Evans et al., 1983). Later it was confirmed that MPF was a complex of a cyclin with another protein (Lohka et al., 1988).

The identity of the second protein has been elucidated by Paul Nurse and colleagues by using yeast genetics (Nurse et al., 1976) (Thuriaux et al., 1978). They identified multiple *Schizosaccharomyces pombe* (*S. pombe*) mutants that could not undergo nuclear division. Amongst them, they discovered gene *cdc2* and they showed the protein encoded by gene *cdc2* was cyclin-dependent kinase 1 (Cdk1). After years of research, Nurse lab also identified human homolog of Cdk1

encoded by CDC2 gene. Remarkably, Nurse and colleagues could also show that CDC2 was able to complement the role of the *cdc2* gene in *S. pombe*, which demonstrated that the role of Cdk enzymes is conserved from yeast to human (Lee and Nurse, 1987).

Nowadays, we know that Cdks lie at the heart of the cell cycle regulation. Cyclin-dependent kinases are heterodimeric enzymes with a catalytic serine/threonine kinase domain and a regulatory cyclin subunit. Cdks not bound to cyclins are inactive and the interaction with cyclins triggers structural changes in the Cdk catalytic subunit (Morgan, 1997). Protein levels of Cdks remain relatively constant during the cell cycle, but their activity is dependent on the associated cyclin subunits, the concentrations of which oscillate. Moreover, binding to different cyclin subunits affects the specificity of Cdks, thus driving the cell through the cell cycle stages by phosphorylating different substrates (Figure 2) (Jeffrey et al., 1995) (Kitagawa et al., 1996) (Ubersax et al., 2003) (Loog and Morgan, 2005).

Cell cycle progression in yeast relies on a single Cdk only (Cdc2 in *S. pombe* and Cdc28 in *Saccharomyces cerevisiae* [*S. cerevisiae*]). Higher eukaryotes express more than ten different Cdks, but only two of them are essential for the cell cycle transitions Cdk1 (Cdc2) and Cdk2. This suggests that the combinatorial action of Cdks with different cyclins is crucial for progression through the cell cycle. Years of research led to formulation of the classical model of the cell cycle (Morgan, 1997). According to this model, Cdk4 and Cdk6 bind to D-type cyclins to promote the start of the cell cycle in early G1 by phosphorylation of proteins from the retinoblastoma protein family – Rb, p107 and p130 (Matsushime et al., 1994) (Sherr and Roberts, 1999). This leads to activation of E2F transcribed genes, including cyclin E and cyclin A. Subsequently, in late G1, Cdk2-Cyclin E complex further phosphorylates Rb proteins and thus promotes more transcription of E2F genes, which results in the transition from G1 to S phase (Weinberg, 1995) (Dyson, 1998) (Lundberg and Weinberg, 1998).

Cdk1 and Cdk2 in complex with cyclin A (A1 and A2 in vertebrates) drives the progression of the cell through S phase by phosphorylating targets involved in DNA replication (Girard et al., 1991) (Walker and Maller, 1991) (Tanaka and Araki, 2010).

S phase cyclins are synthesized in late G1 but stay inactive due to interaction with protein inhibitors p21 and p27 belonging to the Cip/Kip family (Sic1 inhibitor in yeast) (Schneider et al., 1996) (Nakayama and Nakayama, 1998). Cdk2-cyclin E-mediated phosphorylation targets these inhibitors for degradation by the SCF ubiquitin ligase complex, which promotes S phase progression (Pagano et al., 1995) (Verma et al., 1997).

Cyclin B is the main mitotic cyclin, synthesized mainly in G2 phase. In mammals there are two B cyclins – B1 and B2, but only B1 is essential (Brandeis et al., 1998). Cdk1-cyclin B1 complex activity is suppressed by Cdk inhibitors and inhibitory phosphorylation on Cdk1 (Morgan, 1997). An active Cdk1-cyclin B1 complex drives cells to division by phosphorylating a large number of substrates affecting all aspects of mitosis and cytokinesis, which will be discussed in greater detail in the following chapters (Nigg, 1993) (Errico et al., 2010) (Pagliuca et al., 2011). After chromosome segregation, APC degrades the mitotic cyclin B and Cdk1 substrates are dephosphorylated, which elicits mitotic exit and completes the cell cycle (Sullivan and Morgan, 2007).

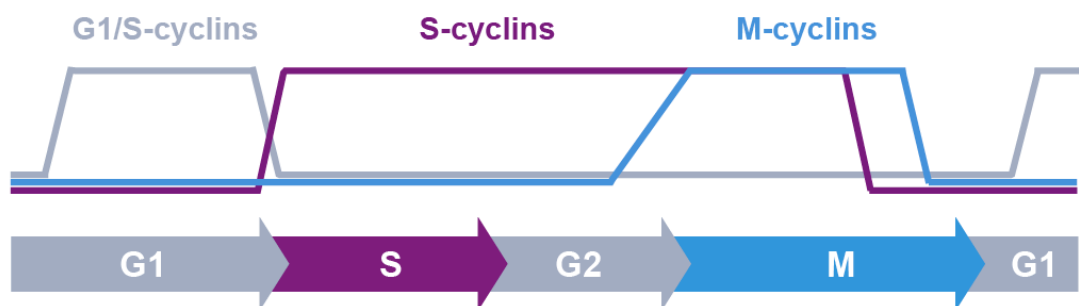


Figure 2 Cell cycle regulation by cyclins

A schematic depiction showing the levels of different cyclins during the cell cycle and how they coincide with the distinct transitions. Adapted from (Morgan, 2006).

The classical model presented above has been challenged by results emerging from mouse models. Interestingly, Cdk2 knockout mice are viable but sterile, suggesting that Cdk2 is crucial for meiosis but dispensable for mitotic cycles in somatic cells (Ortega et al., 2003) (Berthet et al., 2003). Furthermore, Cdk1 was shown to be able to substitute for Cdk2 during G1/S transition and in S phase (Aleem et al., 2005) (Hochegger et al., 2007). Following studies by Santamaria et al.

showed that Cdk1 is the only Cdk that is truly essential for cell division in somatic cells, as the cell cycle was functional in mouse lacking all interphase Cdks (Cdk2, Cdk3, Cdk4 and Cdk6) (Santamaria et al., 2007b). All these results have changed the classical model of the cell cycle and have shown the Cdks and cyclins are more redundant than previously anticipated (Satyanarayana and Kaldis, 2009). Results obtained in yeasts further strengthen this concept, as introduction of a single fusion protein consisting of *cdc2* and B-type cyclin *cdc13* inserted into the genome can rescue deletion of endogenous *cdc2* and *cdc13* and drive the cell cycle progression in *S. pombe* in the absence of any other cyclin (Coudreuse and Nurse, 2010). Currently, researchers use mathematical modelling together with data generated by high-throughput approaches (e.g. mass spectrometry [MS] or siRNA screens) to build a minimal model for the regulation of the eukaryotic cell cycle (Gerard et al., 2015).

1.2 Mitosis

The father of cytology, Walter Flemming, coined the name mitosis in the late 19th century (Flemming, 1882). The word itself originates from a Greek word for thread – mitos. Flemming studied the process of cell division using cells obtained from gills and fins of salamanders and drew incredibly accurate sketches of the process, showing the separation of the chromosomes. He also named chromatin, based on the fact that it strongly absorbed aniline dyes (chroma means colour in Greek) and also observed its nuclear localization (Zacharias, 2001) (Morgan, 2006). Different stages of mitosis are schematically depicted in Figure 3 and described below.

1.2.1 Stages of mitosis

Mitosis starts in prophase, when replicated DNA undergoes large-scale condensation induced partially by the multisubunit protein complex condensin (Hirano and Mitchison, 1994) (Hirano, 2012). At the same time, the two centrosomes move apart to opposite poles of the cell and the structure of the mitotic spindle starts to assemble, orchestrated by motor proteins (Rusan et al., 2001) (Tanenbaum and Medema, 2010). The bipolar mitotic spindle is fully assembled by prometaphase and after nuclear envelope breakdown the

microtubules of the spindle start capturing the chromosomes via kinetochores on sister chromatids (Cheeseman, 2014). Microtubules pull on kinetochores and are thought to create a tension that is opposed by sister chromatid cohesion (Nasmyth and Haering, 2009, Peters and Nishiyama, 2012).

The metaphase stage of the cell cycle is reached when all the chromosomes are aligned at the metaphase plate in the middle of the cell. Metaphase is also the stage when the mitotic rounding of the cell is complete and the typical cultured cell has a shape resembling a sphere. The rounding starts at the onset of mitosis and requires a massive remodelling of the actin cytoskeleton, which is closely linked to the mitotic spindle formation. The round shape of the cell helps establish a symmetrical division of the cell material (Cramer and Mitchison, 1997) (Lancaster and Baum, 2014). After all the chromosomes are correctly aligned and attached to the opposite poles, the spindle assembly checkpoint is satisfied and anaphase promoting complex is activated. APC activation marks the onset of anaphase by ubiquitination and rapid proteasome-mediated degradation of the regulatory proteins securin and mitotic cyclin B (Pines, 2011). Securin degradation releases the cysteine-protease separase, which cleaves the Scc1 subunit of the cohesin complex, thus allowing the sisters chromatids to segregate to the opposite poles (Funabiki et al., 1996) (Uhlmann et al., 1999).

During the first part of anaphase (anaphase A), sister chromatids are pulled to the poles by shortening of kinetochore microtubules. In the subsequent anaphase B, the mitotic spindle elongates and the distance between the poles is increased, which further separates the two sets of chromosomes (Morgan, 2006). During anaphase, sets of non-kinetochore microtubules overlap with their plus ends in the middle of the cell by action of multiple microtubule bundling factors and motor proteins. This creates a signalling platform called the spindle midzone, or central spindle, which together with astral microtubules directs the cytokinetic division (Glotzer, 2009) (D'Avino et al., 2015). During the final stage of mitosis called telophase, the nuclear envelope reassembles, the chromosomes decondense and the mitotic spindle is dissolved. Cytokinesis starts at anaphase with the ingression of a cleavage furrow between the two sets of segregated chromosomes, until the two daughter cells remain connected only by a narrow intercellular bridge.

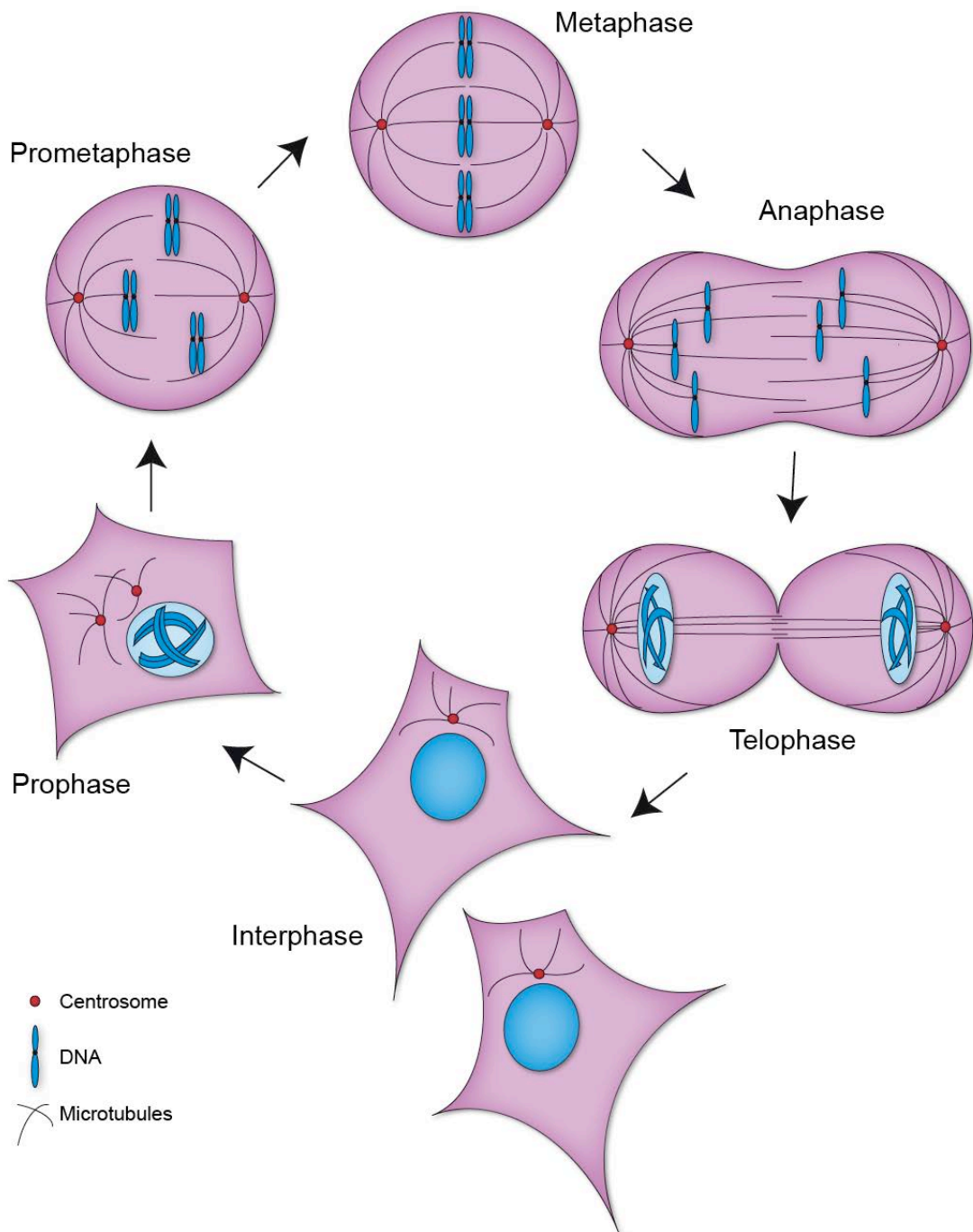


Figure 3 Mitotic stages

Schematic illustration of the cell division cycle with open mitosis. Late interphase cells have duplicated DNA, centrosomes and other cellular components. As cell enters mitosis, the DNA starts to condense and the chromosomes become visible. Centrosomes move apart to the opposite poles and build the mitotic spindle. In prometaphase, the nuclear envelope breaks down and chromosomes are captured by kinetochore microtubules. After all chromosomes are correctly attached and bioriented on the metaphase plate, the anaphase starts and the chromosomes segregate to opposite poles. Afterwards, the two daughter cells are physically separated by cytokinesis and the cells exit mitosis and enter G1 phase again.

This connection is severed by the process of abscission at the end of telophase (Mierzwa and Gerlich, 2014).

1.2.2 Mechanisms of mitotic regulation

To successfully finish the cell cycle, a cell needs to divide into two identical daughter cells. Equal segregation of duplicated chromosomes is especially important to ensure genome stability in daughter cells. Therefore the process of mitosis is under close supervision by various control mechanisms. As mitosis is a series of highly dynamic and ordered steps, the regulatory mechanisms need to act at equally high speed. Thus, most of the transitions are controlled by post-translational modifications, mainly protein phosphorylation by mitotic kinases (Morgan, 2006). Recently, research of mitotic regulation has turned to protein phosphatases and showed that phosphatases and dephosphorylation events are likely as important for mitotic regulation as mitotic kinases (Barr et al., 2011). Another layer of control is provided by ubiquitin-mediated proteolysis of various targets, as precisely timed proteolysis drives the mitotic progression and ensures irreversibility of the transitions (Pines, 2011).

1.2.2.1 Mitotic kinases and phosphatases

For many years, cell cycle research has focused on mitotic kinases and their regulation, and it showed that Cdk1, Plk1 and Aurora kinases are the main mitotic kinases. Due to their key role in cell division regulation, these kinases are also promising targets for anti-cancer therapies (Salmela and Kallio, 2013) (Domenech and Malumbres, 2013). Cdk1, Plk1 and Aurora kinases will be discussed further below, together with their phosphatase counterparts.

Cdk1

Cdk1 is a proline-directed kinase with a preference for the consensus sequence S/TP-X-K/R, however, it can also phosphorylate targets carrying the minimal consensus sequence S/T-P or even non-S/T-P sites (Ubersax et al., 2003) (Errico et al., 2010) (Satterwhite et al., 1992) (Egelhofer et al., 2008). To be catalytically active, Cdk1 must bind a regulatory cyclin subunit. In mammals, cyclin B1 is the main mitotic cyclin, but early mitotic events are also regulated by Cdk1-cyclin A

complex. Additionally, the Cdk1-cyclin A complex seems to work upstream of Cdk1-cyclin B and mediate its activation (Mitra and Enders, 2004) (Fung et al., 2007) (Gong et al., 2007). Cyclin binding is necessary but not sufficient for Cdk1 activation, as a threonine residue close to the active site also needs to be phosphorylated by Cdk-activating kinase (CAK) comprised of Cdk7, cyclin H and Mat1 (Malumbres, 2014). Interestingly, CAK activity remains constant throughout the cell cycle, so it does not exert any temporal control over the Cdk1-cyclin B complex activation.

Cdk1-cyclin B complex accumulates throughout G2 phase, but it is kept inactive until mitosis by two important inhibitory phosphorylation events on T14 and Y15 residues by Wee1 and Myt1 kinases (Russell and Nurse, 1987) (Parker et al., 1992) (Mueller et al., 1995). Phosphorylation of these residues probably prevents substrate binding and also changes the orientation of the ATP molecule (Atherton-Fessler et al., 1993) (Welburn et al., 2007). To fully activate Cdk1-cyclin B complex, these phosphorylations need to be removed by Cdc25 phosphatases to trigger mitotic entry (Dunphy and Kumagai, 1991, Kumagai and Dunphy, 1991) (Rhind and Russell, 2012). In some cells, e.g. *Xenopus laevis* (*X. laevis*) embryos, this regulatory circuit of Wee1 and Cdc25 is enough to trigger a switch-like response and drive the cell to mitosis. The activity of both Wee1 and Cdc25 is regulated by Cdk1-cyclin B itself, as Cdk1 phosphorylation inhibits Wee1 and activates Cdc25 thus creating a positive feedback loop. This feedback loop system ensures rapid activation of Cdk1-cyclin B complex (Kim and Ferrell, 2007) (Trunnell et al., 2011).

In mammals, there are three isoforms of Cdc25, namely Cdc25A, B and C and all of them have been shown to activate Cdk1-cyclin B complex. Cdc25B activity peaks in prophase but the protein is already active in G2 phase, so it does not trigger mitotic entry, but likely has a role in the initial activation of Cdk1-cyclin B (Lammer et al., 1998) (De Souza et al., 2000). Cdc25A/C are both activated in prophase and their action is important for the activation of Cdk1-cyclin B complex at the onset of mitosis (Hoffmann et al., 1993) (Strausfeld et al., 1994). Cdk1 phosphorylation stabilizes Cdc25A and activates Cdc25C (Mailand et al., 2002) (Hoffmann et al., 1993). Additionally, Wee1 is targeted for proteasome destruction after Cdk1 phosphorylation, and Myt1 is inhibited by Plk1 phosphorylation

(Watanabe et al., 1995) (Booher et al., 1997) (Nakajima et al., 2003). This mechanism forms a part of the regulatory system of feedback loops regulating the mitotic entry. Gradual increase of Cdk1-cyclin B activity seems to be important for temporal regulation as different levels of Cdk1 activity trigger different mitotic events (Gavet and Pines, 2010) (Wieser and Pines, 2015).

Another way to control Cdk1-cyclin B activity is the localization of the complex. Cdk1-cyclin B can shuttle between the nucleus and the cytoplasm. Throughout G2, the complex is cytoplasmic, in early prophase it starts to localize to the duplicated centrosomes, and at the end of prophase the complex suddenly translocates to the nucleus (Morgan, 2006). Plk1 phosphorylates cyclin B on S147 to promote the import to the nucleus (Toyoshima-Morimoto et al., 2001). Inhibitory kinase Wee1 is located in the nucleus and it inactivates Cdk1-cyclin B complex, causing export of the complex back to the cytoplasm. When the nuclear concentration of Cdk1-cyclin B reaches certain threshold to counteract the Wee1 inhibition, the nuclear concentration rapidly increases. Consequently, Cdk1 can phosphorylate its nuclear targets including lamins, which leads to nuclear envelope breakdown and onset of early mitotic events (Li et al., 1997) (Lindqvist et al., 2007) (Guttinger et al., 2009). In the cytoplasm, Cdk1-cyclin B complex phosphorylates numerous substrates to promote cell rounding, assembly of the mitotic spindle, the segregation of multiple organelles and others (Matthews et al., 2012) (Nigg et al., 1996) (Jongsma et al., 2015).

Cdk1-cyclin B activation and modification of its substrates is necessary for mitotic progression, but for Cdk1 substrate phosphorylation events to be stable during mitosis, the counteracting phosphatases need to be inactivated at the same time. Budding yeast rely on Cdc14 to dephosphorylate Cdk1 targets (D'Amours and Amon, 2004). This role of Cdc14 is not conserved in other eukaryotes where PP2A and PP1 phosphatase families were identified as important for mitotic progression, in particular for the mitotic exit (Kinoshita et al., 1990) (Chen et al., 2007) (Mochida et al., 2009) (Schmitz et al., 2010). During early mitosis, Cdk1 substrates are dephosphorylated by PP2A-B55 δ (Vandre and Wills, 1992) (Burgess et al., 2010). Research in *X. laevis* embryos showed PP2A activity is controlled by a protein kinase called Greatwall (Gwl) (Castilho et al., 2009). Microtubule-associated

serine/threonine kinase-like enzyme (MASTL) is a human homologue of Gwl, and seems to have the same role (Burgess et al., 2010). Interestingly, Gwl does not inhibit PP2A directly, but acts via activation of two small protein inhibitors ENSA and ARPP-19, which bind specifically to PP2A when in complex with the regulatory subunit B55 δ (Mochida et al., 2010) (Gharbi-Ayachi et al., 2010) (Rangone et al., 2011).

By anaphase onset, after cell starts to segregate its chromosomes, the Cdk1-cyclin B complex has fulfilled its purpose and it is inactivated via proteolytic degradation of cyclin B. Cyclin B contains a D-box recognized by APC complex, which polyubiquitinates cyclin B and targets it for degradation (Pines, 2011). Cdk1 inactivation, concurrent with the activation of PP1 and PP2A phosphatases reverses Cdk1 phosphorylations and thereby triggers mitotic exit (Schmitz et al., 2010) (Wurzenberger and Gerlich, 2011). PP1 is targeted to many cell structures, for example the Repo-Man regulatory subunit brings PP1 to segregated chromosomes and starts their decondensation (Vagnarelli et al., 2011). Inactivation of Cdk1-cyclin B is also a necessary signal for subsequent cytokinesis (Niiya et al., 2005) (Potapova et al., 2006).

Plk1

Polo kinase was identified in 1988 in *Drosophila melanogaster* (*D. melanogaster*) and its role in cell division was proposed when *Polo* mutant cells showed aberrant mitosis and meiosis (Sunkel and Glover, 1988). Polo is well conserved amongst eukaryotes, and the human genome encodes five Polo-like kinases (Plks). Plk1 is a human homologue of Polo in *D. melanogaster*, Plo1 in *S. pombe* and Cdc5 in *S. cerevisiae*. Plk1 is a serine/threonine protein kinase carrying its kinase domain at the N-terminus. At the C-terminus there are two Polo box regions that together form a Polo box domain (PBD), which binds phosphorylated proteins (Archambault and Glover, 2009). The substrates are usually phosphorylated by Cdk1 to create a docking site, but Plk1 can also self-prime its targets (Elia et al., 2003) (Neef et al., 2007).

PBD binding provides selective targeting of Plk1 to specific places within a cell, which is important for its functions. During interphase, Plk1 localizes to the nucleus,

and in late G2 phase it translocates to the cytoplasm. Plk1 has a regulatory role for the timing of mitotic onset, and inhibition of Plk1 leads to a delay in mitotic entry as well as to a prominent cell arrest in prophase afterwards (Lenart et al., 2007). Plk1 together with Cdk1 targets Wee1 phosphatase for degradation and it promotes the nuclear localization of Cdc25C and cyclin B (Watanabe et al., 1995) (Kumagai and Dunphy, 1996) (Toyoshima-Morimoto et al., 2001). After export from the nucleus, Plk1 is localized to centrosomes. Plk1 activity is crucial for centrosome maturation, as it promotes recruitment of pericentriolar material (PCM) (Lane and Nigg, 1996). Moreover, Plk1 is also required for the assembly of the mitotic spindle (Sumara et al., 2004). Recently, a surveillance mechanism that controls the position of the mitotic spindle was discovered. LGN/NuMA/dynein pathway controls the position and orientation of the spindle and is necessary for the symmetric division into two equally sized daughter cells. Plk1 negatively regulates the cortical localization of dynein that pulls on the astral microtubules (Kiyomitsu and Cheeseman, 2012).

In metaphase, Plk1 is also targeted to kinetochores, where it regulates kinetochore-microtubule attachments. Notably, Plk1 phosphorylates BUBR1 (a kinase important for the SAC) and while not crucially involved in the checkpoint function, the phosphorylation promotes stable attachments of kinetochores to the microtubules (Elowe et al., 2007). Plk1 together with Aurora B kinase are also responsible for removing the cohesin complex from the chromosome arms in prophase and prometaphase by phosphorylating the complex and thus lowering its affinity for chromatin (Sumara et al., 2002). Loss of centromeric cohesion is prevented by shugoshin, which recruits phosphatase PP2A-B56 to oppose Plk1 and Aurora B phosphorylations (Salic et al., 2004) (Kitajima et al., 2004) (Kitajima et al., 2006) (Tang et al., 2006b).

After the separation of sister chromatids, Plk1 is recruited to the spindle midzone by interaction with Prc1, a microtubule bundling protein for spindle midzone (Schuyler et al., 2003) (Neef et al., 2007). Studies of the role of Plk1 in the final stages of mitosis were not possible because of the essential roles that Plk1 plays in early mitosis. Development of small molecule inhibitors, however, uncovered the role of Plk1 in cytokinesis. Plk1 activity is necessary for cleavage furrow formation and timely abscission, and this function will be discussed later (Santamaria et al.,

2007a) (Burkard et al., 2007) (Petronczki et al., 2007) (Brennan et al., 2007) (Bastos and Barr, 2010). Eventually, during mitotic exit, Plk1 is degraded by the APC pathway (Lindon and Pines, 2004). A counteracting phosphatase for Plk1 is supposed to be PP1C, which is targeted to Plk1 via direct binding of its regulatory subunit MYPT1 (Yamashiro et al., 2008). The crucial role of Plk1 for cell division makes it an interesting target for anti-cancer treatments (Strebhardt, 2010) (Murugan et al., 2011) (Gjertsen and Schoffski, 2015).

Aurora kinases

The Aurora kinase family is another group of important mitotic kinases. Like Plk1, they have been discovered in *D. melanogaster* when *Aurora* mutants failed to form a bipolar spindle (Glover et al., 1995). Metazoans have at least two Aurora kinases – Aurora A and Aurora B, while yeasts rely only on one isoform, functionally closer to the mammalian Aurora B enzyme, namely Ipl1 in *S. cerevisiae* and Ark1 in *S. pombe* (Carmena et al., 2009) (Chan and Botstein, 1993) (Petersen et al., 2001). Mammals additionally have Aurora C, which is expressed primarily in gonads and plays a role in meiosis (Yanai et al., 1997) (Tang et al., 2006a).

Aurora kinases belong to the serine/threonine kinase family, they have a catalytic domain and non-catalytic regulatory regions. Aurora A and B are very similar both at the level of amino acid sequence and protein structure. Despite these similarities, they have distinct cellular functions and their localization pattern is also different. Differences in the non-catalytic regions and interactions with various regulatory proteins can explain these diverse roles of the two kinases (Carmena et al., 2009) (Morgan, 2006).

Since G2 phase, Aurora A is mainly found on centrosomes and, at low level also at the mitotic spindle during later stages of mitosis (Roghi et al., 1998) (Sugimoto et al., 2002). Phosphorylation of the T-loop, essential for the kinase activity can be mediated by protein kinase A (PKA), or Aurora A also has the ability to auto-phosphorylate itself (Walter et al., 2000) (Cheeseman et al., 2002). Aurora A has a role in mitotic entry, where it indirectly activates Cdk1-cyclin B by means of Cdc25B phosphatase activation, and it also triggers Plk1 activation together with its cofactor Bora (Dutertre et al., 2004) (Macurek et al., 2008) (Seki et al., 2008). The

main functions of Aurora A are in centrosome maturation and bipolar spindle formation.

Aurora A regulates centrosome maturation by recruiting pericentriolar material (Hannak et al., 2001) (Abe et al., 2006). A role in spindle assembly relies on cofactor TPX2 that activates Aurora A and targets it to the spindle microtubules (Tsai and Zheng, 2005). It has been proposed that TPX2 binding also prevents Aurora A dephosphorylation by PP1 phosphatase (Eyers et al., 2003) (Bayliss et al., 2003). Recently, PP6 has been shown as the major phosphatase antagonizing Aurora A activity (Zeng et al., 2010). Assembly of the bipolar spindle requires sliding forces in-between the antiparallel microtubules as well as the cortical forces pulling on the astral microtubules. Aurora A modulates astral microtubule behaviour by phosphorylating Eg5 kinesin, which can slide the microtubules and also MCAK protein, important for the bipolarity of the spindle (Giet et al., 2002) (Kapitein et al., 2005) (Zhang et al., 2008). Aurora A carries a D-box in its sequence and is degraded during mitotic exit by the APC (Honda et al., 2000).

Aurora B is the catalytic subunit of the chromosomal passenger complex (CPC), a protein assembly containing also INCENP, survivin and borealin proteins. Interaction with the CPC is required for Aurora B activation and localization (Adams et al., 2000) (Uren et al., 2000) (Gassmann et al., 2004) (Carmena et al., 2009). INCENP is the scaffold protein of the CPC and it is crucial for Aurora B full activation (Bishop and Schumacher, 2002). In early mitosis, the CPC is found on chromosome arms, later it translocates to the centromeres and kinetochores, and after sister chromatid segregation Aurora B accumulates at the spindle midzone (Carmena et al., 2012).

Aurora B phosphorylates histone H3 on S10, which is a classic epigenetic mark for mitotic chromosomes (Hsu et al., 2000) (Murnion et al., 2001). Consequently, the role of Aurora B in chromosome compaction has been extensively studied, but the level of H3S10 phosphorylation does not correlate with the level of chromosome compaction, and the role for Aurora B in condensation seems to be more relevant for yeast cells (Adams et al., 2001) (Neurohr et al., 2011). One of the main functions of the CPC is to promote chromosome biorientation by destabilization of

incorrect kinetochore-microtubule attachments. A current working model postulates that correctly attached kinetochores are under tension and stretched from the zone of Aurora B phosphorylation (Tanaka et al., 2002) (Andrews et al., 2004) (Liu et al., 2009). Aurora B phosphorylates the outer kinetochore component Ndc80, which leads to destabilization of the attachment and microtubule release (DeLuca et al., 2006) (Cheeseman et al., 2006). Aurora B destabilization of the kinetochore complex is opposed by PP1 γ phosphatase (Liu et al., 2010).

Aurora B activity is crucial for the spindle assembly checkpoint (SAC) and recruitment of its key factors. Moreover, Aurora B also promotes activation of SAC response by other means than error-correction (Carmena et al., 2012) (Santaguida et al., 2011) (Maldonado and Kapoor, 2011). After the SAC is satisfied and the sisters start to segregate, Aurora B translocates to the spindle midzone. This change of localization is important for preventing mitotic checkpoint re-engagement after chromosome segregation (Vazquez-Novelle and Petronczki, 2010). By using a FRET sensor, Fuller et al. have shown there is a gradient of Aurora B phosphorylation with a centre in the middle of the cell during anaphase. They also proposed that this has a role in the cleavage furrow positioning (Fuller et al., 2008). Furthermore, Aurora B also affects abscission, where it can impose an abscission delay when lagging chromatin is found in the way of the cleavage furrow or intercellular bridge (Steigemann et al., 2009). This function will be discussed in more detail in subsequent chapters. Aurora B is targeted for degradation by APC during mitotic exit (Nguyen et al., 2005) (Stewart and Fang, 2005).

Anaphase promoting complex

Another important control of mitotic progression is provided by ubiquitin-mediated proteolysis. Various targets are degraded at specific times, which drives the progression through mitosis and ensures the irreversibility of the transitions. The key ubiquitin ligase (E3 enzyme) for mitosis is APC, also known as the cyclosome (Pines, 2011). APC is a large multisubunit complex that marks its targets by polyubiquitin chains for subsequent proteolysis by the 26S proteasome (Pickart, 2001). APC complex recognizes the substrates through several different degradation sequences or degrons. The most common motif is the destruction box (D-Box) (Glotzer et al., 1991). For the successful interaction with the D-box, APC

needs to be activated by interaction with one of the two important cofactors – Cdc20 and Cdh1 (Passmore and Barford, 2005) (Matyskiela and Morgan, 2009) (Buschhorn et al., 2011) (da Fonseca et al., 2011). During interphase, APC is kept inactive by the inhibitory factor Emi1. At mitotic entry Emi1 is phosphorylated by Plk1 and targeted for degradation by another E3 ligase complex – SCF (Hansen et al., 2004). Interaction with Cdc20 and Cdh1 confers temporal and substrate specificity regulation to the APC, which is crucial for correct mitotic progression.

APC^{Cdc20} complex is activated in mitosis at the same time as the nuclear envelope breaks down (den Elzen and Pines, 2001) (Geley et al., 2001). Activation of APC^{Cdc20} depends on Cdk1-cyclin B phosphorylation, but the exact nature of the regulation is unclear (Rudner and Murray, 2000) (Wieser and Pines, 2015). APC^{Cdc20} is activated at the end of prophase, but its main substrates, securin and cyclin B, are not degraded until the end of metaphase. This delay is caused by the activation of spindle assembly checkpoint. As a response to unattached kinetochores, checkpoint proteins form a mitotic checkpoint complex (MCC) composed of MAD2, BUBR1 and BUB3 that inhibits APC^{Cdc20} complex formation by binding the Cdc20 cofactor (De Antoni et al., 2005) (Sudakin et al., 2001) (Kulukian et al., 2009). Interestingly, two APC^{Cdc20} substrates – cyclin A and Nek2A kinase are degraded while the complex is inactivated in prometaphase (den Elzen and Pines, 2001) (Geley et al., 2001) (Hames et al., 2001). Nek2A is a Ser/Thr kinase important for centrosome separation (Faragher and Fry, 2003). Early degradation of cyclin A and Nek2A probably depends on direct interaction with the APC^{Cdc20} complex (Wolthuis et al., 2008) (Di Fiore and Pines, 2010).

In metaphase, after all sister chromatids are correctly attached to kinetochore microtubules and bioriented, the SAC is turned off and the APC^{Cdc20} targets securin and cyclin B for degradation (Clute and Pines, 1999) (Hagting et al., 2002). This results in separase activation, triggering the cleavage of cohesin holding the sister chromatids together and their segregation to opposite poles (Nasmyth and Haering, 2009) (Funabiki et al., 1996) (Uhlmann et al., 1999). In vertebrates, separase activity is additionally regulated by Cdk1 phosphorylation (Stemmann et al., 2001). Cyclin B degradation also leads to dephosphorylation of the Cdh1 cofactor, which allows APC^{Cdh1} complex formation (Kramer et al., 2000) (Hagting et al., 2002)

(Matyskiela and Morgan, 2009) (Listovsky and Sale, 2013). Afterwards, APC^{Cdh1} targets Cdc20, Plk1 and Aurora kinases amongst other substrates for degradation (Sivakumar and Gorbsky, 2015). Cyclin B degradation inactivates Cdk1 kinase, and the activity of PP1 and PP2A phosphatases results in dephosphorylation of mitotic substrates in turn leading to cytokinesis and mitotic exit (Schmitz et al., 2010) (Wurzenberger and Gerlich, 2011).

1.3 Cytokinesis

Cytokinesis is the process of the final separation of two nascent daughter cells during which cellular material including sister genomes are partitioned. It starts during anaphase, just after the segregation of sister chromatids, which implies that cytokinesis is coordinated with Cdk1 inactivation. Molecular signals coming from the anaphase spindle to the cell cortex induce the formation of an actomyosin ring. Contraction of the ring then leads to the ingression of the cleavage furrow and membrane deposition, which separates the cytoplasm into two parts. After that, the two cells remain connected by a thin intercellular bridge, until it is ultimately severed by the process of abscission (Fededa and Gerlich, 2012) (D'Avino et al., 2015) (Morgan, 2006).

The key players in cytokinesis are evolutionarily conserved, and most organisms require actin, myosin and microtubules to successfully finish the cell division. Interestingly though, the mechanism and the timing of the steps vary in different organisms. In animal cells, the position of the cleavage furrow is established during anaphase based on positional signals emerging from the anaphase spindle. Conversely, the site of cleavage in yeast is determined before mitosis. In budding yeast, the bud, which specifies the division plane appears in G1. Fission yeast mark the cleavage site in early mitosis by using the position of the nucleus (Balasubramanian et al., 2004) (Barr and Gruneberg, 2007). Plants do not form an actomyosin ring, but instead assemble a membrane and cell wall to separate the two cells by using a specialized structure called the phragmoplast (Jurgens, 2005).

For a successful cell division, cytokinesis needs to occur after chromosome segregation and at the equatorial part of the cell in symmetrically dividing cells.

Tight temporal and spatial regulation of cytokinesis prevents cytokinesis failure, and thus the formation of tetraploid cells. Tetraploid cells carry extra centrosomes and they are genetically unstable due to various complications in subsequent divisions (Ganem et al., 2009) (Ganem et al., 2007). Injection of tetraploid cells has been shown to promote tumour growth in a mouse model (Fujiwara et al., 2005), and deregulation of cytokinesis has been linked to multiple diseases including cancer (Lacroix and Maddox, 2012).

Polyploidy, however, is not always a sign of disease, as many tissues require presence of polyploid cells to be functional (Lacroix and Maddox, 2012). Classic examples include liver cells hepatocytes. In adult human liver 30% of hepatocytes are polyploid (mostly tetraploid) (Kudryavtsev et al., 1993). Hepatocytes become polyploid because of controlled cytokinesis failure caused by a disorganized cytoskeleton and defective RhoA activation. The cells are able to further divide as they can cluster their supernumerary centrosomes and form a bipolar spindle (Guidotti et al., 2003) (Celton-Morizur et al., 2009). Interestingly, tumorigenic hepatocytes proliferate as diploid (Saeter et al., 1988). Other examples of adjusted cell cycle can be seen during development, for example in the *D. melanogaster* embryo. Fertilized *D. melanogaster* embryos undergo thirteen fast rounds of division without any cytokinesis, which creates a large syncytium (Lee and Orr-Weaver, 2003). This event is followed by a process of cellularization, whereby the thousands of nuclei are packaged to form individual cells (Mazumdar and Mazumdar, 2002). Cellularization is a specialized form of cytokinesis and it uses some of the same molecular components. In the rest of the chapter, the main focus will be on the typical cytokinesis in animal cells.

1.3.1 Central spindle assembly

At anaphase onset, Cdk1 inactivation allows formation of the central spindle, a signalling platform crucial for cell division. The structure of mitotic spindle completely changes as cells progress from metaphase to later stages, kinetochore microtubules shorten to segregate the chromosomes to the opposite poles, and astral microtubules elongate (Tournebize et al., 2000) (Rusan et al., 2001). The central spindle is an array of interdigitated antiparallel microtubules that overlap

with their plus ends at the equatorial part of the cell (Glotzer, 2009) (Mastrorarde et al., 1993). It is partially formed from interpolar non-kinetochore microtubules of the mitotic spindle but it also requires *de novo* polymerisation of microtubules. Newly formed microtubules assemble through non-centrosomal pathway on pre-existing interpolar microtubules and this assembly requires the augmin complex (Uehara et al., 2009) (Uehara and Goshima, 2010) (Kamasaki et al., 2013).

The structure of the central spindle is stabilized by many proteins binding to the overlap zone. The key factor is a bundling protein Prc1 (protein required for cytokinesis 1). Prc1 homodimers specifically bind and crosslink the antiparallel microtubules (Bieling et al., 2010) (Subramanian et al., 2010). Cdk1 phosphorylation keeps Prc1 in an inactive monomeric form before anaphase onset (Jiang et al., 1998) (Zhu et al., 2006). After Cdk1 inactivation, Prc1 also provides an important docking space for Plk1 recruitment to the spindle midzone (Neef et al., 2007).

Another essential component of central spindle is a protein complex called Centralspindlin, a heterotetramer that consists of a dimer of Mklp1 and two molecules of MgcRacGAP (Mishima et al., 2002) (Pavicic-Kaltenbrunner et al., 2007). Mklp1, also known as KIF23, is a kinesin-6 motor protein. Research on the orthologs of Mklp1, Pavarotti in *D. melanogaster* and ZEN-4 in *C. elegans*, uncovered a role for Mklp1 in the bundling of antiparallel microtubules and cytokinesis progression (Adams et al., 1998) (Powers et al., 1998). MgcRacGAP (RACGAP1) was discovered in human cells as a new Rho family GAP factor (Toure et al., 1998). Study involving the *C. elegans* ortholog CYK4 revealed a role in the central spindle assembly and cytokinesis (Jantsch-Plunger et al., 2000).

Subsequent research showed that only the full Centralspindlin complex is able to bind and bundle microtubules (Mishima et al., 2002) (Pavicic-Kaltenbrunner et al., 2007). Recent data demonstrated that MgcRacGAP binding to Mklp1 changes the conformation of the two motor domains within the Mklp1 dimer, which creates a structure suitable for antiparallel microtubule bundling (Davies et al., 2015). Additionally, Centralspindlin activity is regulated on several levels. Cdk1 phosphorylates the motor domains of Mklp1, which reduces their affinity to

microtubules before anaphase onset (Mishima et al., 2004). Conversely, Aurora B phosphorylation of Mklp1 stabilizes the structure of the central spindle (Kaitna et al., 2000) (Guse et al., 2005). Aurora B phosphorylation enables formation of higher-order clusters of the Centralspindlin complex, which promotes microtubule bundling and transport of the complex to the overlap zone (Hutterer et al., 2009). The clustering of Centralspindlin is negatively regulated by 14-3-3 protein inhibitory interaction with Mklp1, which is released after Aurora B phosphorylation (Douglas et al., 2010).

Aurora B activity supports central spindle assembly as already mentioned. At anaphase onset, the CPC complex translocates from centromeres to the central spindle, and this translocation depends on Mklp2 (Gruneberg et al., 2004). Mklp2 is kinesin-6 motor protein like Mklp1 and it also helps Plk1 targeting to the central spindle, where it regulates cytokinesis (Hill et al., 2000) (Neef et al., 2003) (Petronczki et al., 2007) (Burkard et al., 2009) (Wolfe et al., 2009). CPC interaction with Mklp2 is enabled after Cdk1 inhibitory phosphorylation is removed from INCENP protein (Hummer and Mayer, 2009). It has been proposed that the CPC complex also helps to build the central spindle by bundling the microtubules, but its main role is likely focused on delivering the catalytic subunit Aurora B to the spindle midzone in order to regulate different components of the spindle midzone by phosphorylation, such as Centralspindlin complex (Glotzer, 2009) (Guse et al., 2005).

Since the central spindle serves as a signalling platform for the later stages of cytokinesis it needs to be a stable structure. All the components mentioned above help to stabilize this platform throughout division. The length of the overlap zone is controlled by the kinesin KIF4A, which brings Prc1 to the antiparallel overlap in order to stabilize it (Zhu and Jiang, 2005) (Subramanian et al., 2010). Aurora B-mediated phosphorylation activates KIF4A ATPase activity that suppresses polymerization and dynamic instability of the microtubules to restrict the midzone (Bieling et al., 2010) (Hu et al., 2011) (Nunes Bastos et al., 2013). Another kinesin regulated by Aurora B is KIF2A, which depolymerises microtubules from their minus ends. Aurora B gradient keeps it inactive at the spindle midzone to prevent over-shortening of the microtubules (Uehara et al., 2013).

In order to successfully complete cytokinesis, it is, however, not sufficient to only assemble and stabilize the spindle, as it also needs to be positioned correctly in the dividing cell. This phenomenon has been studied mainly during asymmetric divisions in *D. melanogaster* and *C. elegans* (Gonczy, 2008) (Sansregret and Petronczki, 2013). However, it is also important for symmetric divisions, where the spindle needs to be placed in the centre of the cell to produce two daughter cells of equal size. Astral microtubules serve as a connection between the spindle and the polar cell cortex, and they play an important role in the spindle positioning. They work in parallel with dynein-dynactin complexes at the cell cortex that can exert pulling forces on the spindle (Busson et al., 1998) (O'Connell and Wang, 2000) (Kotak et al., 2012). Dynein is recruited to the polar cortex by interaction with NuMA, while NuMA is positioned by binding to LGN and Gai proteins (Blumer et al., 2006) (Du and Macara, 2004) (Woodard et al., 2010). Recent work has demonstrated that centrosomal Plk1 activity antagonizes the interaction of dynein with NuMA, which spatially modulates dynein pulling activity and helps positioning the spindle in the middle of the cell. Chromosome-derived RanGTP gradient further restricts the lateral localization of LGN/Gai-NuMA complex and thus also regulates the spindle position (Kiyomitsu and Cheeseman, 2012). Furthermore, the RanGTP gradient supports proper spindle positioning also via asymmetric membrane elongation (Kiyomitsu and Cheeseman, 2013).

The central spindle assembly marks the beginning of cytokinesis in anaphase. Cdk1 inactivation and re-localization of Aurora B and Plk1 kinases are crucial for proper spindle assembly and positioning.

1.3.2 Cleavage plane determination

The cleavage plane is specified by the anaphase spindle signalling to the cell cortex, which provides an important spatial and temporal coupling with the segregation of sister chromatids (Rappaport, 1996) (Burgess and Chang, 2005). Early seminal studies were performed in echinoderm eggs, large cells suitable for micromanipulation. Raymond Rappaport performed his classic micromanipulation experiments using sand dollar eggs. One of these experiments clearly showed that the spindle induces formation of the cleavage furrow and regulates its position. Just

after the egg started to cleave, he physically shifted the spindle to a new position. Regression of the original furrow and formation of a new furrow above the spindle midplane was observed and remarkably, this could be repeated several times in the same cell (Rappaport and Ebstein, 1965) (Rappaport, 1985).

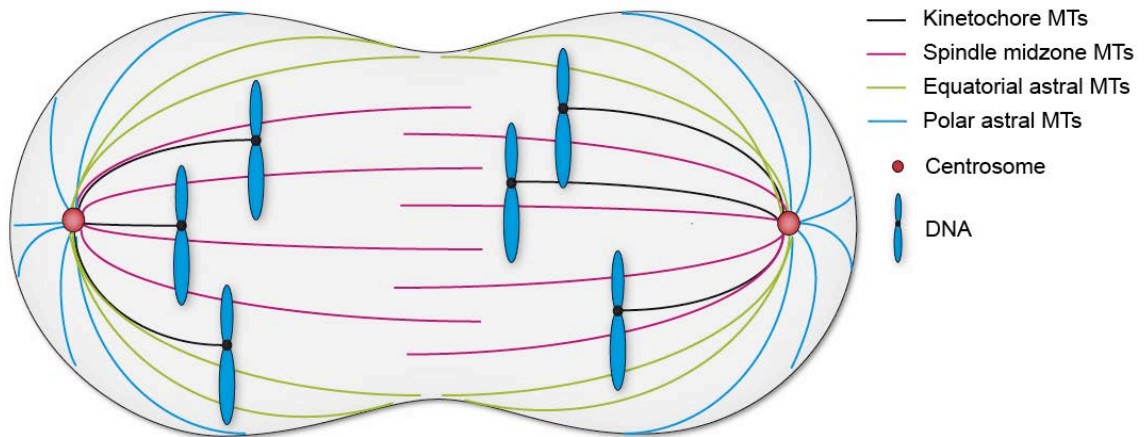


Figure 4 Microtubule organization in a human anaphase cell

Schematic representation showing the different types of microtubules (MTs) in an anaphase cell. Chromosomes are pulled to the cell poles by kinetochore microtubules. Spindle midzone microtubules are antiparallel microtubules that overlap with their plus ends in the middle of the cell. Astral microtubules also emanate from the centrosomes but they reach to the cell cortex. Polar astral microtubules grow towards the cell poles, while equatorial asters grow towards the furrow. Adapted from (Burgess and Chang, 2005).

How exactly does the spindle control the position of the cleavage furrow, however, still remains a key question field of cell division research and cell biology in general. Different models have emerged throughout the years, but none of them could reconcile all the results obtained in the different model organisms. Nonetheless, a consensus has emerged regarding the convergence of these signals, suggesting that the signals from the spindle lead to the activation of a key player in cytokinesis, the small GTPase RhoA that can promote the formation and contraction of the cleavage furrow (Piekny et al., 2005) (Bement et al., 2005) (Jordan and Canman, 2012).

Do microtubules promote the contractility of the cell cortex or do they inhibit the contractile forces? Are all microtubules affecting contractility equally or do subpopulations of fibers differ (Figure 4)? A series of seminal experiments performed by Raymond Rappaport, including the classic “torus experiment”,

supported the stimulation model (Rappaport, 1996) (Burgess and Chang, 2005). Briefly, by pushing a glass sphere through the sand dollar egg, Rappaport created a toroidal shaped cell (Figure 5). During next division, two spindles formed two normal cleavage furrows just above the spindle midplanes, but importantly, also a third furrow (later named as the Rappaport furrow) emerged a few minutes later in-between the astral microtubules of the two spindles (Rappaport, 1961). Other researchers expanded these experiments and their results further support the notion that only the presence of astral microtubules, but not the chromosomes or the midzone microtubules is crucial for furrowing (Hiramoto, 1971) (Zhang and Nicklas, 1996). Conversely, results from *D. melanogaster* showed the importance of central spindle signalling. *D. melanogaster* cells with a mutated *asterless* gene that lack the astral microtubules are able to form a furrow (Bonaccorsi et al., 1998) (Giansanti et al., 2001). Only if the central spindle assembly was disrupted simultaneously, furrow formation was blocked (Adams et al., 1998).

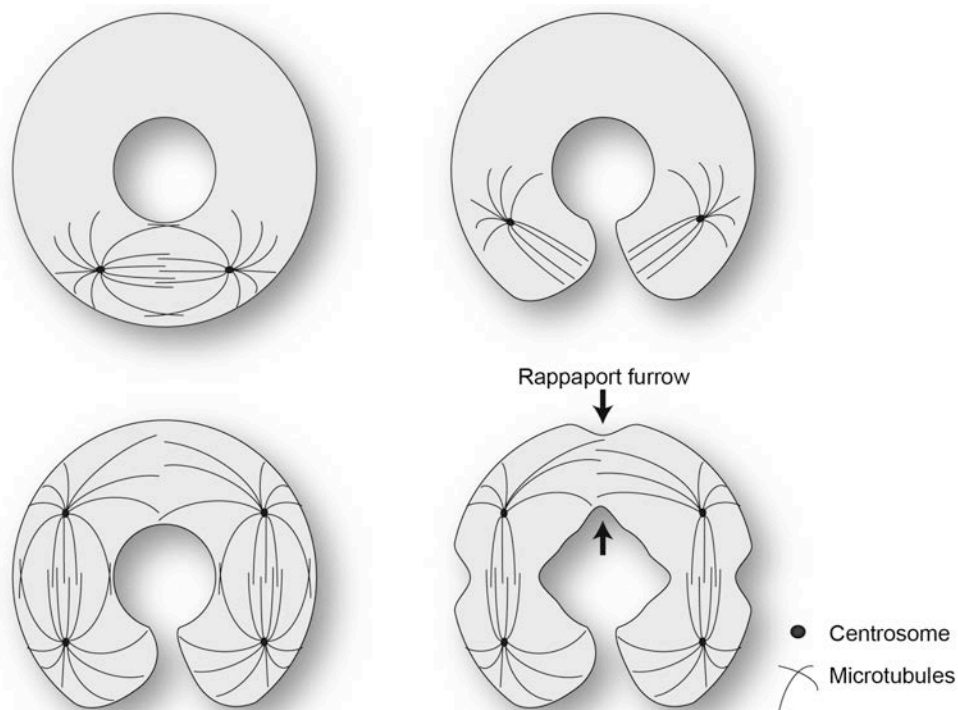


Figure 5 Rappaport “torus experiment”

Schematic representation of classic Rappaport “torus experiment” in sand dollar eggs described in the text. Results supported astral stimulation model of cleavage plane specification.

The polar relaxation model postulates that astral microtubules inhibit cortical tension at the poles and thus “relax” the cortex (Figure 6) (Wolpert, 1960) (White and Borisy, 1983). This inhibition of contractility at the polar regions could then lead to cleavage in the middle of the cell. It has been shown (Asnes and Schroeder, 1979) and theoretically modelled (Yoshigaki, 2003) that there are less astral microtubules contacting the furrow than at the poles, which supports this notion.

In 2003, Dechant and Glotzer attempted to reconcile the different models and explain the conflicting results obtained in different model organisms. It had been demonstrated before that in *C. elegans* embryos, Centralspindlin is necessary for the central spindle assembly, but that it is not crucial for cleavage furrow formation (Powers et al., 1998) (Jantsch-Plunger et al., 2000). Dechant and Glotzer showed that the central spindle becomes essential for furrow formation in *C. elegans* embryos if the spindle is not elongated to the normal extent and the two centrosomes are in close proximity (Dechant and Glotzer, 2003). Consequently, they proposed that both the central spindle and the asters redundantly contribute to positioning and formation of the cleavage furrow by creating a local minimum of the microtubule density. This model was later expanded with the notion that astral microtubules negatively regulate the recruitment of cortical myosin, which could explain why they inhibit furrowing (Werner et al., 2007). However, other studies could not identify the local minimum of the microtubule density in *C. elegans* embryos (Motegi et al., 2006) (Verbrugghe and White, 2007).

A subsequent study from Bringmann and Hyman used laser microdissection to sever astral microtubules in order to separate the roles of the central spindle and the asters for furrow positioning in *C. elegans*. After shifting the position of the spindle midzone, they observed two separate furrows – one in-between the asters, and the second one close to the midzone. These experiments suggested the existence of two redundant signals that influence the furrow positioning, a notion consistent with the results obtained in Glotzer lab: the first signal emerging from the astral microtubules, and the second correction signal arising from the central spindle (Bringmann and Hyman, 2005).

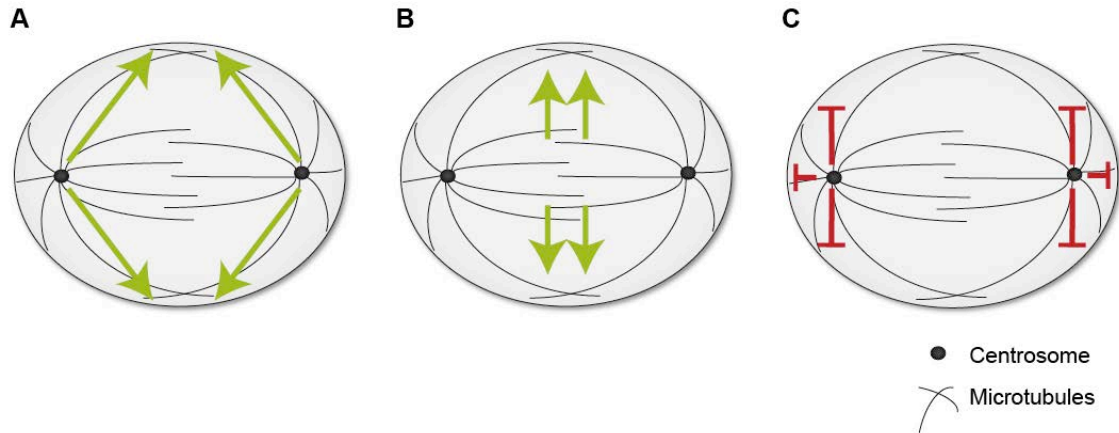


Figure 6 Different models for cleavage furrow positioning

A Astral stimulation model – equatorial asters deliver the stimulatory signal.

B Central spindle model – the spindle midzone provides the cleavage signal.

C Polar relaxation model – polar astral microtubules inhibit contractility at the cell poles.

Another model does not base the different role of microtubules on their geometry but rather on their stability. Canman et al. induced cytokinesis in cells with monopolar spindles. Interestingly, they observed formation of the furrow at the cortex distal to the chromosomes. Additionally, they also determined that microtubules contacting the furrow were more stable than the polar asters. This observation has led the authors to propose that stable microtubules promote furrowing, as opposed to dynamic microtubules that inhibit the contractility (Canman et al., 2003). Further supporting this notion, it was later shown that even a single microtubule stabilized by taxol could induce furrowing (Shannon et al., 2005). In 2008, Foe and Dassow working with sea urchin eggs discovered that a subset of microtubules, mainly equatorial asters, became more stable during anaphase. Moreover, plus-end tips of these stabilized microtubules matched the localization of activated myosin (Foe and von Dassow, 2008). These observations bring about the conceptual question of why should the stable microtubules be better than dynamic ones in furrowing stimulation? Their increased ability to bring and concentrate factors necessary for furrowing to the cortex was suggested as an explanation (Carvalho et al., 2003) (Odell and Foe, 2008), however, this model also has caveats. Further research with sea urchin eggs suggested that the dynamic state of asters is not crucial for furrow formation, at least in this system, as various drugs affecting the microtubule dynamics did not affect their competency to stimulate furrowing (Strickland et al., 2005).

The last model argues that the stimulatory signal may be coming from the spindle midzone rather than the asters. It was originally postulated after micromanipulation studies in grasshopper neuroblasts, which showed that the cleavage furrow always formed at the middle of the spindle (Kawamura, 1960) (Kawamura and Carlson, 1962). In support of this model, presence of a barrier in-between the spindle midzone and the cortex prevented the formation of the furrow in rat kidney cells (Cao and Wang, 1996). Likewise, the aforementioned results from *D. melanogaster* are in line with the notion that the midzone is providing the signal that stimulates furrowing (Bonaccorsi et al., 1998) (Giansanti et al., 2001) (Adams et al., 1998). The spindle midzone model can be viewed as a spinoff from the equatorial stimulation model, because both propose that an array of overlapping microtubules in the middle of the cell provides the stimulatory signal. In small cells, the spindle midzone might be close enough to the cortex to provide such signal. In large cells, equatorial astral microtubules could cooperate with the midzone (Su et al., 2014). Spindle midzone microtubules are stable, so they also fit the dynamics model (Foe and von Dassow, 2008).

Molecular details of how the spindle midzone contributes to the formation of the active RhoA zone are better understood than the elusive role of asters (Figure 7). The crucial activator of RhoA during cytokinesis is a RhoGEF factor called Ect2. Ect2 interacts with the spindle midzone through its N-terminal BRCT domains that bind to MgcRacGAP (Somers and Saint, 2003) (Yuce et al., 2005) (Nishimura and Yonemura, 2006). The interaction requires Plk1 to phosphorylate MgcRacGAP and this phosphorylation event is crucial for cytokinesis progression (Petronczki et al., 2007) (Wolfe et al., 2009) (Burkard et al., 2009) (Zou et al., 2014) (Kim et al., 2014). During later anaphase, Ect2 also interacts with the plasma membrane and this interaction is coordinated with chromosome segregation through Cdk1 inhibitory phosphorylation (Su et al., 2011) (Chalamalasetty et al., 2006). Combined, these findings resulted in a model, which proposes that the spindle midzone regulates the furrow position by activating RhoA at the equatorial part of the membrane through localised accumulation of Ect2 (Su et al., 2011).

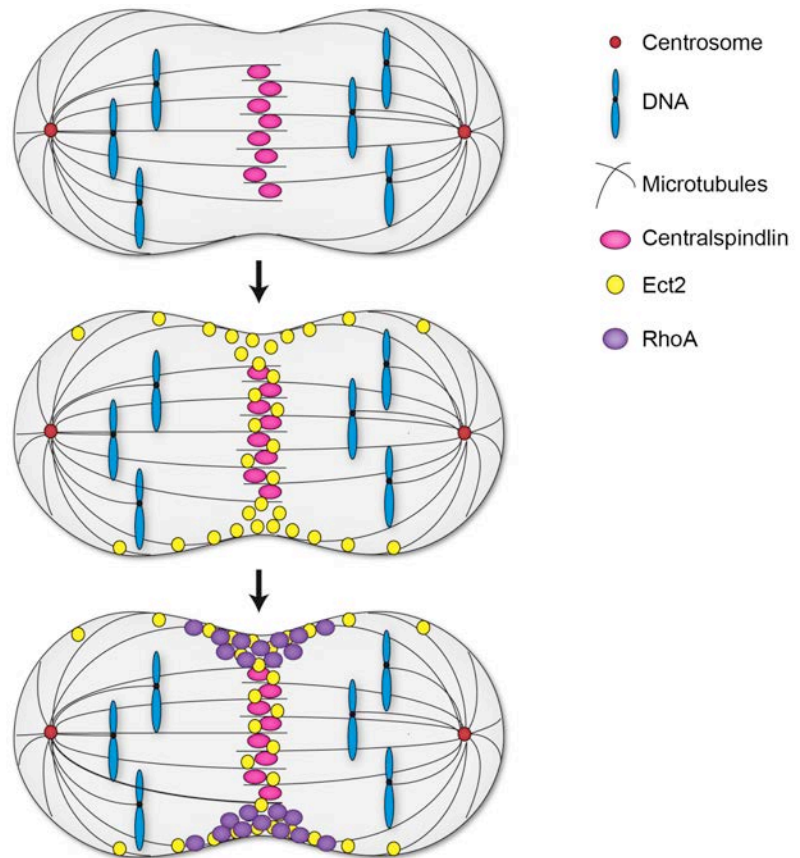


Figure 7 Molecular details of central spindle model of cleavage plane specification

After anaphase onset, Centralspindlin complex binds to antiparallel overlap of midzone microtubules. Protein Ect2 localizes to spindle midzone by interaction with Centralspindlin. Ect2 also binds plasma membrane, which creates concentration gradient of Ect2 at the equatorial part of the membrane. Central spindle model propose that this specific localization of Ect2, main activator of RhoA leads to preferential activation of RhoA in the equatorial part of plasma membrane.

As outlined above, despite many years of research, there is currently no simple model that could reconcile all the results from the different model organisms. Most likely, there is no simple answer and multiple redundant pathways could specify the position of the cleavage furrow to make the system robust. Alternative explanation is that the mechanism that plays major role varies in different organism and in cells of different size. Finally, the possibility that another player may be involved in the process cannot be formally excluded.

1.3.3 Activation of RhoA

RhoA is a master regulator of cytokinesis. Together with Rac1 and Cdc42, RhoA belongs to the family of Rho GTPases, acting as molecular switches (Dvorsky and Ahmadian, 2004). The first experiments that showed RhoA has a crucial role in cytokinesis were performed in *X. laevis* embryos, where the specific inhibition of RhoA by C3 toxin impaired cleavage furrow formation and cytokinesis (Kishi et al., 1993). Further experiments confirmed the importance of RhoA for cell division in other organisms, like *D. melanogaster* and *C. elegans* (Crawford et al., 1998) (Prokopenko et al., 1999) (Jantsch-Plunger et al., 2000). The use of fluorescent probes in sea urchin and HeLa cells, demonstrated that active RhoA localizes to the cleavage plane and its accumulation precedes the furrow formation (Yoshizaki et al., 2003) (Bement et al., 2005). However, experiments with other mammalian cell lines were less clear, as some of the cell types failed the division completely, while others showed a less penetrant phenotype (Moorman et al., 1996) (O'Connell et al., 1999). This could be caused by vertebrate paralogs of RhoA, namely RhoB and RhoC, which may be able to partially complement RhoA functions (Jordan and Canman, 2012).

Experiments in sea urchins using fluorescent probes also suggested that microtubules of the anaphase spindle control the localization of cleavage plane during cytokinesis via controlling the zone of active RhoA. Displacement of the spindle resulted in a corresponding shift of the zone of active RhoA. Importantly, this provided the link between the spindle and RhoA activity, and demonstrated causal connection between the spindle and furrowing (Bement et al., 2005).

Intrinsic GTPase activity of RhoA is very low and it needs to be activated by interaction with regulatory factors. Guanine nucleotide exchange factors (GEFs) stimulate the dissociation of inactive GDP-bound complex and thus activate the GTPase and its effectors. GEF interaction with the GTPase affects the nucleotide-binding site of the GTPase, which triggers nucleotide release. The concentration of GTP in the cytoplasm is around ten-times higher than GDP, favouring the GTP binding and subsequent RhoA activation (Bos et al., 2007). Conversely, GTPase activating proteins (GAPs) promote efficient GTP hydrolysis,

and consequently stimulate GTPase activity, resulting in the return of the GTPase to its inactive state (Vetter and Wittinghofer, 2001) (Bos et al., 2007). Originally, the consensus was that GEFs activate RhoA to initiate furrowing and GAPs inactivate RhoA at the end of cytokinesis. Afterwards, the so-called “flux” model was proposed, which suggests constant cycling of RhoA between GTP and GDP states (Bement et al., 2006) (Miller and Bement, 2009).

The main GEF factor for RhoA during cytokinesis is Ect2 and its mutation or depletion causes a failure in contractile ring assembly and cleavage furrow formation (Tatsumoto et al., 1999) (Prokopenko et al., 1999) (Somers and Saint, 2003) (Yuce et al., 2005). However, other GEFs were also proposed to participate in RhoA activation during cytokinesis. MyoGEF localizes to the central spindle and spindle poles. Depletion of MyoGEF by siRNA led to mild cytokinetic defects (Wu et al., 2006). MyoGEF activity was proposed to affect Ect2 and RhoA localization, but was not shown to directly activate RhoA, which might explain the mild cytokinetic defects (Asiedu et al., 2009). Another GEF factor with a possible role in RhoA activation during cytokinesis is GEF-H1, which is localized to spindle microtubules during mitosis. Similarly to MyoGEF, GEF-H1 depletion caused mild cytokinetic defects, while GEF-H1 activity was dispensable for the initiation of furrowing. Consequently, it was proposed to stimulate RhoA during ingression of the cleavage furrow (Birkenfeld et al., 2007).

In the cytokinesis field, the most intensely studied GAP factor is MgcRacGAP (called CYK-4 in *C. elegans* and RacGAP50 in *D. melanogaster*). MgcRacGAP is a part of Centralspindlin complex and plays a crucial role in central spindle assembly (Mishima et al., 2002) (Pavicic-Kaltenbrunner et al., 2007). How and whether MgcRacGAP affects RhoA activity is, however, controversial. The first study suggesting its role in RhoA activation was in *C. elegans* embryos, when *cyk-4* mutant embryos initiated furrowing but afterwards failed to complete cytokinesis (Jantsch-Plunger et al., 2000). Therefore, CYK-4 was proposed to be the GAP factor for RhoA (Jantsch-Plunger et al., 2000) (Lee et al., 2004). In line with this notion, in *X. laevis* embryos GAP-defective mutants of MgcRacGAP led to a broader RhoA zone (Miller and Bement, 2009). Conversely, MgcRacGAP was shown as a poor GAP for RhoA, and was much more efficient towards Rac1 and

Cdc42 (Toure et al., 1998) (Jantsch-Plunger et al., 2000). To reconcile these contradictory results, it was suggested MgcRacGAP becomes efficient towards RhoA after Aurora B phosphorylation (Minoshima et al., 2003). However, other researchers disputed this notion, and showed that MgcRacGAP was still not an efficient RhoGAP even after treatment with Cdk1, Aurora B and Plk1 inhibitors (Bastos et al., 2012). MgcRacGAP inhibition of Rac GTPase was proposed to prevent branched actin formation via Rac effector Arp2/3 complex, which could otherwise disrupt the action of the contractile ring (Canman et al., 2008) (D'Avino et al., 2004). Another possibility was suggested by Bastos et al., arguing that the Rac activity may be crucial for cell adhesion and the spreading. Thus, Rac activity needs to be inhibited at the site of the cleavage furrow and MgcRacGAP could serve this purpose (Bastos et al., 2012). Recently, it was also proposed that Rac1 inhibition is necessary to reduce cortical tension to allow furrow formation (Loria et al., 2012).

Moreover, MgcRacGAP might promote RhoA activation indirectly through activation of other cytokinetic factors. For example, MgcRacGAP binding to N-terminal part of Ect2 was proposed to relieve autoinhibition of Ect2 protein (Kim et al., 2005) (Yuce et al., 2005). Recent work from Zhang et al. suggested that MgcRacGAP activates RhoA function through Ect2 activation, and proposed a complex formation between Ect2, MgcRacGAP and RhoA allows the highest stimulation of RhoA (Zhang and Glotzer, 2015).

Other GAPs were shown to have a role in cytokinesis too, namely p190RhoGAP and MP-GAP. p190RhoGAP can regulate RhoA activation as a classic GAP factor, as its overexpression led to cytokinesis failure and formation of multi-nucleated cells (Su et al., 2003). It was proposed that p190RhoGAP could oppose Ect2 GEF activity and thus regulate RhoA activation, however, the phenotype of p190RhoGAP depletion was not very penetrant, suggesting p190RhoGAP is probably not the main GAP factor for RhoA (Mikawa et al., 2008) (Su et al., 2009). Notably, inhibition of MP-GAP (ARHGAP11A), a homolog of *C. elegans* Rga-3 and Rga-4, led to excessive contractility of the cell cortex and formation of large protrusions. Additionally, MP-GAP was shown to stimulate GTPase activity of RhoA

in vitro. Interestingly, MP-GAP restricted RhoA zone but only in the sensitized background of cells lacking astral microtubules (Zanin et al., 2013).

1.3.4 Contractile ring assembly and contraction

The active GTP-bound form of RhoA promotes contractile ring formation and contraction by simultaneous activation of actin assembly and non-muscle myosin II activity (Figure 8) (Piekny et al., 2005) (Jordan and Canman, 2012). RhoA binding to diaphanous-related formins causes release of their autoinhibition (Otomo et al., 2005). Subsequently, formins together with profilin can nucleate and elongate linear actin filaments, which are thought to be crucial for contractile ring assembly and ingression (Castrillon and Wasserman, 1994) (Watanabe et al., 1997) (Severson et al., 2002) (Watanabe et al., 2008). Furthermore, RhoA indirectly activates myosin II via ROCK activation and inhibition of MYPT phosphatase (Matsumura, 2005). Rho-associated protein kinase (ROCK) is a serine/threonine kinase that phosphorylates Ser19 of myosin II regulatory light chain (rMLC), which results in myosin II thick filament formation and activates the ATPase activity of its motor domain (Amano et al., 1996) (Kosako et al., 2000).

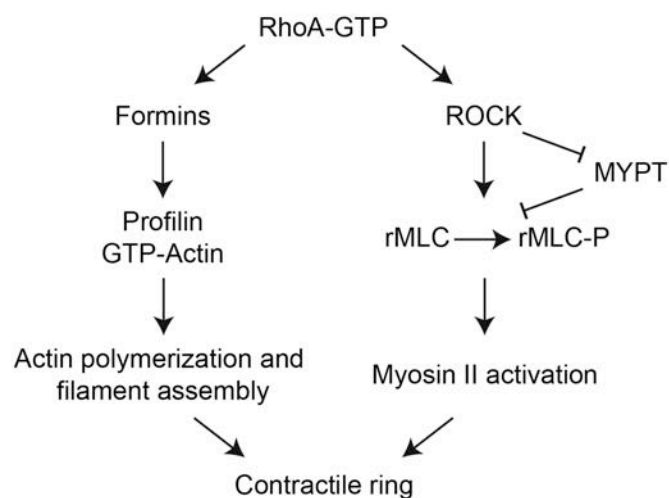


Figure 8 How RhoA activation leads to contractile ring formation and furrow ingression

Activation of small GTPase RhoA is a key step during cytokinesis. This scheme represents the two main downstream pathways that forms actomyosin contractile ring and activates cleavage furrow ingression.

MYPT is a myosin phosphatase that dephosphorylates Ser19, therefore it needs to be inhibited by ROCK phosphorylation to allow the formation of the contractile ring (Kimura et al., 1996) (Piekny and Mains, 2002). Furthermore, ROCK indirectly stabilizes actin filaments by inactivation of the actin binding protein cofilin, which otherwise disassembles the filaments (Amano et al., 2002) (Geneste et al., 2002). Another proposed RhoA target and effector is Citron kinase, which can di-phosphorylate myosin II at Ser19 and Thr18 (Yamashiro et al., 2003). However, recent data obtained with the Citron kinase ortholog in *D. melanogaster* called Sticky, suggest that Citron kinase is not a true effector of RhoA as its activity is independent of RhoA status (Bassi et al., 2011). Citron kinase functions later during abscission and was also proposed to work as a scaffolding factor of the contractile ring (Gai et al., 2011) (Bassi et al., 2013) (D'Avino et al., 2015).

An important scaffolding factor for the contractile ring is Anillin, a highly conserved multi-domain protein interacting with many proteins important for cytokinesis (Piekny and Maddox, 2010). Anillin is able to interact with actin (Miller et al., 1989), myosin (Straight et al., 2005), RhoA (Piekny and Glotzer, 2008), septins (Field et al., 2005a), MgcRacGAP (D'Avino et al., 2008) (Gregory et al., 2008) and Ect2 (Frenette et al., 2012). Anillin is thought to provide a signalling platform and link the contractile ring with the plasma membrane (Liu et al., 2012). Depletion of Anillin does not prevent cleavage furrow ingression, but the furrow is not stable and it regresses later, resulting in formation of multi-nucleated cells. In some cell types, contractile ring oscillations and excessive blebbing are observed, which further supports the scaffolding role of Anillin (Straight et al., 2005) (Piekny and Glotzer, 2008) (Hickson and O'Farrell, 2008).

Septins (Sept1-10 in mammals) are GTPases that assemble into bundles and filaments required for the contractile ring formation (Neufeld and Rubin, 1994) (Kinoshita et al., 1997). Apart from the aforementioned interaction with Anillin, septins also bind actin and myosin II (Joo et al., 2007) (Mavrakis et al., 2014). Septins were shown to bundle actin filaments to form rings *in vitro*, and therefore they might help to bend the filaments *in vivo* as well (Mavrakis et al., 2014).

Actin and myosin II form an actomyosin ring that surrounds cell equator just beneath the cell cortex (Maupin and Pollard, 1986) (Kamasaki et al., 2007). At first it appears as a broad equatorial zone, which later narrows down (Mabuchi, 1994) (Hu et al., 2011) (Lewellyn et al., 2011). Actin and myosin can assemble on site or travel to the equator by cortical flow (Murthy and Wadsworth, 2005) (Yumura et al., 2008) (Zhou and Wang, 2008) (Uehara et al., 2010). How exactly the actomyosin ring generates the force to ingress the furrow is not very well understood. The classic model also known as “purse string” theory postulates that myosin II slides the antiparallel actin filaments similarly to the way muscle contraction works, which shrinks the diameter of the ring and causes the ingression of the surrounding membrane (Schroeder, 1972) (Satterwhite and Pollard, 1992) (Biron et al., 2005). This model requires the alignment of the filaments with the cleavage plane, which was observed experimentally in some organisms (Schroeder, 1972) (Tucker, 1971) (Maupin and Pollard, 1986) (Kamasaki et al., 2007). However, other studies did not confirm this filaments organization (Fishkind and Wang, 1993) (Reichl et al., 2008). Moreover, recent study showed that mutant version of myosin II, which cannot slide actin filaments is able to rescue cytokinesis in COS-7 cells (Ma et al., 2012).

Other models have been proposed to explain this conundrum, and they suggest that depolymerisation of actin together with cross-linking proteins' activity could be sufficient to generate the contractile force (Zumdieck et al., 2007) (Vogel et al., 2013) (Reichl et al., 2008). Experiments demonstrated that actin filaments shorten and the contractile ring disassembles during contraction (Murthy and Wadsworth, 2005) (Kamasaki et al., 2007) (Carvalho et al., 2009). Most of the models to date have focused on the contractile forces in the equatorial part of the cell. But experimental work also showed that cell shape and contractility of the polar cortex also affects the furrow ingression (Zhang and Robinson, 2005) (Sedzinski et al., 2011). Further research is necessary to explain how the contractile ring is organized and how the actomyosin contractility generates the force necessary for furrow ingression.

1.3.5 Membrane trafficking and cytokinesis

Cytokinetic research mostly focused on the role of microtubules and actomyosin systems in cytokinesis. However, in the last decade, the role of the plasma membrane has come into focus as well. As the cleavage furrow ingresses, new membrane needs to be added to the cleavage site to allow the growth of cell surface. Thus, secretory and endocytic pathways have a crucial role in furrow ingression and abscission. Moreover, it was also proposed that vesicles could bring various factors to the cleavage site and therefore directly regulate cytokinesis progression (Neto et al., 2011) (Skop et al., 2004) (Tang, 2012) (Shuster and Burgess, 2002).

Golgi-derived secretory vesicles move and accumulate at the cleavage furrow and midbody region and fuse with the growing membrane (Goss and Toomre, 2008). The role of secretory vesicles trafficking was further confirmed by various experiments. Brefeldin A (BFA) is a fungal antibiotic, which disrupts the secretory pathway by inhibiting protein transport from endoplasmic reticulum to Golgi. BFA treatment led to late cytokinesis failure in *C. elegans* (Skop et al., 2001) and *D. melanogaster* cells (Kitazawa et al., 2012). Further studies in *D. melanogaster* showed that depletion of various regulatory proteins involved in membrane trafficking, e.g. SNARE complexes, caused problems during cell division (Xu et al., 2002) (Farkas et al., 2003) (Robinett et al., 2009).

A functional endocytic pathway is also necessary for correct cytokinesis progression. For instance, the large GTPase dynamin that is involved in vesicle budding and scission was shown to accumulate at the spindle midzone and at the furrow, and its depletion led to cytokinesis failure (Praefcke and McMahon, 2004) (Wienke et al., 1999) (Thompson et al., 2002). The small GTPases Rab11, Arf6 and Rab35 that are crucial for endocytic recycling were recognized for their role in cytokinesis as well (Schiel and Prekeris, 2013). In *D. melanogaster* spermatocytes, Rab11 depletion caused accumulation of Golgi-derived vesicles in the furrow. These vesicles did not fuse with the furrow and this resulted in defective ingression of the contractile ring (Giansanti et al., 2007). FIP3 protein binds to Rab11-positive endosomes and FIP3-Rab11 seems to regulate the endocytic targeting important

for abscission (Wilson et al., 2005). Interestingly, FIP3 was shown to bind MgcRacGAP in late telophase, and this binding was competing with Ect2's interaction with MgcRacGAP. These results suggest a regulation of abscission timing by MgcRacGAP's sequential and mutually exclusive interaction with Ect2 and FIP3 (Simon et al., 2008). All these results support a close relationship between secretory pathways and cytokinesis, and it will be interesting to see the further development of this field.

1.3.6 Lipids and cytokinesis

Given the importance of the plasma membrane for cytokinesis, it is logical that the composition of the membrane will affect the process through influencing physical properties of the cell envelope and mediating the interaction of cytokinetic factors with the plasma membrane. In most membranes, different lipids are asymmetrically distributed, and they can also form specialized domains that affect localization of membrane-binding and transmembrane proteins. Thus, an increasing amount of studies have focused on how lipid composition affects cell division (Neto et al., 2011) (Brill et al., 2011) (Echard, 2012) (Atilla-Gokcumen et al., 2014).

It was reported that multiple lipids accumulate in the cleavage furrow, for example phosphatidylinositol 4,5-bisphosphate (PIP₂) or phosphatidylethanolamine (PE) (Emoto et al., 2005) (Field et al., 2005b) (Emoto et al., 1996). PE specifically accumulates at the outer leaflet of the equatorial plasma membrane at the later stages of cytokinesis. Inhibition of the PE transport to the outer layer of the plasma membrane prevented the contractile ring disassembly during abscission and caused cytokinetic failure (Emoto et al., 1996) (Emoto and Umeda, 2000). Sterol-rich lipid rafts were also observed to localize to the furrow in late cytokinesis, both in yeast and mammalian cells (Wachtler et al., 2003) (Ng et al., 2005). These rafts were enriched for ganglioside GM1, cholesterol and signalling molecules like phospholipase C. Notably, they required actin, myosin II and microtubules in order to form. Disruption of these rafts caused major cytokinetic defects (Ng et al., 2005).

Phosphatidylinositol phosphates (PIPs) form another group of lipids with a reported function in cytokinesis (Brill et al., 2011) (Echard, 2012). Phosphatidylinositol

4,5-bisphosphate (PIP₂) was repeatedly shown to specifically accumulate at the equatorial membrane (Emoto et al., 2005) (Field et al., 2005b) (Wong et al., 2005). Disrupting the PIP₂ localization as well as preventing its hydrolysis caused cytokinetic failure in *D. melanogaster* and mammalian cells (Wong et al., 2005) (Emoto et al., 2005). Importantly, PIP₂ binding targets septins (Zhang et al., 1999) (Bertin et al., 2010) and Anillin (Liu et al., 2012) to the plasma membrane therefore helping to organize the furrow. PIP₂ is also an interaction partner for MgcRacGAP and this binding links the microtubules to the plasma membrane during cytokinesis (Lekomtsev et al., 2012).

Mutation in the *fwd* gene in *D. melanogaster* spermatocytes caused contractile ring instability and subsequent cytokinesis failure. *fwd* gene encodes phosphatidylinositol 4-kinase β (PI4K β), which is required for synthesis of phosphatidylinositol 4-phosphate (PI4P) and formation of PI4P positive vesicles (Brill et al., 2000). These vesicles also contain Rab11, a small GTPase important for endocytic recycling. PI4P targets Rab11-containing vesicles to the spindle midzone, which is believed to bring regulatory factors to control cytokinesis progression (Polevoy et al., 2009). Phosphatidylinositol 3-phosphate (PI3P) positive vesicles were observed in the intercellular bridge between two nascent cells. PI3P accumulation seems to be important for abscission, as depletion of the main phosphatidylinositol 3-kinase VPS34 caused abscission delays and failure (Thoresen et al., 2010) (Sagona et al., 2010).

1.3.7 Abscission

Constriction of the contractile ring continues until the midzone is around 1.5 μm in diameter. The narrow intercellular bridge connects the two daughter cells for some time, before they are finally split during abscission. At the centre of the bridge lies an electron-dense structure called the midbody that forms in telophase and originates from compressed spindle midzone microtubules. The midbody serves as a signalling platform that controls abscission, and more than one hundred proteins were found to associate with the midbody (Mierzwa and Gerlich, 2014) (Skop et al., 2004). Different proteins localize to various places within the midbody structure. KIF4 and Prc1 remain associated with the microtubules in the midbody core (Hu et

al., 2012), while other proteins including Centralspindlin, Ect2, Anillin, RhoA, septins and Citron kinase localize to the midbody ring that surrounds the core (Gai et al., 2011) (Hu et al., 2012) (Kechad et al., 2012). But this ring-like organization of various proteins is likely an artifact due to the inaccessibility of the antibodies to the dense core of the midbody (Elad et al., 2011). Last group includes e.g. Mklp2, Aurora B and CENP-E, which localize to tightly packed microtubules flanking the midbody (Gruneberg et al., 2004) (Hu et al., 2012) (Yen et al., 1991).

After cleavage furrow ingression is complete, the actomyosin ring disassembles. Notably, actin was shown to be dispensable for abscission (Guizetti et al., 2011). RhoA needs to be inactivated to allow the ring disassociation (Emoto et al., 2005). The mechanism for RhoA inactivation is currently unknown, but p50RhoGAP was shown to be important for the clearing of actin filaments from the bridge, making it a suitable candidate (Schiel et al., 2012). At the same time, Ect2, the main RhoA activator, is sequestered in the reforming nucleus and degraded via the APC pathway (Prokopenko et al., 1999) (Tatsumoto et al., 1999) (Liot et al., 2011). During late cytokinesis, protein kinase C ϵ (PKC ϵ) accumulates at the furrow and participates in RhoA inactivation via an unknown mechanism (Saurin et al., 2008). After the contractile ring disassembly, the furrow area is stabilized by multiple mechanisms to ensure the two daughter cells stay connected by the intercellular bridge for the required amount of time until abscission occurs (Mierzwa and Gerlich, 2014). One such mechanism is MgcRacGAP interaction with PIs, which anchors the central spindle to the midbody membrane (Lekomtsev et al., 2012). Additionally, Mklp1, the second part of the Centralspindlin complex, also stabilizes the structure by direct binding to Arf6, a small GTPase involved in endocytic trafficking to the midbody (Schweitzer and D'Souza-Schorey, 2002). Interestingly, Arf6 also takes over the role of Aurora B in telophase and counteracts the 14-3-3 protein binding of Mklp1, which would otherwise disrupt the Centralspindlin clustering and would consequently lead to its dissipation and midbody destabilization (Joseph et al., 2012). Scaffolding factors Anillin and Citron kinase also help to connect various midbody proteins, and link them to the plasma membrane (Gai et al., 2011) (El Amine et al., 2013) (Piekny and Maddox, 2010) (Bassi et al., 2013).

Secretory and endocytic vesicles are thought to play a crucial role in abscission. Vesicles accumulate in the ingressing furrow and they surround the midbody, and fuse with the membrane before the final cut occurs (Gromley et al., 2005) (Goss and Toomre, 2008) (Schiel et al., 2011). The intercellular bridge further narrows down during maturation until it reaches about half of its initial width (Guizetti et al., 2011) (Schiel et al., 2012). Before the actual separation, the cortex adjacent to the midbody constricts even further on both sides of the bridge, and afterwards the full constriction produces two separate daughter cells and a midbody remnant (Elia et al., 2011) (Guizetti et al., 2011) (Mullins and Biesele, 1977). The midbody remnant has different fates in different cell types (Ettinger et al., 2011). Some cells cut on both sides of the midbody, which is then released to the extracellular space (Elia et al., 2011) (Guizetti et al., 2011). Other cells cut only on one side, which results in retention of the midbody by one daughter cell. In the latter case, the midbody remnant is usually degraded by autophagy (Pohl and Jentsch, 2009).

Electron microscopy allowed researchers to observe 17 nm filaments forming a large membrane-associated helix at the place of the secondary constriction (Guizetti et al., 2011). The identity of the 17 nm filaments is still not confirmed, but the main candidate is the endosomal sorting complex required for transport (ESCRT), especially ESCRT-III that is essential for the process of abscission. ESCRT-III colocalizes with the secondary constriction zones, and is required for the formation of 17 nm filaments (Carlton and Martin-Serrano, 2007) (Morita et al., 2007) (Elia et al., 2011) (Guizetti et al., 2011).

ESCRT-III functions in mediating the constriction and fission of cell membranes, and it has a role in various cell processes such as virus budding or autophagy (Hurley and Hanson, 2010). ESCRT-III localization depends on multiple regulators. Centrosomal protein Cep55 binds to Mklp1, and this interaction is negatively regulated by Plk1, until the kinase is degraded during mitotic exit (Bastos and Barr, 2010). Cep55 then recruits ESCRT-III targeting factors ALIX and Tsg10, which belong to ESCRT-I complex (Carlton and Martin-Serrano, 2007) (Morita et al., 2007). How exactly the ESCRT-III complex mediates the secondary constriction is not known (Mierzwa and Gerlich, 2014). Once the intercellular bridge is formed, microtubules are dispensable for abscission, and their disassembly is a rate-limiting

step for the final cut (Guizetti et al., 2011) (Green et al., 2013). The disassembly is executed by microtubule-severing protein spastin (Yang et al., 2008) (Connell et al., 2009). Spastin is targeted to the midbody by interaction with CHMP1B, a part of the ESCRT-I complex (Reid et al., 2005) (Yang et al., 2008).

Abscission is tightly regulated by Plk1 and Aurora B kinases. Plk1 prevents premature ESCRT-III accumulation at the midbody (Bastos and Barr, 2010). In the cells with persisting chromosome bridges, Aurora B remains active in the cleavage furrow and inhibits the furrow regression and abscission in order to prevent the formation of tetraploid cells (Steigemann et al., 2009) (Norden et al., 2006). Aurora B phosphorylates CHMP4C, which has been proposed to prevent the ESCRT-III assembly via unknown mechanism, however, the exact role of CHMP4C in abscission control is still controversial (Capalbo et al., 2012) (Carlton et al., 2012). A recent paper proposed another level of regulation by an unknown sensor that can sense the tension exerted on the intercellular bridge. Cutting the bridge by laser caused tension release, which promoted ESCRT-III assembly and membrane fission (Lafaurie-Janvore et al., 2013).

1.4 Ect2

Ect2 or epithelial cell transforming sequence 2 is an essential protein and highly conserved throughout animal kingdom with orthologs in *D. melanogaster* (Pebble/Pbl), *C. elegans* LET-21 and *X. laevis* (XEct2). Ect2 and its orthologs are required for the formation of the cleavage furrow (Prokopenko et al., 1999) (Tatsumoto et al., 1999) (Dechant and Glotzer, 2003) (Yuce et al., 2005).

Ect2 was first identified in *D. melanogaster* by genetic screening, and the *pbl* gene was shown to be essential, as mutations in *pbl* resulted in embryonic lethality (Jürgens et al., 1984). Subsequent studies proposed the role of Ect2 in cytokinesis as the *pbl* mutant embryos failed to assemble the contractile ring, and failed to undergo cell division after cellularization (Lehner, 1992) (Hime and Saint, 1992). Mammalian Ect2 was identified as a protooncogene in a screen for transforming genes in NIH3T3 cells, and it was shown to bind RhoA and Rac (Miki et al., 1993). Ensuing *in vitro* studies defined Ect2 as a putative GEF factor for small GTPases

RhoA, Rac and Cdc42 (Tatsumoto et al., 1999). Studies in *D. melanogaster* showed Pbl localized to the cleavage furrow. Overexpression of Pbl caused modified eye morphology in *D. melanogaster*, which was suppressed by a Rho1 mutation (RhoA ortholog in *D. melanogaster*), providing genetic *in vivo* evidence for the interaction. As a single missense mutation in the Pbl catalytic GEF domain led to cytokinesis failure, reminiscent of Rho1 phenotype, Prokopenko et al. proposed Pbl acts as GEF factor for RhoA, and Ect2-dependent activation of RhoA was proposed to be a key step in cytokinesis (Prokopenko et al., 1999) (Tatsumoto et al., 1999) (Kimura et al., 2000).

A recent study evaluated the role of Ect2 in development and cell proliferation in a mouse model. Cook et al. generated an Ect2 knockout mouse. As expected, homozygous deletion of Ect2 was embryonically lethal. Mouse embryo fibroblasts (MEFs) obtained from conditional Ect2 knockout mice showed impaired proliferation and cell migration. Ect2-depleted MEFs also accumulated in G2/M transition and formed large multi-nucleated cells, which is consistent with its essential role in cytokinesis (Cook et al., 2011).

1.4.1 Ect2 protein domains and their function

Human Ect2 protein consists of 883 amino acids and has multiple structural domains (Figure 9). The domain responsible for the guanine nucleotide exchange activity is a Dbl-homology (DH) type GEF domain (Rossman et al., 2005). The crucial role of Ect2 GEF activity was first shown in *D. melanogaster*, where a single mutation (V513D) in the conserved CR3 helix, important for RhoA binding, led to cytokinesis failure (Prokopenko et al., 1999) (Rossman et al., 2005). In human cells, replacement of the endogenous Ect2 with a version carrying mutations of four highly conserved residues within the C3 helix (565PVQR568) caused cytokinetic defects, and the mutations were shown to abolish the GEF exchange activity *in vitro* (Su et al., 2011). Furthermore, GEF domain mutations also blocked the transforming activity of Ect2 (Saito et al., 2004).

DH domains are usually coupled with pleckstrin homology (PH) domains and, in line with that arrangement, Ect2 also contains a PH domain. PH domains normally

target the protein to the plasma membrane via interaction with phosphoinositides in the inner leaflet of the cell membrane (Lemmon, 2008).

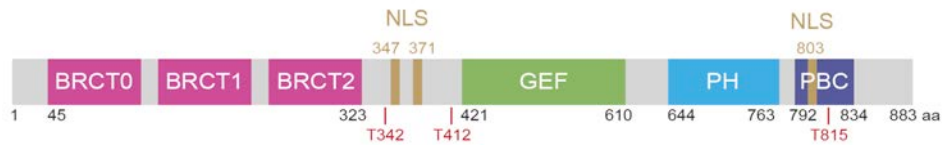


Figure 9 Ect2 domain structure

Schematic domain organization of human Ect2 protein. N-terminal tandem BRCA1 C terminal domains (BRCT), the guanine nucleotide exchange factor (GEF) domain, the C-terminal pleckstrin homology (PH) and cluster of basic amino acids (PBC) are highlighted. Nuclear localization signals (NLS) are depicted in brown. Cdk1 phosphorylation sites with proposed regulatory role are shown in red. The amino acid numbering refers to the human protein. Adapted from (Su et al., 2011) and (Zou et al., 2014).

Full-length Ect2 as well as its C-terminal fragment were observed at the cell cortex by fixed cell analysis, and the PH domain was shown to act as a membrane-targeting domain (Chalamalasetty et al., 2006) (Nishimura and Yonemura, 2006).

A recent study used a genetic complementation system in HeLa cells, which allowed Su et al. to follow Ect2 localization in live cells. They confirmed the interaction of Ect2 with the plasma membrane and showed that Ect2 localized to the plasma membrane shortly after anaphase onset. Deletion analysis revealed that the PH domain was responsible for the membrane targeting of the protein together with a cluster of basic amino acids (polybasic tail, PBC) localized at the very end of the protein. Notably, deletion of the C-terminal part of Ect2 (PH domain and PBC) abrogated RhoA activation, cleavage furrow ingression and cytokinesis, which suggested that the membrane association of Ect2 could be an important step for cell division (Su et al., 2011).

Two BRCT domains are present at the N-terminus of Ect2 – BRCT1 and BRCT2. Recently, a crystal structure of the N-terminal part of Ect2 was resolved and a third BRCT domain called BRCT0 was found, located before the BRCT1 domain (Zou et al., 2014). BRCT (BRCA1 C terminal) domains are specialized interaction domains that bind phosphorylated peptides, DNA and poly(ADP-ribose) (Leung and Glover, 2011). The binding partner of Ect2 BRCT domains was found to be MgcRacGAP, a subunit of the Central spindle complex (Somers and Saint, 2003) (Yuce et al.,

2005) (Zhao and Fang, 2005). Importantly, this interaction takes place only during anaphase, targets Ect2 to the central spindle, and is dependent on phosphorylation (Yuce et al., 2005). The phosphorylation is mediated by the Plk1 kinase that phosphorylates residues in the N-terminal part of MgcRacGAP (Burkard et al., 2009) (Wolfe et al., 2009). The exact identity of the phosphorylated residue is currently controversial as first studies favoured pS157 (Burkard et al., 2009) (Wolfe et al., 2009). Later, Zou et al. proposed pS164 as the only crucial residue (Zou et al., 2014), and Kim et al. suggested that both the pS157 and pS164 might be important for the Ect2-MgcRacGAP interaction (Kim et al., 2014). Mutation of these serine residues prevents the interaction of Ect2 with MgcRacGAP *in vitro* and *in vivo* (Burkard et al., 2009) (Wolfe et al., 2009). Moreover, replacing the endogenous MgcRacGAP with non-phosphorylatable version prevented RhoA accumulation and cytokinetic progression (Burkard et al., 2009) (Wolfe et al., 2009). These results offer an explanation for why Plk1 activity is important for cytokinesis (Petronczki et al., 2007) (Burkard et al., 2009) (Wolfe et al., 2009).

Binding of Ect2 to MgcRacGAP brings Ect2 to central spindle and this interaction plays a crucial role in central spindle model of cytokinesis (Figure 7) (Yuce et al., 2005) (Petronczki et al., 2007) (Wolfe et al., 2009) (Su et al., 2011) (Green et al., 2012) (Mierzwa and Gerlich, 2014). Interestingly, orthologs of Ect2 in *D. melanogaster* (Pebble) and *C. elegans* (LET-21) do not localize to the spindle midzone (Prokopenko et al., 1999) (Green et al., 2012), even though Pebble was shown to interact with RacGAP50C (MgcRacGAP) (Somers and Saint, 2003). Both Pebble and LET-21 localize to the cleavage furrow and the plasma membrane and are crucial for cytokinetic progression (Prokopenko et al., 1999) (Dechant and Glotzer, 2003). Binding of Ect2 to spindle midzone and its role in cytokinesis is thus likely restricted to vertebrates (Green et al., 2012).

1.4.2 Regulation of Ect2 activity

Ect2 activity is regulated on several levels. Expression of Ect2 is induced in S-phase and peaks at G2-M transition (Seguin et al., 2009). Localization of Ect2 regulates the accessibility of the protein for its binding partners – in interphase, Ect2 is sequestered in the nucleus by tandem nuclear localization sequences

(NLS) between the BRCT2 and the GEF domain, and a third NLS inside the PBC (Prokopenko et al., 1999) (Tatsumoto et al., 1999). Overexpression of Ect2's N-terminal fragment containing the BRCT repeats caused late cytokinetic defects (Tatsumoto et al., 1999) (Chalamalasetty et al., 2006). Longer fragments including the NLS signals did not replicate the multi-nucleation phenotype, suggesting that nuclear sequestration might regulate RhoA activation (Chalamalasetty et al., 2006). Moreover, expression of full-length Ect2 with mutated NLS sequences also triggered ectopic rounding (Matthews et al., 2012).

Ect2 activity is regulated by post-translational modifications, mainly phosphorylations. Ect2 is phosphorylated in G2, and the extent of phosphorylation increases during mitosis. The phosphorylation events are necessary for the Ect2's catalytic GEF activity *in vitro* (Tatsumoto et al., 1999). Cdk1 phosphorylates Ect2 on multiple sites, but results regarding the functional outcome of phosphorylation at individual sites are conflicting.

Threonine 342 (T342) is phosphorylated before anaphase onset, and this phosphorylation inhibits the binding to MgcRacGAP. Yuce et al. proposed that Cdk1 is responsible for this modification and that it is important for correct temporal regulation of RhoA activation (Yuce et al., 2005). Conversely, Hara et al. suggested an activatory role for pT342, as they observed a slight enhancement of RhoA activity with the phospho-mimetic mutant. Hara et al. proposed that the phosphorylation causes conformational change of Ect2, which allows the interaction with other proteins that might then fully activate it (Hara et al., 2006). The existence of the T342 phosphorylation *in vivo* was confirmed by a large phosphoproteomic screen (Dephoure et al., 2008). Recent research confirmed that Cdk1 indeed phosphorylates T342 together with the adjacent site S345 (non-S/T-P site). Both sites are close to NLS signals and the phospho-mimetic mutants abolished Ect2 interaction with importin β , which shuttles proteins to nucleus, suggesting that the phosphorylation might be able to counteract the effects of the nuclear localization signals (Suzuki et al., 2015). This might not be relevant for cytokinesis, as the nuclear membrane breaks down at the mitotic entry, but it can affect the role of Ect2 for mitotic rounding, which will be discussed later (Suzuki et al., 2015) (Matthews et al., 2012).

Cdk1 also phosphorylates T412, which might be important for the catalytic activity of Ect2, as the non-phosphorylatable T421A mutant exhibits lower GEF activity. Phosphorylated T412 also creates a docking site for Plk1, which might further regulate Ect2 or other important cytokinetic factors (Niiya et al., 2006) (Petronczki et al., 2007). Another Cdk1-phosphorylated residue is T815 as demonstrated *in vitro* (Niiya et al., 2006) and by phosphoproteomic analysis *in vivo* (Dephoure et al., 2008). T815 is located within the polybasic cluster, which facilitates Ect2 interaction with the plasma membrane (Su et al., 2011). Su et al. speculated that this Cdk1 phosphorylation might regulate the interaction of Ect2 with the plasma membrane that coincides with the anaphase onset. Remarkably, the C-terminal fragment of Ect2 containing the T815A mutation was enriched at the plasma membrane as soon as the cells entered mitosis lending further support to this notion. Moreover, acute inhibition of Cdk1 by flavopiridol caused the rapid translocation of the protein to the plasma membrane. Cdk1 activity thus inhibits Ect2-cell membrane interaction until the anaphase onset possibly via targeting T815 (Su et al., 2011).

The ability of the N-terminus to bind and inhibit the catalytically active C-terminal domain is a common mode of regulation amongst different GEFs (Rossman et al., 2005). Autoinhibitory regulation of Ect2 activity was first proposed by Saito et al. In their study, they demonstrated the interaction between Ect2 N-terminus and C-terminus *in vitro*. Moreover, co-expression of different N-terminal fragments inhibited the transforming activity of the C-terminal Ect2 fragment (Saito et al., 2004). A subsequent study showed that the BRCT domains are responsible for the autoinhibitory interaction with the C-terminal part of Ect2 (Kim et al., 2005). Mutation of highly conserved tryptophan in BRCT2 (W340R) abolished this interaction and enhanced the catalytic GEF activity towards RhoA *in vitro*. A complementation assay, however, showed that BRCT domains have more than this inhibitory function, as the W340R mutant failed to rescue cytokinesis after endogenous Ect2 depletion (Kim et al., 2005).

Discovery of Ect2's association with the phosphorylated MgcRacGAP via the BRCT domains led to a model of MgcRacGAP activating Ect2 by relieving its autoinhibition (Yuce et al., 2005) (Wolfe et al., 2009) (Zou et al., 2014). Recent

work from Zhang et al. provided a further evidence for this model, when they showed the C-termini of Ect2 and MgcRacGAP could also interact *in vitro*. The authors proposed a complex formation between Ect2, MgcRacGAP and RhoA at the equatorial plasma membrane, which leads to induction of Ect2's full activity followed by RhoA activation and the cleavage furrow formation (Zhang and Glotzer, 2015).

Another level of Ect2 regulation is provided by protein-protein interactions. The main binding partner of Ect2 is MgcRacGAP, and the role of this interaction was discussed in the previous paragraphs. Additionally, a study demonstrated that PH domain of Ect2 could interact with the scaffolding factor Anillin at the cell cortex. Frenette et al. proposed this interaction might stabilize the connection between the spindle midzone and the equatorial cell cortex, and promote furrowing (Frenette et al., 2012).

Finally, during mitotic exit Ect2 activity is also controlled by degradation. A sequence within the PBC is ubiquitinated by APC^{Cdh1} and this targets Ect2 for degradation, while a smaller pool of Ect2 translocates back into the nucleus (Liot et al., 2011).

1.4.3 Other functions of Ect2

Apart from its crucial role in cytokinesis, Ect2 also plays a role in other cellular processes. Firstly, Ect2 activity was implicated in the process of cell rounding. After a cell enters mitosis, it starts to detach from the substrate surface, and in metaphase the cell is almost perfectly round. This process is important, as cell rounding affects mitotic spindle assembly and positioning (Kunda and Baum, 2009). Proper cell rounding requires a small pool of Ect2 exported from the nucleus in prophase. Cytosolic Ect2 then activates RhoA and its effectors to induce the cytoskeleton remodelling and stiffening of the cell cortex (Matthews et al., 2012).

Myosin II activation through centralspindlin-Ect2-RhoA pathway is not restricted to cytokinesis. In interphase cells, this pathway is important for the integrity of adherens junctions (Smutny et al., 2010) (Ratheesh et al., 2012). α -catenin is an

adhesion protein linking the actin filaments with cadherins at the junction (Padmanabhan et al., 2015). α -catenin also targets Centralspindlin to the junctions to support the junction stability by myosin II recruitment via the Centralspindlin-Ect2-RhoA pathway (Ratheesh et al., 2012).

Another role for Ect2 lies in cell polarity regulation. Ect2 was shown to interact with the cell polarity complex Par6/Par/aPKC, crucial for establishing the anterior-posterior polarity in *C. elegans* and apical-basal polarity in *D. melanogaster* (Liu et al., 2004) (Cox et al., 2001) (Drubin and Nelson, 1996). Expression of dominant negative N-terminal fragment or constitutively active C-terminus of Ect2 abolished cell polarity establishment in 3D cultures (Liu et al., 2006). In *C. elegans* embryos, Ect2 is localized to the cell cortex with the exception of area around the centrosomes, where it is excluded. This asymmetric localization influences the cortical flow and polarizes the Par proteins and Cdc42 in order to establish the anterior-posterior polarity (Motegi and Sugimoto, 2006). The same pathway was also shown to allow the correct assembly of the actomyosin cortex in *D. melanogaster* cells (Rosa et al., 2015).

The *X. laevis* ortholog of Ect2, XEct2, was proposed to regulate spindle assembly. Interestingly, in a cell free *X. laevis* egg extract system, expression of the N-terminal XEct2 caused formation of monopolar and multipolar spindles. As the only GTPase that showed the same phenotype was Cdc42, Tatsumoto et al. suggested that Ect2 might regulate the spindle assembly via Cdc42 activation (Tatsumoto et al., 2003). The notion that Ect2 can act as a GEF factor for Cdc42 found support in mammalian cells too, where Ect2 activated Cdc42 in metaphase and depletion of Ect2 or Cdc42 in HeLa cells, resulted in a delay in prometaphase and impaired kinetochore attachments (Oceguera-Yanez et al., 2005).

Finally, Ect2 was also proposed to have a role in Wnt signalling. In both *D. melanogaster* and mammalian cells, Ect2 can negatively regulate Wnt pathway (Greer et al., 2013). Ect2 was originally described as a protooncogene, and its involvement in Wnt signalling can be relevant for its role in tumour growth (Fields and Justilien, 2010).

1.5 Goal of this research

The structure of the mitotic spindle determines the location of the cleavage plane. Despite many years of research, the exact mechanism is still not fully understood. A crucial step during cytokinesis is the activation of the small GTPase RhoA, which triggers contractile ring formation and cleavage furrow ingression. As Ect2 is the main activatory factor for RhoA, it lies at the heart of cytokinesis regulation. Recent results led to formation of a model that could explain, why most mammalian cells place the cleavage furrow in the middle of the cell. In anaphase cells, the ability of Ect2 to interact with the spindle midzone and the plasma membrane creates a concentration gradient at the equatorial plasma membrane, which can result in preferential activation of RhoA at the equator and the formation of the furrow at the right place (Figure 10). The aim of this research is to find out (1) whether the plasma membrane engagement and (2) the spindle midzone interaction of Ect2 are essential prerequisites for cytokinesis and (3) whether Ect2's equatorial enrichment at the cell membrane is the primary signal for furrow placement and formation in somatic mammalian cells. By addressing these key questions we hope to decisively test prevailing models of cytokinesis and expand our understanding of the principles that underlie the process in mammalian cells.

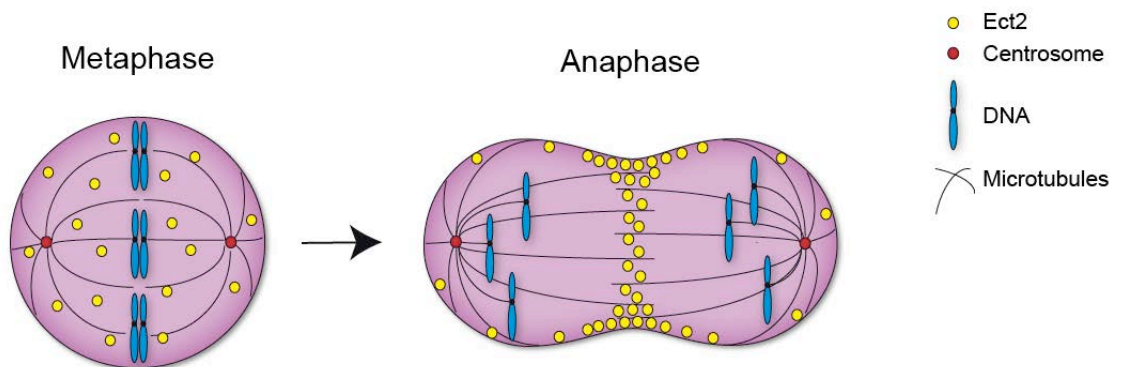


Figure 10 Ect2 localization during mitosis

In metaphase Ect2 is cytoplasmic. After anaphase onset Ect2 is targeted to the spindle midzone and later in anaphase Ect2 also localizes to the plasma membrane with enrichment in the equatorial area.

Chapter 2. Materials & Methods

2.1 Plasmids and cell lines

To prepare tagged variants of various transgenes to express in human cells, the transgenes were amplified by PCR (Phusion High-Fidelity DNA Polymerase, Finnzymes) either from plasmids available in the laboratory (Su et al., 2011) (Lekomtsev et al., 2012) or bought from Addgene (Steigemann et al., 2009) (Kennedy et al., 2010). PCR products were inserted into pCR2.1-TOPO vector (Invitrogen). If necessary, point mutations were produced in pCR2.1-TOPO plasmids by site directed mutagenesis with QuikChange II Site-Directed Mutagenesis Kit (Stratagene) or Phusion Site-Directed Mutagenesis Kit (Finnzymes). Subsequently, the insert was cloned into pIRESpuro3 vector (Clontech), with N-terminal AcGFP-FLAG tag (GFP from *Aequorea coerulea* coupled to FLAG tag) using AgeI and EcoRI restriction enzymes (NEB). These final plasmids were suitable for mammalian expression controlled by puromycin. Some plasmids (see Table 1) were kindly provided by Kuan-Chung Su (Su et al., 2011) or Sergey Lekomtsev (Lekomtsev et al., 2012).

Table 1 List of plasmids used in this study

	Name	Description	Source
1	pIRESpuro3	Original vector used for mammalian expression of the transgenes, puromycin resistance	Clontech
2	pIRES-AcFL-Ect2CT	C-terminal fragment of Ect2 (414-883 aa) tagged with AcGFP-FLAG	(Su et al., 2011)
3	pIRES-eGFP-PLC δ -PH	PH domain from phospholipase C δ tagged with eGFP	Lab database
4	pIRES-eGFP-AKT-PH	PH domain from protein kinase B tagged with eGFP	Lab database

5	pC1-mRFP-FKBP-PJ	Used for hybrid phosphatases system, FKBP-PJ tagged with mRFP	Addgene ID 37999
6	pN1-Lyn11-FRB-mCh	Used for hybrid phosphatases system, Lyn-FRB tagged with mCherry	Addgene ID 38004
7	pIRES-AcFL-C1B	C1B domain from PKC α tagged with AcGFP-FLAG	This study
8	pIRES-AcFL-C1B ^{Q27G}	C1B domain from PKC α carrying Q27G mutation and tagged with AcGFP-FLAG	This study
9	pIRES-AcFL-C1B ^{P11G}	C1B domain from PKC α carrying P11G mutation and tagged with AcGFP-FLAG	This study
10	pIRES-AcFL-Ect2r- Δ PH Δ Tail-C1B	siRNA-resistant Ect2-C1B tagged with AcGFP-FLAG	Kuan-Chung Su
11	pIRES-AcFL-Ect2r- Δ PH Δ Tail-C1B ^{Q27G}	siRNA-resistant Ect2-C1B ^{Q27G} tagged with AcGFP-FLAG	This study
12	pIRES-AcFL-GEF-C1B	GEF domain from Ect2 fused to C1B domain and tagged with AcGFP-FLAG	This study
13	pH2B-mCherry-IRESneo3	Used to visualize chromosomes, histone H2B tagged with mCherry	Addgene ID 21044
14	pCry2PHR-mCh-N1	PHR domain of Cry2 protein tagged with mCherry	Addgene ID 26866
15	pCIBN(deltaNLS)-pmGFP	N-terminal fragment of CIB domain (CIBN), tagged with eGFP and membrane-targeting CAAX signal	Addgene ID 26867
16	pIRES-Cry2-mCh-CAAX	Cry2PHR inserted into pIRES plasmid and tagged with mCherry and CAAX signal	This study

17	pIRES-Cry2-mCh-15aa-CAAX	Cry2PHR tagged with mCherry and CAAX signal with 15 aa linker in-between	This study
18	pIRES-CIBN-GEF-FLAc	CIBN fragment fused to GEF domain from Ect2 and tagged with FLAG-AcGFP	This study
19	pIRES-CIBN-Ect2r- Δ PH Δ Tail-FLAc	CIBN fragment fused to siRNA-resistant Ect2- Δ PH Δ Tail fragment and tagged with FLAG-AcGFP	This study
20	pIRES-Cry2-mCh-Ect2r- Δ PH Δ Tail	Cry2PHR fused to siRNA-resistant Ect2- Δ PH Δ Tail fragment and tagged with mCherry	This study
21	pIRES-AcFL-Ect2r-BRCTTK	siRNA-resistant full-length Ect2 transgene with T153A and K195M mutations and tagged with AcGFP-FLAG	This study
22	pIRES-PM-FLAc	MyrPalm membrane marker tagged with FLAG-AcGFP	Lab database
23	pIRESneo3-MRGr- Δ C1-FLmCh	siRNA-resistant MgcRacGAP transgene with C1 domain deletion and tagged with FLAG- mCherry	(Lekomtsev et al., 2012)
24	pIRESneo3-MRGr-K292L-FLmCh	siRNA-resistant MgcRacGAP transgene with K292L mutation and tagged with FLAG- mCherry	(Lekomtsev et al., 2012)

HeLa 'Kyoto' (HeLaK) and HEK-293T cells were used in this study. HEK-293T cells were used only for a few lipid-related experiments, so unless otherwise specified, HeLaK cells were used. Cells were grown in 25 cm² flasks (Nunc) in the incubator maintained at 37°C and 5% CO₂ in Dulbecco's modified eagle medium (DMEM, Gibco) supplemented with 10% foetal calf serum (FCS, Sigma) and 1% Pen Strep

(Gibco). In order to establish stable cell lines, HeLaK cells were seeded at suitable density in 10 cm dishes (Nunc). Next day, cells were transfected with a transfection mixture prepared from the appropriate plasmid mixed with FuGENE 6 DNA Transfection Reagent (Promega) in 1:3 ratio and diluted in Opti-MEM (reduced serum medium, Gibco). The transfection mixture was incubated for 15 minutes at room temperature before it was added to cells. 48 hours post-transfection, the media was supplemented with 0.3 µg/ml puromycin (Sigma) to select for the cells expressing the transgenes from pIRESpuro3 plasmids. To select for the expression of pIRESneo3 plasmids (mCherry tagged transgenes) or pCIBN(deltaNLS)-pmGFP, 400 µg/ml Geneticin (G418, Gibco) was added to the medium. Monoclonal cell lines were isolated after two weeks of antibiotic selection. Cell lines were characterized by IF and western blotting. Some cell lines (see Table 2) were kindly provided by Kuan-Chung Su (Su et al., 2011). For experiments requiring transient expression of transgenes, the same transfection protocol was followed, but with X-tremeGENE 9 DNA Transfection Reagent (Roche).

Table 2 List of stable cell lines used in this study

	Name	Description	Source
1	AcFL-tag	Control cell line expressing only the AcGFP-FLAG tag	(Su et al., 2011)
2	AcFL-Ect2r	Cell line expressing siRNA-resistant full-length WT Ect2, tagged with AcGFP-FLAG	(Su et al., 2011)
3	AcFL-Ect2r- ΔPHΔTail	Cell line expressing siRNA-resistant Ect2 with deleted PH domain and C-terminal tail, tagged with AcGFP-FLAG	(Su et al., 2011)
4	AcFL-Ect2r- ΔPHΔTail-C1B	Cell line expressing siRNA-resistant Ect2 with deleted PH domain and C-terminal tail fused to C1B domain, tagged with AcGFP-FLAG	This study
5	AcFL-Ect2r- ΔPHΔTail-C1B ^{Q27G}	Cell line expressing siRNA-resistant Ect2 with deleted PH domain and C-terminal tail fused to C1B domain with Q27G mutation, tagged with AcGFP-FLAG	This study

6	AcFL-GEF-C1B	Cell line expressing GEF domain from Ect2 fused to C1B domain, tagged with AcGFP-FLAG	This study
7	CIBN-eGFP-CAAX	Cell line expressing CIBN domain, tagged with eGFP and membrane-targeting CAAX signal	This study
8	AcFL-Ect2r, H2B-mCherry	Cell line expressing siRNA-resistant full-length WT Ect2, tagged with AcGFP-FLAG and histone H2B tagged with mCherry	(Su et al., 2011)
9	AcFL-Ect2r-BRCT ^{TK} , H2B-mCherry	Cell line expressing siRNA-resistant full-length Ect2 with T153A and K195M mutations, tagged with AcGFP-FLAG and histone H2B tagged with mCherry	This study
10	AcFL-Ect2r-BRCT ^{TK}	Cell line expressing siRNA-resistant full-length Ect2 with T153A and K195M mutations, tagged with AcGFP-FLAG	This study
11	AcFL-Ect2r-GEF ^{4A}	Cell line expressing siRNA-resistant full-length Ect2 with 565PVQR568AAAA mutations, tagged with AcGFP-FLAG	(Su et al., 2011)
12	AcFL-Ect2r-BRCT ^{TK} , MgcRacGAPr- Δ C1-FLmCh	Cell line expressing siRNA-resistant full-length Ect2 with T153A and K195M mutations, tagged with AcGFP-FLAG and siRNA-resistant full-length MgcRacGAP with C1 domain deletion, tagged with mCherry	This study
13	AcFL-Ect2r-BRCT ^{TK} , MgcRacGAPr-K292L-FLmCh	Cell line expressing siRNA-resistant full-length Ect2 with T153A and K195M mutations, tagged with AcGFP-FLAG and siRNA-resistant full-length MgcRacGAP with K292L mutation in C1 domain, tagged with mCherry	This study

2.2 siRNA transfection

Transfections with siRNA were performed with Lipofectamine RNAiMax reagent (Invitrogen) using reverse transfection as by the manual. siRNAs were diluted to 20 μ M concentration in RNase-free 1x siRNA buffer (prepared from 5x siRNA buffer and RNase-free water, Thermo). To transfect cells in 1 well of a 12-well plate (Corning), 1.5 μ l of siRNA was mixed with 2.5 μ l of Lipofectamine RNAiMax and diluted in Opti-MEM. The mixture was scaled up or down appropriately, for different volumes. The mixture was incubated for 5 minutes at room temperature, and subsequently it was mixed with the cells and plated. The final concentration of siRNA in the medium was 20 nM. The medium was changed 6 hours after transfection. The following siRNA duplexes were used in this study: control siRNA (NTC) (Thermo Scientific siGenome Non-Targeting siRNA #1 D-001210-01 and #4 D-001210-04), Ect2 siRNA (Thermo Scientific siGenome D-006450-02) and MgcRacGAP siRNA (Invitrogen Stealth HSS120934).

2.3 Cell synchronization and drug treatments

To synchronize the majority of the cells in anaphase (Figure 26), 2.5 mM thymidine (Sigma) was added to the medium 6 hours after siRNA transfection. After 20 hours of incubation with thymidine, the medium was changed to normal cell medium for 6 hours to allow cells to progress through S phase. After that, cells were treated with nocodazole at 50 ng/ml (Sigma) for 4.5 hours. Cells were in prometaphase after the nocodazole washout. Proteasome inhibitor MG132 at 10 μ M was added for 2 hours, which allowed the cells to reach metaphase. Afterwards, cells were released from MG132 and 45 minutes later either DMSO as a control or 1 μ M 12-O-Tetradecanoylphorbol-13-acetate (TPA, Sigma) was added and live-cell imaging was started right after. Same synchronization protocol was used for low nocodazole treatment to deplete astral microtubules from anaphase cells (Figure 51). Similarly, 45 minutes after MG132 washout, DMSO as a control or 50 nM nocodazole was added to cells. 10 minutes later, cells were fixed and analysed by immunofluorescence analysis (IF) or followed by live-cell imaging.

To enrich the culture for metaphase cells (Figure 31), cells were treated with 50 ng/ml concentration of nocodazole for 4.5 hours. One hour after the release from nocodazole, DMSO or 1 μ M TPA was added and the cells were fixed 5 minutes later.

Single thymidine block was used to obtain anaphase cells for IF analysis (Figure 41). Cells were transfected with Ect2 siRNA and 6 hours later, thymidine at 2.5 mM was added to the medium. After 20 hours of thymidine block, cells were washed and let to recover and grow. Cells were fixed after 9.5 hours, when the culture was enriched for anaphase cells.

Ionomycin treatment (Figure 12): Cells were transiently transfected with eGFP-PLC δ -PH and AcFL-Ect2CT plasmids. 48 hours post-transfection, cells were imaged with the fluorescent confocal microscope. Firstly, Opti-MEM was added for 10 minutes as a control. To activate phospholipase C and deplete PIP2 and PI4P from the cell membrane, cells were treated with 10 μ M ionomycin (Sigma) together with 1 mM CaCl₂ for 6.5 minutes during the imaging (phenotype was analysed after 3 minutes). Subsequently, 10 mM EGTA was added for 15 minutes (phenotype was analysed after 12 minutes). The experiment with neomycin followed similar protocol: after 10 minutes with Opti-MEM, cells were treated with 50 mM neomycin (Sigma) for 20 minutes and afterwards 10 μ M ionomycin and 1 mM CaCl₂ were added for 6 minutes.

PI3Ks inhibitors (Figure 14): HEK-293T cells were transiently transfected with eGFP-AKT-PH and AcFL-Ect2CT plasmids. 24 hours post-transfection, cells were imaged with the fluorescent confocal microscope. Firstly, Opti-MEM was added for 10 minutes as a control. To deplete phosphatidylinositol 3-phosphate, phosphatidylinositol 3,4-bisphosphate and phosphatidylinositol 3,4,5-trisphosphate from the plasma membrane, cells were treated with 25 μ M LY294002 (Sigma) or 100 nM wortmannin (Sigma) for 30 minutes.

Rapamycin treatment (Figure 17): HeLaK and HEK-293T cells were transiently transfected with Lyn-FRB-mCh, mRFP-FKBP-PJ and eGFP-PLC δ -PH or AcFL-Ect2CT plasmids. Cells were imaged with the fluorescent confocal

microscope 48 hours after transfection. PJ hybrid phosphatase was targeted to the plasma membrane by treatment with 10 μ M rapamycin (Sigma) during live-cell imaging.

Phorbol ester treatment: TPA was used for artificial membrane targeting of hybrid C1B proteins. 10 nM concentration was used for long-term rescue experiments and 1 μ M concentration was used during initial testing and for imaging purposes. DMSO was always used as a control.

2.4 Cell lysates preparation and western blotting (WB)

Cells were transfected with siRNA or plasmid DNA and treated as appropriate. After 48 hours, cells were harvested by trypsinization, i.e. washed with PBS buffer and detached from the surface by Trypsin-EDTA solution (Sigma) treatment for 3 minutes at 37°C. Subsequently, cells were pelleted down by centrifugation and washed with cold PBS buffer (4°C). To prepare the whole cell lysate, the cell pellet was directly resuspended in Laemmli buffer (12.5 ml 4x SDS-PAGE stacking buffer [0.5 M Tris-HCl, pH 6.8, 0.4% SDS w/v], 10 ml glycerol, 20 ml SDS [10% w/v], 2.5 ml β -mercaptoethanol and 2.5 ml bromophenol blue [1% w/v]). Afterwards, lysates were boiled for 5 minutes and sonicated 3 times for 10 seconds.

After the preparation of cell lysates, the protein concentration was measured by Bradford assay using the Bradford's reagent (BioRad) and serial dilution of BSA standard (Sigma). Subsequently, 30 μ g of each sample was loaded in a precasted gel (Criterion XT, 3-8% Tris-Acetate, BioRad) or (NuPAGE Novex 3-8% Tris-Acetate, Invitrogen) and the SDS-PAGE was performed. Separated proteins were transferred onto Immobilon PVDF membrane (Millipore) by semi-dry blotting for 1 hour at room temperature. Subsequently, the membrane was blocked with 5% milk in TBST buffer (Tris-buffered saline [50 mM Tris-HCl, pH 7.5, 150 mM NaCl] with 0.1% Tween-20) for 1 hour and then incubated with the selected primary antibody diluted in 5% milk in TBST o/n at 4°C. The membrane was washed 3 times for 5 minutes with TBST buffer and subsequently incubated with the appropriate secondary antibody conjugated with HRP (horseradish peroxidase) diluted in 5% milk in TBST buffer. After another round of TBST washes, the protein

signals were detected using ECL chemiluminescence reaction (GE Healthcare) on ECL-sensitive film (GE Healthcare).

2.5 Immunofluorescence microscopy (IF)

Cells were seeded and treated appropriately onto coverslips of 18 mm diameter and thickness 1 (Assistant). Afterwards, they were fixed in ice cold methanol (-20°C) for 2 hours or o/n (Figure 23, Figure 29, Figure 31, Figure 41 and Figure 47) or in 4% PFA (paraformaldehyde, Thermo) diluted in PBS for 10 minutes at 37°C (Figure 47 AcFL-tag sample) or with 10% TCA (trichloroacetic acid) on ice for 15 minutes (Figure 50). After the fixation process was finished, the samples were washed 3 times for 5 minutes with PBST buffer (PBS with 0.01% Triton X-100), then permeabilized with 0.2% Triton X-100 in PBS for 10 minutes on rocking platform. Then, the samples were washed again 3 times with PBST and subsequently incubated with the blocking solution (3% BSA diluted in PBS with 0.01% Triton X-100) for 1 hour. Afterwards, the coverslips were incubated with selected primary antibodies diluted in the blocking solution in the wet chamber o/n at 4°C. Samples were washed 3 times with PBST and incubated for 45 minutes in the dark at room temperature with appropriate secondary antibodies conjugated with fluorescent dyes and diluted in the blocking solution. Following this incubation, the samples were washed again 3 times with PBST and mounted on microscopic slides (Thermo) using the antifade mountant ProLong Gold or ProLong Diamond (Molecular Probes). The samples were dried at room temperature, o/n and in the dark.

IF images were acquired on a Zeiss Axio Imager M1 or M2 microscope using a Plan Neofluor 40x/1.3 oil objective lens (Figure 23, Figure 29, Figure 40 and Figure 47) or Plan Aplanachromat 63x/1.4 oil objective lens (Figure 31, Figure 41 and Figure 50) (both from Zeiss) equipped with an ORCA-ER camera (Hamamatsu) and controlled by Volocity 6.1 software (Improvision).

2.6 Antibodies and dyes

The following primary antibodies were used in this study: mouse monoclonal anti-AcGFP (Clontech JL8, WB 1:1000), rabbit polyclonal anti-Ect2 (raised against

Ect2 1-421 aa, WB raw serum 1:2000), rabbit monoclonal anti- β -tubulin (Cell Signaling 9F3, WB 1:2000), mouse monoclonal anti-MgcRacGAP (Abnova M01 1G6, WB 1:500), rabbit polyclonal anti-AcGFP (Clontech 632592, IF 1:2000), rat monoclonal α -tubulin (AbD Serotec MCA78G, IF 1:1000), mouse monoclonal anti-Mklp1 (Santa Cruz Biotechnology 24, IF 1:500), rabbit polyclonal anti-Anillin (kindly provided by Michael Glotzer, 1:2000) and mouse monoclonal anti-RhoA (Santa Cruz Biotechnology 26C4, IF 1:75). Secondary antibodies conjugated to Alexa Fluor 488 or Alexa Fluor 594 (Molecular Probes, IF 1:500) were used for immunofluorescence detection. DNA was stained with DAPI at 1 μ g/ml (Molecular Probes). HRP-conjugated secondary antibodies (polyclonal goat anti-mouse P0447 and polyclonal anti-rabbit P0488, Dako) were used at 1:5000 dilution to detect protein signals on PVDF membrane.

2.7 Live-cell imaging

For live-cell imaging of fluorescently-tagged proteins, cells were grown in Lab-Tek chambers (Lab-Tek chambered coverglass, Nunc). Before the imaging, the cell medium was changed to sterile-filtered imaging medium (CO₂ independent medium [Gibco], 20% FCS, 1% Pen Strep and 0.2 mM L-glutamine [Gibco]). For all experiments in Chapter 3, the imaging medium was supplemented only with 10% FCS and cells were seeded on poly-L-lysine (Sigma) coated Lab-Tek chambers. Appropriate volume of poly-L-lysine solution was added to cover the surface of the chambers. After 5 minutes incubation, the chambers were washed 3 times with sterile-filtered water, and left to dry for 1 hour at room temperature.

Images for Figure 12, Figure 14, Figure 17, Figure 18 and Figure 34 were acquired at 37°C on an Olympus FV1000D (Inverted Microscope IX81) laser confocal scanning microscope using an UPlanFIU 40x/1.30 Oil Sc objective lens (Olympus) controlled by FV10-ASW software. The same microscope was used for Figure 19, but with a PlanApoN 60x/1.40 oil Sc objective lens (Olympus). Images for Figure 21, Figure 28 and Figure 42 were obtained at 37°C on a PerkinElmer ERS Spinning disc system equipped with a Nikon TE2000 microscope, an Apo TIRF 60x/1.49 oil objective lens (Nikon), a CSU22 spinning disc scanner (Yokogawa) and a

IEEE1394 Digital CCD C4742-80-12AG camera (Hamamatsu), controlled by Volocity 5.5.1 software (Perkin Elmer).

Images for Figure 35, Figure 36, Figure 37 and Figure 38 were acquired at 37°C on Invert780 Zeiss LSM multi-photon confocal system equipped with Zeiss Axio Observer.Z1 microscope, a Plan-Apochromat 63x/1.46 oil objective lens and a GaAsP spectral detector all controlled by Zen2012 software. The plasma membrane interaction of Cry2-mCh-Ect2 was triggered by scanning with a 488 nm laser in the case of Figure 35. More spatially selective targeting of Cry2-mCh-Ect2 was triggered by illumination with a 488 nm laser inside two small circular regions of 20 pixels in diameter placed at both sides of the equatorial cortex every 5 minutes (Figure 36). Unilateral targeting of Cry2-mCh-Ect2 was achieved by illumination inside one small circle every 2 minutes on one side of the equatorial cortex for Figure 37 and at one cell pole for Figure 38.

Phase contrast images in Figure 24, Figure 26 and Figure 48 were obtained by using an IncuCyte FLR integrated live-cell imaging system (Essen Bioscience). Cells were imaged every 10 minutes in a regular cell medium.

2.8 Image quantification

Images were quantified using ImageJ software version 1.46r (<http://rsbweb.nih.gov/ij/>). For Figure 13, Figure 15 and Figure 32, mean GFP intensities were measured (function Measure in ImageJ) for each time point. The membrane signal value was obtained by averaging six manually placed circular regions of 9 pixels in diameter at the cell periphery. The cytoplasmic signal was measured by averaging three manually selected circular regions of 50 pixels in diameter in the cytoplasm. The mean background signal was obtained by averaging three manually selected circular regions of 50 pixels in diameter outside of the cell. The mean value of the background signal was subtracted from the membrane and cytoplasmic values and after that, the ratio of cell periphery to cytoplasmic average signals was calculated for each cell analyzed (Figure 11). For Figure 45, the ratio of mean AcGFP signal at equatorial periphery to polar periphery was determined. The equatorial periphery signal was obtained by

averaging 2 manually placed circular regions 12 pixels in diameter at the cell periphery at both sides of the furrow. The polar periphery signal was obtained by averaging 2 manually placed circular regions of 12 pixels in diameter at the cell periphery at both cell poles. Mean background signal was obtained by averaging three manually selected circular regions of 50 pixels in diameter outside of the cell. The mean value of the background signal was subtracted from the equatorial and polar periphery values and after that, the ratio of equatorial periphery to polar periphery average signals was calculated for each cell analyzed.

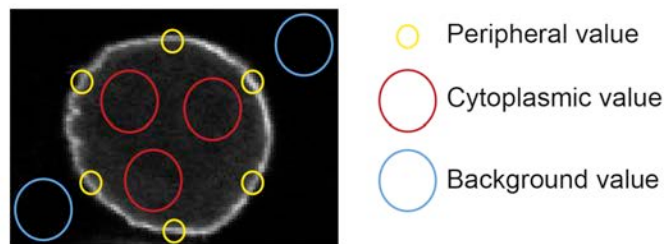


Figure 11 Image quantification - mean intensity ratio cell periphery/cytoplasm
Schematic representation of image quantification to calculate mean ratio of intensity at the cell periphery to cytoplasmic intensity. Yellow circle - peripheral value; red circle - cytoplasmic value; blue circle - background value.

The cell periphery signal for Figure 43 was obtained by measuring the intensity profile of the AcGFP signal along the line manually placed along the cell periphery in ImageJ (function Plot profile). The cytoplasmic signal was measured by averaging three manually selected circular regions of 50 pixels in diameter in the cytoplasm. The mean background signal was obtained as described above and the value was subtracted from the cell periphery and cytoplasmic values, and after that the ratio of cell periphery to cytoplasmic average signals was calculated for each cell analyzed. The same quantification was used for Figure 50, the measured signal being RhoA and Anillin peripheral intensity. Images were processed with ImageJ 1.46r and Adobe Photoshop CS5.1. All graphs presented in this study were made using the GraphPad Prism version 6.0a. Structural alignment from Figure 39B was done using UCSF Chimera software version 1.8.1.

Chapter 3. Results 1 - Investigating the lipid requirements for the association of Ect2 with the plasma membrane

An increasing body of evidence indicates that lipids, especially phosphoinositides play an important role in cell division and cytokinesis (Neto et al., 2011) (Brill et al., 2011) (Echard, 2012) (Atilla-Gokcumen et al., 2014). Previous studies in our laboratory have shown that Ect2 protein localizes to the plasma membrane shortly after anaphase onset (Su et al., 2011). Translocation of Ect2 to the plasma membrane is dependent on the protein's pleckstrin homology (PH) domain and a cluster of basic amino acid residues (polybasic cluster, PBC) located at the C-terminus of the protein. *In vitro* experiments have also demonstrated the ability of Ect2's C-terminal region to interact with phosphoinositides (Su et al., 2011). However, the requirement of specific lipid species for the recruitment of Ect2 to the plasma membrane in a cellular context, and the role and distribution of these lipids during cytokinesis are currently unknown. Therefore, we set out to determine which lipid species are required for the membrane localization of Ect2.

3.1 Ionomycin•Ca²⁺ treatment abrogates the localization of Ect2CT to the plasma membrane

In order to gain insight into which lipids mediate the interaction of Ect2 with the plasma membrane, we decided to first use pharmacological agents to manipulate the composition of the plasma membrane *in vivo*. We focused our studies on phosphoinositides for two reasons. Generally, PH domains and polybasic clusters are known to interact with phosphoinositides (Heo et al., 2006) (Lemmon, 2008). Furthermore, previous results from our laboratory indicated that phosphoinositides could interact with Ect2's C-terminal region in biochemical assays (Su et al., 2011). Firstly, we used a treatment regime to deplete phosphatidylinositol 4,5-bisphosphate (PIP₂) and phosphatidylinositol 4-phosphate (PI4P) from the inner surface of the cell membrane. The method is based on the calcium-induced activation of phospholipase C (PLC), which results in the hydrolytic cleavage of PIP₂ and PI4P into diacylglycerol and inositol 1,4,5-triphosphate and inositol

1,4-diphosphate (Varnai and Balla, 1998) (Hammond et al., 2012). Ionomycin serves as an ionophore, transferring calcium ions across the cell membrane and consequently raising their intracellular concentration. Calcium chloride was added together with ionomycin to enrich the medium for calcium ions. The effect of ionomycin and calcium treatment can be reversed by addition of a chelating agent for divalent cations, such as EGTA.

To test the ionomycin effect on Ect2 localization in cells, we transiently expressed a GFP-tagged truncated version of Ect2 protein (AcFL-Ect2CT) in HeLa Kyoto cells (HeLaK) (Figure 12A). Ect2CT contains the GEF domain, the C-terminal PH domain and the PBC region but it lacks the N-terminal part including the BRCT repeats. Ect2CT has been shown to localize to the plasma membrane in a PH and PBC-dependent manner when transiently expressed in cells (Su et al., 2011). The rationale for our experiment was that the ionomycin•Ca²⁺ treatment should release Ect2CT from the plasma membrane if Ect2 membrane binding involves interaction with PIP2 or PI4P. We observed the consequences of ionomycin•Ca²⁺ addition in live cells by fluorescence confocal microscopy. The GFP-tagged PH domain of phospholipase C δ (eGFP-PLC δ -PH) that is known to bind to PIP2 and requires this lipid for its membrane localization was used as a positive control (Rebecchi et al., 1992). Treatment of cells with ionomycin•Ca²⁺ triggered rapid release of both PLC δ -PH and Ect2CT proteins from the plasma membrane (Figure 12B and Figure 13A). We confirmed that this effect was dependent on calcium ions, because it could be at least partially reversed by the addition of EGTA. Further results were obtained by experiments with neomycin, which has been shown to bind and protect PIP2 from degradation by phospholipase C (Wang et al., 2005). Pre-treatment with neomycin before the addition of ionomycin•Ca²⁺ abolished the release of PLC δ -PH protein from the plasma membrane, which confirmed the specific interaction of PLC δ -PH with PIP2 (Figure 13B). In case of Ect2CT, neomycin partially prevented the release of the protein from the cell membrane. Taken together, our data strongly suggest that Ect2's association with the plasma membrane requires and involves the polyanionic phosphoinositides PIP2 and PI4P.

3.2 PI3Ks inhibitor treatment does not prevent Ect2CT recruitment to the plasma membrane

To analyze if Ect2 binding to the plasma membrane is dependent on the phosphoinositides with a phosphorylated hydroxyl in position 3 of the inositol ring, we tested the phenotype of phosphoinositide 3-kinases (PI3Ks) inhibitors wortmannin and LY294002. Wortmannin is a strong irreversible inhibitor of PI3Ks, LY294002 is less potent but reversible inhibitor (Powis et al., 1994) (Vlahos et al., 1994). PI3Ks inhibition results in depletion of phosphatidylinositol 3-phosphate, phosphatidylinositol 3,4-bisphosphate and phosphatidylinositol 3,4,5-trisphosphate (PI3P) from the cell membrane. As a positive control sensor for the PI3Ks inhibition, we used a GFP-tagged PH domain from protein kinase B (eGFP-Akt-PH), which is known to bind phosphatidylinositol 3,4,5-trisphosphate and phosphatidylinositol 3,4-bisphosphate (Franke et al., 1997) (James et al., 1996). Akt-PH expressed in HeLaK cells does not localize to the plasma membrane, possibly due to the low abundance of phosphatidylinositol 3,4,5-trisphosphate and phosphatidylinositol 3,4-bisphosphate within the inner leaflet of the plasma membrane. Therefore we used HEK-293T cells for these experiments (Santi and Lee, 2010). After incubation with the PI3Ks inhibitors wortmannin and LY294002, the PH domain of Akt was efficiently displaced from the plasma membrane (Figure 14 and Figure 15). Conversely, Ect2CT membrane localization did not change after the treatment with LY294002 or wortmannin (Figure 14 and Figure 15). These results suggest that the membrane localization of Ect2 does not require the interaction with phosphatidylinositol 3-phosphate, phosphatidylinositol 3,4,5-trisphosphate or phosphatidylinositol 3,4-bisphosphate. Notably, Ect2CT protein localization to the plasma membrane was less pronounced in HEK-293T cells as compared to HeLaK cells (Figure 13 and Figure 15) and HEK-293T cells did not tolerate the expression of Ect2CT fragment as well as the HeLaK cells.

3.3 Attempt to study Ect2 membrane localization using a chemically controlled lipid phosphatases

In order to deplete specific phosphoinositide species from the plasma membrane and to individually assess their role in Ect2 binding (e.g. PIP2 versus PI4P), we

employed a system of chemically controlled hybrid phosphatases, which can selectively hydrolyze different phosphoinositides at the plasma membrane (Hammond et al., 2012). The hybrid phosphatase, pseudojanin (PJ), consists of polyphosphate-5-phosphatase E (INPP5E), which hydrolyses PIP2 to PI4P, and *S. cerevisiae* Sac1 phosphatase (Sac), which dephosphorylates PI4P to generate phosphatidylinositol (PI) (Figure 16). Thus, sequential action of INPP5E and Sac converts PIP2 to PI. Acute membrane targeting of the hybrid phosphatase PJ is achieved by the FKBP-FRB chemical dimerizing system (Rivera et al., 1996). FRB fragment is fused to N-terminal peptide from Lyn kinase, which serves as a myristoylation and palmitoylation signal so FRB is constitutively associated with the cell membrane (Raucher et al., 2000). Rapamycin binds to FKBP and triggers dimerization of FKBP protein with FRB fragment. As it is possible to target PJ with catalytically inactive Sac and/or INPP5E phosphatase domains, the system can help discriminate between the effects of PIP2 and PI4P loss (Hammond et al., 2012) and can confirm which one is important for Ect2 targeting to the plasma membrane.

First, we tested the hybrid phosphatases system in HeLaK cells, where Ect2CT association with the plasma membrane can be easily assessed and quantified (Figure 12 and Figure 13). After co-transfection with eGFP-PLC δ -PH, Lyn-FRB-mCh and mRFP-FKBP-PJ plasmids, we added rapamycin and followed its effect by fluorescence confocal microscopy. Surprisingly, rapamycin treatment did not release the PLC δ -PH control protein from the plasma membrane (Figure 17A). Conversely, repetition of the same experiment in HEK-293T cells showed translocation of PLC δ -PH to the cytoplasm after rapamycin addition, consistently with the published data on PJ system (Hammond et al., 2012) (Lekomtsev et al., 2012). This result can be explained by previously reported limitations of the rapamycin-induced dimerization system in HeLaK and other cell types (Coutinho-Budd et al., 2013) (Ballister et al., 2014). Some cell types including HeLaK cells express high levels of endogenous FKBP protein, which can compete with the exogenous hybrid protein mRFP-FKBP-PJ and thus prevents efficient translocation to the plasma membrane. Therefore, we used HEK-293T cells, in which the successful use of rapamycin system has been reported (Hammond et al., 2012) (Lekomtsev et al., 2012) (Figure 17A). Unfortunately, and in line with what we

observed before during experiments with PI3Ks inhibitors, we were unable to identify enough cells successfully co-transfected with all three plasmids (AcFL-Ect2CT, Lyn-FRB-mCh and mRFP-FKBP-PJ) and the Ect2CT fragment exhibited poor enrichment at the plasma membrane in comparison to HeLaK cells. Nevertheless, in the few HEK-293T cells that we could test, Ect2CT membrane localization was reduced after treatment with rapamycin (Figure 17B). The number of cells analysed and the poor enrichment of Ect2CT at the plasma membrane, however, did not allow us to draw any firm conclusions from the experiments with hybrid PJ phosphatase nor did they allow us to differentiate between the effect of PIP2 and PI4P depletion.

3.4 Conclusions - The lipid requirements for Ect2 plasma membrane association

Membrane lipids interact with various membrane-associated proteins that drive cleavage furrow formation (Neto et al., 2011) (Brill et al., 2011) (Echard, 2012) (Atilla-Gokcumen et al., 2014). Consequently, the presence and distribution of lipids within the cell membrane can affect cell division. To increase our understanding about the role of lipids during cytokinesis, we set out to determine which lipid species target Ect2 to the plasma membrane.

As previous *in vitro* biochemical experiments in our lab have shown that Ect2 can associate with phosphoinositides, they were in the centre of our focus during this study. We have successfully employed several pharmacological treatments to deplete different phosphoinositides from the plasma membrane and assessed the phenotype after the depletion. Firstly, we used ionomycin and calcium treatment to activate phospholipase C in order to deplete PIP2 and PI4P. Experiments with ionomycin•Ca²⁺ treatment combined with neomycin pre-treatment, which specifically inhibits PIP2 depletion, strongly suggested that Ect2 engagement with PIP2 promotes membrane localization of the protein with a possible contribution of an interaction with PI4P.

Two different PI3Ks inhibitors, LY294002 and wortmannin released the positive control Akt-PH from the plasma membrane of HEK-293T cells, but had no effect on

membrane localization of Ect2CT protein. Due to the technical limitations with Ect2CT expression assays in HEK-293T cells it is difficult to rule out the possibility of a minor contribution of phosphoinositides with a phosphorylated hydroxyl in position 3 to plasma membrane binding of Ect2. However, our data do not support any major contribution mediated by these lipid species.

We experienced other technical difficulties with the rapamycin system of hybrid phosphatases, which we planned to use to distinguish between Ect2 binding to PIP2 and PI4P. The system is not functional in HeLaK cells, possibly because of high cytosolic concentration of endogenous FKBP protein (Coutinho-Budd et al., 2013) (Ballister et al., 2014). We observed plasma membrane displacement of the PLC δ -PH control protein in HEK-293T cells, but we could not reliably replicate the experiment using Ect2CT, because of very poor transfection efficiency with all three plasmids at once (Ect2CT, Lyn-FRB-mCh and mRFP-FKBP-PJ) and a reduced association of Ect2CT with the cell membrane in HEK-293T cells. We attempted to overcome these problems by using different cell types like U2OS and RPE cells, but we encountered similar difficulties.

In summary, our results suggest that phosphatidylinositol 4,5-bisphosphate (PIP2) and phosphatidylinositol 4-phosphate (PI4P) as the main lipid species interacting with Ect2 and mediating the protein's membrane association during cytokinesis. Importantly, PIP2 is the most abundant phosphoinositide in the inner cell membrane (Balla, 2013). The polyanionic lipids PIP2 and PI4P contribute to plasma membrane identity and PIP2 has been shown to accumulate in the cleavage furrow and its depletion impairs cytokinesis (Emoto et al., 2005) (Field et al., 2005b). Our experiments using Ect2CT are consistent with the biochemical lipid interaction assays (Su et al., 2011). Structural and mutational studies will be required to dissect whether the protein's PH domain and PBC region engage with the same lipids to promote the plasma membrane association. Although, Ect2CT contains all known membrane engagement regions of Ect2, using transient and ectopic Ect2CT expression in interphase cells, as a surrogate assay for Ect2 membrane localization, is artificial. Under normal conditions, Ect2 interacts with the plasma membrane only after anaphase onset, so cells expressing full-length Ect2 and synchronized in cytokinesis would be a better model for future lipid studies.

There is also a possibility that Ect2 interacts with another lipid species that is specifically present in the plasma membrane during cytokinesis. Using anaphase-synchronized cells would also allow us to identify this possible interacting lipid. And by using the full-length Ect2 should overcome the problem with ectopic expression of the Ect2CT, a highly active GEF and activator of RhoA (Su et al., 2011) (Su et al., 2014). To test the requirement of PIP2 and PI4P for Ect2 membrane localization during cell division, pharmacological interventions and enzymatic lipid depletions should be set up in cells that undergo cytokinesis and that express GFP-tagged full-length Ect2 at endogenous level.

Another way to study the lipids important for Ect2 membrane binding during cytokinesis would be to employ biochemical techniques and *in vitro* approach, using recombinantly expressed Ect2 protein (Su et al., 2011). Possible techniques include liposome-binding experiments, which study interaction with artificially prepared liposomes containing different lipid species. Various methods are used to study interaction of isolated proteins with liposomes, including isothermal titration calorimetry (ITC), vesicle sedimentation approaches, and surface plasmon resonance (SPR) (Narayan and Lemmon, 2006).

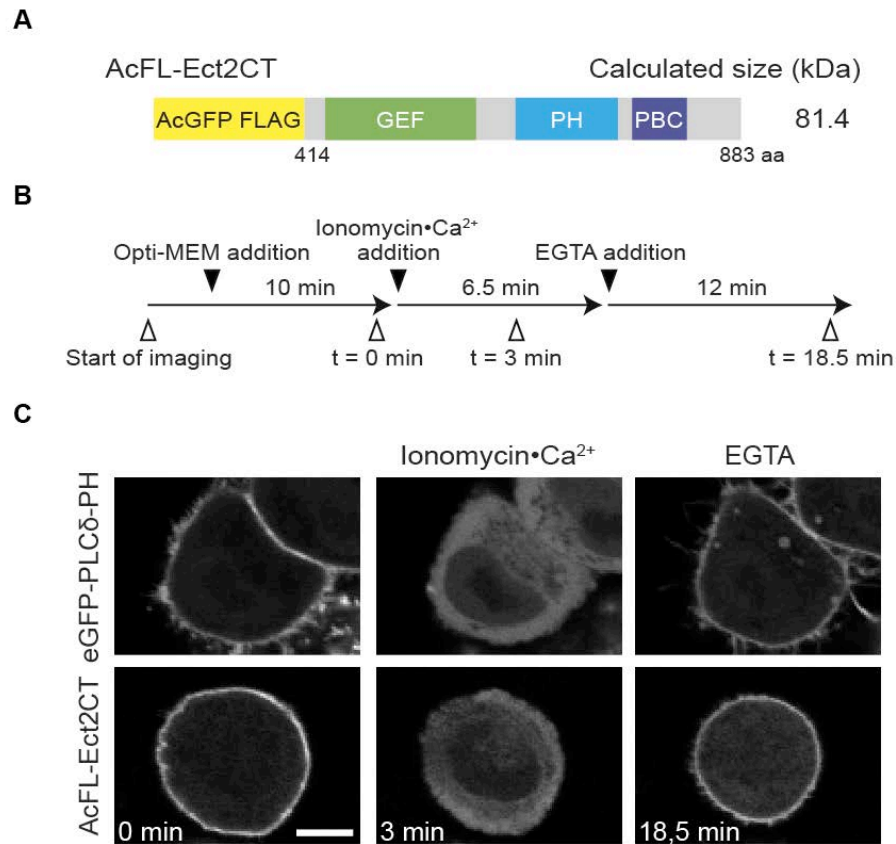


Figure 12 Ionomycin•Ca²⁺ treatment releases PLCδ-PH and Ect2CT from the plasma membrane

A Schematic representation of the domain organization of the Ect2CT fragment used for the lipid manipulation experiments. Numbering of amino acid residues corresponds to positions in human full-length Ect2 protein.

B Timeline representation of ionomycin•Ca²⁺ experiment shown in Figure 12C and Figure 13.

C Stills from confocal imaging of HeLaK cells transiently transfected with plasmids encoding GFP-tagged PLCδ-PH and Ect2CT. 48 hours post-transfection, the cells were treated with 10 μM ionomycin and 1 mM CaCl₂ and subsequently with 10 mM EGTA. t = 0 min was set to the frame prior to ionomycin•Ca²⁺ addition. Scale bar represents 10 μm.

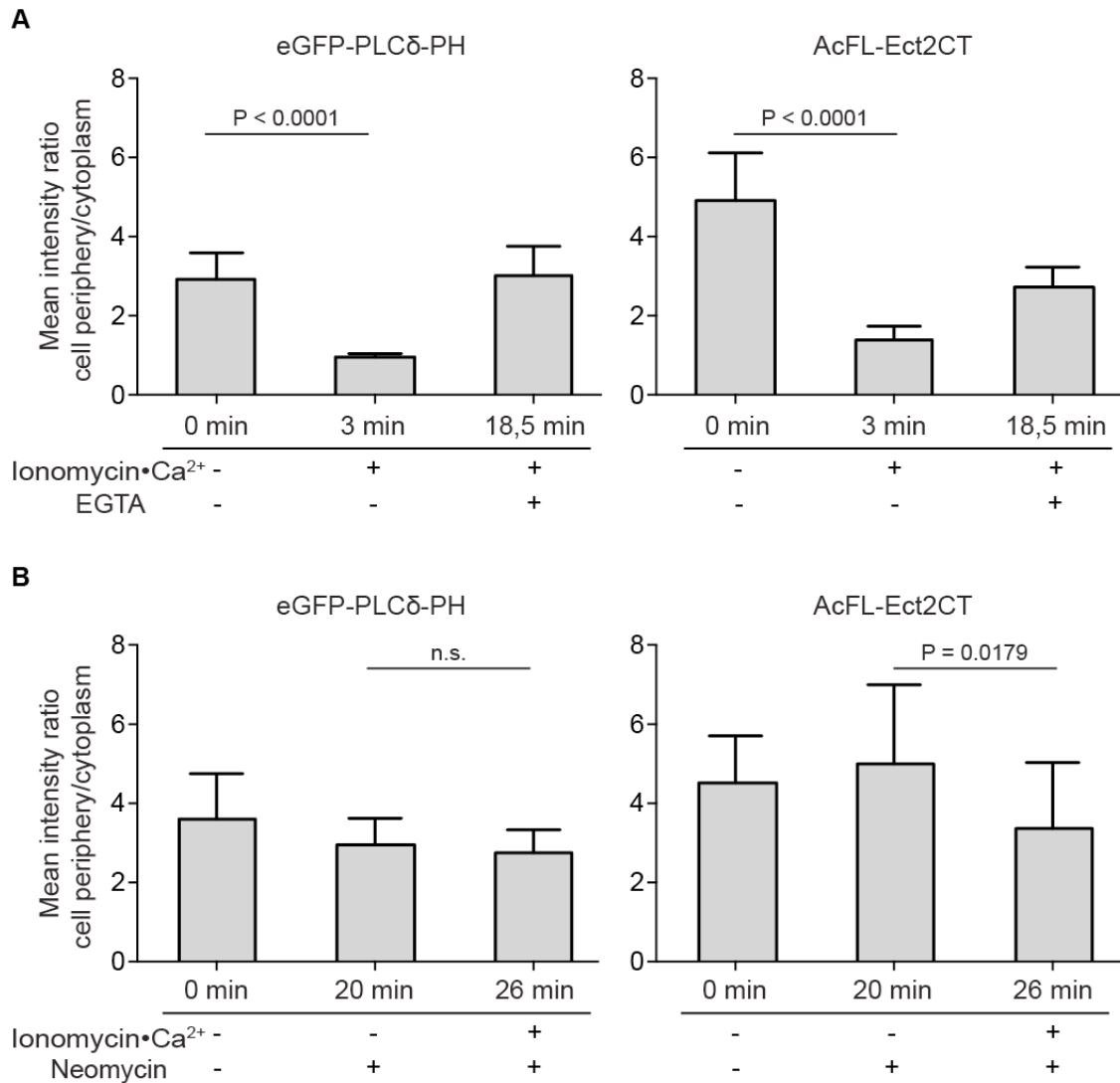


Figure 13 Analysis of Ect2CT membrane localization after ionomycin•Ca²⁺ treatment

A Quantification of Ect2CT localization to the plasma membrane after ionomycin•Ca²⁺ treatment (Figure 12B and C). Graph shows the ratio of the GFP fluorescence signal at the cell periphery and in the cytoplasm for PLC δ -PH and Ect2CT, which were measured as shown in Figure 11. ($n > 10$, bars represent mean \pm SD, Student's t-test)

B Quantification of Ect2CT localization to the plasma membrane after ionomycin•Ca²⁺ addition including the neomycin pre-treatment. Graph shows the ratio of the GFP fluorescence signal at the cell periphery and in the cytoplasm for PLC δ -PH and Ect2CT. ($n > 10$, bars represent mean \pm SD, Student's t-test)

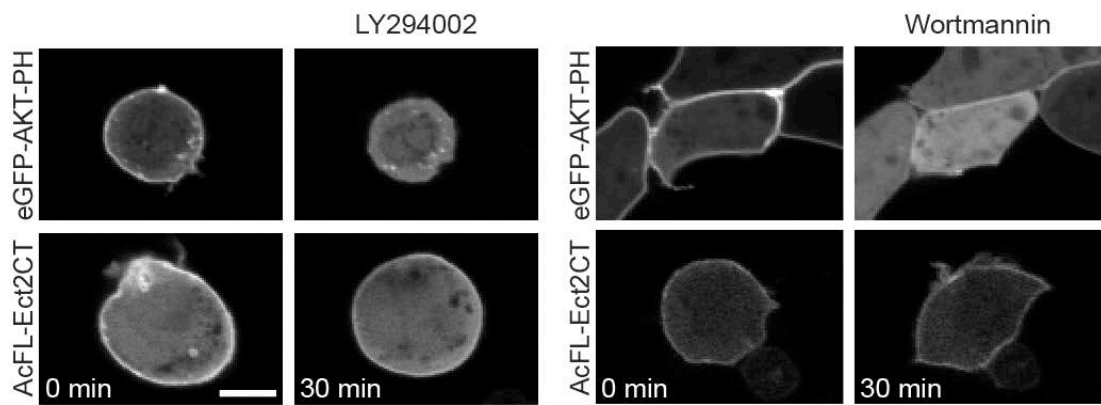


Figure 14 PI3Ks inhibitors do not affect membrane localization of Ect2

Confocal images of HEK-293T cells treated with PI3Ks inhibitors Ly294002 and wortmannin. Cells were transfected with plasmids encoding GFP-tagged Akt-PH and Ect2CT and treated with 25 μ M Ly294002 and 100 nM wortmannin 24 hours post transfection. t = 0 min was set to the frame prior to addition of inhibitors. Scale bar represents 10 μ m.

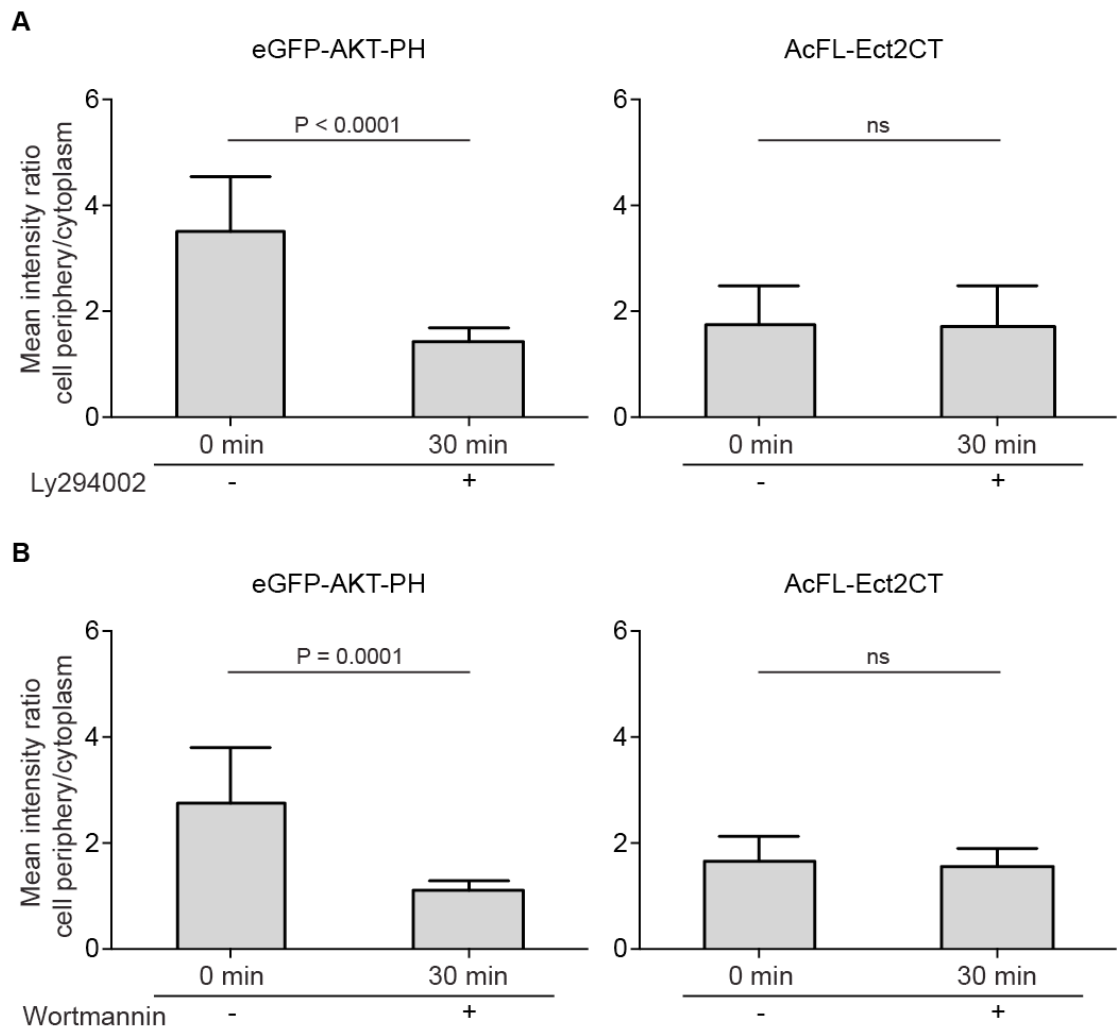


Figure 15 Analysis of Ect2CT membrane localization after treatment with PI3Ks inhibitors

A Quantification of Ect2CT localization to the plasma membrane after Ly294002 treatment. Graph shows the ratio of the GFP fluorescence signal at the cell periphery and in the cytoplasm for Akt-PH and Ect2CT. (n = 10, bars represent mean \pm SD, Student's t-test)

B Quantification of Ect2CT localization to the plasma membrane after wortmannin treatment. Graph shows the ratio of the GFP fluorescence signal at the cell periphery and in the cytoplasm for Akt-PH and Ect2CT. (n = 10, bars represent mean \pm SD, Student's t-test)

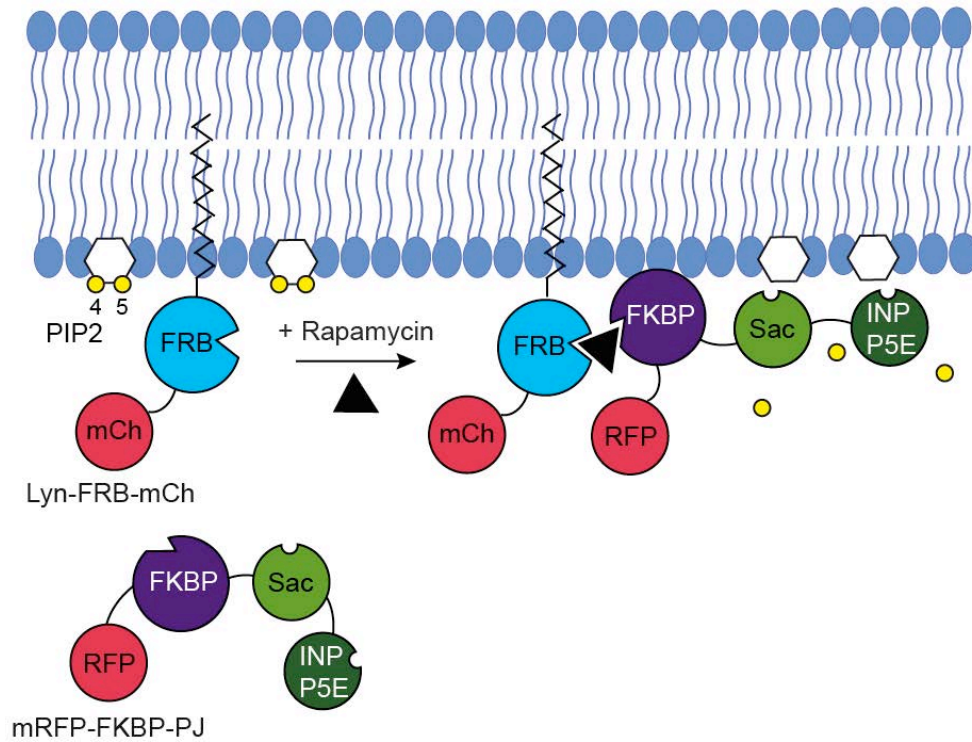


Figure 16 System of rapamycin-controlled hybrid phosphatases for specific depletion of phosphoinositides from the plasma membrane

Schematic representation of the hybrid phosphatase system based on rapamycin-induced dimerization of FRB and FKBP fragments (Hammond et al., 2012). Rapamycin binds to FKBP and triggers dimerization of FKBP protein with FRB fragment, which brings PJ to the plasma membrane. Sequential action of INPP5E and Sac converts PIP₂ to PI.

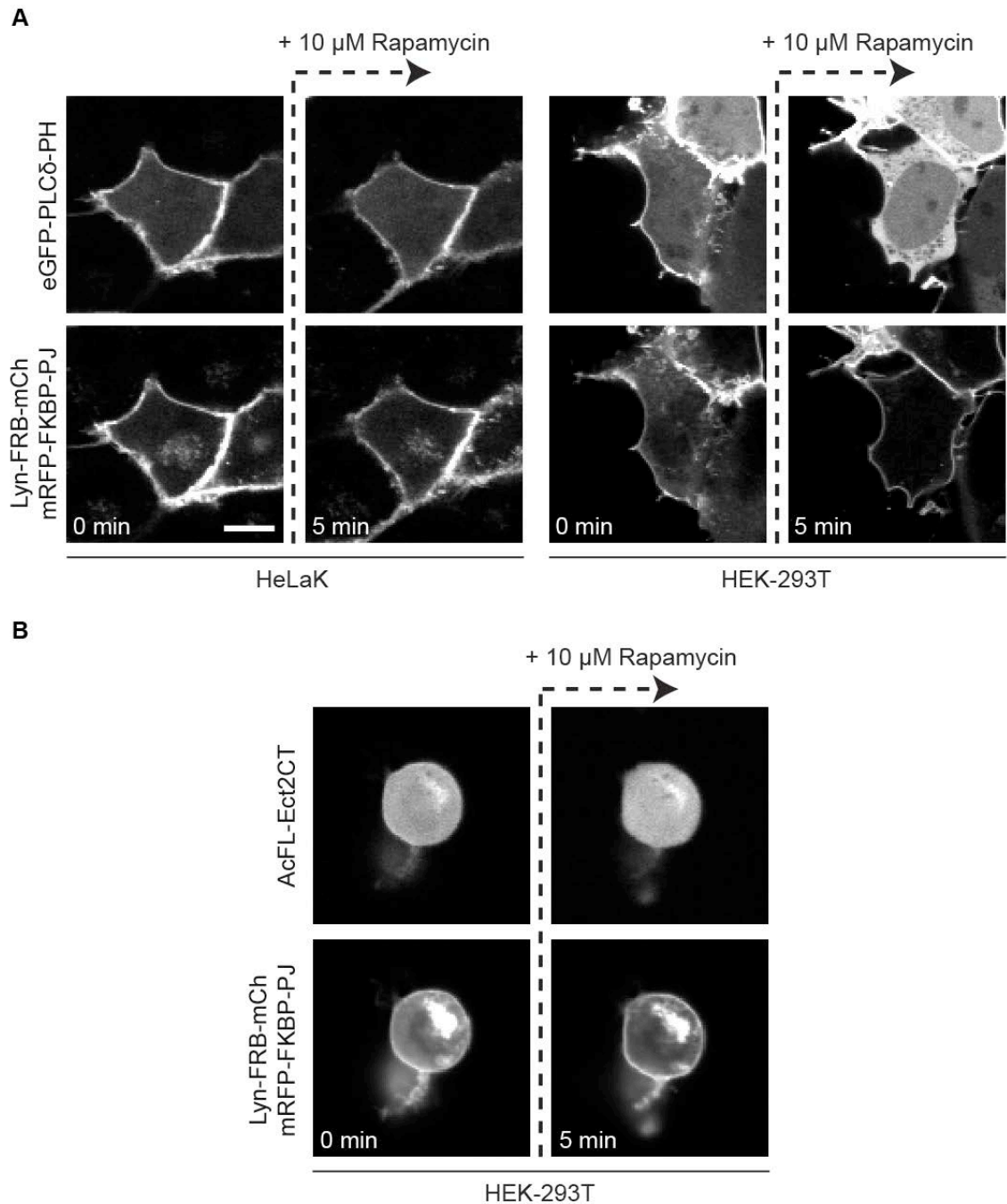


Figure 17 Action of rapamycin-controlled hybrid PJ phosphatase displaces PLC δ -PH from the plasma membrane in HEK-293T but not HeLaK cells

A Confocal images of HeLaK cells (left panels) and HEK-293T cells (right panels) treated with rapamycin. Both cell lines were co-transfected with eGFP-PLC δ -PH, Lyn-FRB-mCh and mRFP-FKBP-PJ. Cells were imaged after treatment with 10 μ M rapamycin 48 hours post transfection. t = 0 min was set to the frame prior to rapamycin treatment. Scale bar represents 10 μ m.

B Confocal images of HEK-293T cells transfected with AcFL-Ect2CT, Lyn-FRB-mCh and mRFP-FKBP-PJ. Cells were treated with 10 μ M rapamycin 48 hours post transfection.

Chapter 4. Results 2 - Using hybrid proteins and chemical genetic system to artificially target Ect2 to the plasma membrane

Previous work in our laboratory has demonstrated that Ect2 protein localizes to the plasma membrane shortly after anaphase onset. Ect2 membrane translocation is dependent on its pleckstrin homology (PH) domain and a cluster of basic amino acid residues (polybasic tail, PBC) located in the C-terminus of the protein (Su et al., 2011). An Ect2 version lacking both the PH domain and PBC in the C-terminal part of Ect2 (Ect2- Δ PH Δ Tail) is unable to support RhoA activation and cleavage furrow formation and ingression, which suggests that Ect2 membrane translocation could be an important step for cytokinesis in mammalian cells (Su et al., 2011). C-terminal deletion abrogates both the membrane localization and the furrow formation providing a correlative link between the two phenomena but not a causative relationship. Ect2- Δ PH Δ Tail construct lacks two hundred and fifty-two C-terminal amino acids, which raises the possibility that this drastic change can affect other functions of Ect2 than the membrane targeting. To decisively test whether the association of Ect2 with the plasma membrane is a prerequisite for cleavage furrow formation in human cells, we decided to set up a chemical genetic system that will allow us to artificially control the association of Ect2 with the plasma membrane. Such system will also allow us to probe the temporal requirement of Ect2-plasma membrane interaction during cell division and to test whether this interaction represents a rate-limiting step for the cleavage furrow formation.

4.1 Construction of the system for Ect2 plasma membrane artificial targeting

We started by generating a chemical genetic system based on hybrid proteins fused to the C1B domain from human protein kinase C α (PKC α) (Colon-Gonzalez and Kazanietz, 2006). This system was previously employed in our laboratory to investigate the importance of the plasma membrane binding of the Central spindle subunit MgcRacGAP (Lekomtsev et al., 2012). Typical C1 domains bind the

plasma membrane via interaction with diacylglycerol (DAG) or with phorbol esters, pharmacological mimetics of DAG. Thus proteins containing a C1B domain can be artificially targeted to the plasma membrane by addition of phorbol esters (Colon-Gonzalez and Kazanietz, 2006). To utilise this system, a chimeric Ect2 construct was generated in our laboratory by Kuan-Chung Su, in which the entire C-terminal part containing PH domain and PBC was removed and replaced with the C1B domain from human PKC α . The construct allows stable transgenic expression of the fluorescently tagged and siRNA-resistant Ect2-C1B hybrid protein in human cells (AcGFP-FLAG-Ect2r- Δ PH Δ Tail-C1B).

To obtain a negative control for our experiments, we sought to generate an Ect2-C1B hybrid construct carrying a point mutation in the C1B domain that abolishes the interaction with phorbol esters and consequently the plasma membrane localization of C1B. After a literature search, we decided to mutate two residues, proline in position 11 (P11G) and glutamine 27 (Q27G). Both residues are highly conserved in typical C1 domains from different proteins (Figure 18A), and both have been reported to significantly reduce phorbol ester binding when mutated (Colon-Gonzalez and Kazanietz, 2006) (Bogi et al., 1999). In order to test the effect of P11G and Q27G on membrane targeting of C1B independent of Ect2, we introduced the mutations separately into C1B domain tagged with AcGFP-FLAG (AcFL-C1B) and the mutated C1B constructs were transiently expressed in HeLaK cells. Subsequently, the phorbol ester 12-O-Tetradecanoylphorbol-13-acetate (TPA) was added to cells while protein localization was tracked by fluorescence confocal microscopy (Figure 18B). WT version of C1B domain translocated to the plasma membrane in less than 10 min. In striking contrast, both mutations abolished or greatly reduced recruitment of the reporter protein to the cell periphery. In cells expressing the P11G mutant of C1B domain we could still observe weak plasma membrane localization, while the Q27G mutation appeared to completely inhibit the membrane localization so we focused on Q27G mutation (Figure 18B). Image analysis over time revealed that the WT C1B domain quantitatively translocated to the plasma membrane within 5 minutes after 1 μ M TPA addition (Figure 19). The enrichment of C1B domain at the plasma membrane was completely abolished by the Q27G mutation confirming that this alteration indeed prevents the phorbol ester-induced targeting of C1B domain to the membrane (Figure 19). Our work has

identified the C1B^{Q27G} as a suitable negative control for artificial membrane recruitment experiments using Ect2-C1B hybrid proteins. Therefore we cloned the construct for expression of AcGFP-FLAG-Ect2r- Δ PH Δ Tail-C1B^{Q27G} in human cells (Figure 20). For simplicity, we will refer to the constructs and proteins AcGFP-FLAG-Ect2r- Δ PH Δ Tail-C1B and AcGFP-FLAG-Ect2r- Δ PH Δ Tail-C1B^{Q27G} as Ect2-C1B and Ect2-C1B^{Q27G} respectively.

In order to assess the importance of Ect2 membrane targeting, we generated cell lines stably expressing either WT or Q27G mutant hybrid Ect2-C1B protein. The Q27G hybrid Ect2 protein was expressed at similar level as the WT hybrid (Figure 20B). For both C1B hybrid transgenic proteins, the expression level was higher than that of endogenous Ect2 and the transgenic full-length Ect2 protein. The phenomenon that Ect2 alleles lacking the C-terminal part are expressed at a higher level was observed previously in our laboratory (Su et al., 2011). The effect of the siRNA-induced endogenous Ect2 depletion is not easily visible on the WB of hybrid proteins-expressing cells, as both the endogenous Ect2 and the hybrids have the same electrophoretic mobility. However, the strong efficacy of the siRNA depletion is easily seen in control cell lines (AcFL and AcFL-Ect2r) (Figure 20B). We completed our set with cell lines generated previously (Su et al., 2011), expressing the AcFL-tag only (AcFL), the full-length version of Ect2 (AcFL-Ect2r) and the truncated Ect2 protein without PH domain and polybasic tail (AcFL-Ect2r- Δ PH Δ Tail). All transgenes contain an N-terminal AcGFP-FLAG tag to track the transgenic proteins in cellular and biochemical assays and they are resistant to Ect2 siRNA due to introduction of synonymous mutations in the siRNA binding site (Su et al., 2011). The domain structure of all proteins used in subsequent experiments is depicted in Figure 20A.

Next, we tested whether the hybrid Ect2-C1B protein expressed in the stable transgenic cell lines were capable of plasma membrane localization after TPA treatment. Upon addition of TPA, we observed a rapid (within 1 min) translocation of the Ect2-C1B hybrid protein to the plasma membrane in anaphase cells (Figure 21). Conversely, the Ect2-C1B^{Q27G} hybrid protein failed to accumulate at the cell periphery. In both hybrid proteins the localization to the spindle midzone, which is mediated by Ect2's N-terminal BRCT repeats (Somers and Saint, 2003) (Yuce et

al., 2005) was maintained upon TPA addition. Thus, we have succeeded in setting up an experimental system based on C1B-hybrid proteins and TPA phorbol ester treatment that will allow us to artificially induce and temporally modulate the plasma membrane recruitment of Ect2 during cell division.

4.2 Artificial plasma membrane targeting of Ect2 can bypass the requirement for the protein's PH domain and PBC

In order to first assess whether TPA addition can restore cytokinesis in hybrid cell lines and to determine the optimal phorbol ester concentration for the rescue experiments, we depleted endogenous Ect2 in the Ect2-C1B cell line and six hours later added increasing concentrations of TPA ranging from 1 nM to 1 μ M. Two days after siRNA transfection the cells were fixed and analysed by immunofluorescence (IF) microscopy. As a readout for successful or failed cytokinesis, we quantified the percentage of multi-nucleated cells (Figure 22A). Interestingly, we observed a significant decrease in the level of multi-nucleation in TPA-treated cells. 77% of DMSO-treated cells were multinucleated. TPA addition lowered the multi-nucleation level to 32% (10 nM TPA) and 38% (100 nM TPA). This first observation raised the possibility that artificial recruitment of Ect2-C1B hybrid protein can restore cytokinesis in the absence of Ect2's native membrane engagement domains. For subsequent in-depth experiments we decided to use the concentration of 10 nM TPA.

In order to exclude that the TPA treatment is affecting cytokinesis by lowering the effectivity of the Ect2 siRNA depletion, we examined the protein levels of the Ect2 hybrids with or without TPA treatment. WB analysis showed that TPA addition did not change the expression levels of Ect2 hybrid proteins (Figure 22B). Unfortunately, the same electrophoretic mobility of the Ect2 hybrid proteins and endogenous Ect2 complicated the analysis for the endogenous protein, but there was no obvious difference in expression levels between DMSO and TPA treatment in Ect2 siRNA treated cells (Figure 22B). Furthermore, we observed only a minor reduction in cytokinesis failure upon depletion of endogenous Ect2 in a cell line expressing only the AcFL tag after addition of TPA (Figure 23).

Using the setup described above, we conducted rescue experiments with artificial membrane targeting of Ect2. We assessed the results using IF staining and measuring the level of multi-nucleation (Figure 23). All cell lines showed a background level of multi-nucleation, characteristic for HeLaK cells transfected with non-targeting control siRNA (NTC) (Figure 23B). Depletion of endogenous Ect2 in cell expressing only the AcFL tag caused a dramatic cytokinetic defect resulting in high multi-nucleation levels. As published previously, expression of the full-length wild type Ect2 transgene was able to fully complement the loss of the endogenous protein (Su et al., 2011). Removal of the PH domain and PBC (AcFL-Ect2r- Δ PH Δ Tail) abrogated this rescue activity. Addition of TPA did not strongly affect the observed phenotypes for the above transgenic cell lines when compared to addition of the solvent control (DMSO). We calculated the difference in multi-nucleation levels between DMSO and TPA treated cells and we subtracted the background level of multinucleation obtained from cells transfected with control siRNA. We observed that TPA treatment caused a small reduction in the level of multi-nucleation in control cell lines, 18% for tag-only cells, 17% for AcFL-Ect2r- Δ PH Δ Tail and 19% for cells expressing Ect2-C1B^{Q27G}. This minor reduction was very similar between the different control cell lines and we propose this is caused by extension of the cell cycle time by TPA treatment and this issue is addressed in subsequent experiments (Figure 24 and Figure 25). Strikingly, TPA addition considerably suppressed cytokinetic failure in cells expressing the hybrid Ect2-C1B protein with 53% drop in multi-nucleation levels (Figure 23B). Importantly, TPA addition had no effect on the multi-nucleation score in the cell line expressing Ect2-C1B^{Q27G} when compared to the cells expressing the same transgene without the C1B domain (AcFL-Ect2r- Δ PH Δ Tail).

To further establish that artificial membrane targeting of Ect2-C1B can complement the role that PH domain and PBC play during cytokinesis, we examined the rescue effect using live-cell imaging (Figure 24 and Figure 25). The results confirmed that TPA-induced membrane targeting of Ect2 could partially rescue cytokinetic defects after endogenous Ect2 depletion. Notably, more than 60% of cell expressing Ect2-C1B successfully divided, while close to 100% of Ect2-C1B^{Q27G} expressing cells failed cell division. The live-cell imaging experimental setup proved to be more suitable than the end-point IF analysis, as we could focus only on the cells that

undergo cell division. Live-cell imaging analysis thus eliminated the small difference in multi-nucleation levels between DMSO and TPA-treated control cell lines, detected by IF analysis (Figure 23B). Examples of TPA-treated cells undergoing cytokinesis are shown in Figure 24. Collectively, these results suggest that TPA-induced targeting of Ect2 hybrids can partially restore cytokinesis in the absence of Ect2's native membrane engagement domains when TPA is added in a long-term fashion to asynchronously growing cells.

Normally, Ect2 localizes to the plasma membrane only shortly after anaphase onset (Su et al., 2011). In order to replicate this temporal regulation, we targeted Ect2 to the plasma membrane specifically at the metaphase-to-anaphase transition using a previously described synchronisation protocol (Petronczki et al., 2007). Cells depleted for endogenous Ect2 were arrested in metaphase by addition of proteasome inhibitor MG132, released from the block and forty-five minutes later DMSO as a control or 10 nM TPA was added to the cell medium and cells going through division were imaged. Notably, 50% of the cells expressing Ect2-C1B successfully divided after TPA addition, while 99% of cells expressing Ect2-C1B^{Q27G} failed to divide (Figure 26). These data formally demonstrate that Ect2's localization to the plasma membrane is essential and sufficient for cytokinesis from metaphase onwards, even though it possibly only plays a role after anaphase onset.

4.3 Artificial targeting of Ect2's GEF domain alone to the plasma membrane cannot support cytokinesis

The GEF domain is the catalytic domain of Ect2, which exerts the nucleotide exchange activity on RhoA and thus promotes cleavage furrow formation (Tatsumoto et al., 1999) (Prokopenko et al., 1999) (Su et al., 2011). Therefore, we decided to determine if targeting of only the GEF domain to the plasma membrane is sufficient to rescue cytokinesis. This experiment addresses whether the only key functions of Ect2 during cytokinesis are the GEF activity and the plasma membrane engagement. To this end we prepared a monoclonal stable cell line expressing the construct only covering the GEF domain of Ect2 fused to C1B domain (GEF-C1B) (Figure 27) and tested its TPA-induced membrane targeting, which we followed by

fluorescence microscopy (Figure 28). Notably, GEF-C1B translocation to the plasma membrane was more effective than that of the Ect2-C1B hybrid, likely as a result of the increased mobility of the smaller protein and due to higher expression level of GEF-C1B protein (Figure 27B). Afterwards, we repeated the rescue experiments with the GEF-C1B cell line. Importantly, artificial membrane targeting of the GEF domain alone did not complement for the loss of endogenous Ect2 like the Ect2-C1B hybrid (Figure 29). We tested several TPA concentrations to prevent cytokinesis failure due to an overactivation of RhoA and hypercontractility of the cortex but obtained no rescue activity using the GEF-C1B fusion protein (Figure 30). This result indicates that the N-terminal part of Ect2 plays an important role in the cleavage furrow formation, and while the GEF activity of Ect2 is essential (Prokopenko et al., 1999) (Tatsumoto et al., 1999) (Somers and Saint, 2003) (Yuce et al., 2005) (Su et al., 2011), it is not sufficient to target only the GEF domain to the plasma membrane for successful cytokinesis progression. One caveat of the above experiments is that rescue activity of the GEF-C1B hybrid may be masked by hyperactivation of RhoA due to higher expression of the construct.

4.3 Precocious artificial membrane targeting of Ect2

We have shown that the interaction of Ect2 with the plasma membrane is indispensable function for cytokinesis in human cells. During cytokinesis Ect2's translocation to the plasma membrane occurs at the time of anaphase onset when Cdk1 activity declines (Su et al., 2011). Having established a system for Ect2 artificial membrane targeting, we sought next to determine whether the interaction of Ect2 with the plasma membrane is a rate-limiting step for the timing of cleavage furrow formation. This experiments aimed at determining whether the only or main reason why cytokinesis is inhibited in metaphase cells is due to the inability of Ect2 to engage with the cell periphery. To this end we targeted Ect2 to the plasma membrane prematurely in metaphase and scored the cells for signs of contractility. During cytokinesis the active pool of RhoA, which drives the cleavage furrow formation, localizes to the equatorial part of the cell cortex (Piekny et al., 2005) (Bement et al., 2005). Anillin, a key scaffolding protein of the contractile ring, directly interacts with RhoA and stabilizes its cortical localization (Piekny and Glotzer, 2008) (Liu et al., 2012). In order to follow possible upregulation of

cytokinetic contractility after premature membrane targeting of Ect2, we analysed the cells for membrane enrichment of RhoA and Anillin.

We synchronized Ect2 hybrid cell lines in metaphase, treated them with DMSO or TPA and analysed them by immunofluorescence microscopy (Figure 31). Consistent with our previous results, we observed the Ect2-membrane interaction after TPA treatment in the case of Ect2-C1B and GEF-C1B hybrids, while no change in localization of Ect2-C1B^{Q27G} protein could be detected. To assess the plasma membrane enrichment of RhoA and Anillin after Ect2 membrane targeting, we quantified the ratio of fluorescence intensity on the cell periphery and in the cytoplasm for both proteins (Figure 32). Interestingly, we observed a small, but significant increase of RhoA and Anillin plasma membrane signal after Ect2-C1B membrane targeting. GEF-C1B TPA-induced translocation led to even more significant enrichment of RhoA and Anillin at the plasma membrane. GEF-C1B expressing cells also exhibited signs of hypercontractility with irregular shape of plasma membrane and membrane blebbing (Figure 31), a phenotype not observed after Ect2-C1B membrane targeting. This difference could be explained by the more efficient membrane translocation of the smaller GEF-C1B protein, but it may also suggest a negative regulatory role of the Ect2's N-terminus, missing in the GEF-C1B fusion protein, possibly resulting in uncontrolled RhoA activation. These results suggest that forcing Ect2 to localize at the plasma membrane in metaphase can increase the levels of downstream cortical cytokinetic regulators but does not result in precocious ectopic furrow formation.

4.4 Conclusions - Chemical genetic system to artificially target Ect2 to the plasma membrane

We developed a system for the artificial membrane targeting of Ect2 using fusion proteins with C1B domain from PKC α substituting the role of PH domain and polybasic tail present in endogenous Ect2. This system allows rapid, chemically induced membrane translocation of Ect2 by addition of phorbol esters (TPA) directly to the cell medium. We have generated a set of stable cell lines expressing various versions of the hybrid Ect2 proteins and used them to test the role and regulation of Ect2 association with the plasma membrane for cytokinesis.

In summary, the cells expressing Ect2 protein lacking PH domain and polybasic tail are unable to properly form the cleavage furrow and fail cytokinesis after depletion of the endogenous Ect2 protein. Importantly, these cytokinetic defects can be partially (50-60% efficiency) rescued by artificial membrane targeting of Ect2-C1B hybrid protein, which we have shown by end-point analysis of fixed cells as well as by live-cell imaging experiments. The rescue effect is dependent on the C1B interaction with TPA at the plasma membrane, as the Q27G mutation in C1B domain, which prevents phorbol ester recognition, also abolishes the rescue effect. Additionally, acute membrane targeting of Ect2 in synchronized cells entering anaphase can also rescue cytokinetic division, demonstrating that Ect2 membrane interaction is important only from metaphase onwards. These results unambiguously demonstrate that membrane localization of Ect2 is an essential, non-redundant step for the execution of cytokinesis in human cells. Thus, our observations combined with previous results using GEF domain point mutants (Prokopenko et al., 1999) (Su et al., 2011), firmly establish GEF activity and plasma membrane engagement as two key and indispensable properties of Ect2 for cytokinesis.

Artificial membrane targeting of Ect2 during the metaphase-to-anaphase transition was able to rescue cleavage furrow formation to the same extent as chronic treatment with the phorbol ester. This result strongly suggests that the interaction of Ect2 with the plasma membrane is only required from metaphase onwards, and possibly only after anaphase onset, when the interaction normally occurs (Su et al., 2011). It has been previously shown that Ect2 activity is required for the establishment of a stiff mitotic cell cortex and timely mitotic cell rounding (Matthews et al., 2012) (Kunda and Baum, 2009). Our acute TPA-induced Ect2-C1B targeting experiments showed that mitotic cell rounding and the establishment of a stiff mitotic cortex do not require Ect2 interaction with the plasma membrane.

Interestingly, we found that the GEF-C1B fusion protein was unable to complement the role of endogenous Ect2 causing GEF-C1B expressing cells to fail cytokinesis after depletion of endogenous Ect2, despite efficient TPA-induced membrane targeting. On the other hand, premature targeting of GEF-C1B in metaphase cells shows signs of RhoA overactivation. Taken together, these results suggest a

crucial regulatory role of the N-terminal part of the Ect2 protein. Previous observations in human cells and echinoderm embryos suggest that massive delocalized RhoA hyperactivation by expression of Ect2CT can block cleavage furrow ingression (Su et al., 2011) (Su et al., 2014). Thus, the cytokinetic rescue activity of the GEF-C1B fusion protein upon TPA addition may be masked by RhoA hyperactivation. However, arguing against this possibility is the fact that we were unable to detect cytokinetic rescue activity even at much reduced concentrations of TPA.

Finally, precocious targeting of Ect2-C1B in metaphase leads to a slight enrichment of RhoA and Anillin localization at the plasma membrane, but does not cause cells to become hypercontractile. We conclude that Ect2 translocation to the plasma membrane might help regulate the timing of cytokinesis, but other temporal control mechanisms that restrain contractility in metaphase are likely to exist.

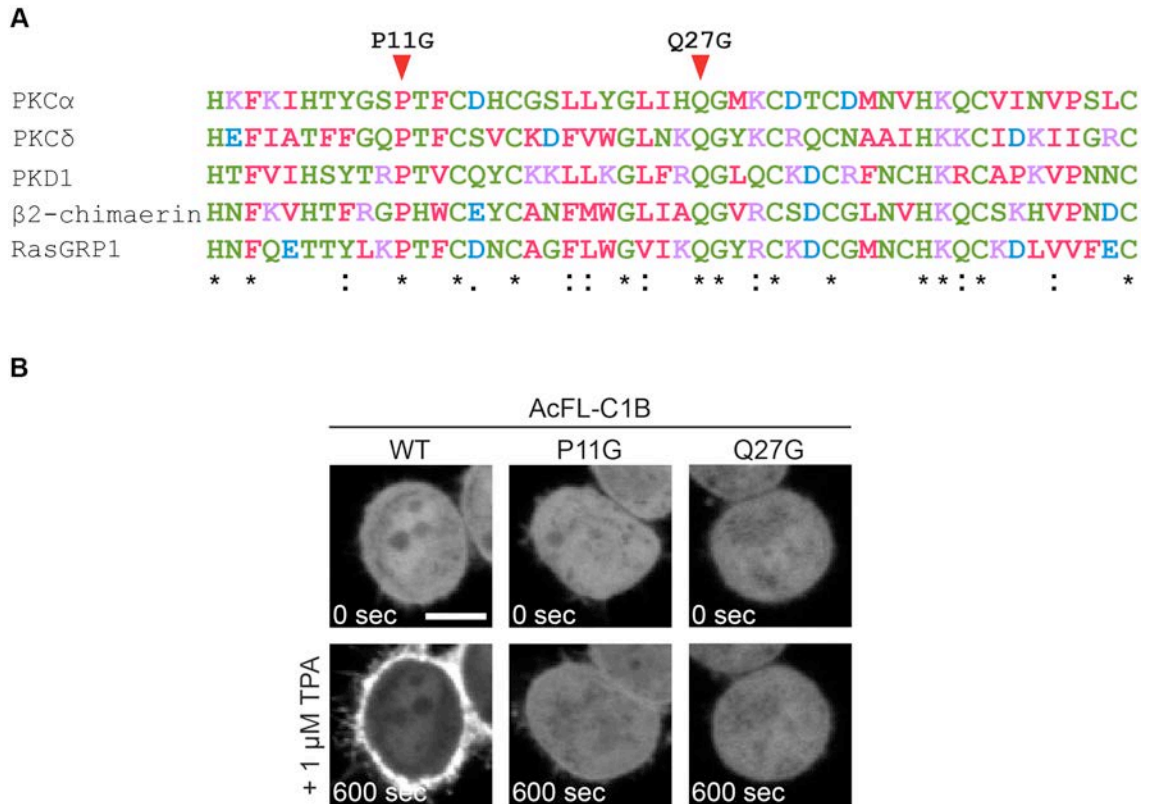


Figure 18 C1B domain mutations

A Sequence alignment of human C1 domains from indicated proteins. The first sequence belongs to the C1B domain from PKC α , which was used for construction of hybrid proteins. Highlighted are the residues, which were mutated to glycine.

B Stills from confocal imaging of HeLaK cells transiently transfected with GFP-tagged wild type or mutant C1B domains (AcFL-C1B). The cells were treated with 1 μ M TPA 48 hours after transfection. $t = 0$ sec is set to the frame prior to TPA addition. Scale bar represents 10 μ m.

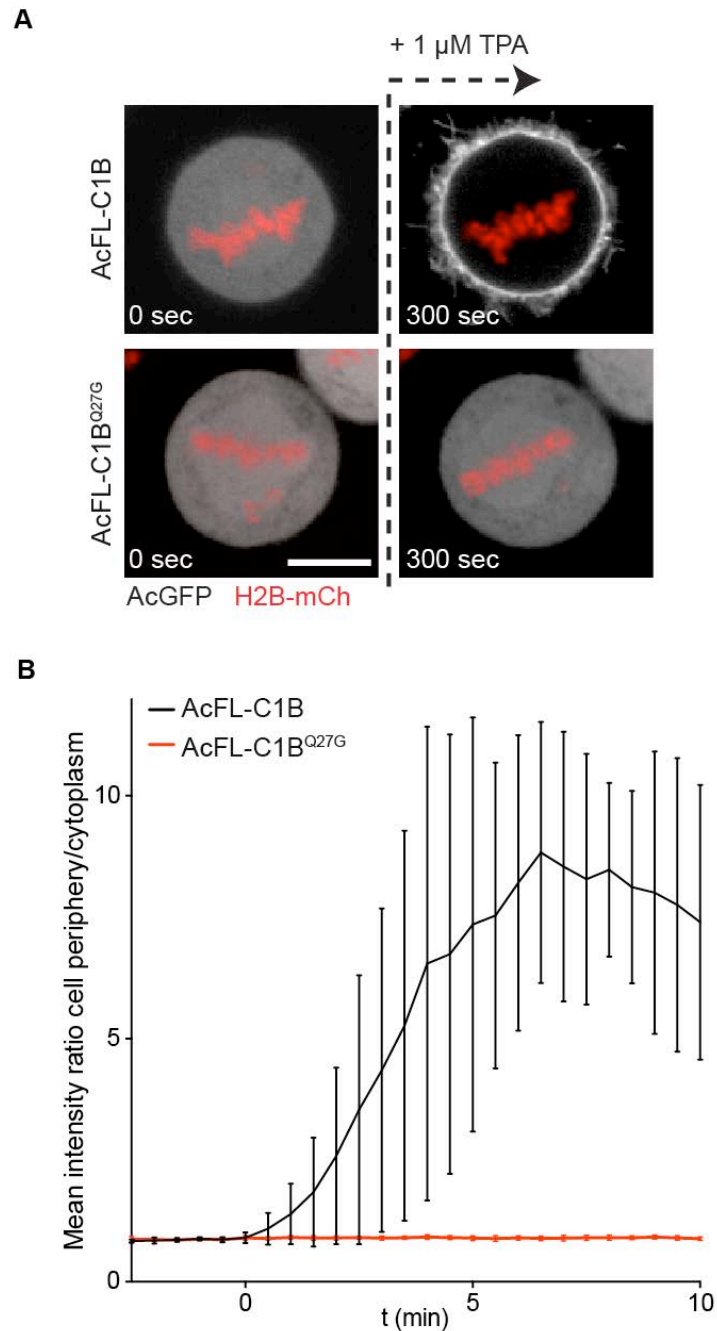


Figure 19 The mutation of Q27 abrogates TPA-induced membrane recruitment of the C1B domain

A Confocal images of the HeLaK cells transiently transfected with AcFL-C1B or AcFL-C1B^{Q27G} together with H2B-mCherry. Cells were treated with 1 μ M TPA 48 hours after transfection. $t = 0$ sec is set to the frame prior to TPA addition. Scale bar represents 10 μ m.

B Quantification of C1B domains translocation to the plasma membrane after the TPA treatment as shown in Figure 19A. Graph shows ratio of the GFP signal at the cell periphery and in the cytoplasm from -2.5 minutes to 10 minutes with $t = 0$ min set as the TPA addition time. ($n = 6$, bars represent mean \pm SD)

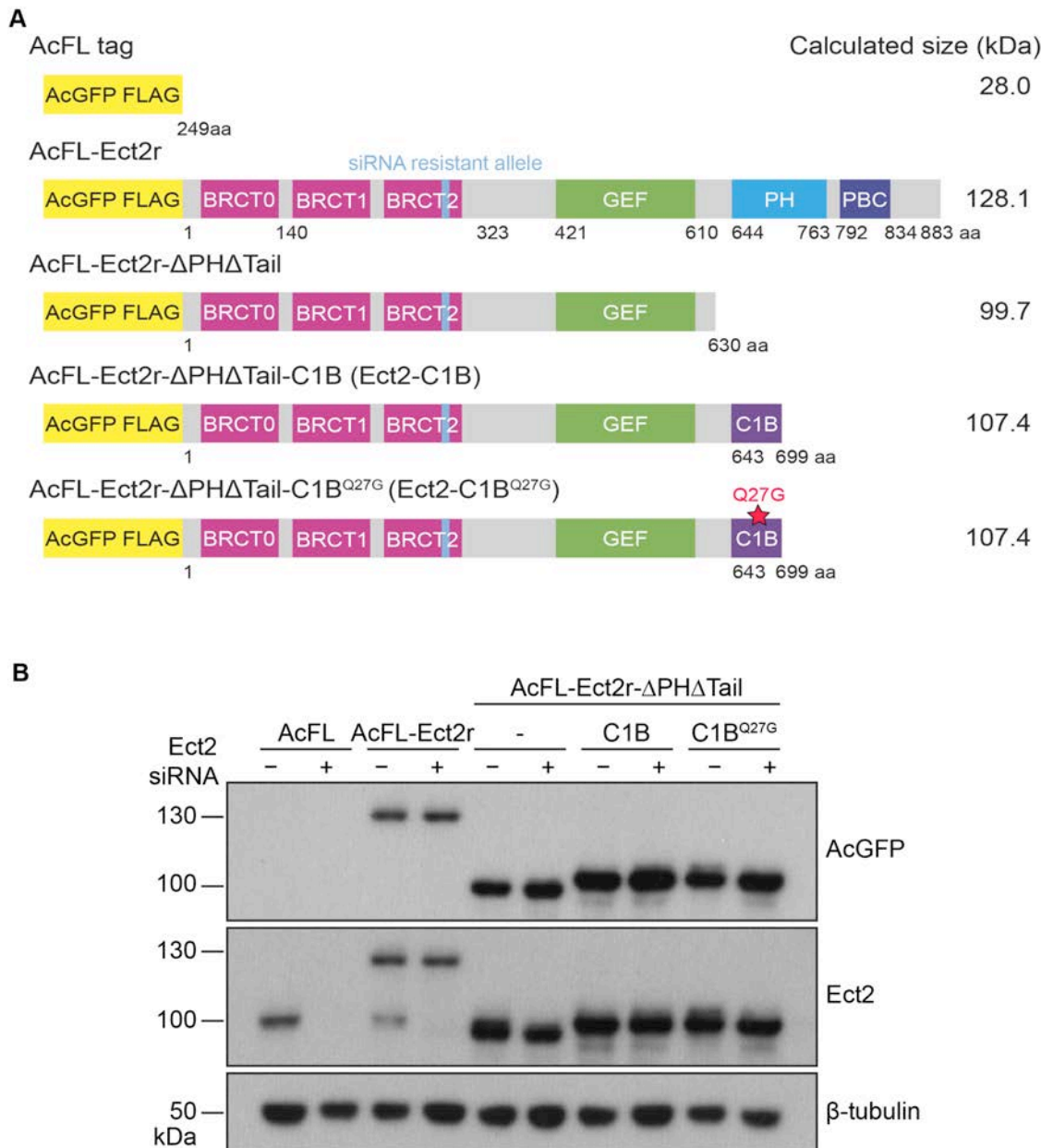


Figure 20 System for artificial membrane targeting of Ect2

A Schematic representation of the domain organization of different Ect2 constructs used to generate monoclonal HeLaK cell lines for testing the role of Ect2's interaction with the plasma membrane. Numbering of amino acid residues corresponds to their positions in human full-length Ect2 protein.

B Immunoblot analysis of protein lysates from the HeLaK cell lines stably expressing the proteins schematically depicted in panel A. Protein lysates were prepared 48 hours after transfection with NTC (-) or Ect2 siRNA (+). The immunoblot membrane was probed with antibodies directed against AcGFP, Ect2 and β -tubulin. All stable cell lines express the GFP-tagged transgenes in more than > 95% of the cell population.

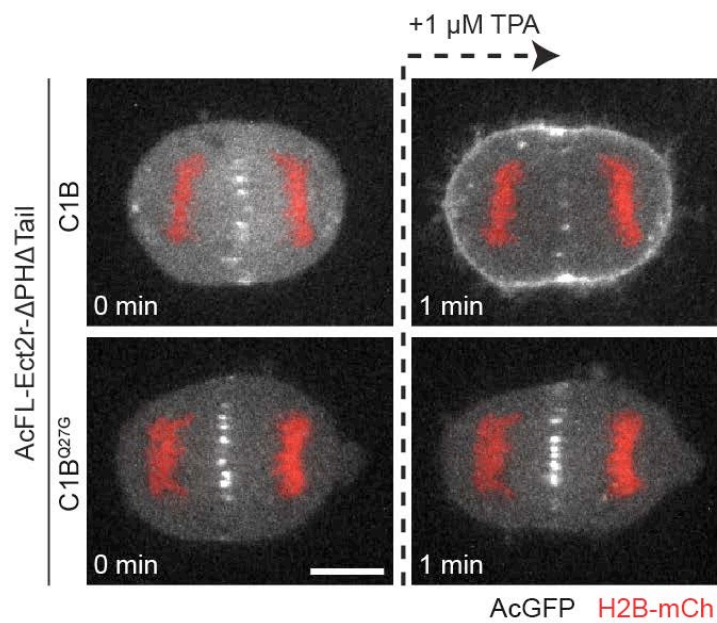


Figure 21 Membrane translocation of Ect2 hybrid proteins after TPA addition in anaphase

Confocal images from spinning disk confocal microscopy depicting the hybrid Ect2-C1B protein interacting with plasma membrane after the TPA treatment. Stable cell lines expressing AcGFP-FLAG-Ect2r- Δ PH Δ Tail-C1B (Ect2-C1B) or the Q27G-mutated version (Ect2-C1B^{Q27G}) were transiently transfected with H2B-mCherry. Cells were treated with 1 μ M TPA and imaged 48 hours after transfection. $t = 0$ min is set to the time of TPA addition. Scale bar represents 10 μ m.

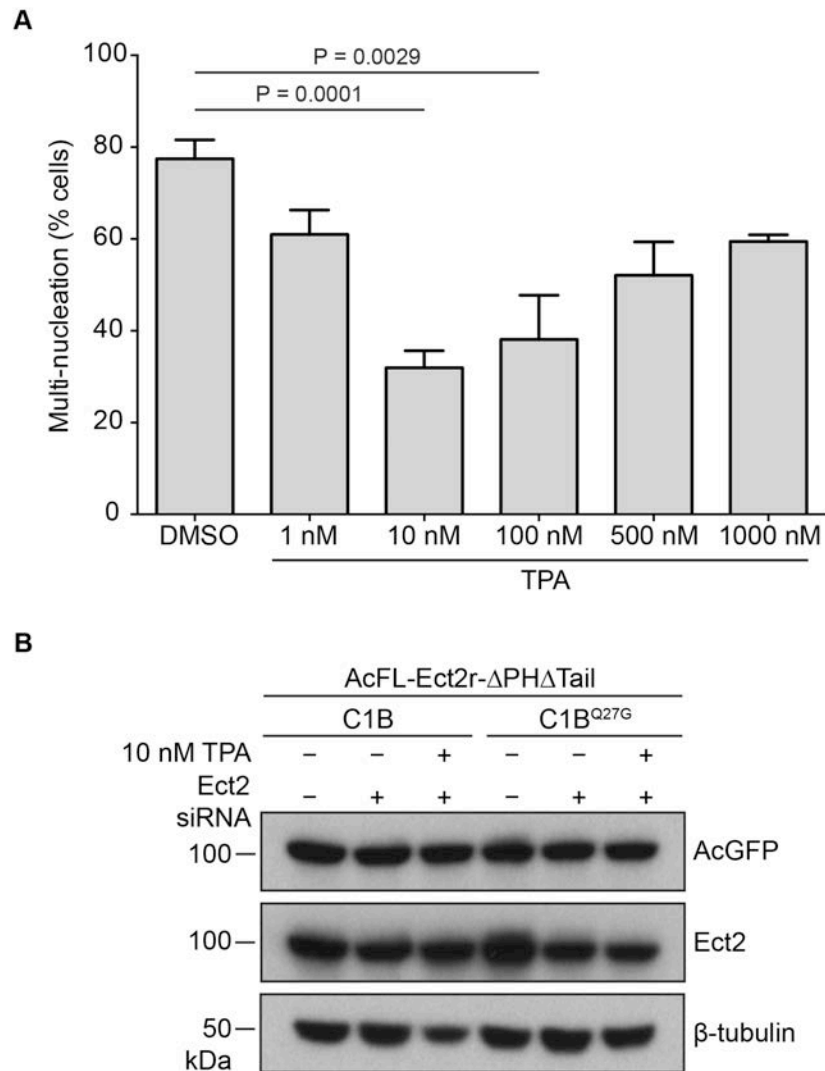


Figure 22 TPA concentration optimization

A Quantification of the percentage of multi-nucleated interphase cells. The stable cell line expressing Ect2-C1B was transfected with Ect2 siRNA. After 6 hours, the medium was changed and indicated concentrations of TPA or DMSO as a negative control were added. Cells were analysed by IF 48 hours after the siRNA transfection. (n > 300, bars represent mean \pm SD of three independent experiments, Student's t-test)

B Immunoblot analysis of cell lines stably expressing Ect2-C1B and Ect2-C1B^{Q27G} hybrid proteins. Protein lysates were prepared 48 hours after transfection with NTC (-) or Ect2 siRNA (+). 10 nM TPA (+) or DMSO (-) was added 6 hours post siRNA transfection. The immunoblot membrane was probed with antibodies directed against AcGFP, Ect2 and β -tubulin.

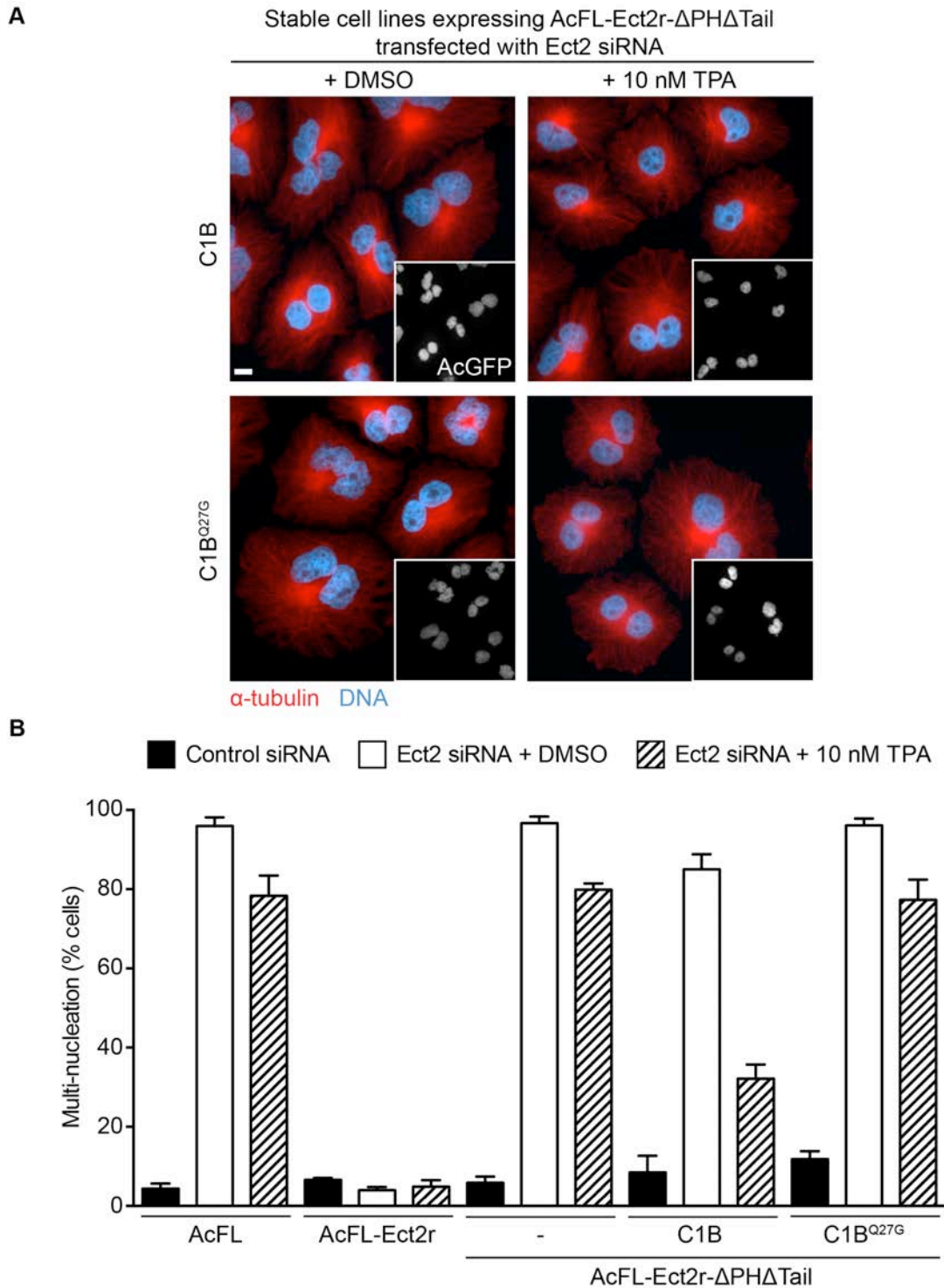


Figure 23 Analysis of cellular phenotype after artificial membrane targeting of Ect2

A IF analysis of Ect2-C1B and Ect2-C1B^{Q27G} hybrid proteins expressing cell lines. Cells were transfected with Ect2 siRNA. After 6 hours, the medium was changed and 10 nM TPA or DMSO was added. Cells were fixed and stained with antibodies directed against AcGFP, α -tubulin and with DAPI 48 hours after siRNA transfection. Scale bar represents 10 μ m.

B Quantification of multi-nucleation levels for rescue experiments with hybrid cell lines. Indicated cell lines were treated as described above (panel A). (n > 300, bars represent mean \pm SD of three independent experiments, Student's t-test).

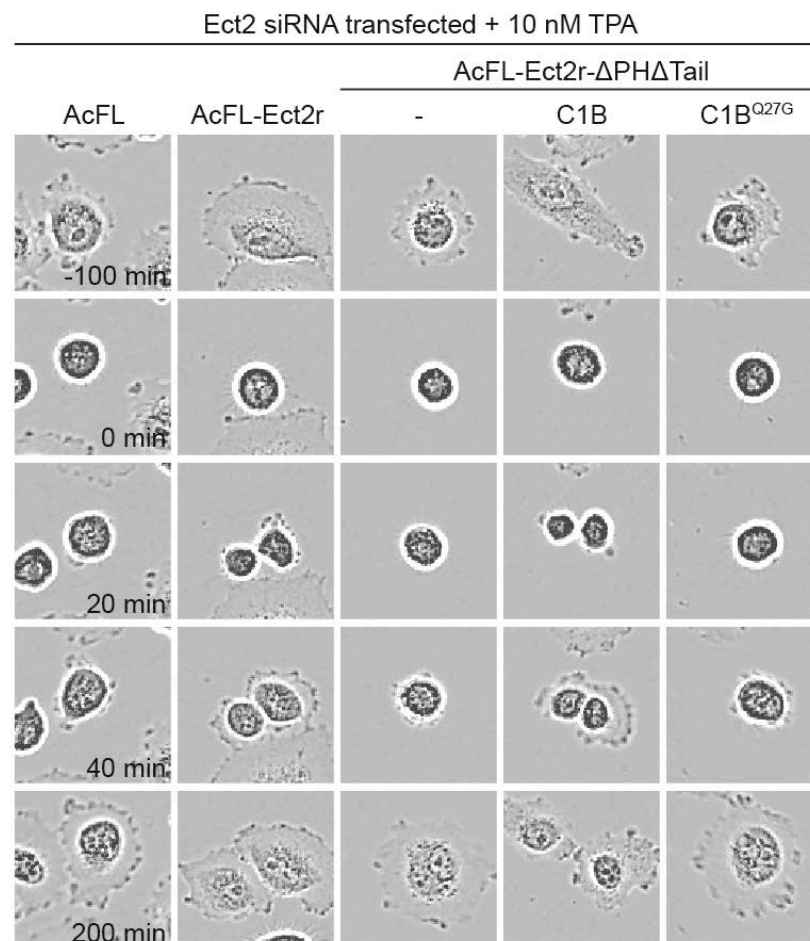


Figure 24 Live-cell imaging analysis of cytokinesis after artificial membrane targeting of Ect2

Representative images showing cytokinetic phenotypes for the whole set of cell lines (Figure 20A) after Ect2 siRNA transfection and TPA treatment. Cells were transfected with Ect2 siRNA and after 6 hours the medium was changed and 10 nM TPA was added. Cells were imaged with bright field microscopy starting 24 hours after siRNA transfection. Time point t = 0 min was set to metaphase to anaphase transition.

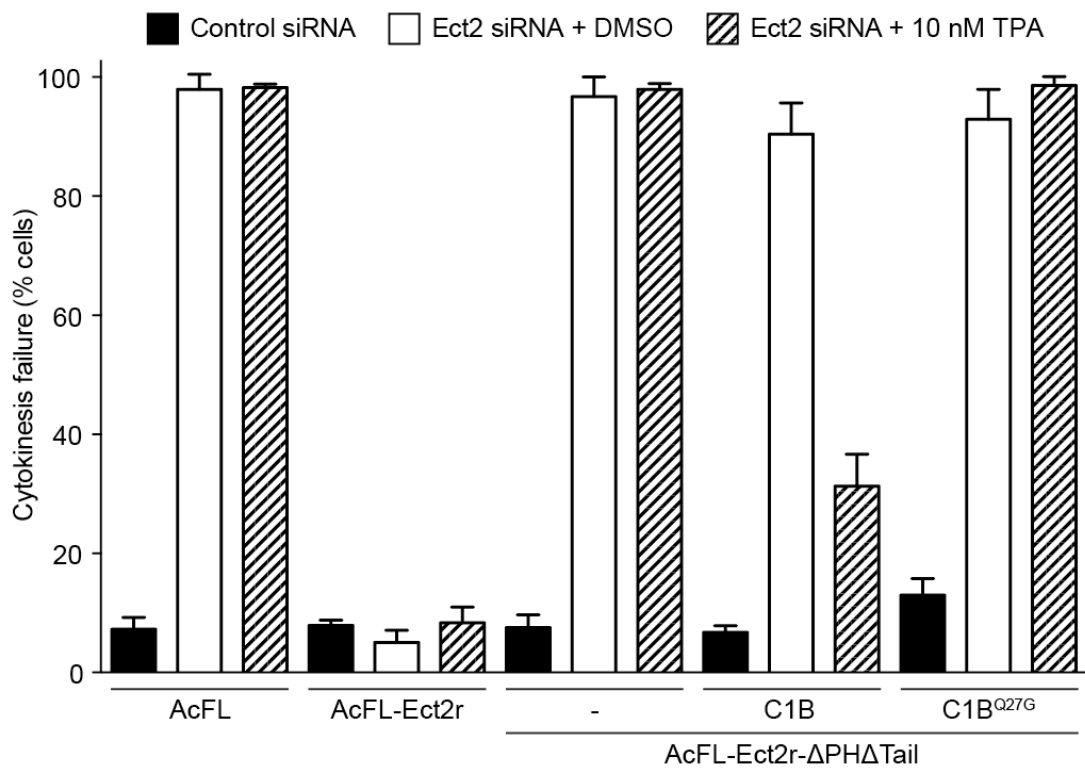
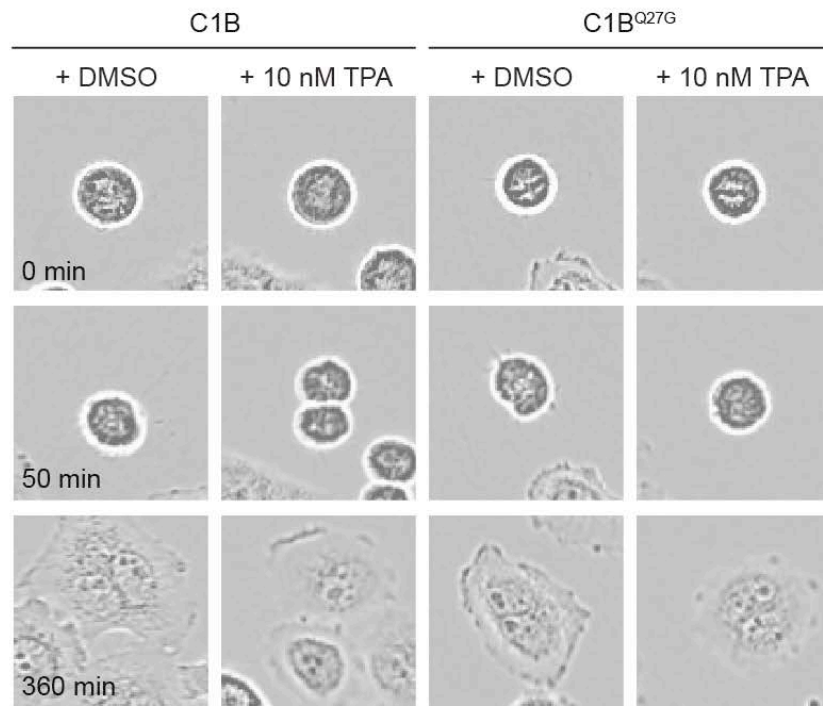


Figure 25 Live-cell imaging analysis of cytokinetic phenotype after artificial membrane targeting of Ect2 - quantification

Quantification of cytokinetic failure for Ect2 hybrid cell lines using live-cell imaging analysis. Indicated cell lines were treated as described above (Figure 24). Mono-nucleate cells undergoing cell division were scored from 24 to 72 hours post-transfection. ($n > 100$, bars represent mean \pm SD of three independent experiments).

A Stable cell lines expressing AcFL-Ect2r- Δ PH Δ Tail, transfected with Ect2 siRNA



B

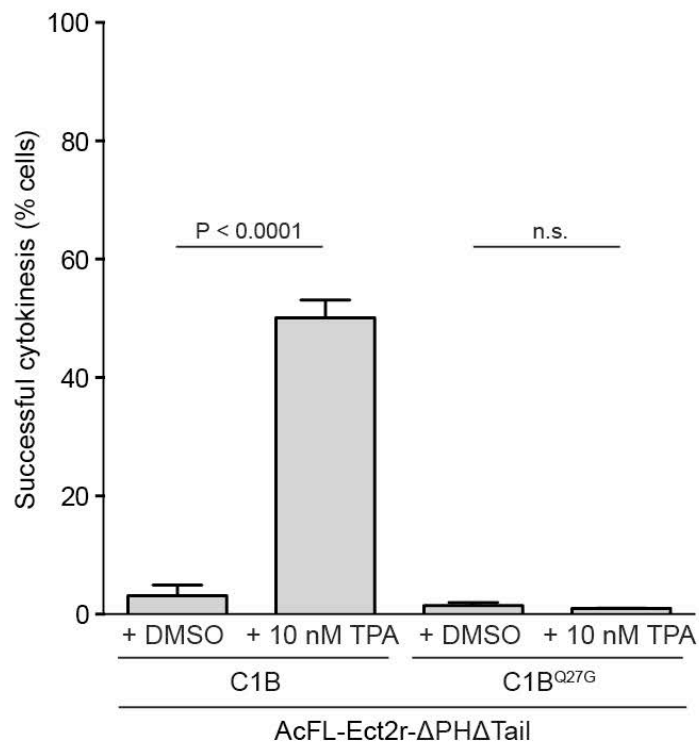


Figure 26 Live-cell imaging analysis of cytokinetic phenotype after artificial membrane targeting of Ect2 in anaphase

A Representative images showing cytokinetic phenotypes for Ect2-C1B and Ect2-C1B^{Q27G} hybrid stable cell lines. After Ect2 siRNA depletion, cells were synchronized in metaphase using previously described synchronization protocol (Petronczki et al., 2007). 45 minutes after release from the metaphase block, the

cells were treated with DMSO or 10 nM TPA and imaged with bright field microscopy right after. Time point $t = 0$ min was set to metaphase to anaphase transition.

B Quantification of cytokinetic phenotype after artificial membrane targeting of hybrid Ect2 proteins in anaphase. Time-lapse movies were obtained as described above (panel A). Mono-nucleated cells that were in metaphase at the beginning of the time-lapse imaging were scored. ($n > 200$, bars represent mean \pm SD of three independent experiments, Student's t-test).

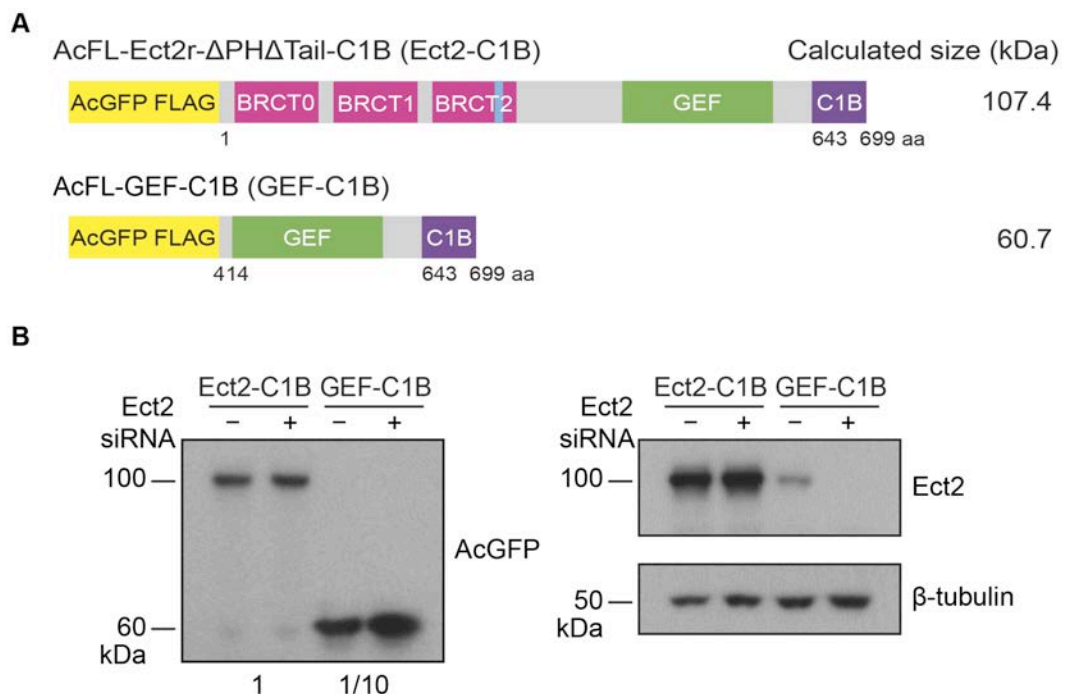


Figure 27 System for artificial membrane targeting of Ect2's GEF domain

A Schematic representation of the domain organization of the GEF domain only hybrid construct (GEF-C1B) and the Ect2-C1B construct. Numbering of amino acid residues corresponds to their positions in human full-length Ect2 protein.

B Immunoblot analysis of Ect2-C1B and GEF-C1B hybrid stable cell lines. Protein lysates were prepared 48 hours after transfection with NTC (-) or Ect2 siRNA (+). The immunoblot membrane was probed with antibodies directed against AcGFP, Ect2 and β -tubulin. For the GEF-C1B sample 1/10 of lysate was loaded for the blot probed against AcGFP.

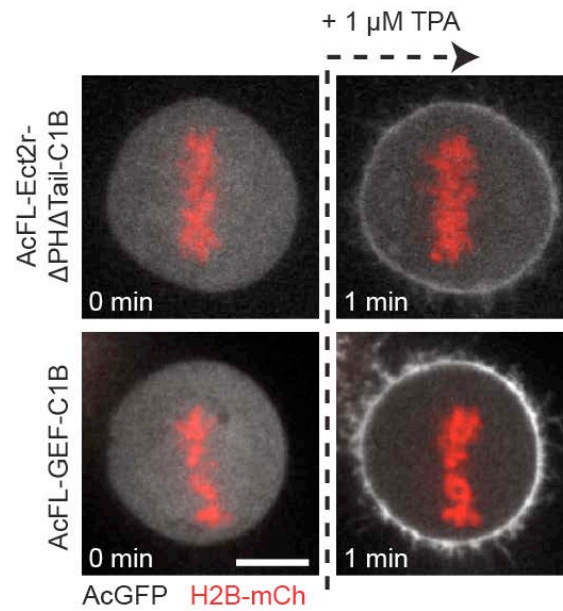


Figure 28 Membrane translocation of Ect2's GEF domain after TPA treatment
 Images from spinning disk confocal microscope depicting the hybrid GEF-C1B and Ect2-C1B proteins interacting with the plasma membrane after TPA treatment. Stable cell lines were transiently transfected with H2B-mCherry to visualise chromosomes. Cells were treated with 1 μ M TPA and imaged 48 hours after transfection. $t = 0$ min is set to the time of TPA addition. Scale bar represents 10 μ m.

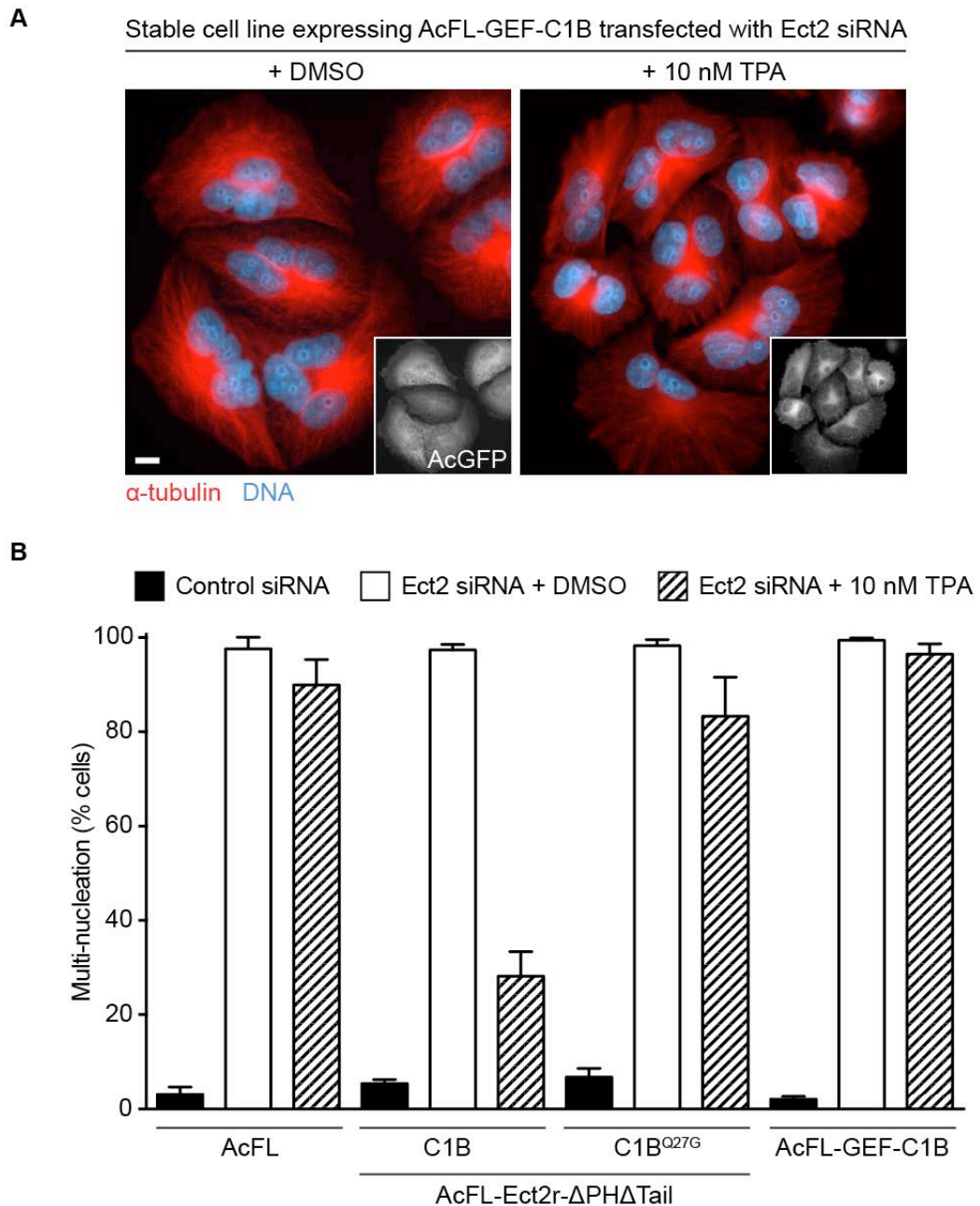


Figure 29 Analysis of cellular phenotype after artificial membrane targeting of GEF-C1B

A IF analysis of cells stably expressing GEF-C1B. Cells were transfected with Ect2 siRNA. After 6 hours, the medium was changed and 10 nM TPA or DMSO was added. Cells were fixed and stained with antibodies directed against AcGFP, α -tubulin and with DAPI 48 hours after siRNA transfection. Scale bar represents 10 μ m.

B Quantification of multi-nucleation levels for the GEF-C1B rescue experiment. Indicated cell lines were treated as described above (panel A). (n > 300, bars represent mean \pm SD of three independent experiments).

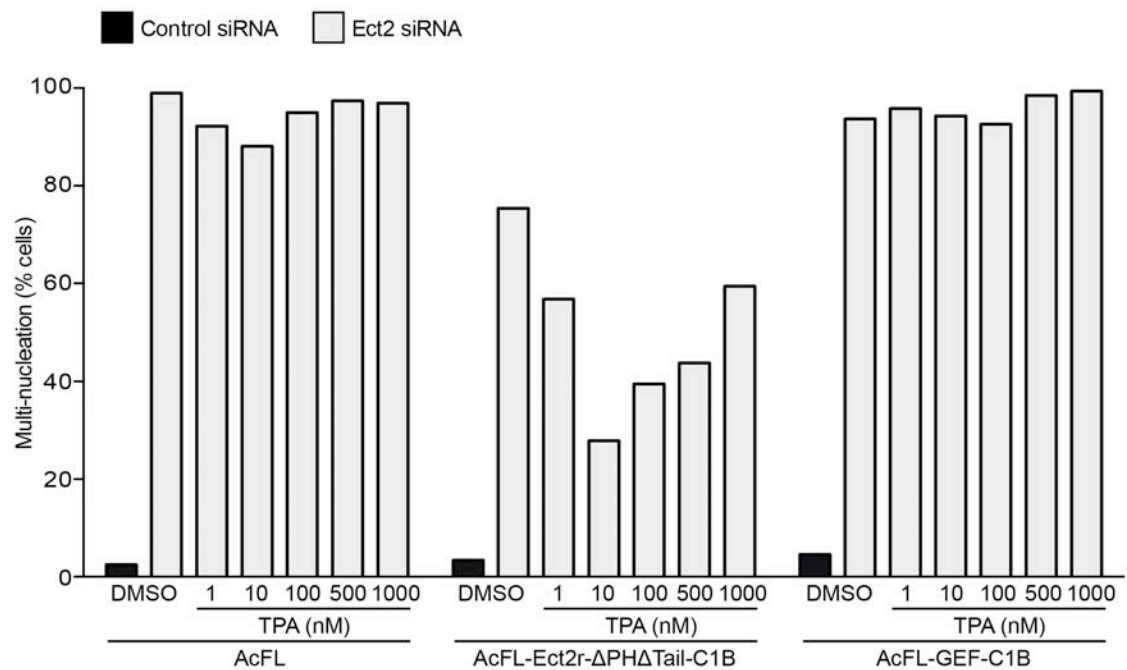


Figure 30 Analysis of cellular phenotype after artificial membrane targeting of GEF-C1B – various TPA concentrations

Quantification of multi-nucleation levels for the GEF-C1B rescue experiment. Cells were expressing AcFL tag, Ect2-C1B and GEF-C1B were transfected with control or Ect2 siRNA. After 6 hours, the medium was changed and DMSO or various TPA concentrations was added. (n > 300, bars represent values of one experiment).

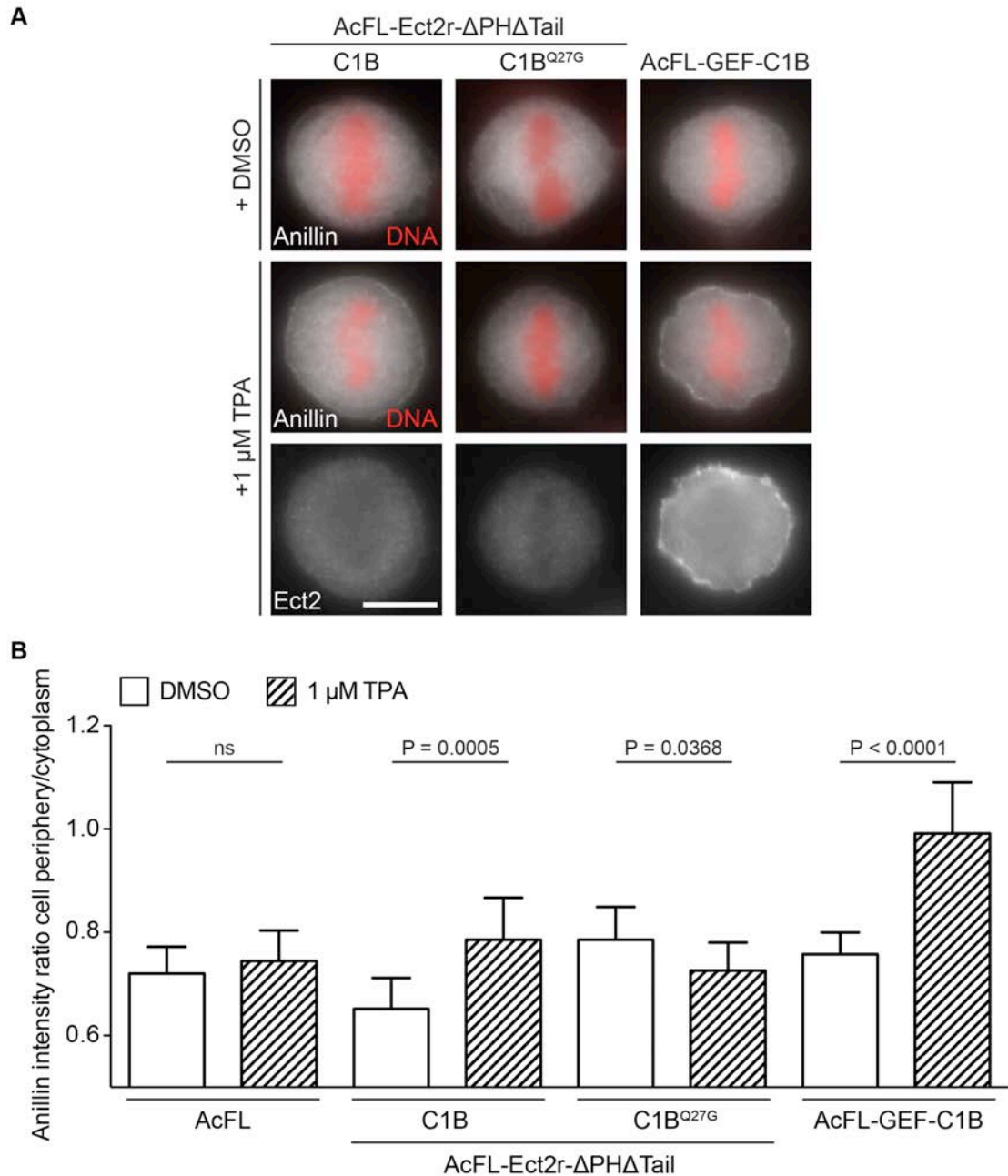


Figure 31 Precocious targeting of Ect2 in metaphase cells – Anillin

A IF analysis of Anillin in cell lines expressing Ect2 hybrid proteins treated with TPA in metaphase. Cells were treated with nocodazole for 4.5 hours to enrich the population of prometaphase cells. 1 hour after nocodazole washout the cells were treated with DMSO or 1 μ M TPA for 5 minutes. After the treatment, the cells were fixed and stained with antibodies directed against Anillin, together with AcGFP and DAPI for DNA. Scale bar represents 10 μ m.

B Quantification of Anillin enrichment at the plasma membrane after TPA treatment. Graph shows the ratio of the fluorescence signal at the cell periphery and in the cytoplasm for Anillin (n = 10, bars represent mean \pm SD, Student's t-test).

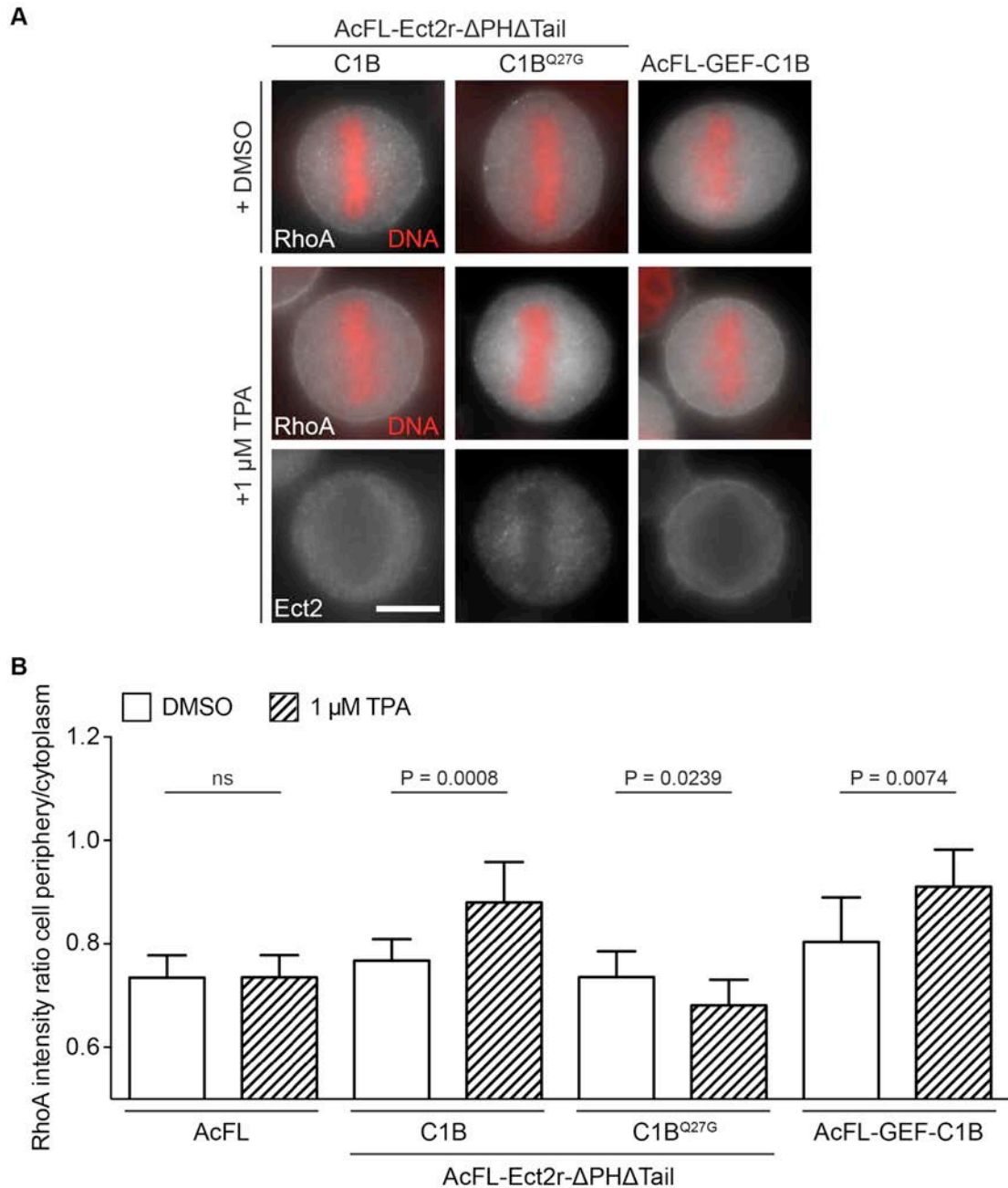


Figure 32 Precocious targeting of Ect2 in metaphase cells – RhoA

A IF analysis of RhoA in cell lines expressing Ect2 hybrid proteins treated with TPA in metaphase. Cells were treated with nocodazole for 4.5 hours to enrich the population of prometaphase cells. 1 hour after nocodazole washout the cells were treated with DMSO or 1 μM TPA for 5 minutes. After the treatment, the cells were fixed and stained with antibodies directed against RhoA, together with AcGFP and DAPI for DNA. Scale bar represents 10 μm.

B Quantification of RhoA enrichment at the plasma membrane after TPA treatment. Graph shows the ratio of the fluorescence signal at the cell periphery and in the cytoplasm for RhoA (n = 10, bars represent mean ± SD, Student's t-test).

Chapter 5. Results 3 - Optogenetic system to study the spatial requirements of Ect2 interaction with the plasma membrane during cytokinesis

Using chemical genetics we have shown that Ect2 membrane translocation is an important step for cytokinesis in mammalian cells. To expand our understanding of Ect2 function and the execution of cytokinesis, we decided to determine the importance of spatial distribution of Ect2 at the cell membrane for the cleavage furrow formation and cytokinesis. The previously employed chemical genetic system that is based on Ect2-C1B hybrid proteins can provide temporal control over Ect2's interaction with the membrane but does not provide spatial resolution. Addition of the compound to the cell medium results in an even distribution of the hybrid protein along the cell membrane. To overcome this limitation, we used a recently developed optogenetic method, which allows control of cellular processes by light stimulus. Importantly, optogenetic techniques offer higher temporal and spatial precision in delivering the activation signal when compared to the chemical genetic methods (Pathak et al., 2013). Our plan was to target Ect2 protein to different parts of the cell membrane and study the consequences for the formation of the cleavage furrow formation in human cells.

5.1 Developing an optogenetic system for spatially confined targeting of Ect2 to the plasma membrane

We took advantage of an optogenetic system based on the photosensitive cryptochrome protein (Cry2) from *Arabidopsis thaliana*. After activation with blue light, Cry2 changes its conformation and interacts with the CIB1 protein, establishing a useful optically controlled dimerizing system (Kennedy et al., 2010). A schematic representation of the original cryptochrome system is shown in Figure 33A and B. The system uses the photolyase homology region (PHR) from Cry2 as a photosensitive moiety, which is tagged with mCherry at the C-terminus to facilitate tracking of the protein in the living cells (Cry2-mCh). The interaction partner for Cry2 is the N-terminal part of CIB1 protein (CIBN). CIBN is tagged with GFP and stably targeted to the inner leaflet of the plasma membrane by addition of

the C-terminal prenylation sequence CAAX (CIBN-eGFP-CAAX). Cry2 binding to CIBN is activated by blue-light illumination with 488 nm laser, the same wavelength normally used to visualize GFP-tagged proteins. The interaction is very rapid, first Cry2 molecules can be detected 300 ms after the laser illumination and within 10 seconds the translocation is almost complete. The binding of Cry2 to CIBN is reversible with slow dissociation over 10 minutes (Kennedy et al., 2010).

In the original reported system, Cry2-mCh protein is present in the cytoplasm. Consequently, when it is activated by blue light, it diffuses very quickly and the interaction with plasma membrane is not exclusively restricted to the activated section. Nevertheless, activation of the Cry2 fusion protein in a subcellular region will result in the enhanced recruitment to the plasma membrane in close proximity to the activated region. Since we wanted to target Ect2 in a site-specific manner we attempted to swap the two interacting partners and to stably localize Cry2-mCh to the plasma membrane in order to restrict the cytoplasmic diffusion of the protein. To this end we generated a construct expressing Cry2-mCh with a C-terminal prenylation signal (Cry2-mCh-CAAX). For the second component, we fused the CIBN to siRNA-resistant AcGFP-tagged version of Ect2 that lacks the native membrane binding domains (Ect2r- Δ PH Δ Tail) or the Ect2's GEF domain only through N-terminus or C-terminus (Figure 33C).

To test the Cry2 system, we transiently transfected HeLaK cells with different combinations of constructs and tracked the mCherry and AcGFP-tagged fusion proteins following the whole-cell illumination with blue light and subsequent Cry2 activation with confocal live-cell imaging. Using the original system, we observed a rapid translocation of Cry2-mCh to the plasma membrane in CIBN-eGFP-CAAX expressing cells following a blue-light stimulus (Figure 34A). Unfortunately, we were not able to replicate this translocation with the adapted Cry2 system. Both proteins were expressed, however, for reasons currently not understood Cry2 protein stably attached to the plasma membrane was unable to attract the CIBN domain after illumination. We tried to overcome this problem by inserting different linkers in-between Cry2-mCh and the CAAX signal (Figure 33C). Unfortunately, the addition of linkers did not trigger the blue-light-induced membrane targeting of CIBN-GEF-FLAc either (Figure 34B).

5.2 Optogenetic targeting of Ect2 to the plasma membrane causes cleavage furrow formation

In light of the results described above, we decided to employ the original and validated setup with cytosolic Cry2-mCh and membrane-bound CIBN, hoping to still achieve a sufficient level of spatial selectivity. To facilitate our experiments for the optogenetic targeting of Ect2 to the plasma membrane, we generated a monoclonal cell line stably expressing CIBN-eGFP-CAXX stably bound to the plasma membrane. Then we fused truncated Ect2 without PH domain and PBC to Cry2-mCh creating a photo-responsive Cry2-mCh-Ect2r- Δ PH Δ Tail fusion protein (Cry2-mCh-Ect2) (Figure 35A). We subsequently transfected the CIBN-expressing cell line with Cry2-mCh-Ect2 and imaged the cells using confocal microscopy. Upon whole-cell illumination with a 488 nm laser, the Cry2-mCh-Ect2 protein rapidly translocated to the plasma membrane and colocalized with the CIBN domain in anaphase cells (Figure 35B). Importantly, blue-light activation and subsequent membrane binding also appeared to stimulate the interaction of Cry2-mCh-Ect2 with the midzone. The effect of Ect2's membrane interaction on midzone binding of the protein has not been explored previously. However, experiments focusing on the localization of the GFP-tagged WT allele of Ect2 during mitosis showed that the Ect2 midzone localization gradually increases during anaphase as does the localization of Ect2 to the equatorial part of the membrane also grows (Su, 2013). This raises the possibility that plasma membrane binding of Ect2 may stimulate the midzone association of the protein, but further research will be necessary to test this. In our optogenetic system this localization pattern could be enhanced due to the weaker midzone localization of Cry2-mCh-Ect2. Reasons for weaker localisation of Cry2-mCh-Ect2 protein to the midzone are currently unknown. One possibility is that the fusion of Ect2 with the large cryptochrome protein blocks the BRCT domains mediated interaction and that this is alleviated after a light-induced conformational switch in Cry2.

As we were able to target Ect2 to the plasma membrane in live cells and directly observe the cleavage furrow formation, we decided to repeat our rescue experiments with the light-controlled system. CIBN-expressing cells were transfected with Cry2-mCh-Ect2 and endogenous Ect2 protein was depleted by

Ect2 siRNA. We focused on metaphase and early anaphase cells and activated the interaction of Cry2-mCh-Ect2 with CIBN in the plasma membrane by repeated illumination with a 488 nm laser in two small circular regions at both sides of the equatorial cortex where the cleavage furrow was expected to form. Upon such illumination the Cry2-mCh-Ect2 protein was partially depleted from the cytoplasm and rapidly translocated to the plasma membrane, enriched at the equatorial periphery. Conversely, we could not detect any plasma membrane recruitment of the fusion protein without the blue-light activation (Figure 36A). Surprisingly, we observed unexpected arrangement of segregating chromosomes (Figure 36A) in approximately half of the cells not activated by blue light. This phenotype of tilted chromosomes suggests defective anaphase spindle, unexpected consequence of Ect2's PH and PBC deletion. Importantly, optogenetic targeting of Cry2-mCh-Ect2 to the plasma membrane could potentially restore cleavage furrow ingression and cytokinesis in more than 70% of cells, despite the absence of Ect2's normally essential membrane engagement domains (Figure 36B). To confirm that the rescue effect is dependent on Ect2, we performed the same experiments with cells expressing only Cry2-mCh. Targeting of Cry2-mCh protein was unable to rescue cytokinesis after depletion of endogenous Ect2 with or without the blue-light activation. In this case, the level of cytokinesis failure was very similar to Cry2-mCh-Ect2 expressing cells not activated by the blue-light illumination (Figure 36B).

5.3 One-sided Ect2 targeting causes formation of unilateral cleavage furrows

After we demonstrated that optogenetic targeting of Cry2-mCh-Ect2 to the plasma membrane could complement the role of PH domain and PBC, we tested the role of the spatial distribution of the Ect2 protein at the cell membrane. In anaphase, Ect2 is mainly accumulated in the equatorial part of the plasma membrane (Su et al., 2011).

Firstly, we tested if Cry2-mCh-Ect2 targeting to only one side of the potential cleavage plane can cause unilateral furrowing. As before, CIBN-expressing cells were transfected with Cry2-mCh-Ect2 and Ect2 siRNA. Anaphase cells were illuminated only on one side of the equatorial periphery (Figure 37A). In 60% of

cases, diffusion of Cry2-mCh-Ect2 along the cell membrane abolished selective accumulation of Ect2 protein. Notably, this Ect2 localization while reminiscent of the bilateral accumulation did not rescue completion of cytokinesis, despite observed bilateral furrowing in a fraction of the cells (Figure 37B). This could be caused by delayed activation of the plasma membrane interaction, an insufficient level of Ect2 at the membrane or could suggest the necessity of the bilateral activation. In the rest of the cells we examined, we observed the one-sided accumulation of Cry2-mCh-Ect2. Strikingly, selective membrane targeting in almost all of these cells led to formation of a unilateral furrow coinciding with the side of Cry2-mCh-Ect2 enrichment (Figure 37). Again we observed the abnormal geometry of the anaphase spindle in approximately half of the cells studied. Moreover this adjusted spindle geometry positively correlated with the unilateral accumulation of Cry2-mCh-Ect2 and might have caused the selective localization. Importantly, this experiment suggests that local activity of Ect2 at the plasma membrane is necessary and sufficient to drive cleavage furrow formation. While one-sided targeting of Ect2 could form unilateral furrow, it was not sufficient to rescue cytokinesis, and the level of cytokinetic failure was very similar to cells not activated by light (Figure 36). These results suggest Ect2 activity is necessary at both sides of the cleavage furrow for successful completion of cytokinesis and that its action at both sides of the furrow has to occur at a similar time.

5.4 Polar activation of Cry2-mCh-Ect2 does not lead to local accumulation of the fusion protein at the plasma membrane

To complete our optogenetic studies, we also tested the effect of targeting Ect2 to the cell poles in anaphase cells. We used the same protocol as above, and activated the membrane targeting of Ect2 always at one pole of anaphase cell (Figure 38). In contrast to the equatorial targeting we never observed strong accumulation of Cry2-mCh-Ect2 at the pole. After activation, the protein diffused quickly and accumulated either on one side of potential furrow or both. These results could imply the existence of an active regulatory mechanism preventing Ect2 accumulation at the cell poles or positive feedback control for enrichment at the equator.

5.5 Conclusions - Optogenetic targeting of Ect2 to the plasma membrane

We have employed a recently developed optogenetic technique to investigate the importance and spatial requirements for Ect2's interaction with the plasma membrane. We have adapted a light-induced dimerization system based on the interaction of the light-sensitive Cry2 protein with CIBN domain only upon illumination with blue light. To render the system more spatially constraint we tried to stably attach the Cry2 protein to the plasma membrane. Unfortunately, despite several attempts and modifications, such as the inclusion of linkers, the Cry2 protein did not interact with the CIBN fragment upon illumination when the former was attached to the plasma membrane. Thus we decided to use the original system and test if we can achieve spatial selectivity by activating cytoplasmic Cry2 in close proximity to plasma membrane regions of interest. Firstly, we genetically fused Ect2 lacking the C-terminal membrane targeting domains to Cry2-mCh and generated a stable HeLaK cell line expressing the GFP-tagged interaction partner CIBN stably targeted to the plasma membrane by addition of C-terminal prenylation sequence. After activation with the blue-light (488 laser), we observed targeting of the Cry2-mCh-Ect2 to the plasma membrane. Blue-light activation also enhanced weak midzone localization of Cry2-mCh-Ect2 protein. The reasons for weak midzone interaction of Cry2-mCh-Ect2 are currently unknown, as the protein has the BRCT domains crucial for this localization of Ect2. The fusion with large cryptochrome might cause some steric clashes and prevent stable interaction of Cry2-mCh-Ect2 with the midzone. Conformational change allowing interaction of Cry2 with CIBN might also allow stable interaction of BRCT domains of Ect2 with the midzone.

With the system set up, we tested if optical targeting of Ect2 can rescue cytokinetic failure after endogenous Ect2 depletion. In metaphase or early anaphase cells, we activated the dimerization by illuminating two small circular regions at the cell equator, the place of presumptive furrow formation. Subsequently, we observed the accumulation of Cry2-mCh-Ect2 at the plasma membrane. Shortly after the activation, the protein diffused along the membrane, however its concentration remained increased in the original place of activation. Remarkably, light-induced

targeting of Ect2 to the membrane could rescue cell division in 70% of the cells tested, while the majority of the non-illuminated cells failed to divide. Thus, we were able to create a condition in which we were able to control cytokinesis by using light. This result is consistent with our chemical genetic experiments and further confirms that the interaction of Ect2 with the plasma membrane is a crucial step for cytokinesis in human cells and perhaps all animal cells. Since the illumination took place in metaphase or early anaphase cells, the optogenetic experiments also provide further support for the notion that Ect2's function at the PM for cytokinesis is critical at or after this point during cell division.

By using two artificial membrane targeting approaches, one controlled by a chemical and one controlled by light, we were able to replace the function of the two known and normally indispensable membrane engagement domains of the protein, the PH domain and the polybasic tail. This indicates that while it is essential for Ect2 to engage with the plasma membrane, the precise manner, interaction mode and lipids involved are possibly less critical.

Interesting observation was that deletion of Ect2's PH domain and PBC caused abnormal arrangement of chromosomes in anaphase and changed the geometry of the anaphase spindle. This phenotype was never described before in human cells, but the role for Ect2 in spindle assembly was proposed in cell free *X. laevis* extract system (Tatsumoto et al., 2003).

To test the spatial requirements of Ect2 interaction with the plasma membrane, we targeted Cry2-mCh-Ect2 only to one side of the potential furrow by unilateral illumination. Lateral diffusion in the plasma membrane prevented unilateral accumulation of the Ect2 fusion protein in 60% of the cells. However, cells that exhibited specific accumulation on one side of the cell formed a unilateral furrow at the activated side. This result proves the specific involvement of Ect2 in RhoA activation and cleavage furrow formation at the plasma membrane. Notably, unilateral accumulation was not sufficient to fully support cytokinesis and majority of the cells failed cytokinesis, suggesting the importance of Ect2 activity and cleavage furrow ingression at both sides of the equatorial cortex in human cells. Our unilateral illumination experiments suggest that Ect2 is required and sufficient

at the equatorial cortex to locally stimulate formation of the cleavage furrow. However, these experiments do not answer the question whether Ect2's equatorial enrichment is the main and essential mechanism for the equatorial placement and formation of the furrow, an aspect that will be investigated in the next result chapter. Importantly, adjusted spindle geometry positively correlated with one-sided accumulation of Cry2-mCh-Ect2 and unilateral furrow formation. This suggests that the changed spindle geometry might have caused the unilateral furrow formation, but we have not observed unilateral furrowing in cells not activated by blue light that showed the same spindle geometry. Thus the unilateral localization of Ect2 seems to be key, but further experiments would be necessary to confirm this.

No specific accumulation or formation of the cleavage furrow was observed when we targeted Ect2 to the cell poles. This observation could indicate the existence of an inhibitory pathway preventing the RhoA activation and furrow formation at the polar regions of the cell. It has been previously shown that astral microtubules provide this inhibitory signal and this might explain the inability of Ect2 to drive the furrow formation at the poles (Dechant and Glotzer, 2003) (Werner et al., 2007) (Foe and von Dassow, 2008). As polar targeting of Ect2 by optogenetic approaches was not possible, it is not clear whether polar accumulation of Ect2 could induce furrowing at the cell poles or whether furrowing would still be suppressed. Testing these questions and hypotheses requires and merits further study.

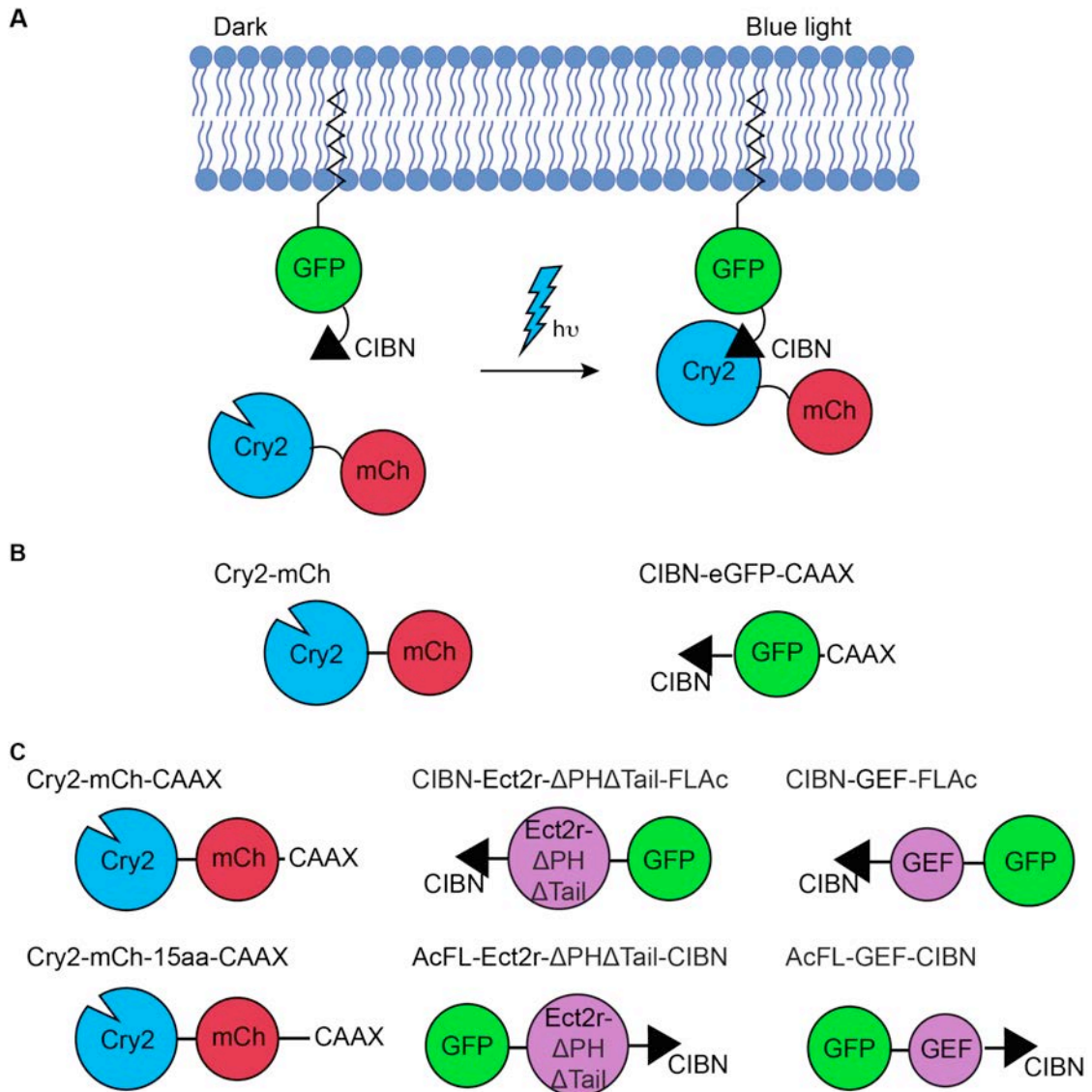


Figure 33 Cry2 optogenetic system

A Schematic depiction of the original Cry2 system, showing the targeting of Cry2-mCh to the plasma membrane after blue-light activation.

B Schematic representation of the constructs used in the original Cry2 system.

C Schematic representation of the adapted optogenetic constructs, designed for spatially-confined optogenetic targeting of Ect2 to the plasma membrane.

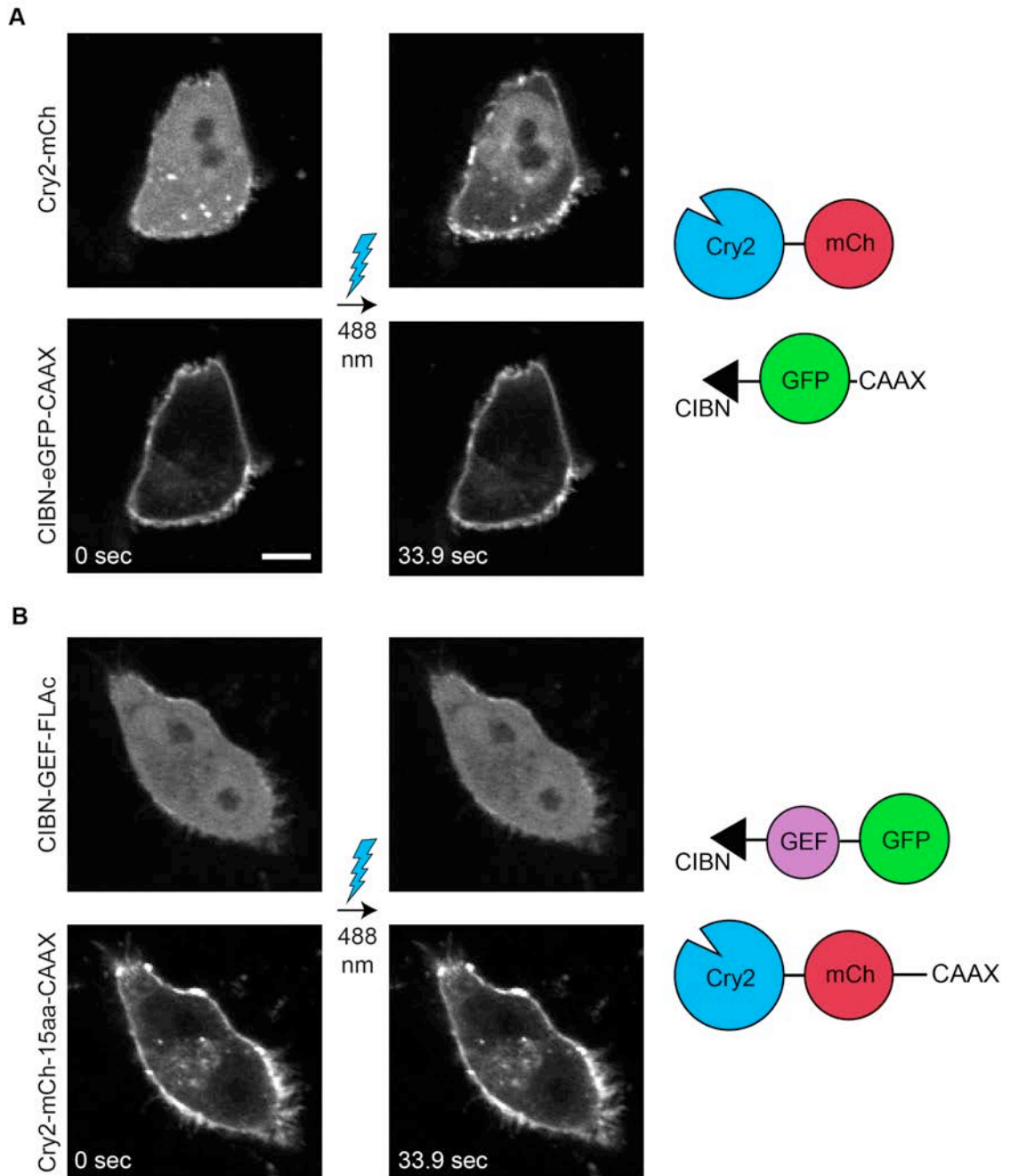


Figure 34 Optogenetic membrane targeting of the adapted Cry2 system with swapped Cry2 and CIBN proteins

A Confocal images showing the translocation of Cry2-mCh to the plasma membrane after blue-light illumination. HeLaK cells were transiently transfected with Cry2-mCh and CIBN-eGFP-CAAX, schematic illustration of the constructs used is shown on the right side. Cells were imaged 48 hours post transfection and activated by whole-field GFP imaging with a 488 nm laser. Scale bar represents 10 μ m.

B Confocal images showing the localization of CIBN-GEF-FLAc and Cry2-mCh-15aa-CAAX proteins after blue-light illumination. The same protocol was used as described in panel A above.

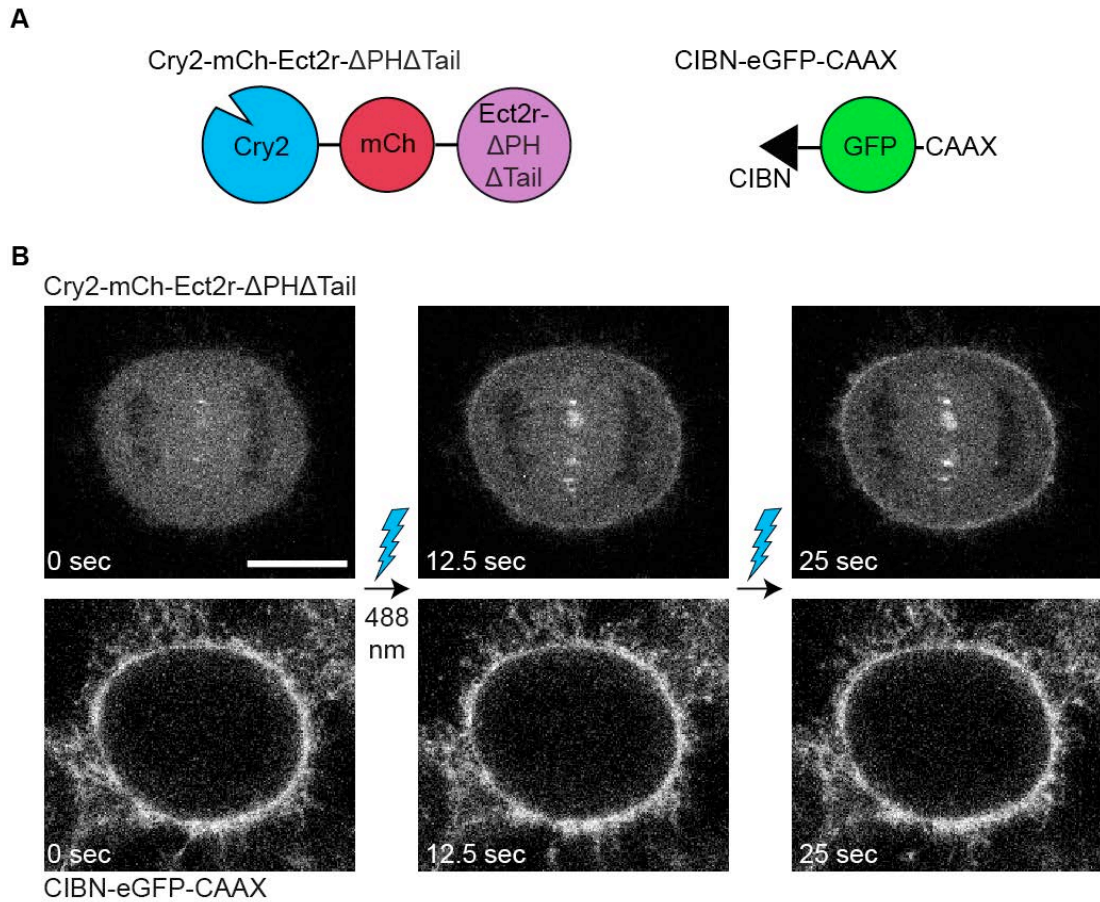


Figure 35 Optogenetic targeting of Cry2-mCh-Ect2 to the plasma membrane

A Schematic representation of the constructs used for the optogenetic targeting of Ect2 to the plasma membrane.

B Confocal microscopy images showing the translocation of Cry2-mCh-Ect2 to the plasma membrane after blue-light illumination. HeLaK cells were transiently transfected with Cry2-mCh-Ect2r- Δ PH Δ Tail and CIBN-eGFP-CAAX. Cells were imaged 48 hours post transfection and the whole fields were activated by GFP imaging with a 488 nm laser. Scale bar represents 10 μ m.

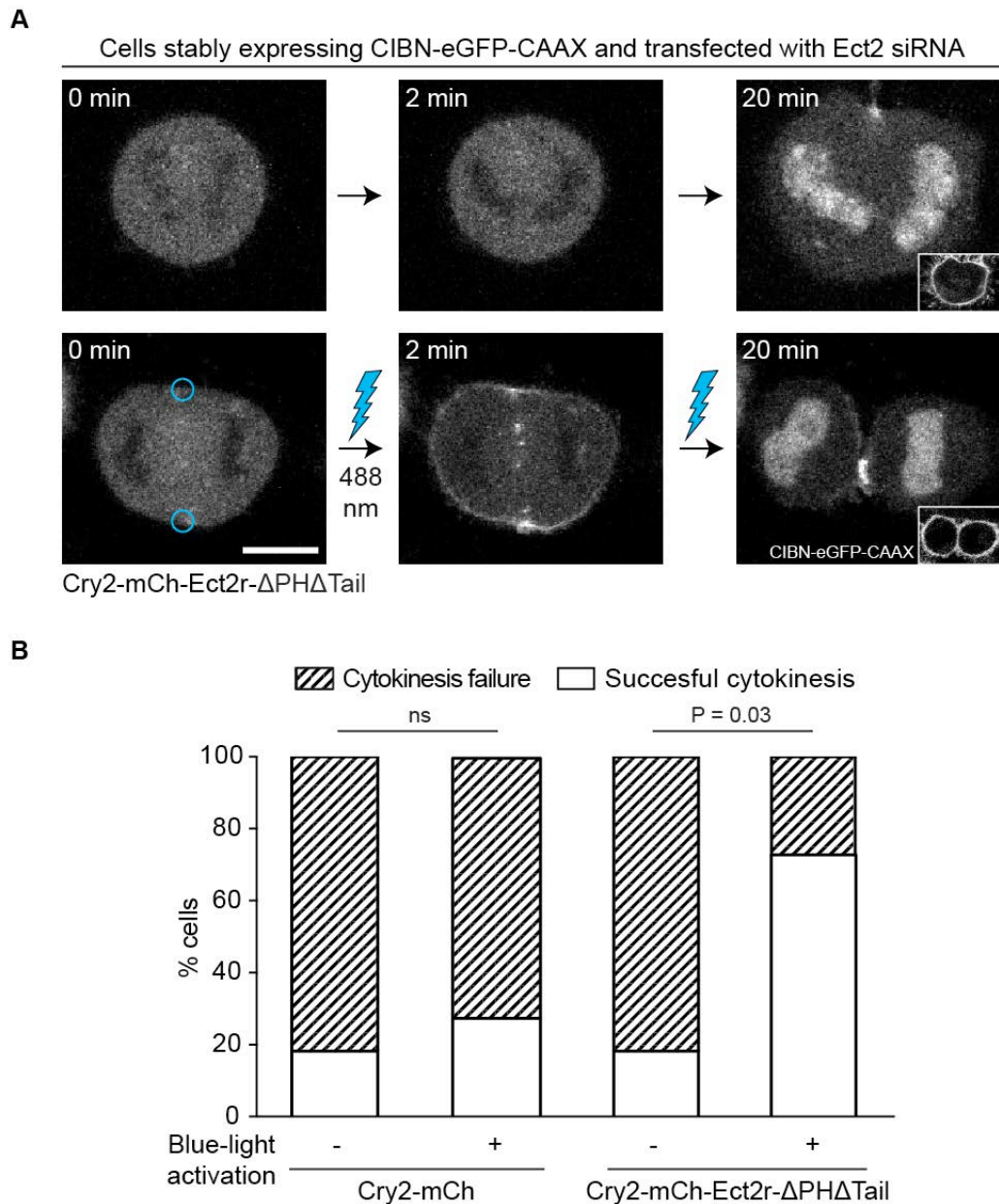
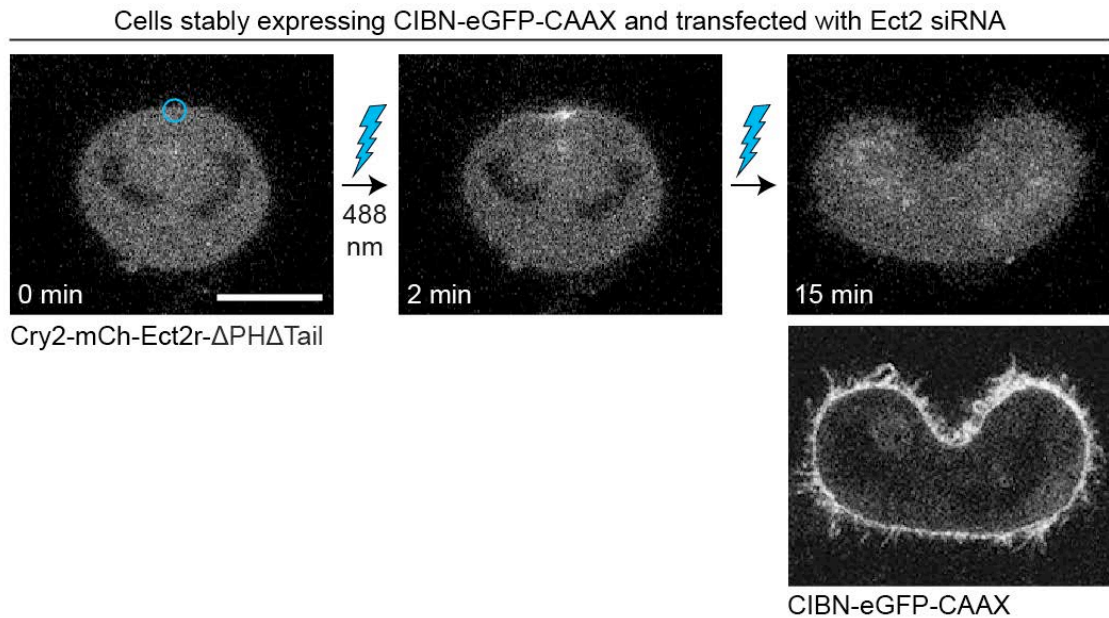


Figure 36 Analysis of the cytokinetic phenotype upon optogenetic targeting of Ect2 to the plasma membrane

A Confocal microscopy images showing the localization of the Cry2-mCh-Ect2 protein with or without blue-light illumination. HeLaK cell line stably expressing CIBN-eGFP-CAAX (inset) was transfected with Cry2-mCh-Ect2r- Δ PH Δ Tail and Ect2 siRNA. Cells were imaged 24 hours after siRNA transfection. Plasma membrane translocation of Cry2-mCh-Ect2 was induced by illumination with a 488 nm laser within two small circular regions at the equatorial periphery as marked in the image above. Scale bar represents 10 μ m.

B Quantification of cytokinetic phenotype after optogenetic membrane targeting of Ect2. Experiments were performed as described above (panel A). Metaphase or early anaphase cells were scored. (n = 11, Fisher's exact test)

A



B

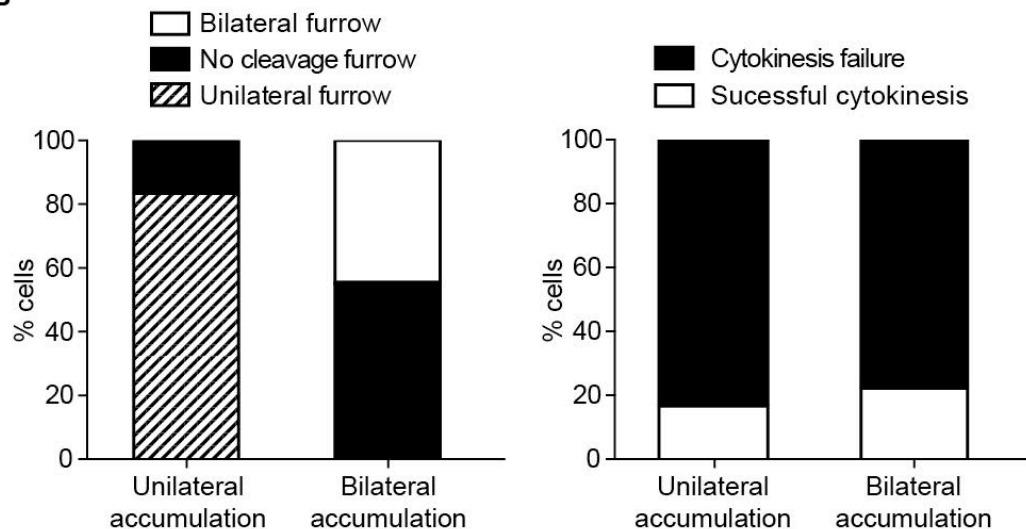


Figure 37 One-sided Ect2 targeting to the plasma membrane causes formation of unilateral cleavage furrow

A Confocal microscopy images showing the localization of Cry2-mCh-Ect2 after unilateral blue-light illumination. HeLaK cells stably expressing CIBN-eGFP-CAAX were transfected with Cry2-mCh-Ect2r- Δ PH Δ Tail and Ect2 siRNA. Cells were imaged 24 hours after siRNA transfection. Plasma membrane translocation of Cry2-mCh-Ect2 was induced by illumination with a 488 nm laser within the circular region at the equatorial periphery as marked in the image above. Scale bar represents 10 μ m.

B Quantification of the protein localization pattern and the furrowing phenotype (left) and cytokinetic phenotype (right) after unilateral membrane targeting of Ect2. Experiments were performed as described above (panel A). Anaphase cells were scored. (n = 15)

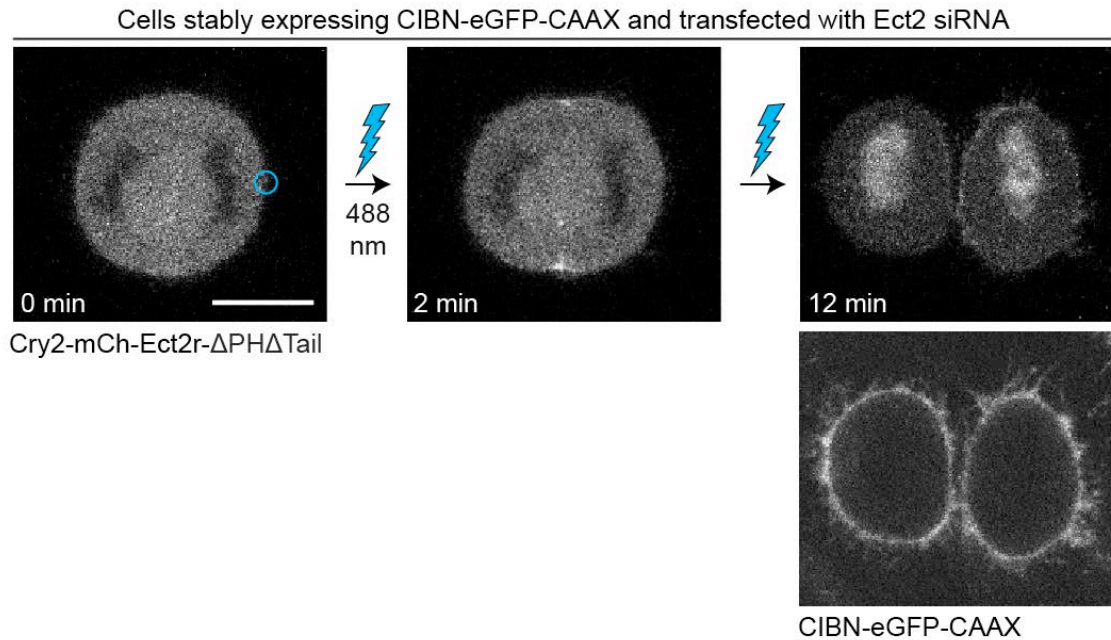


Figure 38 Ect2 protein does not accumulate at the polar cell periphery after optogenetic targeting

Confocal microscopy images showing the localization of Cry2-mCh-Ect2 after unilateral blue-light illumination at the cell pole. HeLaK cell line stably expressing CIBN-eGFP-CAAX was transfected with Cry2-mCh-Ect2r- Δ PH Δ Tail and Ect2 siRNA. Cells were imaged 24 hours after siRNA transfection. Plasma membrane translocation of Cry2-mCh-Ect2 was induced by illumination with a 488 nm laser within the small circular region as marked in the image above. Scale bar represents 10 μ m.

Chapter 6. Results 4 - Investigating the role of Ect2's recruitment to the spindle midzone for cleavage furrow formation

Previous work from our laboratory showing that Ect2 associates with the equatorial part of the plasma membrane during anaphase in a manner that likely requires Ect2's midzone anchor Centralspindlin suggests a model for the placement of the cleavage furrow. The binding to Centralspindlin and subsequent concentration of Ect2 in the equatorial plane could be converted into a protein activity gradient at the plasma membrane, which could specify active RhoA zone and therefore be the main signal to place the cleavage furrow in small somatic cells. The interaction of Ect2 with Centralspindlin in general lies at the heart of many models of cleavage furrow formation and positioning that have been put forward by our laboratory and others (Somers and Saint, 2003) (Yuce et al., 2005) (Petronczki et al., 2007) (Burkard et al., 2009) (Wolfe et al., 2009) (Su et al., 2011). Currently, the Ect2-Centralspindlin interaction is the only molecularly well-characterized event that provides strong hypothesis for how the mitotic spindle might position the cleavage furrow by using the central spindle to stimulate RhoA activity. Other mechanisms by which the mitotic spindle can regulate cleavage plane formation and positioning have been observed and proposed (e.g. polar relaxation by astral microtubules) (Bringmann and Hyman, 2005) (Dechant and Glotzer, 2003) (Yoshigaki, 2003) (Werner et al., 2007). However, their description remains largely phenomenological and therefore difficult to interrogate and test decisively using specific molecular alterations.

This work and previous results demonstrate that GEF activity of Ect2 and binding to the plasma membrane are two properties of the molecule that are essential for cytokinesis (Prokopenko et al., 1999) (Su et al., 2011). Although located at the central position in our models, the importance of the third known property of Ect2, the BRCT domains-mediated interaction with the spindle midzone has not been rigorously interrogated. To test the hypothesis that the Ect2-Centralspindlin interaction plays a key role in the formation of the cleavage furrow, we decided to prevent this interaction by defined molecular changes. At the anaphase onset, Ect2

localize to spindle midzone through the interaction with MgcRacGAP, a subunit of the Centralspindlin complex (Somers and Saint, 2003) (Yuce et al., 2005). The interaction is promoted by Plk1-dependent phosphorylation of the N-terminus of MgcRacGAP (Petronczki et al., 2007) (Burkard et al., 2009) (Wolfe et al., 2009). Ect2 binds phosphorylated MgcRacGAP via tandem BRCT domains located in the N-terminal part of the protein. T153 and K195 residues are conserved throughout different BRCT-containing proteins (Figure 39). T153 and K195 are located in the BRCT1 domain and they have been shown to be crucial residues for MgcRacGAP binding (Wolfe et al., 2009) (Zou et al., 2014). Their mutation prevented MgcRacGAP interaction with a recombinant bacterially expressed N-terminal fragment of Ect2 in cell extracts (Wolfe et al., 2009) or binding of N-terminal Ect2 fragment to synthesized phosphopeptide from MgcRacGAP (Zou et al., 2014) and abolished localization of similar N-terminal fragment of Ect2 when transiently overexpressed in cells (Wolfe et al., 2009).

Therefore, we decided to introduce point mutations in T153A and K195M into the BRCT1 domain of Ect2 and use our transgenic complementation system for Ect2 to investigate the consequences of this alteration. This should allow us to decisively test the importance of Ect2 interaction with the spindle midzone for cytokinesis in human cells.

6.1 Localization of Ect2-BRCT^{TK} protein during cytokinesis

We generated a full-length siRNA-resistant and AcGFP-FLAG-tagged Ect2 construct with the mutations T153A and K195M in the first BRCT domain of the protein (Ect2-BRCT^{TK}) (Figure 40A). To study the localization of the Ect2-BRCT^{TK} protein in live cells, we generated monoclonal stable cell lines expressing GFP-tagged Ect2-BRCT^{TK} together with H2B-mCherry to visualize chromosomes. As a control for our experiments, we used a previously generated cell line expressing the wild-type siRNA-resistant and AcGFP-FLAG-tagged full-length version of Ect2 together with H2B-mCherry (Su et al., 2011). Notably, in both stable cell lines obtained (clone 9 and 21) the transgenic Ect2-BRCT^{TK} protein was expressed at a similar level as the endogenous counterpart and as the Ect2-WT transgene in the control cell line (Figure 40B). The stable cell lines expressing

BRCT^{TK} mutant Ect2 at levels close to the endogenous counterpart provided a suitable system for us to investigate the effect of these mutations on protein localization and cytokinesis.

To test whether the BRCT mutations T153A and K195M abolish Ect2 localization to the spindle midzone, we co-stained the cells for transgenic Ect2 and Mklp1, a part of the Centralspindlin complex. Consistent with a key role of the Ect2-Centralspindlin interaction in the recruitment of Ect2 to the spindle midzone, Ect2-WT colocalized with Mklp1 in anaphase cells, while Ect2-BRCT^{TK} was not enriched at the midzone (Figure 41).

Our transgenic cell lines also allowed us to track Ect2 protein localization in live cells during cell division. Using live-cell imaging for tracking Ect2 is particularly important, as fixation and staining often precludes the detection of the membrane-associated pool of the protein (Su et al., 2011). Both WT and BRCT-mutated Ect2 were cytoplasmic in metaphase cells (Figure 42). After anaphase onset, Ect2-WT accumulated at the spindle midzone, whereas the Ect2-BRCT^{TK} protein did not appear to localize at the midzone, although minor residual interaction is difficult to disprove. Both proteins translocated to the plasma membrane soon after anaphase onset with similar kinetics. As described previously (Su et al., 2011), shortly before and during cleavage furrow formation, we observed the enrichment of Ect2-WT protein at the equatorial part of the plasma membrane. This enrichment of Ect2 protein was disrupted in Ect2-BRCT^{TK} expressing cells. After completion of furrow ingression, protein Ect2 localized to the midbody in both cell lines.

To assess the differences in Ect2 enrichment at the equator between Ect2-WT and Ect2-BRCT^{TK}, we quantified the intensity profile of Ect2-WT and Ect2-BRCT^{TK} proteins along the cell periphery during furrow ingression (Figure 43A). We observed more than twofold enrichment of Ect2-WT protein within approximately 10 μm wide equatorial interval (Figure 43B, first graph). This enrichment became even more pronounced as furrow ingression progressed (Figure 43B, second and third graph). This was compared to only a minor increase in the case of Ect2-BRCT^{TK} protein (Figure 43B, first and second graph). But Ect2-BRCT^{TK}

protein also localized to the midbody, so at the later stage there was also equatorial enrichment of Ect2-BRCT^{TK} protein, even though still 1.5-fold smaller than the wild-type protein (Figure 43B, third graph).

We decided to determine if this apparent small enrichment was simply caused by cleavage furrow ingression rather than by a specific property of Ect2-BRCT^{TK} protein. To this end, we compared the plasma membrane localization of Ect2-BRCT^{TK} to MyrPalm-GFP, a membrane-bound fluorescent marker. MyrPalm-GFP is targeted to the plasma membrane by myristoylation signal sequence, which results in even localization of the marker along the cell membrane (Figure 44). We followed the cells expressing Ect2-WT, Ect2-BRCT^{TK} or MyrPalm-GFP proteins from the metaphase-to-anaphase transition until cleavage furrow ingression, and determined the protein intensity ratio at the equatorial membrane to the polar membrane (Figure 45A). Ect2-WT protein showed a gradual enrichment at the equatorial region starting 10 min after anaphase onset and reaching a peak value of fourfold enrichment, consistent with the single frame analysis (Figure 43B). Ect2-BRCT^{TK} protein showed significantly lower equatorial enrichment around twofold equatorial enrichment. Importantly, its profile was very similar to that of the control MyrPalm-GFP marker. Although equatorial accumulation was detected earlier for the MyrPalm-GFP protein than for Ect2-BRCT^{TK}, the magnitude of accumulation was comparable between the two proteins. This indicates that the minor equatorial enrichment observed for the Ect2-BRCT^{TK} could be a non-specific phenomenon, likely caused by membrane indentation. We speculated that the temporal shift between the cell lines could be caused by differences in the speed at which cells progress through cytokinesis (the time from anaphase onset until full cleavage furrow ingression). Indeed, the progression of MyrPalm-GFP expressing cells through cytokinesis was about five minutes faster, compared to Ect2-WT and Ect2-BRCT^{TK} cells (Figure 44, Figure 45B). Notably, there was no difference between the WT and the BRCT-mutated transgene. The reason for the slightly delayed progression through cytokinesis in cells expressing Ect2 transgenes is currently not known, but could be linked to Ect2 siRNA transfection in these cell lines.

Collectively, these data demonstrate that the mutations in the BRCT1 domain of Ect2 protein that are reported to disrupt binding to MgcRacGAP, do abrogate the recruitment of Ect2 to the spindle midzone, and additionally prevent the accumulation of the protein at the equatorial region of the plasma membrane. These results provide the strongest experimental support yet for the two previously proposed aspects of cytokinetic regulation: (1) that Ect2's recruitment to the spindle midzone depends on the interaction with the Centralspindlin subunit MgcRacGAP (Yuce et al., 2005) (Zhao and Fang, 2005) and (2) that Ect2's recruitment to the midzone could be the mechanistic basis for the proteins enrichment at the equatorial membrane (Su et al., 2011).

6.2 The effect of Ect2 BRCT1 domain mutations T153A and K195M on cytokinesis

In order to examine the role of Ect2's targeting to the spindle midzone and equatorial membrane during cell division, we tested the ability of the Ect2-BRCT^{TK} transgene to support cytokinesis. To this end, we generated monoclonal cell lines stably expressing Ect2-BRCT^{TK}, which we used together with previously generated monoclonal cell lines stably expressing various versions of the Ect2 protein, transgene missing the membrane targeting domains PH domain and polybasic tail (AcFL-Ect2r- Δ PH Δ Tail) and catalytically dead transgene carrying mutations in GEF domain (565-568 PVQR to AAAA) (Figure 46A) (Su et al., 2011). WB analysis revealed the two BRCT-mutated cell lines (clone 2 and 5) expressed the Ect2-BRCT^{TK} protein at a level close to the level of the endogenous protein (Figure 46B).

To test if the Ect2-BRCT^{TK} protein was able to replace the endogenous counterpart, we transfected cells with NTC or Ect2 siRNA and analysed the levels of multi-nucleation forty-eight hours after the transfection. Endogenous Ect2 was potently depleted in all cell lines by Ect2 siRNA transfection (Figure 46B). The vast majority of GFP-tag only expressing cells, cells expressing a GEF-defective mutant and cells expressing a truncated Ect2 version lacking PH domain and PBC was converted into multi-nucleated cells after depletion of endogenous Ect2, indicating a failure to support cytokinesis of these transgenes (Figure 47). As shown before,

this phenotype could be fully rescued by expression of the wild-type Ect2 transgene (Su et al., 2011). Unexpectedly, expression of the Ect2-BRCT^{TK} protein was also able to fully rescue cytokinesis after Ect2 depletion in both monoclonal cell lines. There was a small elevation of the multi-nucleation level for the Ect2-BRCT^{TK} 5 cell line. However, this elevation was observed in both NTC and Ect2 siRNA transfected cells indicating that it was not caused by a lack of Ect2, but is either inherent to the particular cell line or represents a semi-dominant effect of the slightly higher expressed transgene.

To further confirm our surprising result, we examined the phenotype of BRCT mutant-expressing cells using live-cell imaging after depletion of endogenous Ect2 (Figure 48). The quantification confirmed Ect2-BRCT^{TK} protein could support cytokinesis in the absence of the endogenous protein, as majority of the cells divided successfully (Figure 49). A small percentage of Ect2-BRCT^{TK} cells that failed to divide was still able to form a cleavage furrow that later regressed, while control cell lines expressing defective versions of Ect2 were unable to form the cleavage furrow in most cases. The less penetrant phenotype with regards to cleavage furrow formation for the GEF4A-mutant allele was reported before (Su et al., 2011). Thus, endpoint IF analysis as well as time-lapse studies indicate the point mutations within Ect2's BRCT1 domain that block midzone recruitment and enrichment at the equatorial membrane of the protein, do not prevent cleavage furrow formation or cytokinesis completion in the vast majority of cells.

Next, we decided to test if BRCT domain mutations and the consecutive changes in Ect2 protein localization affect the distribution of contractile ring proteins. To do that, we transfected GFP-tag, Ect2-WT and Ect2-BRCT^{TK} expressing cell lines with Ect2 siRNA. Cells were synchronized to enrich the cultures for mitotic cells, fixed and stained for RhoA and Anillin. In control anaphase cells, both RhoA and Anillin localized to the plasma membrane and accumulated mostly at the cleavage furrow (Figure 50A). We quantified the equatorial enrichment of RhoA and Anillin by measuring the intensity profile along the cell periphery. Depletion of endogenous Ect2 in the GFP-tag only expressing cells completely disrupted the accumulation of RhoA and Anillin at the equator (Figure 50). As expected, this phenotype was fully

rescued in the Ect2-WT expressing cells. The RhoA and Anillin profiles in Ect2-BRCT^{TK} cells were undistinguishable from the Ect2-WT cells.

Taken together, our data indicate that Ect2's interaction with Centralspindlin, Ect2's recruitment to the spindle midzone, and the enrichment of the protein at the equatorial membrane are likely not essential for cytokinesis in human cells. Furthermore, our observations suggest that the Ect2 gradient at the plasma membrane is not the only or the main signal that places the cleavage furrow in human cells.

6.3 Testing the role of astral microtubules and MgcRacGAP during cytokinesis in Ect2-BRCT^{TK} expressing cells

Our results have suggested that Ect2's recruitment to the spindle midzone, and the enrichment of the protein at the equatorial membrane are not essential for cytokinesis in otherwise unperturbed human cells. This result could indicate that Ect2's binding to the spindle midzone and its consequences acts in a redundant manner with another mechanism to place the cleavage furrow. Therefore, our next experiments represent the first attempts to dissect this additional elusive signal, which may be sufficient to position the furrow during cytokinesis by itself or it may be redundant with the equatorial accumulation of Ect2. Possible signals could act by either stimulating furrowing at the equatorial part of the cell membrane or by inhibiting contractility at the cell poles. We also cannot rule out the possibility of multiple redundant signals working together, which would complicate their identification. The prediction for our experiments was that if a signal was redundant with the equatorial accumulation of Ect2, its inhibition should compromise cytokinesis in cells expressing Ect2-BRCT^{TK} protein but not in cells expressing the wild-type version of Ect2.

Firstly, we focused on the role of astral microtubules for cytokinesis in Ect2-BRCT^{TK} expressing cells. Astral microtubules have been shown to inhibit contractility and were proposed to prevent RhoA activation at the cell poles (Bringmann and Hyman, 2005) (Dechant and Glotzer, 2003) (Werner et al., 2007) (Foe and von Dassow, 2008). To deplete the cells for astral microtubules without destabilizing the spindle

midzone, we employed a treatment with low concentration of nocodazole (Bement et al., 2005) (Foe and von Dassow, 2008) (Zanin et al., 2013). This technique takes advantage of the different stability of astral and midzone microtubules. Short treatment with low concentration of nocodazole results in the preferential depletion of astral microtubules. We needed to optimize the concentration of nocodazole for our system. It has been shown that depletion of astral microtubules leads to formation of broader RhoA and Anillin zone (Bement et al., 2005) (Foe and von Dassow, 2008) (Zanin et al., 2013). As a readout for efficacy of nocodazole treatment we measured the profile of Anillin around the cell periphery in anaphase cells. Anillin distribution acted as a surrogate assay for the analysis of astral microtubules that are difficult to quantify and observe in HeLaK anaphase cells. We treated Ect2-WT-expressing cells that were synchronized at the metaphase-to-anaphase transition with increasing concentrations of nocodazole (from 10 nM to 100 nM) or DMSO as a control. Subsequently, the width of the Anillin zone was analysed using IF and quantified (Figure 51). Concentrations of nocodazole higher than 25 nM led to a slight broadening of the zone of cortical Anillin. For further experiments, we decided to use a dose of 50 nM nocodazole, in order to minimize possible side effects of nocodazole treatment.

Cell lines expressing GFP-tag only, Ect2-WT and Ect2-BRCT^{TK} were synchronized at the metaphase-to-anaphase transition after depletion of endogenous Ect2. Cells were treated with DMSO or 50 nM nocodazole and subsequently, the cytokinetic phenotype was analysed by live-cell imaging. The vast majority of GFP-tag-expressing cells failed cytokinesis after depletion of endogenous Ect2. Notably, nocodazole treatment enhanced the cytokinetic phenotype in GFP-tag only cells, as the majority of the cells (95%) were unable to form a furrow completely, while 40% of the cells treated with DMSO formed a cleavage furrow, which later regressed (Figure 52). However, the addition of a low dose of nocodazole did not result in an increase in cytokinetic defects in cells expressing either Ect2-WT or Ect2-BRCT^{TK} (Figure 52). Thus, our data suggest that compromising astral microtubules with low doses of nocodazole does not cause a significant defect in cytokinesis execution in cells complemented with wild-type or BRCT-mutated Ect2. This suggests that Ect2 recruitment to the spindle midzone

and the action of astral microtubules do not act as the main or only redundant pathways to promote cleavage furrow formation.

Our next analysis focused on MgcRacGAP and its role in furrowing. It was speculated that MgcRacGAP could stimulate Ect2's activity by releasing the inhibitory interaction of N-terminus and C-terminus of the protein (Kim et al., 2005) (Yuce et al., 2005) (Wolfe et al., 2009) (Zou et al., 2014). These studies proposed that the autoinhibitory binding could be relieved by interaction between the BRCT domains of Ect2 and the Plk1-phosphorylated N-terminus of MgcRacGAP. In our study we have shown this interaction is probably not essential for cytokinesis, which renders this possibility unlikely. Nevertheless, MgcRacGAP, like Ect2, is essential for RhoA activation. Recently, it has been shown that MgcRacGAP also interacts with the plasma membrane via its C1 domain and that the C1 domain of MgcRacGAP is also crucial for early and late aspects of cytokinesis (Lekomtsev et al., 2012) (Basant et al., 2015). We speculated that MgcRacGAP could stimulate Ect2 activity in the equatorial region of the plasma membrane via a different mode of interaction. This notion is supported by recent *in vitro* data suggesting that the C-termini of Ect2 and MgcRacGAP interact with each other in order to activate RhoA (Zhang and Glotzer, 2015).

To test if membrane association of MgcRacGAP could control Ect2's GEF activity at the equatorial membrane and act redundantly with the enrichment of Ect2 at the equator, we generated monoclonal cell lines stably co-expressing two siRNA-resistant transgenic proteins: (1) AcGFP-tagged full-length Ect2 with T153A and K195M mutations (Ect2-BRCT^{TK}) and (2) mCherry-tagged MgcRacGAP lacking the membrane-targeting C1 domain (MgcRacGAP- Δ C1) or carrying the K292L mutation that abolishes membrane targeting of MgcRacGAP (MgcRacGAP-K292L) (Figure 53). We attempted to generate a control cell line expressing the wild-type version of MgcRacGAP together with Ect2-BRCT^{TK} protein but failed to obtain double positive clones. We examined the cytokinetic phenotype of described double transgenic cell lines after co-depletion of Ect2 and MgcRacGAP by live-cell imaging. MgcRacGAP depletion in cells expressing only Ect2-BRCT^{TK} resulted in major cytokinetic failure when 50% of the cells failed to form a furrow and 80% of them failed cytokinesis (Figure 54). Expression of

MgcRacGAP- Δ C1/K292L drastically enhanced the furrowing ability of cells, as almost all the cells were able to form a cleavage furrow but most of them failed cytokinesis, consistently with published data (Lekomtsev et al., 2012). Additionally, expression of MgcRacGAP- Δ C1/K292L increased the level of cells that were able to progress through cytokinesis, especially in the case of MgcRacGAP-K292L cell line. Co-depletion of Ect2 and MgcRacGAP resulted only in a slight enhancement of the cytokinetic phenotype, despite the efficient depletion of endogenous Ect2 and MgcRacGAP proteins (Figure 53B). These data suggest that preventing MgcRacGAP's binding to the plasma membrane only weakly enhances the phenotypic severity of cells in which Ect2 no longer associates with the spindle midzone. These data are consistent with Centralspindlin promoting contractility at the plasma membrane but also indicate that the complexes' association with the plasma membrane is not the elusive redundant mechanism driving cytokinesis in Ect2-BRCT^{TK} cells.

6.4 Conclusions - Role of Ect2 midzone recruitment in cleavage furrow formation

We decided to study the role of Ect2 interaction with the spindle midzone in cleavage furrow formation and cytokinesis. Ect2 targeting to spindle midzone requires Plk1 phosphorylation of MgcRacGAP, a subunit of the Centralspindlin complex (Somers and Saint, 2003) (Yuce et al., 2005) (Petronczki et al., 2007) (Burkard et al., 2009) (Wolfe et al., 2009). Ect2 interacts with MgcRacGAP via phosphate binding by its BRCT1 domain. The crucial residues for this are T153 and K195, and their mutation has been shown to prevent the interaction both *in vitro* and *in vivo* (Wolfe et al., 2009) (Zou et al., 2014). Therefore, we generated stable cell lines expressing full-length BRCT-mutated Ect2 protein (Ect2-BRCT^{TK}) to study the importance of the interaction of Ect2 with the spindle midzone.

Firstly, we have shown that Ect2-BRCT^{TK} protein does not localize to spindle midzone using both fixed-cell IF analysis and live-cell imaging. We have followed the localization of Ect2-BRCT^{TK} protein in dividing cells and compared the localization pattern to the wild-type Ect2 protein. Ect2's interaction with the cell membrane was not affected by the BRCT mutations and Ect2-BRCT^{TK} protein

localized to the plasma membrane shortly after anaphase onset like the wild-type Ect2. However, Ect2-BRCT^{TK} mutant showed even distribution along the plasma membrane with only small enrichment at the cell equator, likely a non-specific phenomenon. These results provide the strongest evidence yet that the interaction of Ect2 with Centralspindlin at the spindle midzone is required for and may direct the equatorial enrichment of Ect2 at the plasma membrane.

Subsequently, we interrogated the ability of Ect2-BRCT^{TK} to support cytokinesis. We depleted endogenous Ect2 in Ect2-BRCT^{TK} expressing cells and quantified the level of multi-nucleation levels by IF analysis. Control cells expressing only the GFP-tag became multi-nucleated after depletion of endogenous Ect2. As shown previously, expression of the Ect2-WT could fully rescue cytokinesis defects (Su et al., 2011). Surprisingly, Ect2-BRCT^{TK} transgene could rescue cytokinesis to a similar extent. We confirmed this unexpected result by following the division in live cells after depletion of endogenous Ect2. Additionally, we also demonstrated that distribution of contractile ring proteins, RhoA and Anillin was not affected in Ect2-BRCT^{TK} expressing cells.

Analysis of cytokinetic competency of Ect2-BRCT^{TK} protein demonstrated Ect2-BRCT^{TK} could support cleavage furrow formation at the equator and cytokinesis, despite the apparent inability of the mutant protein to bind Centralspindlin, accumulate at the spindle midzone or at the equatorial plasma membrane. Our results show that Ect2 midzone binding and the enrichment of Ect2 at the equatorial plasma membrane are not crucial for cytokinesis in otherwise unperturbed human cells. Ect2 equatorial accumulation has been proposed to specify the zone of active RhoA and thus position the cleavage furrow (Yuce et al., 2005) (Petronczki et al., 2007) (Su et al., 2011). Our data, however, are not consistent with this hypothesis. Our previous results obtained by chemical genetic and optogenetic systems demonstrate that Ect2 binding to the plasma membrane is essential for cytokinesis and that the local presence at the presumptive cleavage site is likely to be essential. However, the results obtained in BRCT mutant cells suggest that this equatorial enrichment is not essential for cleavage furrow placement and formation. The interaction of Ect2 with Centralspindlin was the best molecular candidate for explaining how the spindle midzone directs equatorial

contractility. Thus, our new results require a reinterpretation of models for cleavage furrow placement and formation as well as reconsidering the role of Plk1 activity in cleavage furrow formation. It is conceivable that the small enrichment of Ect2-BRCT^{TK} protein at the later stages of cytokinesis is enough to drive the cleavage furrow formation on its own, but we do not favour this option, as it would not be a very robust mechanism. One disadvantage of our study is that we were able to follow localization of Ect2 protein but not its activity. It is therefore possible that the small pool of Ect2-BRCT^{TK} that accumulates at the equatorial part of the membrane is the active pool of the protein and it might be sufficient to drive cytokinesis. Nevertheless, there must be a mechanism that specifies the active pool of Ect2, which is currently not known. Further research will be necessary to explore this possibility.

Based on our data, it seems clear that enrichment of the RhoGEF Ect2 at the equatorial plasma membrane at anaphase is insufficient to account for furrow formation. Ect2 binding to Centralspindlin and its accumulation at the equatorial membrane could provide one of the signals that help place the furrow in the middle of the cell, but this signal could be redundant with other mechanisms and signals, at least under conditions used in this study. At this point, it is possible that Ect2's interaction with Centralspindlin plays no important or even redundant role in cytokinesis at all. Given the apparent inconsistency with models put forward by others and us, our results emphasize the importance of renewed efforts to dissect and identify the molecular mechanisms that position the cleavage furrow in animal cells.

Our next experiments attempted to determine the potential redundant mechanisms that specify the position of the cleavage furrow in the Ect2-BRCT^{TK} expressing cells. Firstly, we examined the role of astral microtubules that have been shown to inhibit contractility at the polar regions (Bringmann and Hyman, 2005) (Dechant and Glotzer, 2003) (Werner et al., 2007) (Foe and von Dassow, 2008). We employed the treatment with low concentration of nocodazole that should compromise astral microtubules but not the microtubules of the spindle midzone. Cells expressing Ect2-WT or Ect2-BRCT^{TK} proteins were not affected by low nocodazole treatment at the metaphase-to-anaphase transition and vast majority of the cells successfully

completed cytokinesis without the endogenous Ect2 protein. Therefore, our data suggest that astral microtubules do not cooperate with equatorial accumulation of Ect2. Interestingly, in the control GFP-tagged only cell line, the treatment with low nocodazole strongly enhanced the cytokinetic phenotype and prevented the formation of the cleavage furrow in majority of cells. Our data suggest that astral microtubules do not affect the furrow formation in cells with functional Ect2, but they become important in cells that lack Ect2 protein completely.

Our study suggests that the interaction of Ect2 with MgcRacGAP through the N-terminal BRCT1 domain is not essential in human cells. But this does not rule out the possibility of MgcRacGAP affecting Ect2 or RhoA activity by other mechanisms. Therefore, we tested the hypothesis that MgcRacGAP can specifically activate Ect2 at the equatorial plasma membrane. To this end, we generated double cell lines expressing Ect2-BRCT^{TK} protein together with MgcRacGAP- Δ C1 or with MgcRacGAP-K292L. These cells were unable to target Ect2 to the spindle midzone and MgcRacGAP to the plasma membrane after co-depletion of endogenous Ect2 and MgcRacGAP. Quantification of cytokinetic phenotype after co-depletion of endogenous Ect2 and MgcRacGAP in these cell lines did not result in major enhancement of the cytokinetic failure when combined. Thus, our results do not provide support for a main role of MgcRacGAP's membrane engagement in cleavage plane specification when Ect2 is distributed evenly across the cell membrane.

In summary, we have shown that T153 and K195 mutations in BRCT1 domain of Ect2 majorly disrupt the interaction of Ect2 with Centralspindlin and its recruitment to spindle midzone. Additionally, we confirmed Ect2's equatorial accumulation at the plasma membrane is dependent on the Centralspindlin interaction, and that T153 and K195 mutations abolish this accumulation of the protein. Altogether our data challenge the model that proposes the equatorial Ect2 accumulation is the main signal that specifies the equatorial localization of the cleavage plane in mammalian cells. This is very important result as this was the main model for cleavage plane specification in small somatic cells (Yuce et al., 2005) (Petronczki et al., 2007) (Wolfe et al., 2009) (Su et al., 2011). We propose equatorial accumulation of Ect2 is not the essential signal, but may work as a redundant

signal to help the cleavage furrow formation at the right place. We attempted to identify other possible signals that regulate the positioning of the furrow and studied the role of astral microtubules, MgcRacGAP protein and other cytokinetic factors in our Ect2-BRCT^{TK} expressing cells. Unfortunately, our experiments did not provide any straightforward explanation and further study will be necessary to understand the mechanism that specifies the cleavage plane equatorial localization.

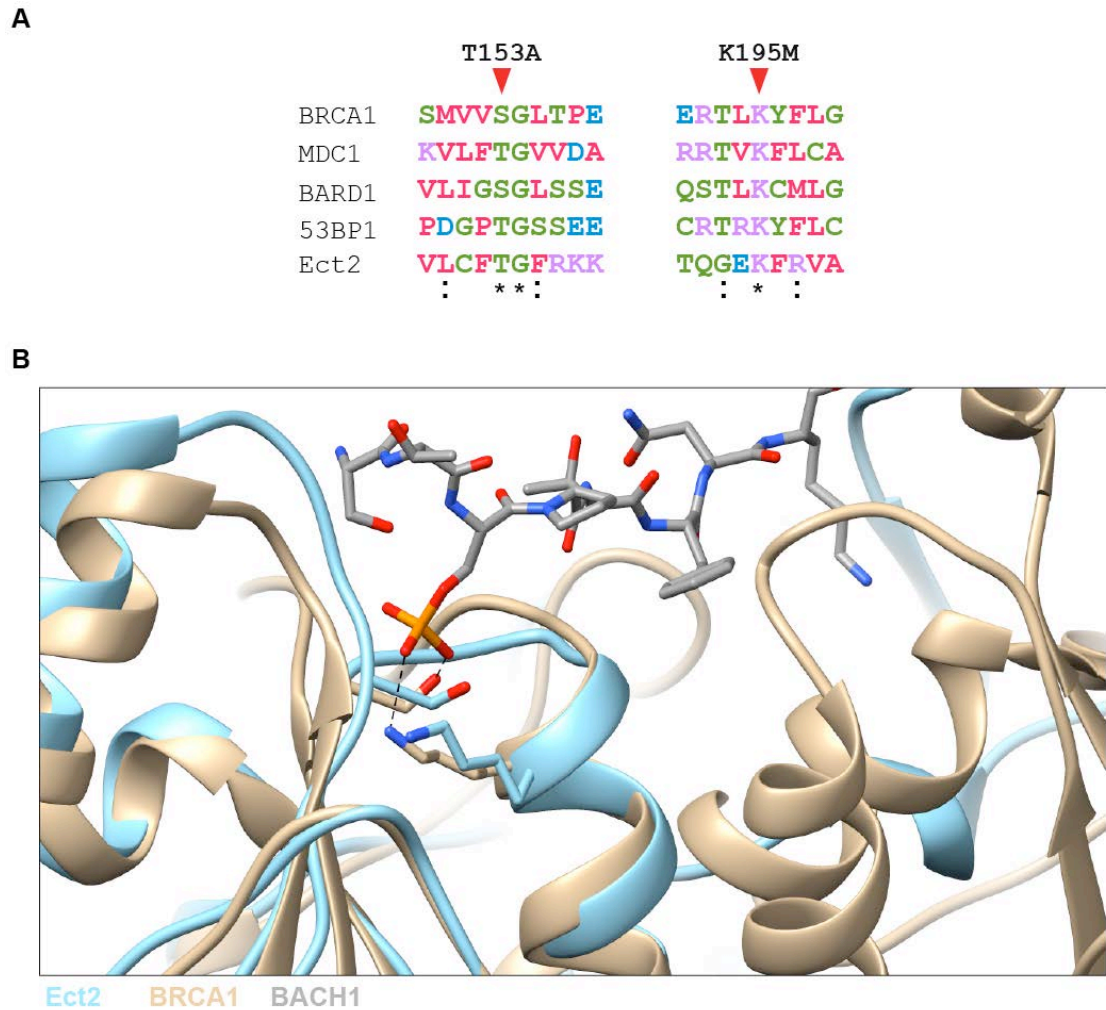


Figure 39 Residues T153 and K195 are conserved in different BRCT domain-containing proteins and they directly coordinate the phosphate from the interacting protein

A Sequence alignment of human BRCT domains from indicated proteins. Highlighted are the conserved residues T153 and K195, which were mutated to prepare the Ect2-BRCT^{TK} construct.

B Crystal structure of N-terminal BRCT domains of Ect2 (PDB ID 4N40; (Zou et al., 2014)) was aligned with a structure of BRCT domains of BRCA1 co-crystalized with bound BACH1 phosphopeptide (PDB ID 1T15; (Clapperton et al., 2004)) using MatchMaker tool in the UCSF Chimera software. Structure of Ect2's BRCT domains is shown in light blue, BRCT domains from BRCA1 in gold. The BACH1 phosphopeptide structure is shown in grey. BRCA1 residues interacting with phosphoserine from BACH1 are highlighted together with their Ect2 counterparts and the hydrogen bonds are shown as dashed lines.

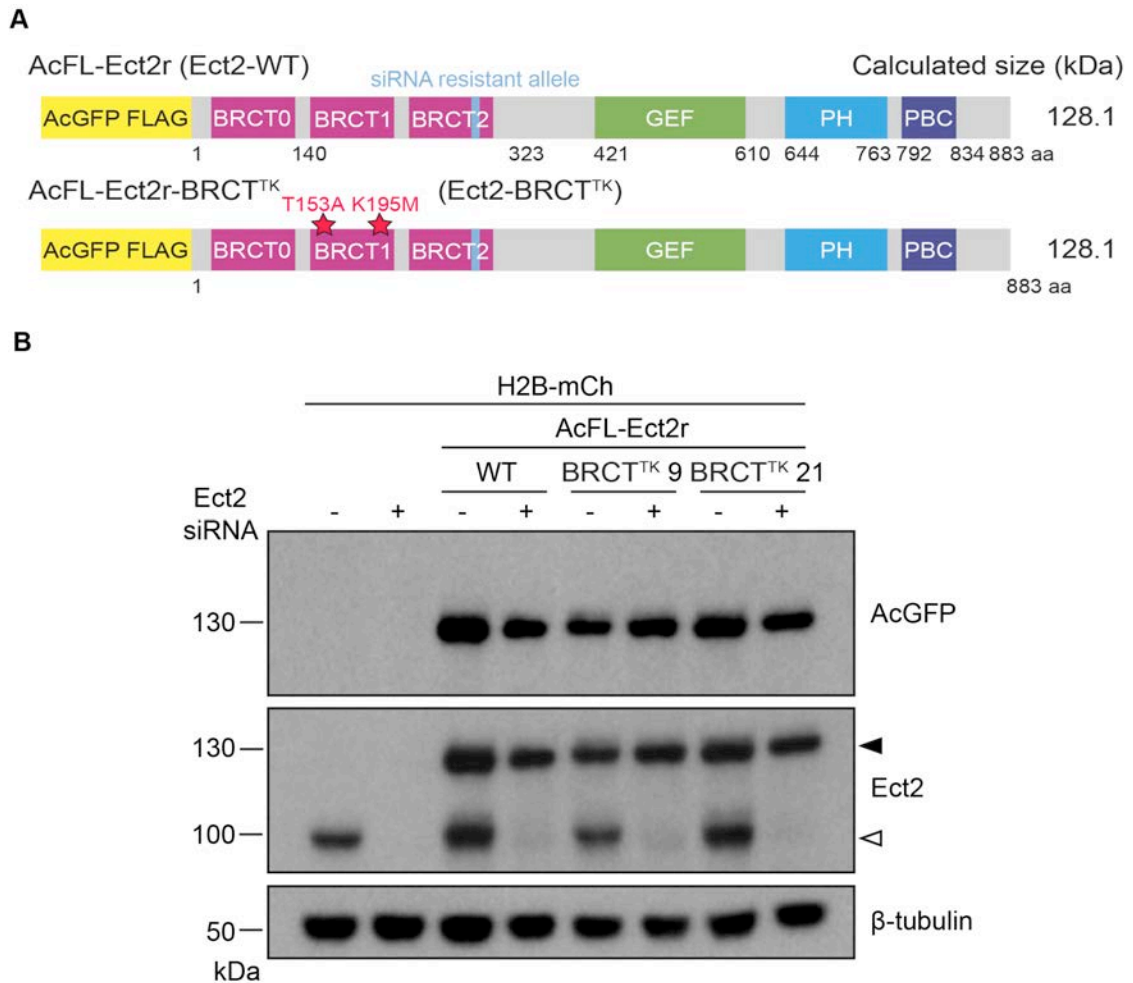


Figure 40 System to study Ect2-BRCT^{TK} localization

A Schematic representation of the domain organization of Ect2-WT and Ect2-BRCT^{TK} constructs used to generate monoclonal HeLaK cell lines for studying the localization of Ect2-BRCT^{TK} protein. Numbering of amino acid residues corresponds to their positions in human full-length Ect2 protein.

B Immunoblot analysis of protein lysates from the indicated cell lines. Protein lysates were prepared 48 hours after transfection with NTC (-) or Ect2 siRNA (+). The immunoblot membrane was probed with antibodies directed against AcGFP, Ect2 and β -tubulin. Endogenous and transgenic Ect2 proteins are indicated by open and filled arrowheads, respectively. > 95% of cells in the transgenic cell lines are GFP positive.

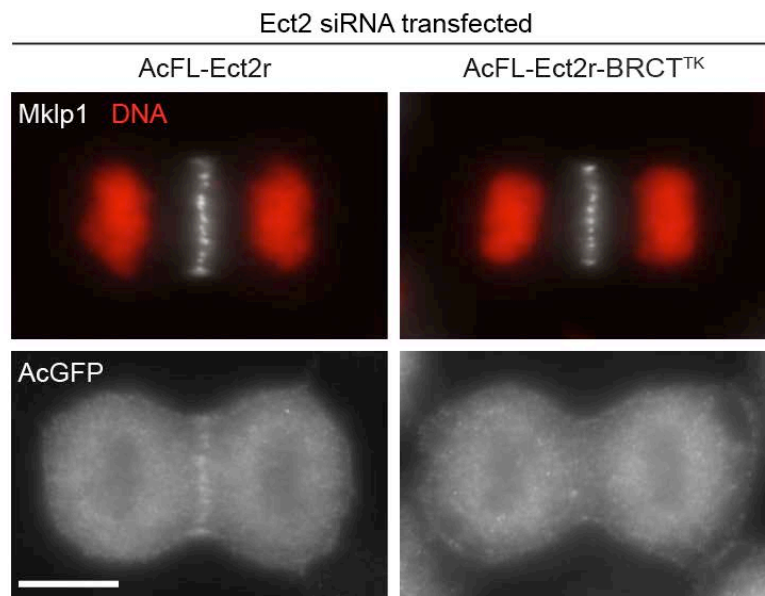


Figure 41 BRCT mutations prevent spindle midzone localization of Ect2

IF analysis of stable cell lines expressing Ect2-WT or Ect2-BRCT^{TK} proteins to show co-localization with the spindle midzone marker Mklp1. Cells were transfected with Ect2 siRNA and synchronized using a thymidine. Cells were released from the thymidine block, fixed and stained with antibodies directed against AcGFP, Mklp1 and with DAPI. Scale bar represents 10 μ m.

Stable cell lines expressing H2BmCherry and transfected with Ect2 siRNA

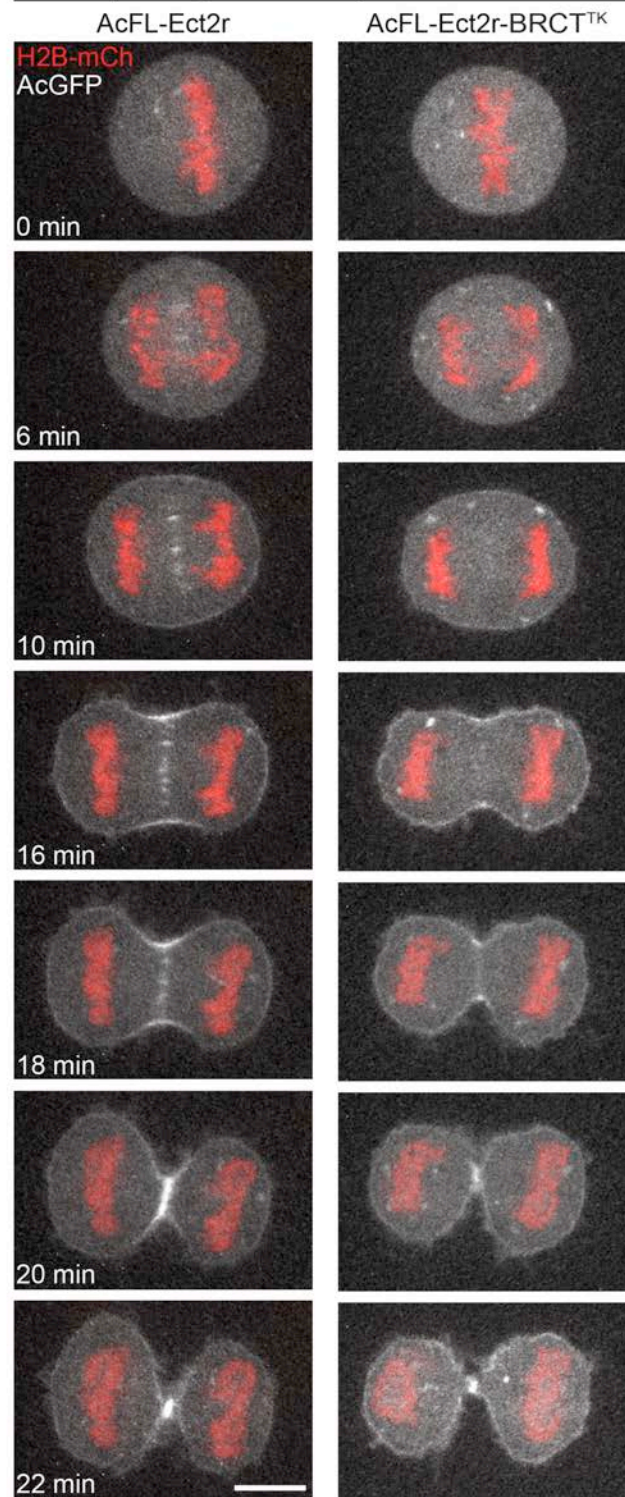


Figure 42 Localization of Ect2-BRCT^{TK} protein during mitosis

Stills from movies obtained on a spinning disk confocal microscope showing the localization of Ect2-BRCT^{TK} protein compared to the wild-type transgene. Stable cell lines were transfected with Ect2 siRNA and imaged 48 hours after transfection. Time point $t = 0$ min was set to the metaphase-to-anaphase transition. Scale bar represents 10 μ m.

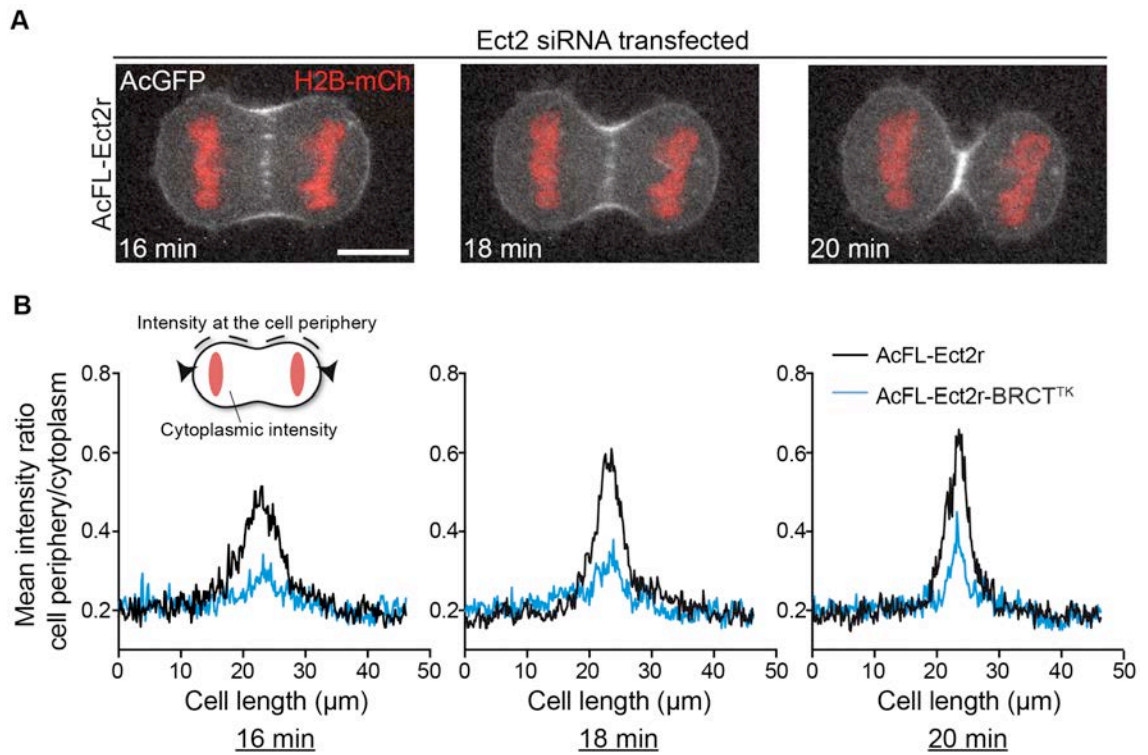


Figure 43 Analysis of peripheral Ect2 localization in anaphase cells

A Representative confocal images used for the analysis in the panel B. The images were obtained as in Figure 42 and they correspond to the graphs in panel B.

B Quantification of the fluorescent intensity profile along the cell membrane for Ect2-WT and Ect2-BRCT^{TK} proteins in cells going through cytokinesis 16, 18 and 20 minutes after anaphase onset. The results are plotted as the mean intensity ratio between the cell periphery and the cytoplasm (schematically depicted in the cartoon) against the measured length. ($n = 6$ for Ect2-WT and $n = 10$ for Ect2-BRCT^{TK}, lines represent mean values)

HeLaK cells expressing H2BmCherry and MyrPalm-GFP

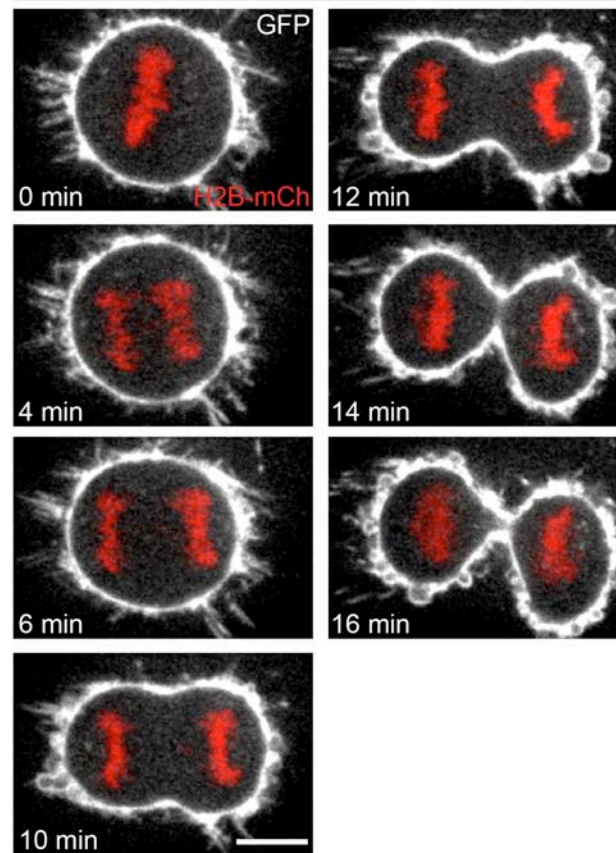


Figure 44 Localization of MyrPalm-GFP protein during mitosis

Stills from movies obtained on a spinning disk confocal microscope showing the localization of MyrPalm-GFP protein. HeLaK cells were transfected with MyrPalm-GFP and H2B-mCherry and imaged 48 hours after transfection. Time point $t = 0$ min was set to the metaphase-to-anaphase transition. Scale bar represents $10 \mu\text{m}$.

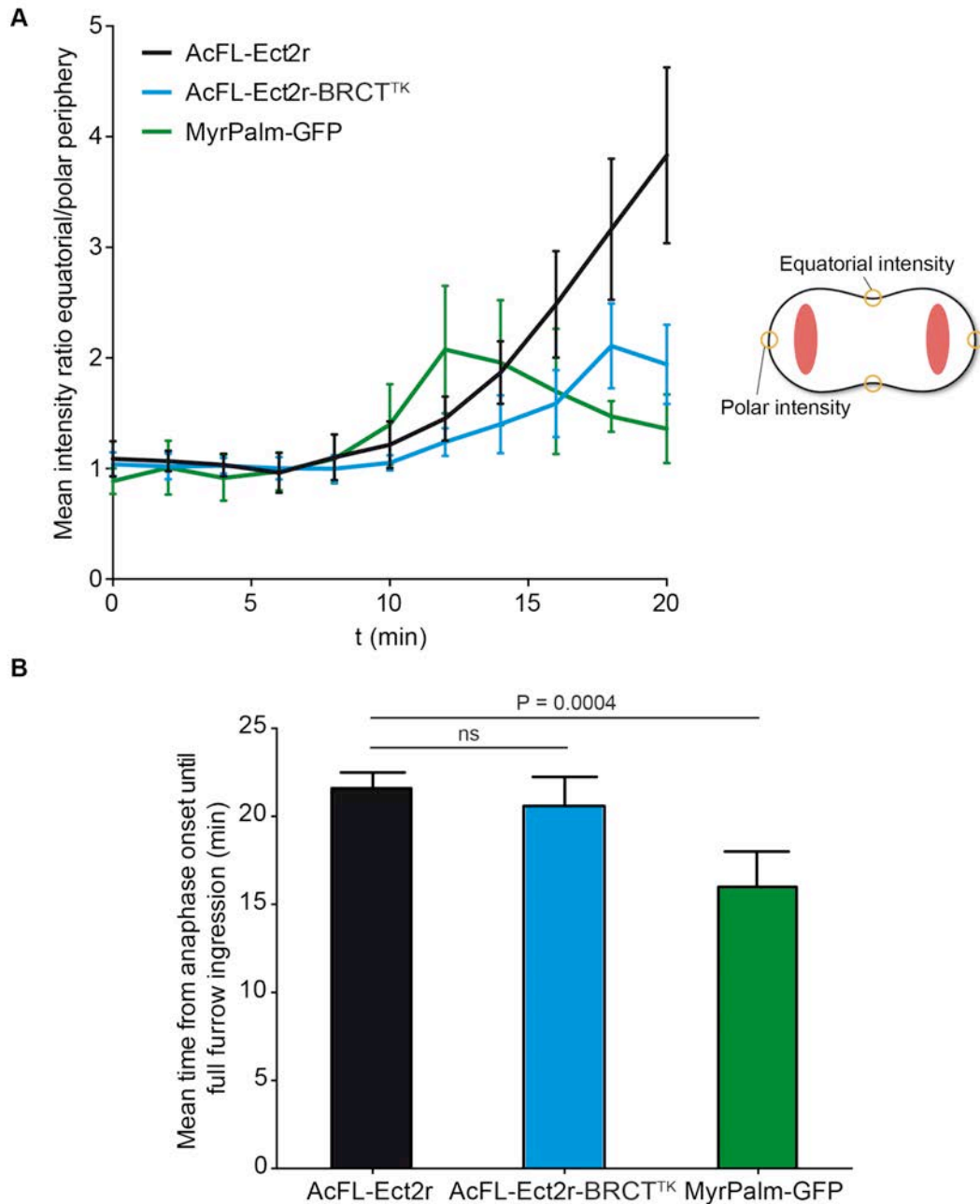


Figure 45 Analysis of the equatorial enrichment of Ect2 at the plasma membrane during mitosis

A Quantification of the equatorial enrichment of Ect2 proteins and MyrPalm-GFP marker over time based on confocal microscope frames (Figure 42, Figure 44). The graph shows the fluorescent intensity ratio between the equatorial and polar membrane, measured from the metaphase-to-anaphase transition ($t=0$ min) until complete furrow ingression. Data were obtained by measuring fluorescence intensity in small circular regions placed as shown on the cartoon on the right side.

B Analysis of the time that indicated cell lines spent in cytokinesis, measured from anaphase onset until full furrow ingression. (Both graphs: $n = 5$ for Ect2-WT and MyrPalm-GFP and $n = 10$ for Ect2-BRCT^{TK}, lines and bars represent mean \pm SD, Student's t-test (B))

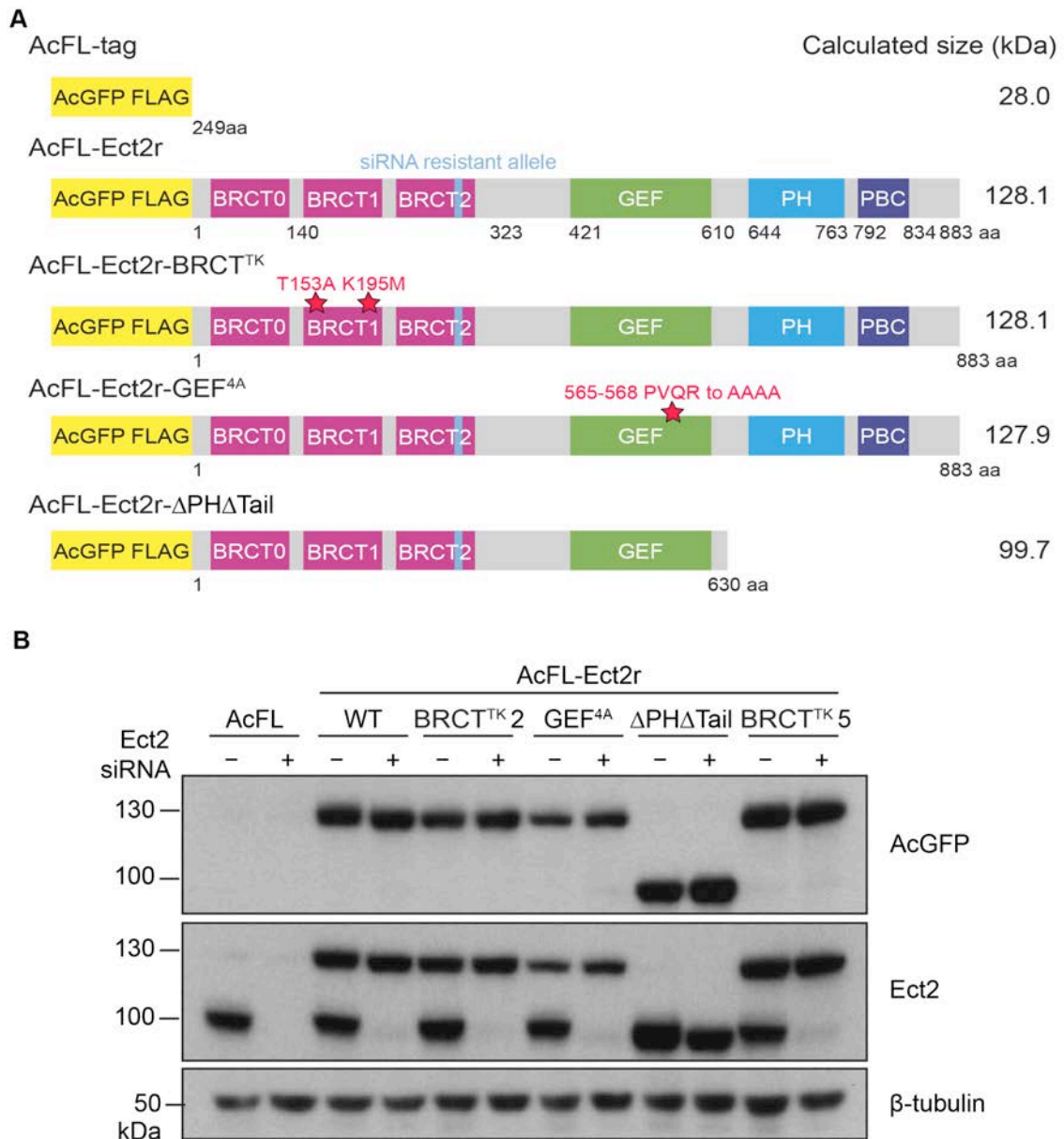


Figure 46 System to study the cytokinetic competency of the Ect2-BRCT^{TK} protein

A Schematic representation of the domain organization of different Ect2 constructs used to generate monoclonal HeLaK cell lines for studying the cytokinetic competency of Ect2-BRCT^{TK} protein. Numbering of amino acid residues corresponds to their positions in human full-length Ect2 protein.

B Immunoblot analysis of protein lysates from the indicated cell lines. Protein lysates were prepared 48 hours after transfection with NTC (-) or Ect2 siRNA (+). The immunoblot membrane was probed with antibodies directed against AcGFP, Ect2 and β -tubulin. > 95% of cells in the cell line populations are GFP-positive.

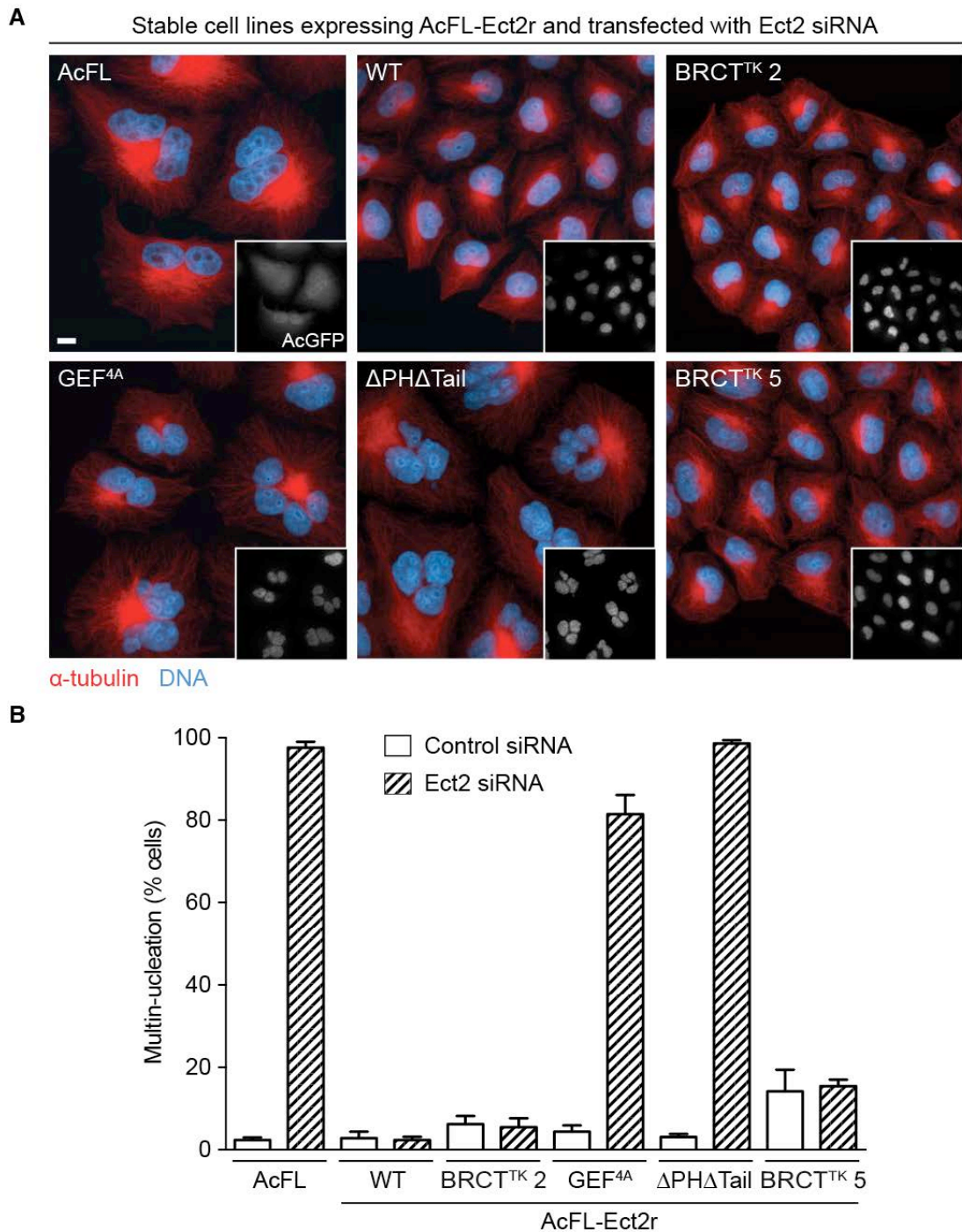


Figure 47 Analysis of the cytokinetic phenotype of Ect2-BRCT^{TK} expressing cells

A IF analysis of indicated stable cell lines. Cells were transfected with Ect2 siRNA and fixed and stained with antibodies directed against AcGFP, α -tubulin and with DAPI 48 hours after siRNA transfection. Scale bar represents 10 μ m.

B Quantification of multi-nucleation levels. Indicated cell lines were treated as described above (panel A). ($n > 300$, bars represent mean \pm SD of three independent experiments).

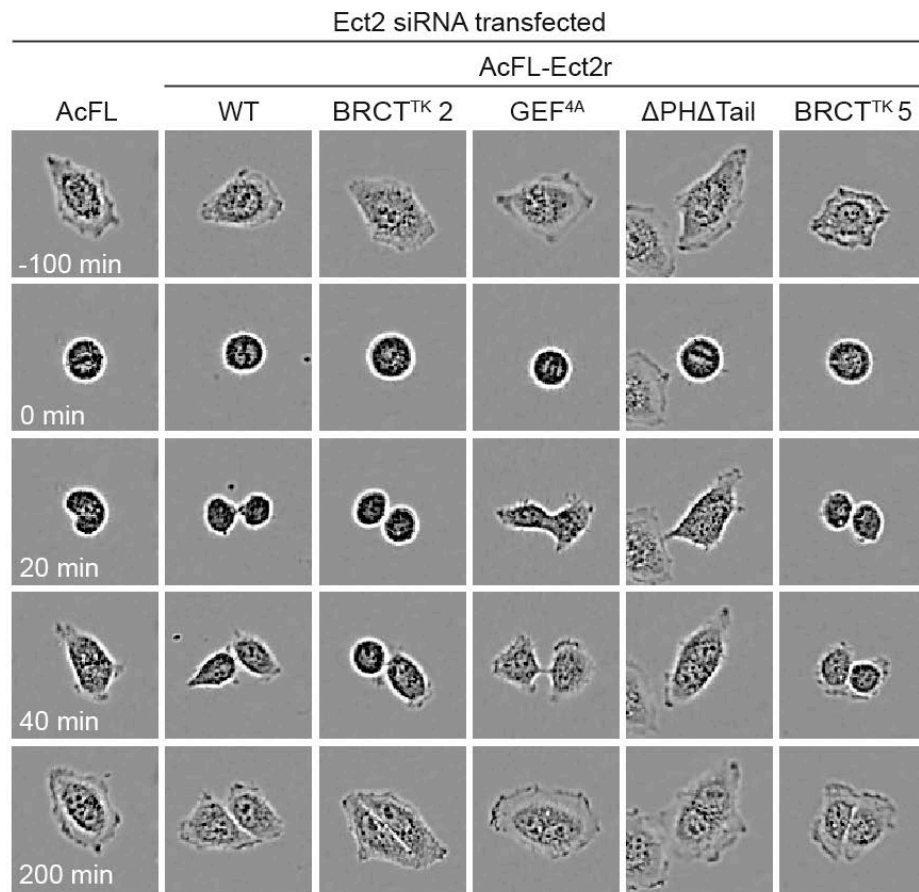


Figure 48 Live-cell imaging analysis of the cytokinetic phenotype of Ect2-BRCT^{TK} expressing cells

Representative images showing cytokinetic phenotypes for the set of cell lines (Figure 46A) after depletion of endogenous Ect2. Cells were transfected with Ect2 siRNA and imaged with BF microscopy starting 24 hours after transfection. Time point $t = 0$ min was set to metaphase-to-anaphase transition.

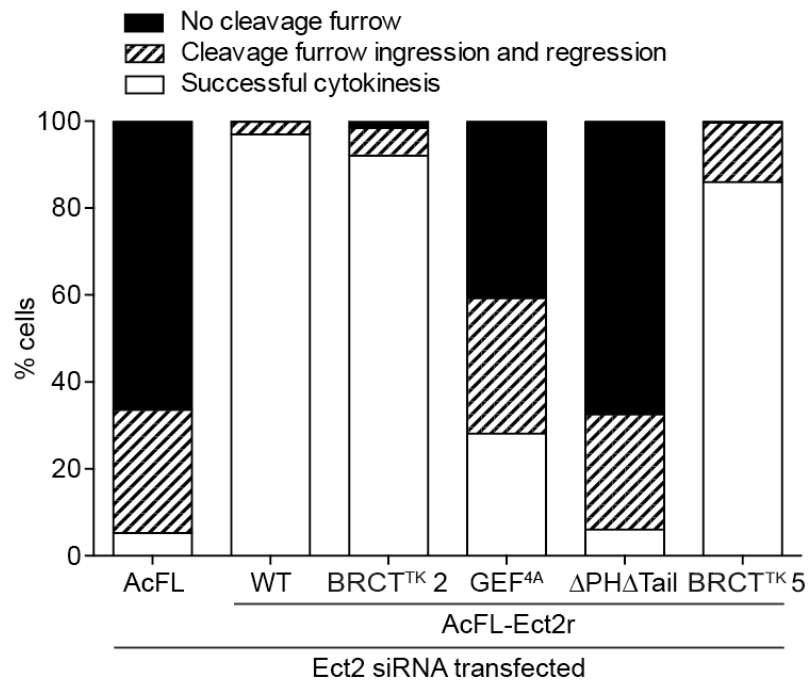


Figure 49 Quantification of the cytokinetic phenotype of Ect2-BRCT^{TK} expressing cells obtained by live-cell imaging

Indicated cell lines were treated as described above (Figure 48). Mono-nucleate cells undergoing cell division were scored from 24 to 48 hours post transfection. (n > 300, bars represent mean values of three independent experiments)

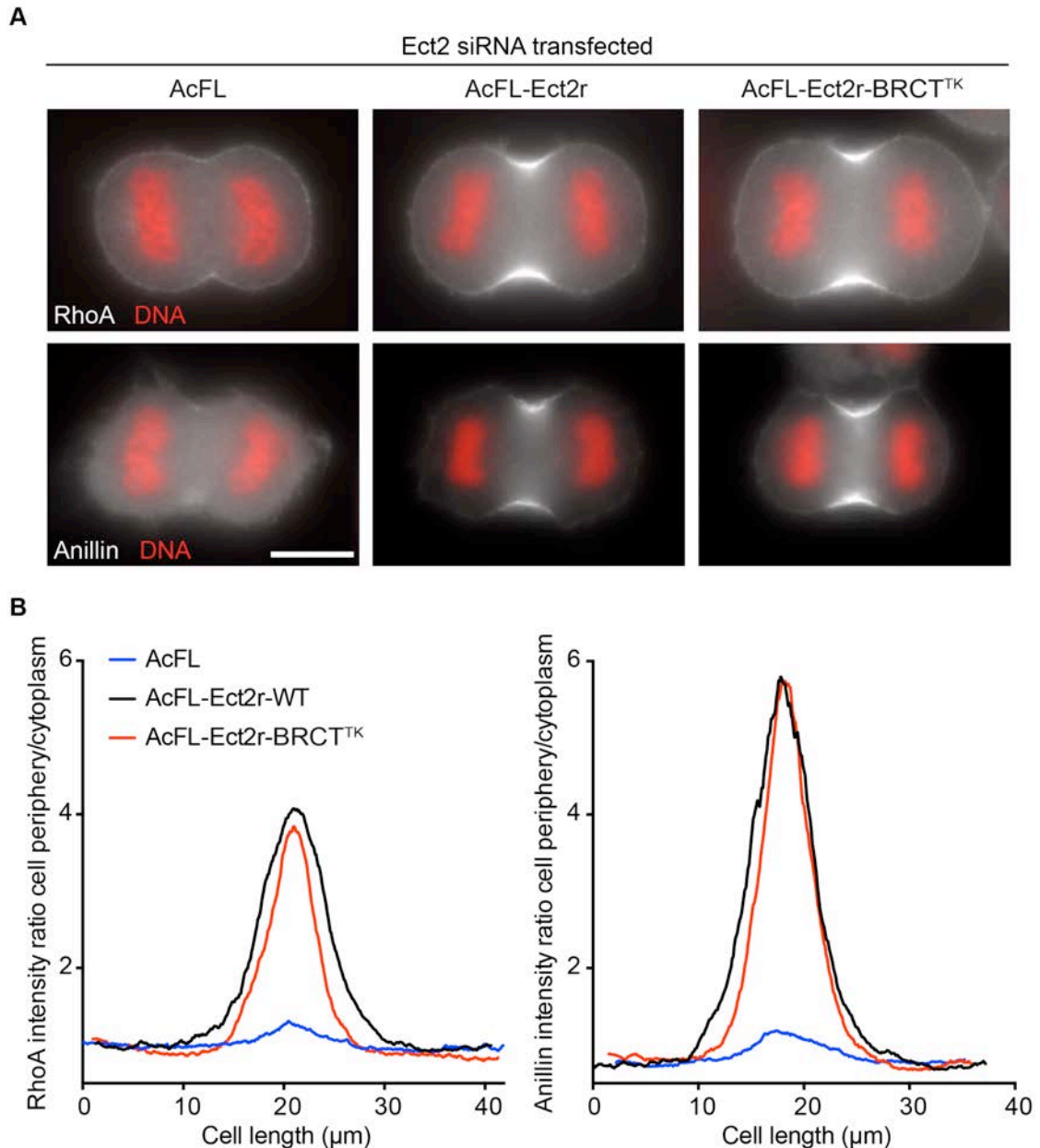


Figure 50 RhoA and Anillin localization in Ect2-BRCT^{TK} expressing cells

A IF analysis of RhoA and Anillin in indicated cell lines. Cells were transfected with Ect2 siRNA and thymidine was added to synchronize the cells in mitosis. Cells were released from the thymidine block, fixed and stained with antibodies directed against RhoA or Anillin, together with AcGFP and DAPI for DNA. Scale bar represents 10 μm .

B Quantification of the fluorescent intensity profile along the cell membrane for RhoA and Anillin in anaphase cells (as shown in panel A). The results are plotted as the mean intensity ratio between the cell periphery and the cytoplasm (as in Figure 43B) against the measured length. ($n = 15$, lines represent mean values)

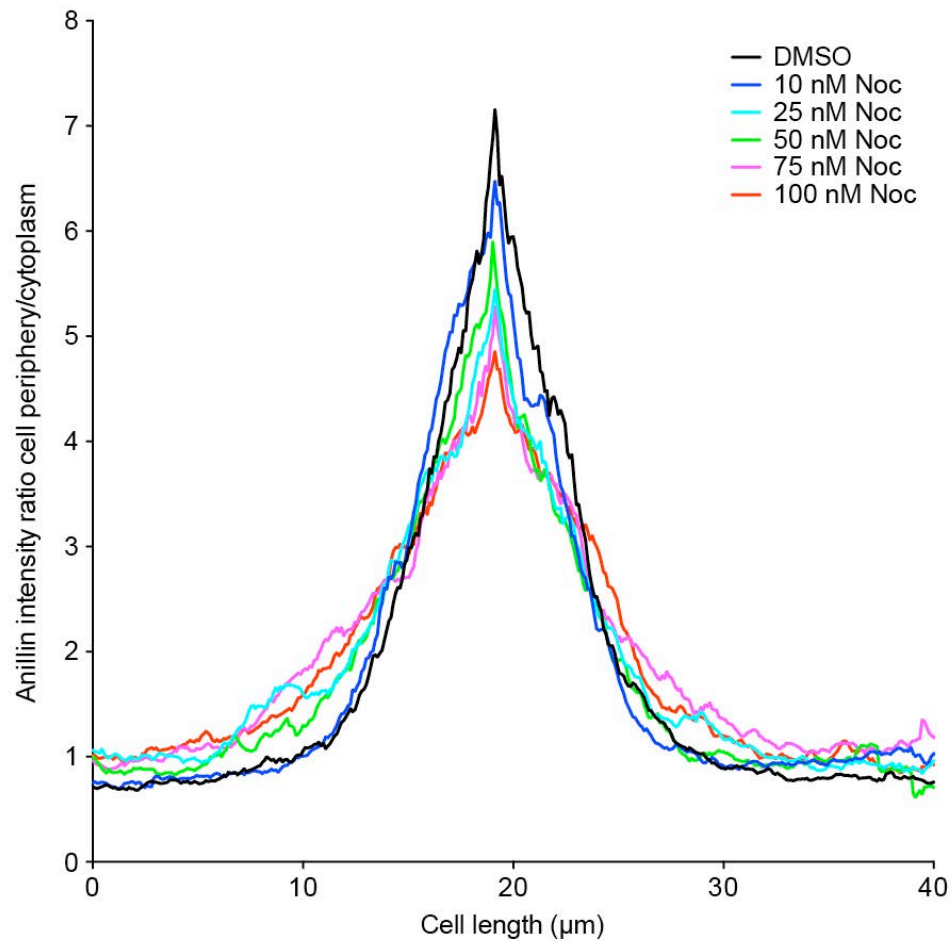


Figure 51 Treatment with low concentration of nocodazole broadens the cortical zone of Anillin in anaphase cells

Quantification of the Anillin fluorescent intensity profile along the cell membrane in anaphase cells treated with different concentration of nocodazole (Noc). After Ect2 siRNA depletion, Ect2-WT expressing cells were synchronized in metaphase using a previously described synchronization protocol (Petronczki et al., 2007). 45 minutes after release from the metaphase block, cells were treated with DMSO or different concentrations of nocodazole and analysed by IF 10 minutes after addition of Noc or DMSO. The results are plotted as the mean intensity ratio between the cell periphery and the cytoplasm against the measured length. (n = 8, lines represent mean values)

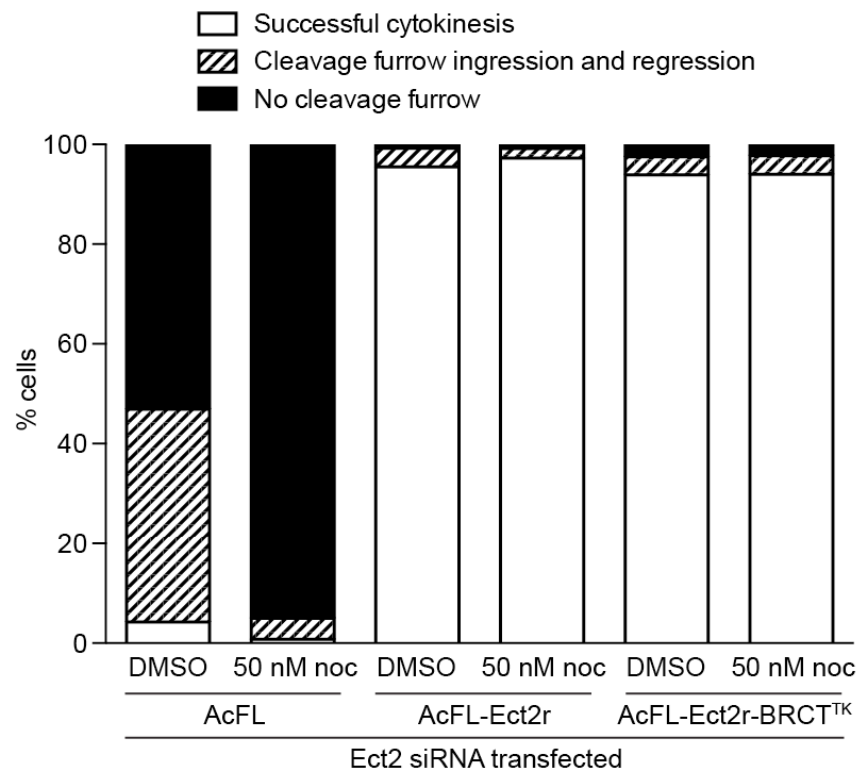


Figure 52 Treatment with low doses of nocodazole does not cause synergistic cytokinetic defects in Ect2-BRCT^{TK} expressing cells

Quantification of cytokinetic phenotype using live-cell imaging analysis after treatment with 50 nM nocodazole during the metaphase-to-anaphase transition. After transfection with Ect2 siRNA, cells were synchronized in metaphase using a previously described synchronization protocol (Petronczki et al., 2007). 45 minutes after release from the metaphase block, the cells were treated with DMSO or 50 nM nocodazole and imaged by BF microscopy. Mono-nucleated cells that were in metaphase at the beginning of the time-lapse imaging were scored ($n > 80$, bars represent mean values of three independent experiments).

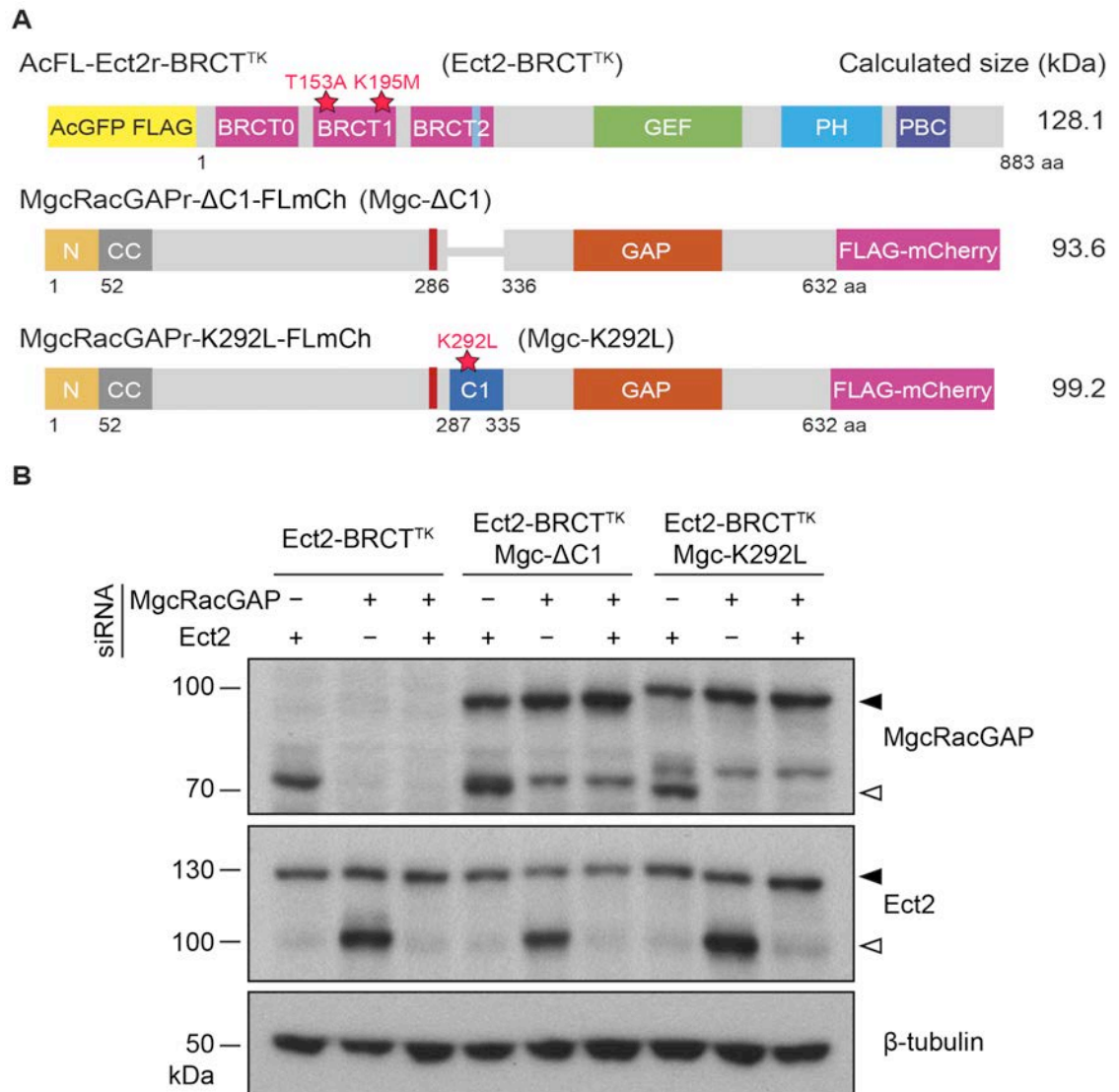


Figure 53 System of double cell lines expressing Ect2-BRCT^{TK} and Mgc-ΔC1/K292L to test the role of MgcRacGAP's membrane interaction for furrowing

A Schematic representation of the domain organization of different constructs used to generate monoclonal HeLaK cell lines expressing Ect2-BRCT^{TK} and Mgc-ΔC1 or Mgc-K292L. Numbering of amino acid residues corresponds to their positions in human full-length Ect2 and MgcRacGAP proteins.

B Immunoblot analysis of protein lysates from the indicated cell lines. Protein lysates were prepared 48 hours after transfection with NTC (-) and MgcRacGAP or Ect2 siRNA (+). The immunoblot membrane was probed with antibodies directed against MgcRacGAP, Ect2 and β-tubulin. Endogenous and transgenic MgcRacGAP or Ect2 proteins are indicated by open and filled arrowheads, respectively. > 95% of cells in the cell line populations are GFP-positive.

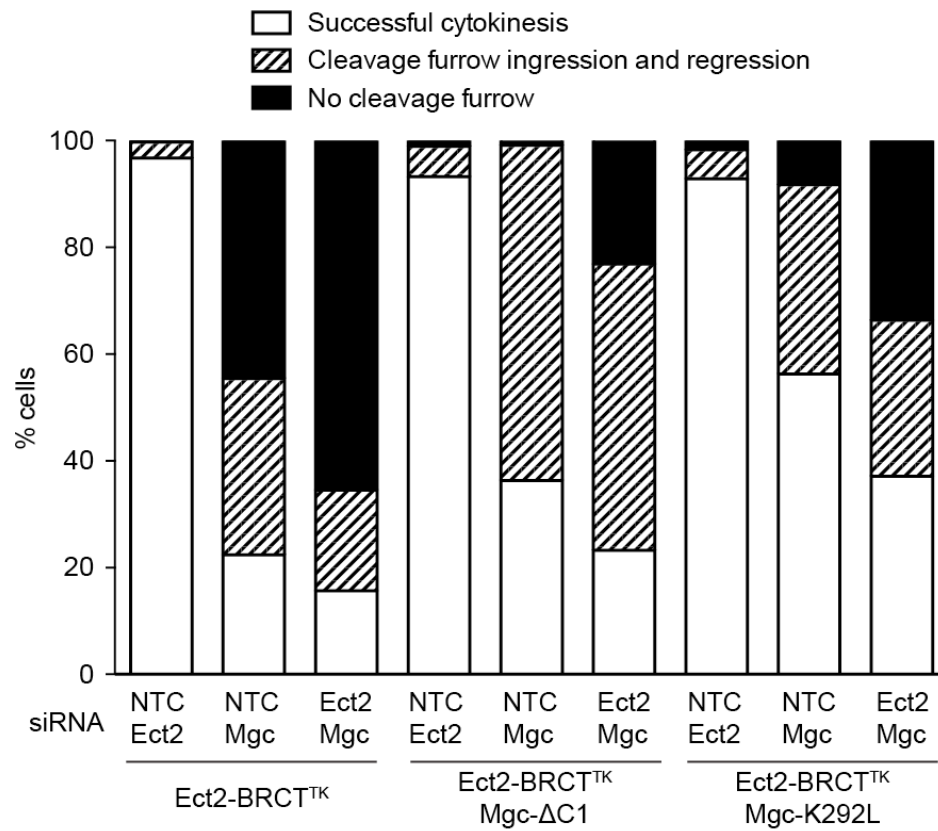


Figure 54 Co-depletion of Ect2 and MgcRacGAP causes minor enhancement of cytokinetic defects in Ect2-BRCT^{TK} and Mgc-ΔC1/K292L expressing cells

Quantification of cytokinetic phenotype using live-cell imaging analysis after depletion of endogenous Ect2 and MgcRacGAP. Cells were transfected with Ect2 and MgcRacGAP siRNA and 6 hours after transfection, the medium was changed. Cells were imaged with BF microscopy starting 24 hours after siRNA transfection. Mono-nucleate cells undergoing cell division were scored from 24 to 60 hours post transfection. (n > 100, bars represent mean values of three independent experiments).

Chapter 7. Discussion

It has previously been demonstrated that the GEF activity of Ect2 is necessary to activate RhoA during cytokinesis (Prokopenko et al., 1999) (Somers and Saint, 2003) (Yuce et al., 2005) (Su et al., 2011). Recent studies from our laboratory have shown that Ect2 interacts with the plasma membrane during anaphase via its PH domain and polybasic cluster located in the C-terminus of the protein (Su et al., 2011). Deletion of both membrane interaction moieties completely blocked the activation of RhoA, cleavage furrow formation and cytokinesis. This indicated that the ability of Ect2 to associate with the plasma membrane is an indispensable and key requirement for cytokinesis. Furthermore, Centralspindlin depletion experiments demonstrated that removal of Ect2's midzone anchor prevents its accumulation at the equatorial plasma membrane during anaphase (Su et al., 2011). This suggested that the interaction with the spindle midzone directs the concentration of Ect2 at the equatorial part of the plasma membrane, and this specific accumulation of Ect2 at the midzone and the cell periphery was proposed to be the main signal for placing the cleavage furrow in the middle of the cell by stimulating RhoA activity around the equator (Somers and Saint, 2003) (Yuce et al., 2005) (Su et al., 2011). Thus, the association of Ect2 with Centralspindlin and the concentration of the RhoGEF protein at the equatorial membrane were predicted to be essential molecular interactions for cleavage plane specification, a key unresolved problem in cell biology. In this study, we have focused on testing this hypothesis experimentally in human cells, in order to expand our knowledge about furrow formation during cytokinesis in animal cells and the role of Ect2 in this process.

7.1 Polyanionic phosphoinositide lipids are implicated in recruiting Ect2 to the plasma membrane

To gain further insight into Ect2's interaction with the plasma membrane, we decided to study which lipids are important for the membrane binding of Ect2. Previous experiments in our laboratory using recombinant proteins and surface-immobilized lipids pinpointed phosphoinositides as the most likely candidates for the interacting lipids (Su et al., 2011). Consequently, in the current

study, we employed several pharmacological treatments to change the lipid composition of the cell membrane and to study the impact of these treatments on Ect2 binding to the plasma membrane by fluorescence confocal microscopy. Our experiments harnessing calcium-dependent activation of phospholipase C strongly suggested PIP2 as the main interacting lipid with a possible contribution of PI4P binding. Conversely, experiments with phosphoinositide 3-kinases inhibitors did not support a strong contribution of phosphoinositides with a phosphorylated hydroxyl group in position 3 to Ect2's membrane interaction, although due to technical difficulties we cannot rule out the possibility that these lipid species may play a minor role. Furthermore, we were unable to distinguish between PIP2 and PI4P contributions to Ect2's membrane binding as we experienced technical difficulties when testing the rapamycin-controlled system of hybrid phosphatases (Hammond et al., 2012). Due to the high transfection efficiency of HEK-293T cells this system is normally more suitable for the genetic lipids manipulation studies than HeLaK cells, however, HEK-293T cells did not tolerate well the ectopic expression of the C-terminal fragment of Ect2 (Ect2CT), a highly active GEF and activator of RhoA (Su et al., 2011) (Su et al., 2014). We speculate that this led to a poor efficiency of obtaining cells co-expressing both components of the rapamycin-controlled hybrid phosphatase system together with Ect2CT. To overcome these hurdles, stable expression of full-length Ect2 GFP-tagged with in HEK-293T cell will be required. This could enable more detailed analysis of the lipid requirements for Ect2's interaction with the plasma membrane using genetic methods specifically in anaphase cells.

Nevertheless, our results supporting the role of PIP2 and PI4P are in line with the biochemical *in vitro* lipid interaction assays performed previously in our laboratory (Su et al., 2011). Recent work has suggested that PIP2 and PI4P together contribute to the identity of the plasma membrane (Hammond et al., 2012). The implication of PIP2 and PI4P in Ect2 binding to the cell membrane suggests that these two polyanionic phosphoinositide species could provide a "postcode" for Ect2 and target it to the equatorial plasma membrane rather than other cellular membrane compartments. This interaction may be prevented in interphase cells and prior to anaphase onset during mitosis by nuclear sequestration of Ect2, intramolecular autoinhibition and Cdk1-mediated phosphorylation (Tatsumoto et al.,

1999) (Chalamalasetty et al., 2006) (Saito et al., 2004) (Kim et al., 2005) (Yuce et al., 2005) (Su et al., 2011). Moreover, PIP2 has been shown to accumulate at the cleavage furrow and its presence is important for cytokinesis progression (Emoto et al., 2005) (Field et al., 2005b). It is tempting to speculate that PIP2 depletion from the equatorial plasma membrane could partially prevent cytokinesis due to compromised Ect2 binding to the membrane and that PIP2 binding can support the equatorial accumulation of Ect2. On the other hand, our experiments with the Ect2-BRCT^{TK} mutant showed that preventing the interaction of Ect2 with the spindle midzone is sufficient to disrupt this preferential accumulation. Thus the membrane lipids provide an interacting partner to allow the membrane interaction of the protein, but probably do not control the spatial distribution of Ect2 at the periphery. Further research will be necessary to show if specific phosphoinositides contribute to cytokinesis by affecting Ect2's recruitment and distribution at the plasma membrane in any way. Additionally, further experiments will have to address which of Ect2's membrane engagement domains binds to which lipid species. PH domains often interact with phosphoinositides (Lemmon, 2008). Although an interesting subject for future studies, the results obtained in our artificial membrane targeting experiments, which are discussed below, indicate that the exact molecular mode of Ect2's interaction with the plasma membrane may not be essential for the action of the molecule during cytokinesis.

7.2 Chemical genetics demonstrate that interaction of Ect2 with the plasma membrane is essential for cytokinesis

In the second part of our study, we focused on the interaction of Ect2 with the plasma membrane and its role for cytokinesis in human cells. We set up a system for the artificial membrane targeting of hybrid Ect2 proteins containing a C1B domain from PKC α that rapidly translocates to the cell membrane upon treatment with phorbol esters such as TPA. We generated a set of stable cell lines expressing Ect2-C1B hybrid proteins, in which the membrane-interacting domains of Ect2 had been replaced with the C1B domain. Both by IF analysis and by live-cell imaging experiments we could demonstrate that artificial membrane targeting of Ect2-C1B can replace the otherwise essential role of PH domain and PBC from Ect2, and at least partially restore cytokinesis upon depletion of the endogenous protein.

Experiments with a C1B mutant version (Ect2-C1B^{Q27G}), which is unable to interact with TPA and to be targeted to the plasma membrane upon phorbol ester treatment, strongly suggested that the observed rescue effect is dependent on the ability of C1B to bind to the plasma membrane. Taken together, these results unequivocally show that the main role for Ect2's PH domain and polybasic tail is to mediate the translocation of the protein to the plasma membrane. Moreover, they demonstrate that membrane translocation of the RhoGEF Ect2 is a crucial step for cytokinesis in human cells. This indicates that both GEF activity and membrane binding of Ect2 are crucial for RhoA activation and cleavage furrow formation (Prokopenko et al., 1999) (Su et al., 2011).

The hybrid versions of Ect2 also enabled us to acutely trigger the recruitment of the protein to the plasma membrane at specific stages of cell division. TPA-induced targeting of Ect2-C1B during the metaphase-to-anaphase transition was sufficient to rescue cleavage furrow formation to the same extent as chronic treatment with the phorbol ester. This result strongly suggests that for the execution of cytokinesis the interaction of Ect2 with the plasma membrane is only required from metaphase onwards, and possibly only after anaphase onset, when the interaction is observed normally. It has been previously shown that Ect2 is required for the establishment of a stiff mitotic cell cortex and timely mitotic cell rounding (Matthews et al., 2012) (Kunda and Baum, 2009). In prophase, Ect2 activates RhoA, which triggers actomyosin remodelling to support the shape transformation from a flat interphase cell into a rounded mitotic cell (Matthews et al., 2012). Importantly though, the experiments dissecting Ect2's role in cell rounding were carried out in HeLa cells grown on a fibronectin-coated substrate. Fibronectin is a large glycoprotein present in the extracellular matrix that is important for cell adhesion (Muro et al., 1999). Therefore, cells seeded on fibronectin-coated plates adhere more strongly to the surface, which might enhance the effect of Ect2 depletion on cell rounding. During our experiments, we did not use the fibronectin coating, and it is thus conceivable that the effect of Ect2 depletion on cell rounding is only clearly observable under conditions where cells adhere more strongly. Therefore, further experiments will be necessary to address if the membrane binding of Ect2 is crucial for mitotic cell rounding. Notwithstanding these considerations, preliminary observations made in collaboration between our laboratory and the laboratory of Buzz Baum, suggested

that deletion of Ect2's plasma membrane engagement domains also impairs mitotic cell rounding (Kuan-Chung Su and Helen Matthews, unpublished data). These observations raised the theoretical possibility that Ect2's action at the plasma membrane was only required to establish a stiff mitotic cell cortex during mitotic rounding and that Ect2 interaction with the plasma membrane was not required during cytokinesis. However, our acute TPA addition experiments addressed this point by temporally separating Ect2-membrane engagement during mitotic entry and later stages such as cytokinesis. The fact that TPA-induced membrane targeting of Ect2-C1B from the metaphase-to-anaphase transition onwards was sufficient to support cytokinesis in most cells, allows us to draw two key conclusions: (1) Ect2 action at the cell envelope is key during cytokinesis and (2) timely mitotic cell rounding and the establishment of a stiff mitotic cortex is not an essential prerequisite for cytokinesis.

7.3 There is more to Ect2 than GEF activity and membrane engagement – a key function of the N-terminal region of Ect2?

Published data (Prokopenko et al., 1999) (Su et al., 2011) together with our experiments described here defined the GEF activity and the plasma membrane binding as two indispensable functions of Ect2 for the correct execution of cytokinesis. However, if these two are the only essential functions of Ect2, it should be sufficient to induce the translocation of the GEF domain of Ect2 to the plasma membrane for successful cytokinesis. To test this hypothesis, we generated a hybrid protein containing only the GEF domain of Ect2 fused to a C1B domain (GEF-C1B) and studied its effects on cleavage furrow formation upon TPA-induced plasma membrane targeting. Artificial membrane targeting of GEF-C1B was not able to restore cytokinesis in cells depleted of endogenous Ect2, despite the fact that the GEF-C1B protein was efficiently expressed and translocated to the cell membrane after TPA treatment. This result suggests an important role for Ect2's N-terminal part, missing from the GEF-C1B protein. Notably, cells expressing GEF-C1B showed signs of RhoA hyperactivation with excessive membrane blebbing and irregular shape of the cell membrane after TPA-induced membrane translocation of GEF-C1B. This result is in line with previous observations in human

cells and echinoderm embryos, which suggested that overexpression of Ect2CT results in RhoA hyperactivation and subsequent cytokinesis failure (Su et al., 2011) (Su et al., 2014). To prevent spatially deregulated RhoA hyperactivation, which might mask the rescue activity of GEF-C1B protein, we titrated the amount of GEF-C1B at the plasma membrane by using lower concentrations of TPA. However, we were unable to identify a concentration of the phorbol ester that would promote cytokinetic rescue in the absence of the endogenous Ect2 protein. This further supports the notion that the N-terminal part of Ect2 plays an important role during cytokinesis, possibly through binding to Centralspindlin via its BRCT domains and/or regulating the catalytic activity of Ect2. A regulatory function of the BRCT domains located in the N-terminal part of Ect2 was suggested previously. *In vitro* experiments supported the hypothesis that the N-terminal and C-terminal parts of Ect2 may interact, which was proposed to regulate its activity during cytokinesis (Saito et al., 2004) (Kim et al., 2005). Further research will be necessary to show if this is indeed the case *in vivo*. Experiments addressing the requirement for BRCT-domain mediated binding of Ect2 to Centralspindlin will be discussed in a later section.

7.4 What prevents a metaphase cell from forming a cleavage furrow?

Previous research in our laboratory showed that Cdk1-mediated phosphorylation on T815 within the polybasic tail of Ect2 can inhibit the membrane interaction of the RhoGEF protein before anaphase onset (Su et al., 2014). This result suggested that the membrane translocation of Ect2 could have a role in the temporal regulation of cytokinesis and might serve as a rate-limiting step for the process. In order to test this hypothesis, we decided to study the consequences of premature targeting of Ect2-C1B to the plasma membrane in metaphase cells using high doses of TPA. We studied the phenotype of premature Ect2 membrane targeting by IF analysis and subsequent quantification of the cortical enrichment of RhoA and Anillin. We observed a minor enhancement of RhoA and Anillin membrane localization when Ect2 was targeted to the membrane in metaphase, but no signs of hypercontractility or ectopic furrowing were detected. This suggests that Ect2 membrane translocation is not the rate-limiting step essential for the temporal

regulation of cytokinesis or at least not the sole one. This indicates that multiple inhibitory mechanisms prevent cleavage furrow formation before anaphase onset. Like Ect2, these mechanisms are likely to be under negative regulation by Cdk1 activity, which is known to inhibit the onset of cytokinesis in mitosis and sharply declines at anaphase onset (Niiya et al., 2005) (Potapova et al., 2006) (Sullivan and Morgan, 2007) (Pines, 2011). Notably, premature translocation of GEF-C1B resulted in higher membrane association of RhoA and Anillin compared to the translocation of Ect2-C1B and also exhibited signs of RhoA hyperactivation. This observation further supports the notion that the N-terminal part of Ect2 may have a regulatory function important for cytokinesis.

7.5 Controlling cleavage furrow formation and cytokinesis using optogenetics

Using chemical genetics we have shown that Ect2 membrane translocation plays a crucial role during cytokinesis. To study the cytokinetic regulatory mechanisms further, we decided to determine the spatial requirements of Ect2's plasma membrane interaction. Our artificial membrane targeting system relies on phorbol ester addition to the cell medium, which can provide temporal but not spatial control over membrane association of the protein of interest. To overcome this limitation, we decided to employ optogenetic techniques that respond to a light stimulus. Light activation can be induced by laser illumination, which provides both high temporal and high spatial resolution.

We took advantage of a recently developed dimerization system based on the light-sensitive cryptochrome protein Cry2, which selectively interacts with the CIB1 protein or its N-terminal fragment (CIBN) after illumination with blue light. The original system was built with the light-sensitive Cry2 protein localized to cytoplasm, which translocates to the plasma membrane after blue-light activation through interaction with the CIBN protein that is stably attached to the cell membrane. In order to avoid rapid diffusion of the activated Cry2 protein in the cytoplasm and to thus render the system more spatially restricted, we attempted to swap the two interacting partners. To achieve this, we stably attached the Cry2 protein to the plasma membrane by adding the prenylation CAAX signal at the C-terminus.

Unfortunately, due to currently unknown reasons, membrane-bound Cry2 lost the ability to attract CIBN protein, despite good expression of both proteins and an illumination stimulus. Consequently, we reverted to the original settings and set up a system for the optogenetic targeting of the Ect2 protein lacking its native membrane-targeting domains (Ect2- Δ PH Δ Tail) and we fused this version of Ect2 to mCherry-tagged Cry2 protein (Cry2-mCh-Ect2). For the interacting partner, we generated a cell line expressing GFP-tagged CIBN fragment that is stably localized to the plasma membrane (CIBN-eGFP-CAAX).

Cry2-mCh-Ect2 rapidly translocated to the cell membrane after blue-light illumination, allowing us to repeat the rescue experiments with a light-inducible system. Membrane targeting of Cry2-mCh-Ect2 in metaphase or anaphase cells by blue-light illumination in two small circular regions at the equatorial cortex triggered accumulation of the protein at the equatorial membrane and was able to partially rescue cytokinetic failure after endogenous Ect2 depletion. The rescue effect was dependent on Ect2's interaction with the plasma membrane, as targeting of the control protein Cry2-mCh to the plasma membrane was unable to restore cytokinesis. These results are in line with our experiments with chemical genetic system and further confirm that membrane association during metaphase-to-anaphase transition is a crucial step for cytokinesis in human cells and possibly all animal cells. Blue-light stimulation also enhanced the midzone localization of Cry2-mCh-Ect2 protein. The wild-type version of Ect2 exhibit similar behaviour, which suggest positive feedback system to promote the equatorial localization of Ect2 (Su et al., 2014) and this study. But with Cry2-mCh-Ect2 the enhancement is more pronounced as the midzone localization of Cry2-mCh-Ect2 is visibly weaker. The reasons for weaker midzone localization are currently unknown, but the fusion with large cryptochrome might cause some steric clashes alleviated by blue-light activation.

Another surprising observation was the "tilted" geometry of the chromosomes in cells that express Cry2-mCh-Ect2 that cannot interact with the plasma membrane. This suggests endogenous Ect2 depletion leads to changed spindle geometry, a phenotype not described previously in human cells. Interestingly, role of Ect2 in spindle assembly was proposed in *X. laevis* egg extract (Tatsumoto et al., 2003).

Further research is necessary to show if Ect2 has a role in spindle assembly in human somatic cells.

In order to test the spatial requirements of Ect2 interaction with the cell membrane we targeted Ect2 only to one side of the equatorial membrane in anaphase cells. Spatially restricted accumulation of Cry2-mCh-Ect2 was complicated by its fast diffusion along the cell periphery, but nevertheless, almost all the cells, in which the one-sided accumulation was observed, developed a unilateral furrow at the side of the illumination. This experiment shows that local Ect2 plasma membrane binding at the equatorial furrow is necessary and at least at the equator sufficient to activate RhoA and trigger cleavage furrow formation. Importantly, one-sided accumulation could support furrowing, but could not rescue successful cytokinesis progression. This suggests that Ect2 and presumably RhoA need to be active on both sides of the cleavage furrow for successful execution of cytokinesis in human cells. This result is consistent with the notion that the equatorial accumulation of Ect2 could act as a main signal for cleavage plane specification and furrow formation, although, it does not prove it. It merely demonstrates that the local presence of Ect2 at the plasma membrane at the presumptive furrowing site is required for furrow initiation. Importantly, adjusted spindle geometry was also observed during experiments with one-sided targeting of Cry2-mCh-Ect2 and this spindle change could be responsible for the unilateral localization of Ect2. Nevertheless, the presence of Ect2 is crucial, as no unilateral furrows were observed in cells without blue-light illumination.

Conversely, after unilateral activation at the polar region of anaphase cells, we neither observed a specific accumulation of Ect2 at the site of the illumination nor furrowing activity at the position. As we were unable to target Cry2-mCh-Ect2 to the poles, the question of whether inducing Ect2 accumulation at the plasma membrane in regions outside the cell equator would result in furrow formation remains unanswered. Our inability to induce accumulation of Ect2 at polar regions in the first place could indicate the existence of an inhibitory mechanism preventing excessive accumulation of Ect2 at the poles, thus potentially contributing to the prevention of RhoA activation at the wrong place. Polar astral microtubules were shown to inhibit furrowing at the polar regions (Bringmann and Hyman, 2005)

(Dechant and Glotzer, 2003) (Werner et al., 2007) (Foe and von Dassow, 2008). Therefore, it is possible that astral microtubules may also inhibit the accumulation of Ect2 at the cell poles, which could partially explain their inhibitory effect on furrowing. However, further research will be necessary to address and test this hypothesis.

7.6 Enrichment of Ect2 at the equatorial membrane is not the main signal that places cleavage furrow in somatic cells

Our experiments showing that interaction of Ect2 with the plasma membrane is sufficient and required for cleavage furrow formation supported the model, which proposes that equatorial accumulation of Ect2 specifies the zone of active RhoA and therefore regulates the placement of the cleavage plane. The spindle midzone interaction of Ect2 was proposed to direct the accumulation of Ect2 preferentially at the equatorial membrane (Su et al., 2011). However, despite the fact that Ect2's interaction with Centralspindlin at the spindle midzone occupies a central position in models for cleavage furrow formation (Yuce et al., 2005) (Petronczki et al., 2007) (Wolfe et al., 2009) (Su et al., 2011), the importance of this interaction and thus the role of the equatorial accumulation of Ect2 have never been decisively tested. A previous study suggested that Ect2 localization to spindle midzone might not be essential for early stages of cytokinesis (Chalamalasetty et al., 2006). Importantly though, this study relied on overexpression of different N-terminal fragments of Ect2, which could have introduced artefacts into the system. We decided for the first time to decisively test the role of the recruitment of the RhoGEF Ect2 to the spindle midzone by introducing previously identified mutations into the first BRCT domain of the protein. The mutations T153A and K195M have been shown not only to prevent the interaction of Ect2 with a phosphorylated form of Centralspindlin but also to abrogate the spindle midzone recruitment of a transiently expressed N-terminal Ect2 fragment containing the BRCT repeats (Wolfe et al., 2009) (Zou et al., 2014).

We have used the genetic complementation system developed in our laboratory to generate monoclonal stable cell lines expressing GFP-tagged siRNA-resistant full-length Ect2 with the mutations T153A and K195M (Ect2-BRCT^{TK}). This allowed us

to study the localization and functionality of Ect2-BRCT^{TK} protein in live cells. Our analysis demonstrated that the Ect2-BRCT^{TK} protein does not localize to the spindle midzone indicating the introduction of these two point mutations in the full-length context of Ect2 indeed blocks the interaction with Centralspindlin *in vivo*. Importantly, our data also show that abolishing the interaction of Ect2 with Centralspindlin disrupts the concentration gradient of the protein and thus compromise the accumulation of Ect2 at the equatorial membrane. Although the spatial pattern of Ect2 at the plasma membrane was lost, the BRCT mutations did not affect the temporal control of Ect2 membrane translocation. These results provide strong support for the previously proposed model that Ect2's interaction with Centralspindlin on equatorial microtubules directs the concentration of the protein at the equatorial plasma membrane (Su et al., 2011).

Strikingly though, the inability of Ect2 to interact with the spindle midzone and get concentrated at the equatorial membrane in anaphase cells did not cause cytokinetic failure. The Ect2-BRCT^{TK} mutant protein was able to fully support cleavage plane specification, cleavage furrow ingression and ultimately cytokinesis, as shown both by end-point IF analysis and by live-cell imaging. Furthermore, Ect2's displacement from the spindle midzone did not change the distribution of contractile ring proteins RhoA and Anillin. Combined, our data suggest that Ect2's interaction with the spindle midzone and the equatorial accumulation of the protein are not essential for cytokinesis in otherwise unperturbed human somatic cells.

Importantly, it is possible that the mutations T153A and K195M do not completely prevent the binding of Ect2 to Centralspindlin. Previous studies have used co-immunoprecipitation and ITC and have showed that the mutations prevent the interaction of Ect2 and MgcRacGAP (Wolfe et al., 2009) (Zou et al., 2014). Both of these studies have used truncated versions of Ect2, which might have influenced the results. Our results from live cell imaging of full-length Ect2-BRCT^{TK} strongly supported that T153A and K195M do abrogate the interaction of Ect2 with Centralspindlin, but more experimental evidence is key to verify our results. It is therefore conceivable that small enrichment of Ect2-BRCT^{TK} is sufficient to drive cleavage furrow formation as the main mechanism. Nevertheless, we do not favour this possibility, as this would make the system less robust. Cytokinesis needs to be

efficiently controlled so more likely explanation is that there are more mechanisms that lead to furrow formation in the equatorial part of cell membrane.

One important limitation of our study is that we could only observe Ect2 protein distribution and not its activity as a GEF factor. This could mean even the apparently small enrichment of Ect2-BRCT^{TK} could be enough to specify furrow formation in the middle of the cell. Additional control mechanisms that would regulate activity of Ect2 might exist and that could explain our observations with Ect2-BRCT^{TK} protein. Previous research in our laboratory has shown only 10% of Ect2 is sufficient for efficient furrowing and cytokinesis, which further supports this notion (Su et al., 2011). Future experiments should be focused on the GEF activity of full-length Ect2 in cells going through cytokinesis and they might explain our surprising results.

Results with Ect2-BRCT^{TK} protein show that Ect2's equatorial accumulation is likely not the only or main signal that places the cleavage furrow in the middle of the cell in small somatic cells. Our new data are in disagreement with the model put forward by our laboratory and others (Yuce et al., 2005) (Petronczki et al., 2007) (Wolfe et al., 2009) (Su et al., 2011) (Fededa and Gerlich, 2012) (Green et al., 2012) (Mierzwa and Gerlich, 2014). These findings have important implications for many aspects of current models of cytokinesis. In the light of our findings several previous observations should be re-interpreted and further studies are required to explain the mechanism of cleavage furrow placement in human somatic cells. Our results suggest that the mechanism of furrow establishment is more similar to *D. melanogaster* and *C. elegans* than we previously thought. Orthologs of Ect2 in *D. melanogaster* (Pebble) and *C. elegans* (LET-21) do not localize to the spindle midzone (Prokopenko et al., 1999) (Green et al., 2012), even though Pebble was shown to interact with RacGAP50C (MgcRacGAP) (Somers and Saint, 2003). So in *D. melanogaster* and *C. elegans* cells, the midzone localization of Ect2 is not crucial and our research suggests that the situation in human cells is similar.

Still, the Ect2-Centralspindlin interaction was the best characterized molecular interaction that could provide a rationale for how spatial control of RhoA activation and cleavage plane specification can be achieved at the cell equator. If our

predictions are correct, our data question the importance of this interaction and leave us with no good alternative molecular hypothesis that could explain, how the cleavage plane is placed at the equator, a key question in cell biology. Renewed efforts have to focus on identifying and characterizing these mechanisms involved. Moreover, our data emphasize the need to constantly question and decisively test models.

Our data with the BRCT-mutated Ect2 allele confirm the conclusion of previous work suggesting that Plk1 phosphorylation of MgcRacGAP is required for the assembly of the Ect2-Centralspindlin complex. Depletion of MgcRacGAP or Ect2 as well as inhibition of Plk1 during anaphase all abrogate cleavage furrow formation (Jantsch-Plunger et al., 2000) (Prokopenko et al., 1999) (Tatsumoto et al., 1999) (Yuce et al., 2005) (Petronczki et al., 2007). These findings together with the fact that Plk1 is required for Ect2-Centralspindlin complex formation suggested that Plk1 regulates cleavage furrow formation in this manner (Petronczki et al., 2007) (Burkard et al., 2009) (Wolfe et al., 2009). This view and model can no longer be fully supported. Thus, Plk1 must phosphorylate additional important targets and regulate additional mechanism to control cytokinesis. In summary, our data demonstrate that the hypothesis that the equatorial concentration of Ect2 at the plasma membrane can account for cleavage furrow placement was simplistic and is probably insufficient to explain the process.

If Ect2's equatorial accumulation contributes to the regulation of cleavage furrow formation, it could work in a redundant manner with another signals or mechanisms. Interestingly, combination of two signals, one from spindle midzone and one from astral microtubules, was previously proposed to regulate the localization of the cleavage furrow and its ingression (Bringmann and Hyman, 2005) (Dechant and Glotzer, 2003) (Werner et al., 2007).

In the light of our results, we decided to perform experiments that would combine the effect of Ect2's BRCT-mutations with depletion or inhibition of other cytokinetic factors to identify a potentially redundant second signalling pathway or mechanism. Firstly, we focused on the role of astral microtubules that could inhibit RhoA and/or myosin at the polar regions of anaphase cells. This would be in line with the notion

that both GEF activity and membrane binding of Ect2 are crucial but the equatorial accumulation of the protein is not, because RhoA or the contractile ring could be activated only in the middle of the cell. However, the experiments have shown that in cells with a wild-type Ect2 allele or the Ect2-BRCT^{TK} allele, the depletion of astral microtubules does not cause enhanced cytokinetic failure. On the other hand, in cells lacking Ect2 entirely, the depletion of asters strongly enhanced the cytokinetic phenotype. This suggests that astral microtubules can contribute to the regulation of furrowing in human cells under severely compromised conditions, however, they do not provide a main signal or signal that is redundant with equatorial concentration of Ect2.

We next tested the possible contribution of MgcRacGAP to cleavage furrow formation. MgcRacGAP interaction with Ect2 was proposed to release Ect2's autoinhibition and thus stimulate its activity (Kim et al., 2005) (Yuce et al., 2005) (Wolfe et al., 2009) (Zou et al., 2014). Previous studies suggested that binding of BRCT domains of Ect2 to Plk1-phosphorylated N-terminus of MgcRacGAP is the interaction that activates Ect2. Our results, however, argue against this hypothesis. Nevertheless, MgcRacGAP could still activate Ect2 and RhoA by another mechanism. Notably, MgcRacGAP also binds to the plasma membrane during anaphase via its C1 domain, and this interaction is important for cytokinesis (Lekomtsev et al., 2012). Moreover, recent work from Zhang et al. showed the C-termini of Ect2 and MgcRacGAP could interact *in vitro* (Zhang and Glotzer, 2015). Thus, we decided to test if MgcRacGAP could activate Ect2 at the equatorial plasma membrane. To this end we generated stable cell lines expressing Ect2-BRCT^{TK} together with MgcRacGAP- Δ C1 or MgcRacGAP-K292L. Deletion of C1 domain or its mutation (K292L) prevents the plasma membrane targeting of the MgcRacGAP transgene. Consequently, after co-depletion of endogenous Ect2 and MgcRacGAP by siRNA, these cells were unable to target Ect2 to the spindle midzone and MgcRacGAP to the plasma membrane. However, the BRCT mutations in Ect2 only slightly enhanced the cytokinetic phenotype observed after interfering with MgcRacGAP's C1 domain. Therefore we do not favour the hypothesis that an Ect2-MgcRacGAP interaction independent of the canonical BRCT domain binding mode is an important signal for cleavage furrow formation. Zhang et al. showed that the two proteins could interact *in vitro* via their GEF and

GAP domains, so further experiments will be necessary to rule out the cooperation completely, as we did not disrupt these domains during our experiments. However, it is conceivable that for the activatory binding of MgcRacGAP-Ect2 to be effective, it should occur either at the midzone or at the equatorial plasma membrane to influence RhoA activity at the right place.

In summary, we were as yet unable to identify a simple redundant mechanism that would explain how is the cleavage furrow positioned at the equator in the Ect2-BRCT^{TK} expressing cells after depletion of the endogenous Ect2. The possibility that there are more than two redundant pathways cannot be ruled out at present, and if that is the case, it will be difficult to dissect these pathways experimentally and test their contributions. Further research will be necessary to understand the molecular mechanisms behind the robust furrow formation in human cells. Contributing phenomena and mechanism might involve polar relaxation by protein phosphatase 1 (Rodrigues et al., 2015), the interaction of astral microtubules with the polar cortex (Dechant and Glotzer, 2003) (Werner et al., 2007), a second stimulatory signal from the spindle midzone (e.g.: Aurora B phosphorylation) or a chromosome-derived inhibitory signal (e.g.: a Ran-GTP gradient). These possibilities have to be explored further in isolation and in combination with the Ect2-BRCT^{TK} allele.

Another interesting question arising from our study is, what is the function of the N-terminal BRCT domains that were proposed to have an important regulatory function. Overexpression of Ect2 version lacking the N-terminal BRCT repeats (Ect2CT) have been to shown to enhance the oncogenic activity of Ect2 (Saito et al., 2004) and to change the morphology of flat interphase cells to rounded cells (Saito et al., 2004) (Su et al., 2011) (Matthews et al., 2012). These phenotypes are probably caused by ectopic activation of RhoA via a constitutively active Ect2. Notably, deletion of the two NLS signals of Ect2 is able to replicate these phenotypes (Saito et al., 2004) (Matthews et al., 2012). It is thus conceivable that the phenotype of Ect2CT is due to its cytoplasmic localization caused by the removal of NLS signals and is not linked to the absence of the BRCT domains. In our study, a potential regulatory function of the N-terminal part of Ect2 was suggested by results with artificial membrane targeting of GEF-C1B. Targeting of

GEF-C1B to the plasma membrane also resulted in the cells showing signs of ectopic RhoA activation. Moreover, artificial membrane targeting of GEF-C1B failed to rescue the cytokinetic failure, in stark contrast to targeting of the hybrid Ect2-C1B protein to the plasma membrane. For future experiments, it would be interesting to examine the rescue effect with a construct similar to GEF-C1B with added part containing the two NLS sequences, but still lacking the BRCT domains. Similarly, it would be intriguing to test the cytokinetic phenotype of full-length Ect2 protein that lacks the two NLS sequences, also in combination with the BRCT mutations. Lastly, it remains possible that the N-terminal region of Ect2 harbours an essential yet elusive additional function or ability. A careful mutational analysis of the first two hundred amino acids of the protein is warranted.

Our study provided important insights into the role of Ect2 for cleavage furrow formation in human cells. We have shown that plasma membrane interaction of Ect2 is crucial for cleavage furrow formation and cytokinesis. However, the equatorial accumulation of Ect2 at the plasma membrane is likely not essential and does not alone specify the zone of active RhoA. Therefore the currently favoured model of cleavage plane localization in somatic human cells is not sufficient to explain the mechanism of cytokinesis and should be re-examined. Given the importance of cytokinesis, it may not come as a surprise that multiple signals are likely to cooperate to restrict the furrowing zone, making the system robust and preventing deleterious mistakes. Further research will be necessary to identify and fully understand these signals and conditions under which some of them might become essential.

Reference List

- ABE, Y., OHSUGI, M., HARAGUCHI, K., FUJIMOTO, J. & YAMAMOTO, T. 2006. LATS2-Ajuba complex regulates gamma-tubulin recruitment to centrosomes and spindle organization during mitosis. *FEBS Lett*, 580, 782-8.
- ADAMS, R. R., MAIATO, H., EARNSHAW, W. C. & CARMENA, M. 2001. Essential roles of Drosophila inner centromere protein (INCENP) and aurora B in histone H3 phosphorylation, metaphase chromosome alignment, kinetochore disjunction, and chromosome segregation. *J Cell Biol*, 153, 865-80.
- ADAMS, R. R., TAVARES, A. A., SALZBERG, A., BELLEN, H. J. & GLOVER, D. M. 1998. pavarotti encodes a kinesin-like protein required to organize the central spindle and contractile ring for cytokinesis. *Genes Dev*, 12, 1483-94.
- ADAMS, R. R., WHEATLEY, S. P., GOULDSWORTHY, A. M., KANDELS-LEWIS, S. E., CARMENA, M., SMYTHE, C., GERLOFF, D. L. & EARNSHAW, W. C. 2000. INCENP binds the Aurora-related kinase AIRK2 and is required to target it to chromosomes, the central spindle and cleavage furrow. *Curr Biol*, 10, 1075-8.
- ALEEM, E., KIYOKAWA, H. & KALDIS, P. 2005. Cdc2-cyclin E complexes regulate the G1/S phase transition. *Nat Cell Biol*, 7, 831-6.
- AMANO, M., ITO, M., KIMURA, K., FUKATA, Y., CHIHARA, K., NAKANO, T., MATSUURA, Y. & KAIBUCHI, K. 1996. Phosphorylation and activation of myosin by Rho-associated kinase (Rho-kinase). *J Biol Chem*, 271, 20246-9.
- AMANO, T., KAJI, N., OHASHI, K. & MIZUNO, K. 2002. Mitosis-specific activation of LIM motif-containing protein kinase and roles of cofilin phosphorylation and dephosphorylation in mitosis. *J Biol Chem*, 277, 22093-102.
- ANDREWS, P. D., OVECHKINA, Y., MORRICE, N., WAGENBACH, M., DUNCAN, K., WORDEMAN, L. & SWEDLOW, J. R. 2004. Aurora B regulates MCAK at the mitotic centromere. *Dev Cell*, 6, 253-68.
- ARCHAMBAULT, V. & GLOVER, D. M. 2009. Polo-like kinases: conservation and divergence in their functions and regulation. *Nat Rev Mol Cell Biol*, 10, 265-75.
- ASIEDU, M., WU, D., MATSUMURA, F. & WEI, Q. 2009. Centrosome/spindle pole-associated protein regulates cytokinesis via promoting the recruitment of MyoGEF to the central spindle. *Mol Biol Cell*, 20, 1428-40.
- ASNES, C. F. & SCHROEDER, T. E. 1979. Cell cleavage. Ultrastructural evidence against equatorial stimulation by aster microtubules. *Exp Cell Res*, 122, 327-38.
- ATHERTON-FESSLER, S., PARKER, L. L., GEAHLEN, R. L. & PIWNICA-WORMS, H. 1993. Mechanisms of p34cdc2 regulation. *Mol Cell Biol*, 13, 1675-85.
- ATILLA-GOKCUMEN, G. E., MURO, E., RELAT-GOBERNA, J., SASSE, S., BEDIGIAN, A., COUGHLIN, M. L., GARCIA-MANYES, S. & EGGERT, U. S. 2014. Dividing cells regulate their lipid composition and localization. *Cell*, 156, 428-39.
- BALASUBRAMANIAN, M. K., BI, E. & GLOTZER, M. 2004. Comparative analysis of cytokinesis in budding yeast, fission yeast and animal cells. *Curr Biol*, 14, R806-18.
- BALLA, T. 2013. Phosphoinositides: tiny lipids with giant impact on cell regulation. *Physiol Rev*, 93, 1019-137.
- BALLISTER, E. R., RIEGMAN, M. & LAMPSON, M. A. 2014. Recruitment of Mad1 to metaphase kinetochores is sufficient to reactivate the mitotic checkpoint. *J Cell Biol*, 204, 901-8.
- BARR, F. A., ELLIOTT, P. R. & GRUNEBERG, U. 2011. Protein phosphatases and the regulation of mitosis. *J Cell Sci*, 124, 2323-34.
- BARR, F. A. & GRUNEBERG, U. 2007. Cytokinesis: placing and making the final cut. *Cell*, 131, 847-60.

- BASANT, A., LEKOMTSEV, S., TSE, Y. C., ZHANG, D., LONGHINI, K. M., PETRONCZKI, M. & GLOTZER, M. 2015. Aurora B kinase promotes cytokinesis by inducing centralspindlin oligomers that associate with the plasma membrane. *Dev Cell*, 33, 204-15.
- BASSI, Z. I., AUDUSSEAU, M., RIPARBELLI, M. G., CALLAINI, G. & D'AVINO, P. P. 2013. Citron kinase controls a molecular network required for midbody formation in cytokinesis. *Proc Natl Acad Sci U S A*, 110, 9782-7.
- BASSI, Z. I., VERBRUGGHE, K. J., CAPALBO, L., GREGORY, S., MONTEBAULT, E., GLOVER, D. M. & D'AVINO, P. P. 2011. Sticky/Citron kinase maintains proper RhoA localization at the cleavage site during cytokinesis. *J Cell Biol*, 195, 595-603.
- BASTOS, R. N. & BARR, F. A. 2010. Plk1 negatively regulates Cep55 recruitment to the midbody to ensure orderly abscission. *J Cell Biol*, 191, 751-60.
- BASTOS, R. N., PENATE, X., BATES, M., HAMMOND, D. & BARR, F. A. 2012. CYK4 inhibits Rac1-dependent PAK1 and ARHGEF7 effector pathways during cytokinesis. *J Cell Biol*, 198, 865-80.
- BAYLISS, R., SARDON, T., VERNOS, I. & CONTI, E. 2003. Structural basis of Aurora-A activation by TPX2 at the mitotic spindle. *Mol Cell*, 12, 851-62.
- BEMENT, W. M., BENINK, H. A. & VON DASSOW, G. 2005. A microtubule-dependent zone of active RhoA during cleavage plane specification. *J Cell Biol*, 170, 91-101.
- BEMENT, W. M., MILLER, A. L. & VON DASSOW, G. 2006. Rho GTPase activity zones and transient contractile arrays. *Bioessays*, 28, 983-93.
- BERTHET, C., ALEEM, E., COPPOLA, V., TESSAROLLO, L. & KALDIS, P. 2003. Cdk2 knockout mice are viable. *Curr Biol*, 13, 1775-85.
- BERTIN, A., MCMURRAY, M. A., THAI, L., GARCIA, G., 3RD, VOTIN, V., GROB, P., ALLYN, T., THORNER, J. & NOGALES, E. 2010. Phosphatidylinositol-4,5-bisphosphate promotes budding yeast septin filament assembly and organization. *J Mol Biol*, 404, 711-31.
- BIELING, P., TELLEY, I. A. & SURREY, T. 2010. A minimal midzone protein module controls formation and length of antiparallel microtubule overlaps. *Cell*, 142, 420-32.
- BIRKENFELD, J., NALBANT, P., BOHL, B. P., PERTZ, O., HAHN, K. M. & BOKOCH, G. M. 2007. GEF-H1 modulates localized RhoA activation during cytokinesis under the control of mitotic kinases. *Dev Cell*, 12, 699-712.
- BIRON, D., ALVAREZ-LACALLE, E., TLUSTY, T. & MOSES, E. 2005. Molecular model of the contractile ring. *Phys Rev Lett*, 95, 098102.
- BISHOP, J. D. & SCHUMACHER, J. M. 2002. Phosphorylation of the carboxyl terminus of inner centromere protein (INCENP) by the Aurora B Kinase stimulates Aurora B kinase activity. *J Biol Chem*, 277, 27577-80.
- BLUMER, J. B., KURIYAMA, R., GETTYS, T. W. & LANIER, S. M. 2006. The G-protein regulatory (GPR) motif-containing Leu-Gly-Asn-enriched protein (LGN) and Galpha3 influence cortical positioning of the mitotic spindle poles at metaphase in symmetrically dividing mammalian cells. *Eur J Cell Biol*, 85, 1233-40.
- BOGI, K., LORENZO, P. S., ACS, P., SZALLASI, Z., WAGNER, G. S. & BLUMBERG, P. M. 1999. Comparison of the roles of the C1a and C1b domains of protein kinase C alpha in ligand induced translocation in NIH 3T3 cells. *FEBS Lett*, 456, 27-30.
- BONACCORSI, S., GIANSAINTI, M. G. & GATTI, M. 1998. Spindle self-organization and cytokinesis during male meiosis in asterless mutants of *Drosophila melanogaster*. *J Cell Biol*, 142, 751-61.

- BOOHER, R. N., HOLMAN, P. S. & FATTAEY, A. 1997. Human Myt1 is a cell cycle-regulated kinase that inhibits Cdc2 but not Cdk2 activity. *J Biol Chem*, 272, 22300-6.
- BOS, J. L., REHMANN, H. & WITTINGHOFER, A. 2007. GEFs and GAPs: critical elements in the control of small G proteins. *Cell*, 129, 865-77.
- BRANDEIS, M., ROSEWELL, I., CARRINGTON, M., CROMPTON, T., JACOBS, M. A., KIRK, J., GANNON, J. & HUNT, T. 1998. Cyclin B2-null mice develop normally and are fertile whereas cyclin B1-null mice die in utero. *Proc Natl Acad Sci U S A*, 95, 4344-9.
- BRENNAN, I. M., PETERS, U., KAPOOR, T. M. & STRAIGHT, A. F. 2007. Polo-like kinase controls vertebrate spindle elongation and cytokinesis. *PLoS One*, 2, e409.
- BRILL, J. A., HIME, G. R., SCHARER-SCHUKSZ, M. & FULLER, M. T. 2000. A phospholipid kinase regulates actin organization and intercellular bridge formation during germline cytokinesis. *Development*, 127, 3855-64.
- BRILL, J. A., WONG, R. & WILDE, A. 2011. Phosphoinositide function in cytokinesis. *Curr Biol*, 21, R930-4.
- BRINGMANN, H. & HYMAN, A. A. 2005. A cytokinesis furrow is positioned by two consecutive signals. *Nature*, 436, 731-4.
- BURGESS, A., VIGNERON, S., BRIOUDES, E., LABBE, J. C., LORCA, T. & CASTRO, A. 2010. Loss of human Greatwall results in G2 arrest and multiple mitotic defects due to deregulation of the cyclin B-Cdc2/PP2A balance. *Proc Natl Acad Sci U S A*, 107, 12564-9.
- BURGESS, D. R. & CHANG, F. 2005. Site selection for the cleavage furrow at cytokinesis. *Trends Cell Biol*, 15, 156-62.
- BURKARD, M. E., MACIEJOWSKI, J., RODRIGUEZ-BRAVO, V., REPKA, M., LOWERY, D. M., CLAUSER, K. R., ZHANG, C., SHOKAT, K. M., CARR, S. A., YAFFE, M. B. & JALLEPALLI, P. V. 2009. Plk1 self-organization and priming phosphorylation of HsCYK-4 at the spindle midzone regulate the onset of division in human cells. *PLoS Biol*, 7, e1000111.
- BURKARD, M. E., RANDALL, C. L., LAROCHELLE, S., ZHANG, C., SHOKAT, K. M., FISHER, R. P. & JALLEPALLI, P. V. 2007. Chemical genetics reveals the requirement for Polo-like kinase 1 activity in positioning RhoA and triggering cytokinesis in human cells. *Proc Natl Acad Sci U S A*, 104, 4383-8.
- BUSCHHORN, B. A., PETZOLD, G., GALOVA, M., DUBE, P., KRAFT, C., HERZOG, F., STARK, H. & PETERS, J. M. 2011. Substrate binding on the APC/C occurs between the coactivator Cdh1 and the processivity factor Doc1. *Nat Struct Mol Biol*, 18, 6-13.
- BUSSON, S., DUJARDIN, D., MOREAU, A., DOMPIERRE, J. & DE MEY, J. R. 1998. Dynein and dynactin are localized to astral microtubules and at cortical sites in mitotic epithelial cells. *Curr Biol*, 8, 541-4.
- CANMAN, J. C., CAMERON, L. A., MADDOX, P. S., STRAIGHT, A., TIRNAUER, J. S., MITCHISON, T. J., FANG, G., KAPOOR, T. M. & SALMON, E. D. 2003. Determining the position of the cell division plane. *Nature*, 424, 1074-8.
- CANMAN, J. C., LEWELLYN, L., LABAND, K., SMERDON, S. J., DESAI, A., BOWERMAN, B. & OEGEMA, K. 2008. Inhibition of Rac by the GAP activity of central spindle is essential for cytokinesis. *Science*, 322, 1543-6.
- CAO, L. G. & WANG, Y. L. 1996. Signals from the spindle midzone are required for the stimulation of cytokinesis in cultured epithelial cells. *Mol Biol Cell*, 7, 225-32.
- CAPALBO, L., MONTEBAULT, E., TAKEDA, T., BASSI, Z. I., GLOVER, D. M. & D'AVINO, P. P. 2012. The chromosomal passenger complex controls the function of endosomal sorting complex required for transport-III Snf7 proteins during cytokinesis. *Open Biol*, 2, 120070.

- CARLTON, J. G., CABALLE, A., AGROMAYOR, M., KLOC, M. & MARTIN-SERRANO, J. 2012. ESCRT-III governs the Aurora B-mediated abscission checkpoint through CHMP4C. *Science*, 336, 220-5.
- CARLTON, J. G. & MARTIN-SERRANO, J. 2007. Parallels between cytokinesis and retroviral budding: a role for the ESCRT machinery. *Science*, 316, 1908-12.
- CARMENA, M., RUCHAUD, S. & EARNSHAW, W. C. 2009. Making the Auroras glow: regulation of Aurora A and B kinase function by interacting proteins. *Curr Opin Cell Biol*, 21, 796-805.
- CARMENA, M., WHEELOCK, M., FUNABIKI, H. & EARNSHAW, W. C. 2012. The chromosomal passenger complex (CPC): from easy rider to the godfather of mitosis. *Nat Rev Mol Cell Biol*, 13, 789-803.
- CARVALHO, A., DESAI, A. & OEGEMA, K. 2009. Structural memory in the contractile ring makes the duration of cytokinesis independent of cell size. *Cell*, 137, 926-37.
- CARVALHO, P., TIRNAUER, J. S. & PELLMAN, D. 2003. Surfing on microtubule ends. *Trends Cell Biol*, 13, 229-37.
- CASTILHO, P. V., WILLIAMS, B. C., MOCHIDA, S., ZHAO, Y. & GOLDBERG, M. L. 2009. The M phase kinase Greatwall (Gwl) promotes inactivation of PP2A/B55delta, a phosphatase directed against CDK phosphosites. *Mol Biol Cell*, 20, 4777-89.
- CASTRILLON, D. H. & WASSERMAN, S. A. 1994. Diaphanous is required for cytokinesis in Drosophila and shares domains of similarity with the products of the limb deformity gene. *Development*, 120, 3367-77.
- CELTON-MORIZUR, S., MERLEN, G., COUTON, D., MARGALL-DUCOS, G. & DESDOUETS, C. 2009. The insulin/Akt pathway controls a specific cell division program that leads to generation of binucleated tetraploid liver cells in rodents. *J Clin Invest*, 119, 1880-7.
- CHALAMALASETTY, R. B., HUMMER, S., NIGG, E. A. & SILLJE, H. H. 2006. Influence of human Ect2 depletion and overexpression on cleavage furrow formation and abscission. *J Cell Sci*, 119, 3008-19.
- CHAN, C. S. & BOTSTEIN, D. 1993. Isolation and characterization of chromosome-gain and increase-in-ploidy mutants in yeast. *Genetics*, 135, 677-91.
- CHEESEMAN, I. M. 2014. The kinetochore. *Cold Spring Harb Perspect Biol*, 6, a015826.
- CHEESEMAN, I. M., ANDERSON, S., JWA, M., GREEN, E. M., KANG, J., YATES, J. R., 3RD, CHAN, C. S., DRUBIN, D. G. & BARNES, G. 2002. Phosphoregulation of kinetochore-microtubule attachments by the Aurora kinase Ipl1p. *Cell*, 111, 163-72.
- CHEESEMAN, I. M., CHAPPIE, J. S., WILSON-KUBALEK, E. M. & DESAI, A. 2006. The conserved KMN network constitutes the core microtubule-binding site of the kinetochore. *Cell*, 127, 983-97.
- CHEN, F., ARCHAMBAULT, V., KAR, A., LIO, P., D'AVINO, P. P., SINKA, R., LILLEY, K., LAUE, E. D., DEAK, P., CAPALBO, L. & GLOVER, D. M. 2007. Multiple protein phosphatases are required for mitosis in Drosophila. *Curr Biol*, 17, 293-303.
- CLAPPERTON, J. A., MANKE, I. A., LOWERY, D. M., HO, T., HAIRE, L. F., YAFFE, M. B. & SMERDON, S. J. 2004. Structure and mechanism of BRCA1 BRCT domain recognition of phosphorylated BACH1 with implications for cancer. *Nat Struct Mol Biol*, 11, 512-8.
- CLUTE, P. & PINES, J. 1999. Temporal and spatial control of cyclin B1 destruction in metaphase. *Nat Cell Biol*, 1, 82-7.

- COLON-GONZALEZ, F. & KAZANIETZ, M. G. 2006. C1 domains exposed: from diacylglycerol binding to protein-protein interactions. *Biochim Biophys Acta*, 1761, 827-37.
- CONNELL, J. W., LINDON, C., LUZIO, J. P. & REID, E. 2009. Spastin couples microtubule severing to membrane traffic in completion of cytokinesis and secretion. *Traffic*, 10, 42-56.
- COOK, D. R., SOLSKI, P. A., BULTMAN, S. J., KAUSELMANN, G., SCHOOR, M., KUEHN, R., FRIEDMAN, L. S., COWLEY, D. O., VAN DYKE, T., YEH, J. J., JOHNSON, L. & DER, C. J. 2011. The ect2 rho Guanine nucleotide exchange factor is essential for early mouse development and normal cell cytokinesis and migration. *Genes Cancer*, 2, 932-42.
- COUDREUSE, D. & NURSE, P. 2010. Driving the cell cycle with a minimal CDK control network. *Nature*, 468, 1074-9.
- COUTINHO-BUDD, J. C., SNIDER, S. B., FITZPATRICK, B. J., RITTINER, J. E. & ZYLKA, M. J. 2013. Biological constraints limit the use of rapamycin-inducible FKBP12-Inp54p for depleting PIP2 in dorsal root ganglia neurons. *J Negat Results Biomed*, 12, 13.
- COX, D. N., SEYFRIED, S. A., JAN, L. Y. & JAN, Y. N. 2001. Bazooka and atypical protein kinase C are required to regulate oocyte differentiation in the Drosophila ovary. *Proc Natl Acad Sci U S A*, 98, 14475-80.
- CRAMER, L. P. & MITCHISON, T. J. 1997. Investigation of the mechanism of retraction of the cell margin and rearward flow of nodules during mitotic cell rounding. *Mol Biol Cell*, 8, 109-19.
- CRAWFORD, J. M., HARDEN, N., LEUNG, T., LIM, L. & KIEHART, D. P. 1998. Cellularization in Drosophila melanogaster is disrupted by the inhibition of rho activity and the activation of Cdc42 function. *Dev Biol*, 204, 151-64.
- D'AMOURS, D. & AMON, A. 2004. At the interface between signaling and executing anaphase--Cdc14 and the FEAR network. *Genes Dev*, 18, 2581-95.
- D'AVINO, P. P., GIANSANTI, M. G. & PETRONCZKI, M. 2015. Cytokinesis in animal cells. *Cold Spring Harb Perspect Biol*, 7, a015834.
- D'AVINO, P. P., SAVOIAN, M. S. & GLOVER, D. M. 2004. Mutations in sticky lead to defective organization of the contractile ring during cytokinesis and are enhanced by Rho and suppressed by Rac. *J Cell Biol*, 166, 61-71.
- D'AVINO, P. P., TAKEDA, T., CAPALBO, L., ZHANG, W., LILLEY, K. S., LAUE, E. D. & GLOVER, D. M. 2008. Interaction between Anillin and RacGAP50C connects the actomyosin contractile ring with spindle microtubules at the cell division site. *J Cell Sci*, 121, 1151-8.
- DA FONSECA, P. C., KONG, E. H., ZHANG, Z., SCHREIBER, A., WILLIAMS, M. A., MORRIS, E. P. & BARFORD, D. 2011. Structures of APC/C(Cdh1) with substrates identify Cdh1 and Apc10 as the D-box co-receptor. *Nature*, 470, 274-8.
- DAVIES, T., KODERA, N., KAMINSKI SCHIERLE, G. S., REES, E., ERDELYI, M., KAMINSKI, C. F., ANDO, T. & MISHIMA, M. 2015. CYK4 promotes antiparallel microtubule bundling by optimizing MKLP1 neck conformation. *PLoS Biol*, 13, e1002121.
- DE ANTONI, A., PEARSON, C. G., CIMINI, D., CANMAN, J. C., SALA, V., NEZI, L., MAPELLI, M., SIRONI, L., FARETTA, M., SALMON, E. D. & MUSACCHIO, A. 2005. The Mad1/Mad2 complex as a template for Mad2 activation in the spindle assembly checkpoint. *Curr Biol*, 15, 214-25.
- DE SOUZA, C. P., ELLEM, K. A. & GABRIELLI, B. G. 2000. Centrosomal and cytoplasmic Cdc2/cyclin B1 activation precedes nuclear mitotic events. *Exp Cell Res*, 257, 11-21.

- DECHANT, R. & GLOTZER, M. 2003. Centrosome separation and central spindle assembly act in redundant pathways that regulate microtubule density and trigger cleavage furrow formation. *Dev Cell*, 4, 333-44.
- DELUCA, J. G., GALL, W. E., CIFERRI, C., CIMINI, D., MUSACCHIO, A. & SALMON, E. D. 2006. Kinetochore microtubule dynamics and attachment stability are regulated by Hec1. *Cell*, 127, 969-82.
- DEN ELZEN, N. & PINES, J. 2001. Cyclin A is destroyed in prometaphase and can delay chromosome alignment and anaphase. *J Cell Biol*, 153, 121-36.
- DEPHOURE, N., ZHOU, C., VILLEN, J., BEAUSOLEIL, S. A., BAKALARSKI, C. E., ELLEDGE, S. J. & GYGI, S. P. 2008. A quantitative atlas of mitotic phosphorylation. *Proc Natl Acad Sci U S A*, 105, 10762-7.
- DI FIORE, B. & PINES, J. 2010. How cyclin A destruction escapes the spindle assembly checkpoint. *J Cell Biol*, 190, 501-9.
- DOMENECH, E. & MALUMBRES, M. 2013. Mitosis-targeting therapies: a troubleshooting guide. *Curr Opin Pharmacol*, 13, 519-28.
- DOUGLAS, M. E., DAVIES, T., JOSEPH, N. & MISHIMA, M. 2010. Aurora B and 14-3-3 coordinately regulate clustering of central spindle during cytokinesis. *Curr Biol*, 20, 927-33.
- DRUBIN, D. G. & NELSON, W. J. 1996. Origins of cell polarity. *Cell*, 84, 335-44.
- DU, Q. & MACARA, I. G. 2004. Mammalian Pins is a conformational switch that links NuMA to heterotrimeric G proteins. *Cell*, 119, 503-16.
- DUNPHY, W. G. & KUMAGAI, A. 1991. The cdc25 protein contains an intrinsic phosphatase activity. *Cell*, 67, 189-96.
- DUTERTRE, S., CAZALES, M., QUARANTA, M., FROMENT, C., TRABUT, V., DOZIER, C., MIREY, G., BOUCHE, J. P., THEIS-FEBVRE, N., SCHMITT, E., MONSARRAT, B., PRIGENT, C. & DUCOMMUN, B. 2004. Phosphorylation of CDC25B by Aurora-A at the centrosome contributes to the G2-M transition. *J Cell Sci*, 117, 2523-31.
- DVORSKY, R. & AHMADIAN, M. R. 2004. Always look on the bright side of Rho: structural implications for a conserved intermolecular interface. *EMBO Rep*, 5, 1130-6.
- DYSON, N. 1998. The regulation of E2F by pRB-family proteins. *Genes Dev*, 12, 2245-62.
- ECHARD, A. 2012. Phosphoinositides and cytokinesis: the "PIP" of the iceberg. *Cytoskeleton (Hoboken)*, 69, 893-912.
- EGELHOFER, T. A., VILLEN, J., MCCUSKER, D., GYGI, S. P. & KELLOGG, D. R. 2008. The septins function in G1 pathways that influence the pattern of cell growth in budding yeast. *PLoS One*, 3, e2022.
- EL AMINE, N., KECHAD, A., JANANJI, S. & HICKSON, G. R. 2013. Opposing actions of septins and Sticky on Anillin promote the transition from contractile to midbody ring. *J Cell Biol*, 203, 487-504.
- ELAD, N., ABRAMOVITCH, S., SABANAY, H. & MEDALIA, O. 2011. Microtubule organization in the final stages of cytokinesis as revealed by cryo-electron tomography. *J Cell Sci*, 124, 207-15.
- ELIA, A. E., CANTLEY, L. C. & YAFFE, M. B. 2003. Proteomic screen finds pSer/pThr-binding domain localizing Plk1 to mitotic substrates. *Science*, 299, 1228-31.
- ELIA, N., SOUGRAT, R., SPURLIN, T. A., HURLEY, J. H. & LIPPINCOTT-SCHWARTZ, J. 2011. Dynamics of endosomal sorting complex required for transport (ESCRT) machinery during cytokinesis and its role in abscission. *Proc Natl Acad Sci U S A*, 108, 4846-51.
- ELOWE, S., HUMMER, S., ULDSCHMID, A., LI, X. & NIGG, E. A. 2007. Tension-sensitive Plk1 phosphorylation on BubR1 regulates the stability of kinetochore microtubule interactions. *Genes Dev*, 21, 2205-19.

- EMOTO, K., INADOME, H., KANAHO, Y., NARUMIYA, S. & UMEDA, M. 2005. Local change in phospholipid composition at the cleavage furrow is essential for completion of cytokinesis. *J Biol Chem*, 280, 37901-7.
- EMOTO, K., KOBAYASHI, T., YAMAJI, A., AIZAWA, H., YAHARA, I., INOUE, K. & UMEDA, M. 1996. Redistribution of phosphatidylethanolamine at the cleavage furrow of dividing cells during cytokinesis. *Proc Natl Acad Sci U S A*, 93, 12867-72.
- EMOTO, K. & UMEDA, M. 2000. An essential role for a membrane lipid in cytokinesis. Regulation of contractile ring disassembly by redistribution of phosphatidylethanolamine. *J Cell Biol*, 149, 1215-24.
- ERRICO, A., DESHMUKH, K., TANAKA, Y., POZNIAKOVSKY, A. & HUNT, T. 2010. Identification of substrates for cyclin dependent kinases. *Adv Enzyme Regul*, 50, 375-99.
- ETTINGER, A. W., WILSCH-BRAUNINGER, M., MARZESCO, A. M., BICKLE, M., LOHMANN, A., MALIGA, Z., KARBANOVA, J., CORBEIL, D., HYMAN, A. A. & HUTTNER, W. B. 2011. Proliferating versus differentiating stem and cancer cells exhibit distinct midbody-release behaviour. *Nat Commun*, 2, 503.
- EVANS, T., ROSENTHAL, E. T., YOUNGBLOM, J., DISTEL, D. & HUNT, T. 1983. Cyclin: a protein specified by maternal mRNA in sea urchin eggs that is destroyed at each cleavage division. *Cell*, 33, 389-96.
- EYERS, P. A., ERIKSON, E., CHEN, L. G. & MALLER, J. L. 2003. A novel mechanism for activation of the protein kinase Aurora A. *Curr Biol*, 13, 691-7.
- FARAGHER, A. J. & FRY, A. M. 2003. Nek2A kinase stimulates centrosome disjunction and is required for formation of bipolar mitotic spindles. *Mol Biol Cell*, 14, 2876-89.
- FARKAS, R. M., GIANSANTI, M. G., GATTI, M. & FULLER, M. T. 2003. The Drosophila Cog5 homologue is required for cytokinesis, cell elongation, and assembly of specialized Golgi architecture during spermatogenesis. *Mol Biol Cell*, 14, 190-200.
- FEDEDA, J. P. & GERLICH, D. W. 2012. Molecular control of animal cell cytokinesis. *Nat Cell Biol*, 14, 440-7.
- FIELD, C. M., COUGHLIN, M., DOBERSTEIN, S., MARTY, T. & SULLIVAN, W. 2005a. Characterization of anillin mutants reveals essential roles in septin localization and plasma membrane integrity. *Development*, 132, 2849-60.
- FIELD, S. J., MADSON, N., KERR, M. L., GALBRAITH, K. A., KENNEDY, C. E., TAHILIANI, M., WILKINS, A. & CANTLEY, L. C. 2005b. PtdIns(4,5)P₂ functions at the cleavage furrow during cytokinesis. *Curr Biol*, 15, 1407-12.
- FIELDS, A. P. & JUSTILIEN, V. 2010. The guanine nucleotide exchange factor (GEF) Ect2 is an oncogene in human cancer. *Adv Enzyme Regul*, 50, 190-200.
- FISHKIND, D. J. & WANG, Y. L. 1993. Orientation and three-dimensional organization of actin filaments in dividing cultured cells. *J Cell Biol*, 123, 837-48.
- FLEMMING, W. 1882. *Zellsubstanz, Kern und Zelltheilung ... Mit ... Tafeln*, Leipzig.
- FOE, V. E. & VON DASSOW, G. 2008. Stable and dynamic microtubules coordinately shape the myosin activation zone during cytokinetic furrow formation. *J Cell Biol*, 183, 457-70.
- FOLEY, E. A. & KAPOOR, T. M. 2013. Microtubule attachment and spindle assembly checkpoint signalling at the kinetochore. *Nat Rev Mol Cell Biol*, 14, 25-37.
- FRANKE, T. F., KAPLAN, D. R., CANTLEY, L. C. & TOKER, A. 1997. Direct regulation of the Akt proto-oncogene product by phosphatidylinositol-3,4-bisphosphate. *Science*, 275, 665-8.
- FRENETTE, P., HAINES, E., LOLOYAN, M., KINAL, M., PAKARIAN, P. & PIEKNY, A. 2012. An anillin-Ect2 complex stabilizes central spindle microtubules at the cortex during cytokinesis. *PLoS One*, 7, e34888.

- FUJIWARA, T., BANDI, M., NITTA, M., IVANOVA, E. V., BRONSON, R. T. & PELLMAN, D. 2005. Cytokinesis failure generating tetraploids promotes tumorigenesis in p53-null cells. *Nature*, 437, 1043-7.
- FULLER, B. G., LAMPSON, M. A., FOLEY, E. A., ROSASCO-NITCHER, S., LE, K. V., TOBELMANN, P., BRAUTIGAN, D. L., STUKENBERG, P. T. & KAPOOR, T. M. 2008. Midzone activation of aurora B in anaphase produces an intracellular phosphorylation gradient. *Nature*, 453, 1132-6.
- FUNABIKI, H., KUMADA, K. & YANAGIDA, M. 1996. Fission yeast Cut1 and Cut2 are essential for sister chromatid separation, concentrate along the metaphase spindle and form large complexes. *EMBO J*, 15, 6617-28.
- FUNG, T. K., MA, H. T. & POON, R. Y. 2007. Specialized roles of the two mitotic cyclins in somatic cells: cyclin A as an activator of M phase-promoting factor. *Mol Biol Cell*, 18, 1861-73.
- GAI, M., CAMERA, P., DEMA, A., BIANCHI, F., BERTO, G., SCARPA, E., GERMENA, G. & DI CUNTO, F. 2011. Citron kinase controls abscission through RhoA and anillin. *Mol Biol Cell*, 22, 3768-78.
- GANEM, N. J., GODINHO, S. A. & PELLMAN, D. 2009. A mechanism linking extra centrosomes to chromosomal instability. *Nature*, 460, 278-82.
- GANEM, N. J., STORCHOVA, Z. & PELLMAN, D. 2007. Tetraploidy, aneuploidy and cancer. *Curr Opin Genet Dev*, 17, 157-62.
- GASSMANN, R., CARVALHO, A., HENZING, A. J., RUCHAUD, S., HUDSON, D. F., HONDA, R., NIGG, E. A., GERLOFF, D. L. & EARNSHAW, W. C. 2004. Borealin: a novel chromosomal passenger required for stability of the bipolar mitotic spindle. *J Cell Biol*, 166, 179-91.
- GAVET, O. & PINES, J. 2010. Progressive activation of CyclinB1-Cdk1 coordinates entry to mitosis. *Dev Cell*, 18, 533-43.
- GELEY, S., KRAMER, E., GIEFFERS, C., GANNON, J., PETERS, J. M. & HUNT, T. 2001. Anaphase-promoting complex/cyclosome-dependent proteolysis of human cyclin A starts at the beginning of mitosis and is not subject to the spindle assembly checkpoint. *J Cell Biol*, 153, 137-48.
- GENESTE, O., COPELAND, J. W. & TREISMAN, R. 2002. LIM kinase and Diaphanous cooperate to regulate serum response factor and actin dynamics. *J Cell Biol*, 157, 831-8.
- GERARD, C., TYSON, J. J., COUDREUSE, D. & NOVAK, B. 2015. Cell cycle control by a minimal Cdk network. *PLoS Comput Biol*, 11, e1004056.
- GERHART, J., WU, M. & KIRSCHNER, M. 1984. Cell cycle dynamics of an M-phase-specific cytoplasmic factor in *Xenopus laevis* oocytes and eggs. *J Cell Biol*, 98, 1247-55.
- GHARBI-AYACHI, A., LABBE, J. C., BURGESS, A., VIGNERON, S., STRUB, J. M., BRIOUDES, E., VAN-DORSSELAER, A., CASTRO, A. & LORCA, T. 2010. The substrate of Greatwall kinase, Arpp19, controls mitosis by inhibiting protein phosphatase 2A. *Science*, 330, 1673-7.
- GIANSANTI, M. G., BELLONI, G. & GATTI, M. 2007. Rab11 is required for membrane trafficking and actomyosin ring constriction in meiotic cytokinesis of *Drosophila* males. *Mol Biol Cell*, 18, 5034-47.
- GIANSANTI, M. G., GATTI, M. & BONACCORSI, S. 2001. The role of centrosomes and astral microtubules during asymmetric division of *Drosophila* neuroblasts. *Development*, 128, 1137-45.
- GIET, R., MCLEAN, D., DESCAMPS, S., LEE, M. J., RAFF, J. W., PRIGENT, C. & GLOVER, D. M. 2002. *Drosophila* Aurora A kinase is required to localize D-TACC to centrosomes and to regulate astral microtubules. *J Cell Biol*, 156, 437-51.

- GIRARD, F., STRAUSFELD, U., FERNANDEZ, A. & LAMB, N. J. 1991. Cyclin A is required for the onset of DNA replication in mammalian fibroblasts. *Cell*, 67, 1169-79.
- GJERTSEN, B. T. & SCHOFFSKI, P. 2015. Discovery and development of the Polo-like kinase inhibitor volasertib in cancer therapy. *Leukemia*, 29, 11-9.
- GLOTZER, M. 2009. The 3Ms of central spindle assembly: microtubules, motors and MAPs. *Nat Rev Mol Cell Biol*, 10, 9-20.
- GLOTZER, M., MURRAY, A. W. & KIRSCHNER, M. W. 1991. Cyclin is degraded by the ubiquitin pathway. *Nature*, 349, 132-8.
- GLOVER, D. M., LEIBOWITZ, M. H., MCLEAN, D. A. & PARRY, H. 1995. Mutations in aurora prevent centrosome separation leading to the formation of monopolar spindles. *Cell*, 81, 95-105.
- GONCZY, P. 2008. Mechanisms of asymmetric cell division: flies and worms pave the way. *Nat Rev Mol Cell Biol*, 9, 355-66.
- GONG, D., POMERENING, J. R., MYERS, J. W., GUSTAVSSON, C., JONES, J. T., HAHN, A. T., MEYER, T. & FERRELL, J. E., JR. 2007. Cyclin A2 regulates nuclear-envelope breakdown and the nuclear accumulation of cyclin B1. *Curr Biol*, 17, 85-91.
- GOSS, J. W. & TOOMRE, D. K. 2008. Both daughter cells traffic and exocytose membrane at the cleavage furrow during mammalian cytokinesis. *J Cell Biol*, 181, 1047-54.
- GOTTIFREDI, V. & PRIVES, C. 2005. The S phase checkpoint: when the crowd meets at the fork. *Semin Cell Dev Biol*, 16, 355-68.
- GREEN, R. A., MAYERS, J. R., WANG, S., LEWELLYN, L., DESAI, A., AUDHYA, A. & OEGEMA, K. 2013. The midbody ring scaffolds the abscission machinery in the absence of midbody microtubules. *J Cell Biol*, 203, 505-20.
- GREEN, R. A., PALUCH, E. & OEGEMA, K. 2012. Cytokinesis in animal cells. *Annu Rev Cell Dev Biol*, 28, 29-58.
- GREER, E. R., CHAO, A. T. & BEJSOVEC, A. 2013. Pebble/ECT2 RhoGEF negatively regulates the Wingless/Wnt signaling pathway. *Development*, 140, 4937-46.
- GREGORY, S. L., EBRAHIMI, S., MILVERTON, J., JONES, W. M., BEJSOVEC, A. & SAINT, R. 2008. Cell division requires a direct link between microtubule-bound RacGAP and Anillin in the contractile ring. *Curr Biol*, 18, 25-9.
- GROMLEY, A., YEAMAN, C., ROSA, J., REDICK, S., CHEN, C. T., MIRABELLE, S., GUHA, M., SILLIBOURNE, J. & DOXSEY, S. J. 2005. Centriolin anchoring of exocyst and SNARE complexes at the midbody is required for secretory-vesicle-mediated abscission. *Cell*, 123, 75-87.
- GRUNEBERG, U., NEEF, R., HONDA, R., NIGG, E. A. & BARR, F. A. 2004. Relocation of Aurora B from centromeres to the central spindle at the metaphase to anaphase transition requires MKlp2. *J Cell Biol*, 166, 167-72.
- GUIDOTTI, J. E., BREGERIE, O., ROBERT, A., DEBEY, P., BRECHOT, C. & DESDOUETS, C. 2003. Liver cell polyploidization: a pivotal role for binuclear hepatocytes. *J Biol Chem*, 278, 19095-101.
- GUIZETTI, J., SCHERMELLEH, L., MANTLER, J., MAAR, S., POSER, I., LEONHARDT, H., MULLER-REICHERT, T. & GERLICH, D. W. 2011. Cortical constriction during abscission involves helices of ESCRT-III-dependent filaments. *Science*, 331, 1616-20.
- GUSE, A., MISHIMA, M. & GLOTZER, M. 2005. Phosphorylation of ZEN-4/MKLP1 by aurora B regulates completion of cytokinesis. *Curr Biol*, 15, 778-86.
- GUTTINGER, S., LAURELL, E. & KUTAY, U. 2009. Orchestrating nuclear envelope disassembly and reassembly during mitosis. *Nat Rev Mol Cell Biol*, 10, 178-91.
- HAGTING, A., DEN ELZEN, N., VODERMAIER, H. C., WAIZENEGGER, I. C., PETERS, J. M. & PINES, J. 2002. Human securin proteolysis is controlled by

- the spindle checkpoint and reveals when the APC/C switches from activation by Cdc20 to Cdh1. *J Cell Biol*, 157, 1125-37.
- HAMES, R. S., WATTAM, S. L., YAMANO, H., BACCHIERI, R. & FRY, A. M. 2001. APC/C-mediated destruction of the centrosomal kinase Nek2A occurs in early mitosis and depends upon a cyclin A-type D-box. *EMBO J*, 20, 7117-27.
- HAMMOND, G. R., FISCHER, M. J., ANDERSON, K. E., HOLDICH, J., KOTECI, A., BALLA, T. & IRVINE, R. F. 2012. PI4P and PI(4,5)P2 are essential but independent lipid determinants of membrane identity. *Science*, 337, 727-30.
- HANNAK, E., KIRKHAM, M., HYMAN, A. A. & OEGEMA, K. 2001. Aurora-A kinase is required for centrosome maturation in *Caenorhabditis elegans*. *J Cell Biol*, 155, 1109-16.
- HANSEN, D. V., LOKTEV, A. V., BAN, K. H. & JACKSON, P. K. 2004. Plk1 regulates activation of the anaphase promoting complex by phosphorylating and triggering SCFbetaTrCP-dependent destruction of the APC Inhibitor Emi1. *Mol Biol Cell*, 15, 5623-34.
- HARA, T., ABE, M., INOUE, H., YU, L. R., VEENSTRA, T. D., KANG, Y. H., LEE, K. S. & MIKI, T. 2006. Cytokinesis regulator ECT2 changes its conformation through phosphorylation at Thr-341 in G2/M phase. *Oncogene*, 25, 566-78.
- HARTWELL, L. H. & WEINERT, T. A. 1989. Checkpoints: controls that ensure the order of cell cycle events. *Science*, 246, 629-34.
- HEO, W. D., INOUE, T., PARK, W. S., KIM, M. L., PARK, B. O., WANDLESS, T. J. & MEYER, T. 2006. PI(3,4,5)P3 and PI(4,5)P2 lipids target proteins with polybasic clusters to the plasma membrane. *Science*, 314, 1458-61.
- HICKSON, G. R. & O'FARRELL, P. H. 2008. Rho-dependent control of anillin behavior during cytokinesis. *J Cell Biol*, 180, 285-94.
- HILL, E., CLARKE, M. & BARR, F. A. 2000. The Rab6-binding kinesin, Rab6-KIFL, is required for cytokinesis. *EMBO J*, 19, 5711-9.
- HIME, G. & SAINT, R. 1992. Zygotic expression of the pebble locus is required for cytokinesis during the postblastoderm mitoses of *Drosophila*. *Development*, 114, 165-71.
- HIRAMOTO, Y. 1971. Analysis of cleavage stimulus by means of micromanipulation of sea urchin eggs. *Exp Cell Res*, 68, 291-8.
- HIRANO, T. 2012. Condensins: universal organizers of chromosomes with diverse functions. *Genes Dev*, 26, 1659-78.
- HIRANO, T. & MITCHISON, T. J. 1994. A heterodimeric coiled-coil protein required for mitotic chromosome condensation in vitro. *Cell*, 79, 449-58.
- HOCHEGGER, H., DEJSUPHONG, D., SONODA, E., SABERI, A., RAJENDRA, E., KIRK, J., HUNT, T. & TAKEDA, S. 2007. An essential role for Cdk1 in S phase control is revealed via chemical genetics in vertebrate cells. *J Cell Biol*, 178, 257-68.
- HOFFMANN, I., CLARKE, P. R., MARCOTE, M. J., KARSENTI, E. & DRAETTA, G. 1993. Phosphorylation and activation of human cdc25-C by cdc2--cyclin B and its involvement in the self-amplification of MPF at mitosis. *EMBO J*, 12, 53-63.
- HONDA, K., MIHARA, H., KATO, Y., YAMAGUCHI, A., TANAKA, H., YASUDA, H., FURUKAWA, K. & URANO, T. 2000. Degradation of human Aurora2 protein kinase by the anaphase-promoting complex-ubiquitin-proteasome pathway. *Oncogene*, 19, 2812-9.
- HSU, J. Y., SUN, Z. W., LI, X., REUBEN, M., TATCHELL, K., BISHOP, D. K., GRUSHCOW, J. M., BRAME, C. J., CALDWELL, J. A., HUNT, D. F., LIN, R., SMITH, M. M. & ALLIS, C. D. 2000. Mitotic phosphorylation of histone H3 is governed by Ipl1/aurora kinase and Glc7/PP1 phosphatase in budding yeast and nematodes. *Cell*, 102, 279-91.

- HU, C. K., COUGHLIN, M., FIELD, C. M. & MITCHISON, T. J. 2011. KIF4 regulates midzone length during cytokinesis. *Curr Biol*, 21, 815-24.
- HU, C. K., COUGHLIN, M. & MITCHISON, T. J. 2012. Midbody assembly and its regulation during cytokinesis. *Mol Biol Cell*, 23, 1024-34.
- HUMMER, S. & MAYER, T. U. 2009. Cdk1 negatively regulates midzone localization of the mitotic kinesin Mklp2 and the chromosomal passenger complex. *Curr Biol*, 19, 607-12.
- HURLEY, J. H. & HANSON, P. I. 2010. Membrane budding and scission by the ESCRT machinery: it's all in the neck. *Nat Rev Mol Cell Biol*, 11, 556-66.
- HUTTERER, A., GLOTZER, M. & MISHIMA, M. 2009. Clustering of centralspindlin is essential for its accumulation to the central spindle and the midbody. *Curr Biol*, 19, 2043-9.
- JAMES, S. R., DOWNES, C. P., GIGG, R., GROVE, S. J., HOLMES, A. B. & ALESSI, D. R. 1996. Specific binding of the Akt-1 protein kinase to phosphatidylinositol 3,4,5-trisphosphate without subsequent activation. *Biochem J*, 315 (Pt 3), 709-13.
- JANTSCH-PLUNGER, V., GONCZY, P., ROMANO, A., SCHNABEL, H., HAMILL, D., SCHNABEL, R., HYMAN, A. A. & GLOTZER, M. 2000. CYK-4: A Rho family gtpase activating protein (GAP) required for central spindle formation and cytokinesis. *J Cell Biol*, 149, 1391-404.
- JEFFREY, P. D., RUSSO, A. A., POLYAK, K., GIBBS, E., HURWITZ, J., MASSAGUE, J. & PAVLETICH, N. P. 1995. Mechanism of CDK activation revealed by the structure of a cyclinA-CDK2 complex. *Nature*, 376, 313-20.
- JIANG, W., JIMENEZ, G., WELLS, N. J., HOPE, T. J., WAHL, G. M., HUNTER, T. & FUKUNAGA, R. 1998. PRC1: a human mitotic spindle-associated CDK substrate protein required for cytokinesis. *Mol Cell*, 2, 877-85.
- JONGSMA, M. L., BERLIN, I. & NEEFJES, J. 2015. On the move: organelle dynamics during mitosis. *Trends Cell Biol*, 25, 112-24.
- JOO, E., SURKA, M. C. & TRIMBLE, W. S. 2007. Mammalian SEPT2 is required for scaffolding nonmuscle myosin II and its kinases. *Dev Cell*, 13, 677-90.
- JORDAN, S. N. & CANMAN, J. C. 2012. Rho GTPases in animal cell cytokinesis: an occupation by the one percent. *Cytoskeleton (Hoboken)*, 69, 919-30.
- JOSEPH, N., HUTTERER, A., POSER, I. & MISHIMA, M. 2012. ARF6 GTPase protects the post-mitotic midbody from 14-3-3-mediated disintegration. *EMBO J*, 31, 2604-14.
- JURGENS, G. 2005. Plant cytokinesis: fission by fusion. *Trends Cell Biol*, 15, 277-83.
- JÜRGENS, G., WIESCHAUS, E., NÜSSLEIN-VOLHARD, C. & KLUDING, H. 1984. Mutations affecting the pattern of the larval cuticle in *Drosophila melanogaster*. *Wilhelm Roux's archives of developmental biology*, 193, 283-295.
- KAITNA, S., MENDOZA, M., JANTSCH-PLUNGER, V. & GLOTZER, M. 2000. Incenp and an aurora-like kinase form a complex essential for chromosome segregation and efficient completion of cytokinesis. *Curr Biol*, 10, 1172-81.
- KAMASAKI, T., O'TOOLE, E., KITA, S., OSUMI, M., USUKURA, J., MCINTOSH, J. R. & GOSHIMA, G. 2013. Augmin-dependent microtubule nucleation at microtubule walls in the spindle. *J Cell Biol*, 202, 25-33.
- KAMASAKI, T., OSUMI, M. & MABUCHI, I. 2007. Three-dimensional arrangement of F-actin in the contractile ring of fission yeast. *J Cell Biol*, 178, 765-71.
- KAPITEIN, L. C., PETERMAN, E. J., KWOK, B. H., KIM, J. H., KAPOOR, T. M. & SCHMIDT, C. F. 2005. The bipolar mitotic kinesin Eg5 moves on both microtubules that it crosslinks. *Nature*, 435, 114-8.
- KAWAMURA, K. 1960. Studies on cytokinesis in neuroblasts of the grasshopper, *Chortophaga viridifasciata* (De Geer). I. Formation and behavior of the mitotic apparatus. *Exp Cell Res*, 21, 1-18.

- KAWAMURA, K. & CARLSON, J. G. 1962. Studies on cytokinesis in neuroblasts of the grasshopper, *Chortophaga viridifasciata* (De Geer). III. Factors determining the location of the cleavage furrow. *Exp Cell Res*, 26, 411-23.
- KECHAD, A., JANANJI, S., RUELLA, Y. & HICKSON, G. R. 2012. Anillin acts as a bifunctional linker coordinating midbody ring biogenesis during cytokinesis. *Curr Biol*, 22, 197-203.
- KENNEDY, M. J., HUGHES, R. M., PETEYA, L. A., SCHWARTZ, J. W., EHLERS, M. D. & TUCKER, C. L. 2010. Rapid blue-light-mediated induction of protein interactions in living cells. *Nat Methods*, 7, 973-5.
- KIM, H., GUO, F., BRAHMA, S., XING, Y. & BURKARD, M. E. 2014. Centralspindlin assembly and 2 phosphorylations on MgcRacGAP by Polo-like kinase 1 initiate Ect2 binding in early cytokinesis. *Cell Cycle*, 13, 2952-61.
- KIM, J. E., BILLADEAU, D. D. & CHEN, J. 2005. The tandem BRCT domains of Ect2 are required for both negative and positive regulation of Ect2 in cytokinesis. *J Biol Chem*, 280, 5733-9.
- KIM, S. Y. & FERRELL, J. E., JR. 2007. Substrate competition as a source of ultrasensitivity in the inactivation of Wee1. *Cell*, 128, 1133-45.
- KIMURA, K., ITO, M., AMANO, M., CHIHARA, K., FUKATA, Y., NAKAFUKU, M., YAMAMORI, B., FENG, J., NAKANO, T., OKAWA, K., IWAMATSU, A. & KAIBUCHI, K. 1996. Regulation of myosin phosphatase by Rho and Rho-associated kinase (Rho-kinase). *Science*, 273, 245-8.
- KIMURA, K., TSUJI, T., TAKADA, Y., MIKI, T. & NARUMIYA, S. 2000. Accumulation of GTP-bound RhoA during cytokinesis and a critical role of ECT2 in this accumulation. *J Biol Chem*, 275, 17233-6.
- KINOSHITA, M., KUMAR, S., MIZOGUCHI, A., IDE, C., KINOSHITA, A., HARAGUCHI, T., HIRAOKA, Y. & NODA, M. 1997. Nedd5, a mammalian septin, is a novel cytoskeletal component interacting with actin-based structures. *Genes Dev*, 11, 1535-47.
- KINOSHITA, N., OHKURA, H. & YANAGIDA, M. 1990. Distinct, essential roles of type 1 and 2A protein phosphatases in the control of the fission yeast cell division cycle. *Cell*, 63, 405-15.
- KISHI, K., SASAKI, T., KURODA, S., ITOH, T. & TAKAI, Y. 1993. Regulation of cytoplasmic division of *Xenopus* embryo by rho p21 and its inhibitory GDP/GTP exchange protein (rho GDI). *J Cell Biol*, 120, 1187-95.
- KITAGAWA, M., HIGASHI, H., JUNG, H. K., SUZUKI-TAKAHASHI, I., IKEDA, M., TAMAI, K., KATO, J., SEGAWA, K., YOSHIDA, E., NISHIMURA, S. & TAYA, Y. 1996. The consensus motif for phosphorylation by cyclin D1-Cdk4 is different from that for phosphorylation by cyclin A/E-Cdk2. *EMBO J*, 15, 7060-9.
- KITAJIMA, T. S., KAWASHIMA, S. A. & WATANABE, Y. 2004. The conserved kinetochore protein shugoshin protects centromeric cohesion during meiosis. *Nature*, 427, 510-7.
- KITAJIMA, T. S., SAKUNO, T., ISHIGURO, K., IEMURA, S., NATSUME, T., KAWASHIMA, S. A. & WATANABE, Y. 2006. Shugoshin collaborates with protein phosphatase 2A to protect cohesin. *Nature*, 441, 46-52.
- KITAZAWA, D., YAMAGUCHI, M., MORI, H. & INOUE, Y. H. 2012. COPI-mediated membrane trafficking is required for cytokinesis in *Drosophila* male meiotic divisions. *J Cell Sci*, 125, 3649-60.
- KIYOMITSU, T. & CHEESEMAN, I. M. 2012. Chromosome- and spindle-pole-derived signals generate an intrinsic code for spindle position and orientation. *Nat Cell Biol*, 14, 311-7.
- KIYOMITSU, T. & CHEESEMAN, I. M. 2013. Cortical dynein and asymmetric membrane elongation coordinately position the spindle in anaphase. *Cell*, 154, 391-402.

- KOPS, G. J., WEAVER, B. A. & CLEVELAND, D. W. 2005. On the road to cancer: aneuploidy and the mitotic checkpoint. *Nat Rev Cancer*, 5, 773-85.
- KOSAKO, H., YOSHIDA, T., MATSUMURA, F., ISHIZAKI, T., NARUMIYA, S. & INAGAKI, M. 2000. Rho-kinase/ROCK is involved in cytokinesis through the phosphorylation of myosin light chain and not ezrin/radixin/moesin proteins at the cleavage furrow. *Oncogene*, 19, 6059-64.
- KOTAK, S., BUSSO, C. & GONCZY, P. 2012. Cortical dynein is critical for proper spindle positioning in human cells. *J Cell Biol*, 199, 97-110.
- KRAMER, E. R., SCHEURINGER, N., PODTELEJNIKOV, A. V., MANN, M. & PETERS, J. M. 2000. Mitotic regulation of the APC activator proteins CDC20 and CDH1. *Mol Biol Cell*, 11, 1555-69.
- KUDRYAVTSEV, B. N., KUDRYAVTSEVA, M. V., SAKUTA, G. A. & STEIN, G. I. 1993. Human hepatocyte polyploidization kinetics in the course of life cycle. *Virchows Arch B Cell Pathol Incl Mol Pathol*, 64, 387-93.
- KULUKIAN, A., HAN, J. S. & CLEVELAND, D. W. 2009. Unattached kinetochores catalyze production of an anaphase inhibitor that requires a Mad2 template to prime Cdc20 for BubR1 binding. *Dev Cell*, 16, 105-17.
- KUMAGAI, A. & DUNPHY, W. G. 1991. The cdc25 protein controls tyrosine dephosphorylation of the cdc2 protein in a cell-free system. *Cell*, 64, 903-14.
- KUMAGAI, A. & DUNPHY, W. G. 1996. Purification and molecular cloning of Plx1, a Cdc25-regulatory kinase from *Xenopus* egg extracts. *Science*, 273, 1377-80.
- KUNDA, P. & BAUM, B. 2009. The actin cytoskeleton in spindle assembly and positioning. *Trends Cell Biol*, 19, 174-9.
- LACROIX, B. & MADDOX, A. S. 2012. Cytokinesis, ploidy and aneuploidy. *J Pathol*, 226, 338-51.
- LAFAURIE-JANVORE, J., MAIURI, P., WANG, I., PINOT, M., MANNEVILLE, J. B., BETZ, T., BALLAND, M. & PIEL, M. 2013. ESCRT-III assembly and cytokinetic abscission are induced by tension release in the intercellular bridge. *Science*, 339, 1625-9.
- LAMMER, C., WAGERER, S., SAFFRICH, R., MERTENS, D., ANSORGE, W. & HOFFMANN, I. 1998. The cdc25B phosphatase is essential for the G2/M phase transition in human cells. *J Cell Sci*, 111 (Pt 16), 2445-53.
- LANCASTER, O. M. & BAUM, B. 2014. Shaping up to divide: coordinating actin and microtubule cytoskeletal remodelling during mitosis. *Semin Cell Dev Biol*, 34, 109-15.
- LANE, H. A. & NIGG, E. A. 1996. Antibody microinjection reveals an essential role for human polo-like kinase 1 (Plk1) in the functional maturation of mitotic centrosomes. *J Cell Biol*, 135, 1701-13.
- LEE, J. S., KAMIJO, K., OHARA, N., KITAMURA, T. & MIKI, T. 2004. MgcRacGAP regulates cortical activity through RhoA during cytokinesis. *Exp Cell Res*, 293, 275-82.
- LEE, L. A. & ORR-WEAVER, T. L. 2003. Regulation of cell cycles in *Drosophila* development: intrinsic and extrinsic cues. *Annu Rev Genet*, 37, 545-78.
- LEE, M. G. & NURSE, P. 1987. Complementation used to clone a human homologue of the fission yeast cell cycle control gene *cdc2*. *Nature*, 327, 31-5.
- LEHNER, C. F. 1992. The pebble gene is required for cytokinesis in *Drosophila*. *J Cell Sci*, 103 (Pt 4), 1021-30.
- LEKOMTSEV, S., SU, K. C., PYE, V. E., BLIGHT, K., SUNDARAMOORTHY, S., TAKAKI, T., COLLINSON, L. M., CHEREPANOV, P., DIVECHA, N. & PETRONCZKI, M. 2012. Centralspindlin links the mitotic spindle to the plasma membrane during cytokinesis. *Nature*, 492, 276-9.
- LEMMON, M. A. 2008. Membrane recognition by phospholipid-binding domains. *Nat Rev Mol Cell Biol*, 9, 99-111.

- LENART, P., PETRONCZKI, M., STEEGMAIER, M., DI FIORE, B., LIPP, J. J., HOFFMANN, M., RETTIG, W. J., KRAUT, N. & PETERS, J. M. 2007. The small-molecule inhibitor BI 2536 reveals novel insights into mitotic roles of polo-like kinase 1. *Curr Biol*, 17, 304-15.
- LEUNG, C. C. & GLOVER, J. N. 2011. BRCT domains: easy as one, two, three. *Cell Cycle*, 10, 2461-70.
- LEWELLYN, L., CARVALHO, A., DESAI, A., MADDOX, A. S. & OEGEMA, K. 2011. The chromosomal passenger complex and centralspindlin independently contribute to contractile ring assembly. *J Cell Biol*, 193, 155-69.
- LI, J., MEYER, A. N. & DONOGHUE, D. J. 1997. Nuclear localization of cyclin B1 mediates its biological activity and is regulated by phosphorylation. *Proc Natl Acad Sci U S A*, 94, 502-7.
- LI, L. & ZOU, L. 2005. Sensing, signaling, and responding to DNA damage: organization of the checkpoint pathways in mammalian cells. *J Cell Biochem*, 94, 298-306.
- LINDON, C. & PINES, J. 2004. Ordered proteolysis in anaphase inactivates Plk1 to contribute to proper mitotic exit in human cells. *J Cell Biol*, 164, 233-41.
- LINDQVIST, A., VAN ZON, W., KARLSSON ROSENTHAL, C. & WOLTHUIS, R. M. 2007. Cyclin B1-Cdk1 activation continues after centrosome separation to control mitotic progression. *PLoS Biol*, 5, e123.
- LIOT, C., SEGUIN, L., SIRET, A., CROUIN, C., SCHMIDT, S. & BERTOGLIO, J. 2011. APC(cdh1) mediates degradation of the oncogenic Rho-GEF Ect2 after mitosis. *PLoS One*, 6, e23676.
- LISTOVSKY, T. & SALE, J. E. 2013. Sequestration of CDH1 by MAD2L2 prevents premature APC/C activation prior to anaphase onset. *J Cell Biol*, 203, 87-100.
- LIU, D., VADER, G., VROMANS, M. J., LAMPSON, M. A. & LENS, S. M. 2009. Sensing chromosome bi-orientation by spatial separation of aurora B kinase from kinetochore substrates. *Science*, 323, 1350-3.
- LIU, D., VLEUGEL, M., BACKER, C. B., HORI, T., FUKAGAWA, T., CHEESEMAN, I. M. & LAMPSON, M. A. 2010. Regulated targeting of protein phosphatase 1 to the outer kinetochore by KNL1 opposes Aurora B kinase. *J Cell Biol*, 188, 809-20.
- LIU, J., FAIRN, G. D., CECCARELLI, D. F., SICHERI, F. & WILDE, A. 2012. Cleavage furrow organization requires PIP(2)-mediated recruitment of anillin. *Curr Biol*, 22, 64-9.
- LIU, X. F., ISHIDA, H., RAZIUDDIN, R. & MIKI, T. 2004. Nucleotide exchange factor ECT2 interacts with the polarity protein complex Par6/Par3/protein kinase Czeta (PKCzeta) and regulates PKCzeta activity. *Mol Cell Biol*, 24, 6665-75.
- LIU, X. F., OHNO, S. & MIKI, T. 2006. Nucleotide exchange factor ECT2 regulates epithelial cell polarity. *Cell Signal*, 18, 1604-15.
- LOHKA, M. J., HAYES, M. K. & MALLER, J. L. 1988. Purification of maturation-promoting factor, an intracellular regulator of early mitotic events. *Proc Natl Acad Sci U S A*, 85, 3009-13.
- LOOG, M. & MORGAN, D. O. 2005. Cyclin specificity in the phosphorylation of cyclin-dependent kinase substrates. *Nature*, 434, 104-8.
- LORIA, A., LONGHINI, K. M. & GLOTZER, M. 2012. The RhoGAP domain of CYK-4 has an essential role in RhoA activation. *Curr Biol*, 22, 213-9.
- LUNDBERG, A. S. & WEINBERG, R. A. 1998. Functional inactivation of the retinoblastoma protein requires sequential modification by at least two distinct cyclin-cdk complexes. *Mol Cell Biol*, 18, 753-61.
- MA, X., KOVACS, M., CONTI, M. A., WANG, A., ZHANG, Y., SELLERS, J. R. & ADELSTEIN, R. S. 2012. Nonmuscle myosin II exerts tension but does not

- translocate actin in vertebrate cytokinesis. *Proc Natl Acad Sci U S A*, 109, 4509-14.
- MABUCHI, I. 1994. Cleavage furrow: timing of emergence of contractile ring actin filaments and establishment of the contractile ring by filament bundling in sea urchin eggs. *J Cell Sci*, 107 (Pt 7), 1853-62.
- MACUREK, L., LINDQVIST, A., LIM, D., LAMPSON, M. A., KLOMPMAKER, R., FREIRE, R., CLOUIN, C., TAYLOR, S. S., YAFFE, M. B. & MEDEMA, R. H. 2008. Polo-like kinase-1 is activated by aurora A to promote checkpoint recovery. *Nature*, 455, 119-23.
- MAILAND, N., PODTELEJNIKOV, A. V., GROTH, A., MANN, M., BARTEK, J. & LUKAS, J. 2002. Regulation of G(2)/M events by Cdc25A through phosphorylation-dependent modulation of its stability. *EMBO J*, 21, 5911-20.
- MALDONADO, M. & KAPOOR, T. M. 2011. Constitutive Mad1 targeting to kinetochores uncouples checkpoint signalling from chromosome biorientation. *Nat Cell Biol*, 13, 475-82.
- MALUMBRES, M. 2014. Cyclin-dependent kinases. *Genome Biol*, 15, 122.
- MALUMBRES, M. & BARBACID, M. 2009. Cell cycle, CDKs and cancer: a changing paradigm. *Nat Rev Cancer*, 9, 153-66.
- MASAI, H., MATSUMOTO, S., YOU, Z., YOSHIZAWA-SUGATA, N. & ODA, M. 2010. Eukaryotic chromosome DNA replication: where, when, and how? *Annu Rev Biochem*, 79, 89-130.
- MASTRONARDE, D. N., MCDONALD, K. L., DING, R. & MCINTOSH, J. R. 1993. Interpolar spindle microtubules in PTK cells. *J Cell Biol*, 123, 1475-89.
- MASUI, Y. 1982. Oscillatory activity of maturation promoting factor (MPF) in extracts of *Rana pipiens* eggs. *J Exp Zool*, 224, 389-99.
- MASUI, Y. & MARKERT, C. L. 1971. Cytoplasmic control of nuclear behavior during meiotic maturation of frog oocytes. *J Exp Zool*, 177, 129-45.
- MATSUMURA, F. 2005. Regulation of myosin II during cytokinesis in higher eukaryotes. *Trends Cell Biol*, 15, 371-7.
- MATSUSHIME, H., QUELLE, D. E., SHURTLEFF, S. A., SHIBUYA, M., SHERR, C. J. & KATO, J. Y. 1994. D-type cyclin-dependent kinase activity in mammalian cells. *Mol Cell Biol*, 14, 2066-76.
- MATTHEWS, H. K., DELABRE, U., ROHN, J. L., GUCK, J., KUNDA, P. & BAUM, B. 2012. Changes in Ect2 localization couple actomyosin-dependent cell shape changes to mitotic progression. *Dev Cell*, 23, 371-83.
- MATYSKIELA, M. E. & MORGAN, D. O. 2009. Analysis of activator-binding sites on the APC/C supports a cooperative substrate-binding mechanism. *Mol Cell*, 34, 68-80.
- MAUPIN, P. & POLLARD, T. D. 1986. Arrangement of actin filaments and myosin-like filaments in the contractile ring and of actin-like filaments in the mitotic spindle of dividing HeLa cells. *J Ultrastruct Mol Struct Res*, 94, 92-103.
- MAVRAKIS, M., AZOU-GROS, Y., TSAI, F. C., ALVARADO, J., BERTIN, A., IV, F., KRESS, A., BRASSELET, S., KOENDERINK, G. H. & LECUIT, T. 2014. Septins promote F-actin ring formation by crosslinking actin filaments into curved bundles. *Nat Cell Biol*, 16, 322-34.
- MAZUMDAR, A. & MAZUMDAR, M. 2002. How one becomes many: blastoderm cellularization in *Drosophila melanogaster*. *Bioessays*, 24, 1012-22.
- MENENDEZ-BENITO, V., VAN DEVENTER, S. J., JIMENEZ-GARCIA, V., ROY-LUZARRAGA, M., VAN LEEUWEN, F. & NEEFJES, J. 2013. Spatiotemporal analysis of organelle and macromolecular complex inheritance. *Proc Natl Acad Sci U S A*, 110, 175-80.
- MIERZWA, B. & GERLICH, D. W. 2014. Cytokinetic abscission: molecular mechanisms and temporal control. *Dev Cell*, 31, 525-38.

- MIKAWA, M., SU, L. & PARSONS, S. J. 2008. Opposing roles of p190RhoGAP and Ect2 RhoGEF in regulating cytokinesis. *Cell Cycle*, 7, 2003-12.
- MIKI, T., SMITH, C. L., LONG, J. E., EVA, A. & FLEMING, T. P. 1993. Oncogene ect2 is related to regulators of small GTP-binding proteins. *Nature*, 362, 462-5.
- MILLER, A. L. & BEMENT, W. M. 2009. Regulation of cytokinesis by Rho GTPase flux. *Nat Cell Biol*, 11, 71-7.
- MILLER, K. G., FIELD, C. M. & ALBERTS, B. M. 1989. Actin-binding proteins from Drosophila embryos: a complex network of interacting proteins detected by F-actin affinity chromatography. *J Cell Biol*, 109, 2963-75.
- MINOSHIMA, Y., KAWASHIMA, T., HIROSE, K., TONOZUKA, Y., KAWAJIRI, A., BAO, Y. C., DENG, X., TATSUKA, M., NARUMIYA, S., MAY, W. S., JR., NOSAKA, T., SEMBA, K., INOUE, T., SATOH, T., INAGAKI, M. & KITAMURA, T. 2003. Phosphorylation by aurora B converts MgcRacGAP to a RhoGAP during cytokinesis. *Dev Cell*, 4, 549-60.
- MISHIMA, M., KAITNA, S. & GLOTZER, M. 2002. Central spindle assembly and cytokinesis require a kinesin-like protein/RhoGAP complex with microtubule bundling activity. *Dev Cell*, 2, 41-54.
- MISHIMA, M., PAVICIC, V., GRUNEBERG, U., NIGG, E. A. & GLOTZER, M. 2004. Cell cycle regulation of central spindle assembly. *Nature*, 430, 908-13.
- MITRA, J. & ENDERS, G. H. 2004. Cyclin A/Cdk2 complexes regulate activation of Cdk1 and Cdc25 phosphatases in human cells. *Oncogene*, 23, 3361-7.
- MOCHIDA, S., IKEO, S., GANNON, J. & HUNT, T. 2009. Regulated activity of PP2A-B55 delta is crucial for controlling entry into and exit from mitosis in Xenopus egg extracts. *EMBO J*, 28, 2777-85.
- MOCHIDA, S., MASLEN, S. L., SKEHEL, M. & HUNT, T. 2010. Greatwall phosphorylates an inhibitor of protein phosphatase 2A that is essential for mitosis. *Science*, 330, 1670-3.
- MOORMAN, J. P., BOBAK, D. A. & HAHN, C. S. 1996. Inactivation of the small GTP binding protein Rho induces multinucleate cell formation and apoptosis in murine T lymphoma EL4. *J Immunol*, 156, 4146-53.
- MORGAN, D. O. 1997. Cyclin-dependent kinases: engines, clocks, and microprocessors. *Annu Rev Cell Dev Biol*, 13, 261-91.
- MORGAN, D. O. 2006. *The cell cycle : principles of control*, London, New Science Press.
- MORITA, E., SANDRIN, V., CHUNG, H. Y., MORHAM, S. G., GYGI, S. P., RODESCH, C. K. & SUNDQUIST, W. I. 2007. Human ESCRT and ALIX proteins interact with proteins of the midbody and function in cytokinesis. *EMBO J*, 26, 4215-27.
- MOTEGI, F. & SUGIMOTO, A. 2006. Sequential functioning of the ECT-2 RhoGEF, RHO-1 and CDC-42 establishes cell polarity in Caenorhabditis elegans embryos. *Nat Cell Biol*, 8, 978-85.
- MOTEGI, F., VELARDE, N. V., PIANO, F. & SUGIMOTO, A. 2006. Two phases of astral microtubule activity during cytokinesis in C. elegans embryos. *Dev Cell*, 10, 509-20.
- MUELLER, P. R., COLEMAN, T. R., KUMAGAI, A. & DUNPHY, W. G. 1995. Myt1: a membrane-associated inhibitory kinase that phosphorylates Cdc2 on both threonine-14 and tyrosine-15. *Science*, 270, 86-90.
- MULLINS, J. M. & BIESELE, J. J. 1977. Terminal phase of cytokinesis in D-98s cells. *J Cell Biol*, 73, 672-84.
- MURNION, M. E., ADAMS, R. R., CALLISTER, D. M., ALLIS, C. D., EARNSHAW, W. C. & SWEDLOW, J. R. 2001. Chromatin-associated protein phosphatase 1 regulates aurora-B and histone H3 phosphorylation. *J Biol Chem*, 276, 26656-65.

- MURO, A. F., CAPUTI, M., PARIYARATH, R., PAGANI, F., BURATTI, E. & BARALLE, F. E. 1999. Regulation of fibronectin EDA exon alternative splicing: possible role of RNA secondary structure for enhancer display. *Mol Cell Biol*, 19, 2657-71.
- MURTHY, K. & WADSWORTH, P. 2005. Myosin-II-dependent localization and dynamics of F-actin during cytokinesis. *Curr Biol*, 15, 724-31.
- MURUGAN, R. N., PARK, J. E., KIM, E. H., SHIN, S. Y., CHEONG, C., LEE, K. S. & BANG, J. K. 2011. Plk1-targeted small molecule inhibitors: molecular basis for their potency and specificity. *Mol Cells*, 32, 209-20.
- MUSACCHIO, A. & SALMON, E. D. 2007. The spindle-assembly checkpoint in space and time. *Nat Rev Mol Cell Biol*, 8, 379-93.
- NAKAJIMA, H., TOYOSHIMA-MORIMOTO, F., TANIGUCHI, E. & NISHIDA, E. 2003. Identification of a consensus motif for Plk (Polo-like kinase) phosphorylation reveals Myt1 as a Plk1 substrate. *J Biol Chem*, 278, 25277-80.
- NAKAYAMA, K. & NAKAYAMA, K. 1998. Cip/Kip cyclin-dependent kinase inhibitors: brakes of the cell cycle engine during development. *Bioessays*, 20, 1020-9.
- NARAYAN, K. & LEMMON, M. A. 2006. Determining selectivity of phosphoinositide-binding domains. *Methods*, 39, 122-33.
- NASMYTH, K. & HAERING, C. H. 2009. Cohesin: its roles and mechanisms. *Annu Rev Genet*, 43, 525-58.
- NEEF, R., GRUNEBERG, U., KOPAJTICH, R., LI, X., NIGG, E. A., SILLJE, H. & BARR, F. A. 2007. Choice of Plk1 docking partners during mitosis and cytokinesis is controlled by the activation state of Cdk1. *Nat Cell Biol*, 9, 436-44.
- NEEF, R., PREISINGER, C., SUTCLIFFE, J., KOPAJTICH, R., NIGG, E. A., MAYER, T. U. & BARR, F. A. 2003. Phosphorylation of mitotic kinesin-like protein 2 by polo-like kinase 1 is required for cytokinesis. *J Cell Biol*, 162, 863-75.
- NETO, H., COLLINS, L. L. & GOULD, G. W. 2011. Vesicle trafficking and membrane remodelling in cytokinesis. *Biochem J*, 437, 13-24.
- NEUFELD, T. P. & RUBIN, G. M. 1994. The *Drosophila* peanut gene is required for cytokinesis and encodes a protein similar to yeast putative bud neck filament proteins. *Cell*, 77, 371-9.
- NEUROHR, G., NAEGELI, A., TITOS, I., THELER, D., GREBER, B., DIEZ, J., GABALDON, T., MENDOZA, M. & BARRAL, Y. 2011. A midzone-based ruler adjusts chromosome compaction to anaphase spindle length. *Science*, 332, 465-8.
- NG, M. M., CHANG, F. & BURGESS, D. R. 2005. Movement of membrane domains and requirement of membrane signaling molecules for cytokinesis. *Dev Cell*, 9, 781-90.
- NGUYEN, H. G., CHINNAPPAN, D., URANO, T. & RAVID, K. 2005. Mechanism of Aurora-B degradation and its dependency on intact KEN and A-boxes: identification of an aneuploidy-promoting property. *Mol Cell Biol*, 25, 4977-92.
- NIGG, E. A. 1993. Cellular substrates of p34(cdc2) and its companion cyclin-dependent kinases. *Trends Cell Biol*, 3, 296-301.
- NIGG, E. A., BLANGY, A. & LANE, H. A. 1996. Dynamic changes in nuclear architecture during mitosis: on the role of protein phosphorylation in spindle assembly and chromosome segregation. *Exp Cell Res*, 229, 174-80.
- NIGG, E. A. & STEARNS, T. 2011. The centrosome cycle: Centriole biogenesis, duplication and inherent asymmetries. *Nat Cell Biol*, 13, 1154-60.
- NIIYA, F., TATSUMOTO, T., LEE, K. S. & MIKI, T. 2006. Phosphorylation of the cytokinesis regulator ECT2 at G2/M phase stimulates association of the mitotic kinase Plk1 and accumulation of GTP-bound RhoA. *Oncogene*, 25, 827-37.

- NIIYA, F., XIE, X., LEE, K. S., INOUE, H. & MIKI, T. 2005. Inhibition of cyclin-dependent kinase 1 induces cytokinesis without chromosome segregation in an ECT2 and MgcRacGAP-dependent manner. *J Biol Chem*, 280, 36502-9.
- NISHIMURA, Y. & YONEMURA, S. 2006. Centralspindlin regulates ECT2 and RhoA accumulation at the equatorial cortex during cytokinesis. *J Cell Sci*, 119, 104-14.
- NORDEN, C., MENDOZA, M., DOBBELAERE, J., KOTWALIWALE, C. V., BIGGINS, S. & BARRAL, Y. 2006. The NoCut pathway links completion of cytokinesis to spindle midzone function to prevent chromosome breakage. *Cell*, 125, 85-98.
- NUNES BASTOS, R., GANDHI, S. R., BARON, R. D., GRUNEBERG, U., NIGG, E. A. & BARR, F. A. 2013. Aurora B suppresses microtubule dynamics and limits central spindle size by locally activating KIF4A. *J Cell Biol*, 202, 605-21.
- NURSE, P. 2000. A long twentieth century of the cell cycle and beyond. *Cell*, 100, 71-8.
- NURSE, P., THURIAUX, P. & NASMYTH, K. 1976. Genetic control of the cell division cycle in the fission yeast *Schizosaccharomyces pombe*. *Mol Gen Genet*, 146, 167-78.
- O'CONNELL, C. B. & WANG, Y. L. 2000. Mammalian spindle orientation and position respond to changes in cell shape in a dynein-dependent fashion. *Mol Biol Cell*, 11, 1765-74.
- O'CONNELL, C. B., WHEATLEY, S. P., AHMED, S. & WANG, Y. L. 1999. The small GTP-binding protein rho regulates cortical activities in cultured cells during division. *J Cell Biol*, 144, 305-13.
- OCEGUERA-YANEZ, F., KIMURA, K., YASUDA, S., HIGASHIDA, C., KITAMURA, T., HIRAOKA, Y., HARAGUCHI, T. & NARUMIYA, S. 2005. Ect2 and MgcRacGAP regulate the activation and function of Cdc42 in mitosis. *J Cell Biol*, 168, 221-32.
- ODELL, G. M. & FOE, V. E. 2008. An agent-based model contrasts opposite effects of dynamic and stable microtubules on cleavage furrow positioning. *J Cell Biol*, 183, 471-83.
- ORTEGA, S., PRIETO, I., ODAJIMA, J., MARTIN, A., DUBUS, P., SOTILLO, R., BARBERO, J. L., MALUMBRES, M. & BARBACID, M. 2003. Cyclin-dependent kinase 2 is essential for meiosis but not for mitotic cell division in mice. *Nat Genet*, 35, 25-31.
- OTOMO, T., OTOMO, C., TOMCHICK, D. R., MACHIUS, M. & ROSEN, M. K. 2005. Structural basis of Rho GTPase-mediated activation of the formin mDia1. *Mol Cell*, 18, 273-81.
- PADMANABHAN, A., RAO, M. V., WU, Y. & ZAIDEL-BAR, R. 2015. Jack of all trades: functional modularity in the adherens junction. *Curr Opin Cell Biol*, 36, 32-40.
- PAGANO, M., TAM, S. W., THEODORAS, A. M., BEER-ROMERO, P., DEL SAL, G., CHAU, V., YEW, P. R., DRAETTA, G. F. & ROLFE, M. 1995. Role of the ubiquitin-proteasome pathway in regulating abundance of the cyclin-dependent kinase inhibitor p27. *Science*, 269, 682-5.
- PAGLIUCA, F. W., COLLINS, M. O., LICHAWSKA, A., ZEGERMAN, P., CHOUDHARY, J. S. & PINES, J. 2011. Quantitative proteomics reveals the basis for the biochemical specificity of the cell-cycle machinery. *Mol Cell*, 43, 406-17.
- PARKER, L. L., ATHERTON-FESSLER, S. & PIWNICA-WORMS, H. 1992. p107wee1 is a dual-specificity kinase that phosphorylates p34cdc2 on tyrosine 15. *Proc Natl Acad Sci U S A*, 89, 2917-21.
- PASSMORE, L. A. & BARFORD, D. 2005. Coactivator functions in a stoichiometric complex with anaphase-promoting complex/cyclosome to mediate substrate recognition. *EMBO Rep*, 6, 873-8.
- PATHAK, G. P., VRANA, J. D. & TUCKER, C. L. 2013. Optogenetic control of cell function using engineered photoreceptors. *Biol Cell*, 105, 59-72.

- PAVICIC-KALTENBRUNNER, V., MISHIMA, M. & GLOTZER, M. 2007. Cooperative assembly of CYK-4/MgcRacGAP and ZEN-4/MKLP1 to form the centralspindlin complex. *Mol Biol Cell*, 18, 4992-5003.
- PETERS, J. M. & NISHIYAMA, T. 2012. Sister chromatid cohesion. *Cold Spring Harb Perspect Biol*, 4.
- PETERSEN, J., PARIS, J., WILLER, M., PHILIPPE, M. & HAGAN, I. M. 2001. The *S. pombe* aurora-related kinase Ark1 associates with mitotic structures in a stage dependent manner and is required for chromosome segregation. *J Cell Sci*, 114, 4371-84.
- PETRONCZKI, M., GLOTZER, M., KRAUT, N. & PETERS, J. M. 2007. Polo-like kinase 1 triggers the initiation of cytokinesis in human cells by promoting recruitment of the RhoGEF Ect2 to the central spindle. *Dev Cell*, 12, 713-25.
- PICKART, C. M. 2001. Mechanisms underlying ubiquitination. *Annu Rev Biochem*, 70, 503-33.
- PIEKNY, A., WERNER, M. & GLOTZER, M. 2005. Cytokinesis: welcome to the Rho zone. *Trends Cell Biol*, 15, 651-8.
- PIEKNY, A. J. & GLOTZER, M. 2008. Anillin is a scaffold protein that links RhoA, actin, and myosin during cytokinesis. *Curr Biol*, 18, 30-6.
- PIEKNY, A. J. & MADDOX, A. S. 2010. The myriad roles of Anillin during cytokinesis. *Semin Cell Dev Biol*, 21, 881-91.
- PIEKNY, A. J. & MAINS, P. E. 2002. Rho-binding kinase (LET-502) and myosin phosphatase (MEL-11) regulate cytokinesis in the early *Caenorhabditis elegans* embryo. *J Cell Sci*, 115, 2271-82.
- PINES, J. 2011. Cubism and the cell cycle: the many faces of the APC/C. *Nat Rev Mol Cell Biol*, 12, 427-38.
- POHL, C. & JENTSCH, S. 2009. Midbody ring disposal by autophagy is a post-abscission event of cytokinesis. *Nat Cell Biol*, 11, 65-70.
- POLEVOY, G., WEI, H. C., WONG, R., SZENTPETERY, Z., KIM, Y. J., GOLDBACH, P., STEINBACH, S. K., BALLA, T. & BRILL, J. A. 2009. Dual roles for the *Drosophila* PI 4-kinase four wheel drive in localizing Rab11 during cytokinesis. *J Cell Biol*, 187, 847-58.
- POTAPOVA, T. A., DAUM, J. R., PITTMAN, B. D., HUDSON, J. R., JONES, T. N., SATINOVER, D. L., STUKENBERG, P. T. & GORBSKY, G. J. 2006. The reversibility of mitotic exit in vertebrate cells. *Nature*, 440, 954-8.
- POWERS, J., BOSSINGER, O., ROSE, D., STROME, S. & SAXTON, W. 1998. A nematode kinesin required for cleavage furrow advancement. *Curr Biol*, 8, 1133-6.
- POWIS, G., BONJOUKLIAN, R., BERGGREN, M. M., GALLEGOS, A., ABRAHAM, R., ASHENDEL, C., ZALKOW, L., MATTER, W. F., DODGE, J., GRINDEY, G. & ET AL. 1994. Wortmannin, a potent and selective inhibitor of phosphatidylinositol-3-kinase. *Cancer Res*, 54, 2419-23.
- PRAEFCKE, G. J. & MCMAHON, H. T. 2004. The dynamin superfamily: universal membrane tubulation and fission molecules? *Nat Rev Mol Cell Biol*, 5, 133-47.
- PROKOPENKO, S. N., BRUMBY, A., O'KEEFE, L., PRIOR, L., HE, Y., SAINT, R. & BELLEN, H. J. 1999. A putative exchange factor for Rho1 GTPase is required for initiation of cytokinesis in *Drosophila*. *Genes Dev*, 13, 2301-14.
- RANGONE, H., WEGEL, E., GATT, M. K., YEUNG, E., FLOWERS, A., DEBSKI, J., DADLEZ, M., JANSSENS, V., CARPENTER, A. T. & GLOVER, D. M. 2011. Suppression of scant identifies Endos as a substrate of greatwall kinase and a negative regulator of protein phosphatase 2A in mitosis. *PLoS Genet*, 7, e1002225.
- RAO, P. N. & JOHNSON, R. T. 1970. Mammalian cell fusion: studies on the regulation of DNA synthesis and mitosis. *Nature*, 225, 159-64.

- RAPPAPORT, R. 1961. Experiments concerning the cleavage stimulus in sand dollar eggs. *J Exp Zool*, 148, 81-9.
- RAPPAPORT, R. 1985. Repeated furrow formation from a single mitotic apparatus in cylindrical sand dollar eggs. *J Exp Zool*, 234, 167-71.
- RAPPAPORT, R. 1996. *Cytokinesis in animal cells*, Cambridge, Cambridge University Press.
- RAPPAPORT, R. & EBSTEIN, R. P. 1965. Duration of Stimulus and Latent Periods Preceding Furrow Formation in Sand Dollar Eggs. *J Exp Zool*, 158, 373-82.
- RATHEESH, A., GOMEZ, G. A., PRIYA, R., VERMA, S., KOVACS, E. M., JIANG, K., BROWN, N. H., AKHMANOVA, A., STEHBENS, S. J. & YAP, A. S. 2012. Centralspindlin and alpha-catenin regulate Rho signalling at the epithelial zonula adherens. *Nat Cell Biol*, 14, 818-28.
- RAUCHER, D., STAUFFER, T., CHEN, W., SHEN, K., GUO, S., YORK, J. D., SHEETZ, M. P. & MEYER, T. 2000. Phosphatidylinositol 4,5-bisphosphate functions as a second messenger that regulates cytoskeleton-plasma membrane adhesion. *Cell*, 100, 221-8.
- REBECCHI, M., PETERSON, A. & MCLAUGHLIN, S. 1992. Phosphoinositide-specific phospholipase C-delta 1 binds with high affinity to phospholipid vesicles containing phosphatidylinositol 4,5-bisphosphate. *Biochemistry*, 31, 12742-7.
- REICHL, E. M., REN, Y., MORPHEW, M. K., DELANNOY, M., EFFLER, J. C., GIRARD, K. D., DIVI, S., IGLESIAS, P. A., KUO, S. C. & ROBINSON, D. N. 2008. Interactions between myosin and actin crosslinkers control cytokinesis contractility dynamics and mechanics. *Curr Biol*, 18, 471-80.
- REID, E., CONNELL, J., EDWARDS, T. L., DULEY, S., BROWN, S. E. & SANDERSON, C. M. 2005. The hereditary spastic paraplegia protein spastin interacts with the ESCRT-III complex-associated endosomal protein CHMP1B. *Hum Mol Genet*, 14, 19-38.
- RHIND, N. & RUSSELL, P. 2012. Signaling pathways that regulate cell division. *Cold Spring Harb Perspect Biol*, 4.
- RIVERA, V. M., CLACKSON, T., NATESAN, S., POLLOCK, R., AMARA, J. F., KEENAN, T., MAGARI, S. R., PHILLIPS, T., COURAGE, N. L., CERASOLI, F., JR., HOLT, D. A. & GILMAN, M. 1996. A humanized system for pharmacologic control of gene expression. *Nat Med*, 2, 1028-32.
- ROBINETT, C. C., GIANANTI, M. G., GATTI, M. & FULLER, M. T. 2009. TRAPP II is required for cleavage furrow ingression and localization of Rab11 in dividing male meiotic cells of *Drosophila*. *J Cell Sci*, 122, 4526-34.
- RODRIGUES, N. T., LEKOMTSEV, S., JANANJI, S., KRISTON-VIZI, J., HICKSON, G. R. & BAUM, B. 2015. Kinetochore-localized PP1-Sds22 couples chromosome segregation to polar relaxation. *Nature*.
- ROGHI, C., GIET, R., UZBEKOV, R., MORIN, N., CHARTRAIN, I., LE GUELLEC, R., COUTURIER, A., DOREE, M., PHILIPPE, M. & PRIGENT, C. 1998. The *Xenopus* protein kinase pEg2 associates with the centrosome in a cell cycle-dependent manner, binds to the spindle microtubules and is involved in bipolar mitotic spindle assembly. *J Cell Sci*, 111 (Pt 5), 557-72.
- ROSA, A., VLASSAKS, E., PICHAUD, F. & BAUM, B. 2015. Ect2/Pbl acts via Rho and polarity proteins to direct the assembly of an isotropic actomyosin cortex upon mitotic entry. *Dev Cell*, 32, 604-16.
- ROSSMAN, K. L., DER, C. J. & SONDEK, J. 2005. GEF means go: turning on RHO GTPases with guanine nucleotide-exchange factors. *Nat Rev Mol Cell Biol*, 6, 167-80.
- RUDNER, A. D. & MURRAY, A. W. 2000. Phosphorylation by Cdc28 activates the Cdc20-dependent activity of the anaphase-promoting complex. *J Cell Biol*, 149, 1377-90.

- RUSAN, N. M., FAGERSTROM, C. J., YVON, A. M. & WADSWORTH, P. 2001. Cell cycle-dependent changes in microtubule dynamics in living cells expressing green fluorescent protein- α tubulin. *Mol Biol Cell*, 12, 971-80.
- RUSSELL, P. & NURSE, P. 1987. Negative regulation of mitosis by *wee1+*, a gene encoding a protein kinase homolog. *Cell*, 49, 559-67.
- SAETER, G., SCHWARZE, P. E., NESLAND, J. M., JUUL, N., PETTERSEN, E. O. & SEGLEN, P. O. 1988. The polyploidizing growth pattern of normal rat liver is replaced by divisional, diploid growth in hepatocellular nodules and carcinomas. *Carcinogenesis*, 9, 939-45.
- SAGONA, A. P., NEZIS, I. P., PEDERSEN, N. M., LIESTOL, K., POULTON, J., RUSTEN, T. E., SKOTHEIM, R. I., RAIBORG, C. & STENMARK, H. 2010. PtdIns(3)P controls cytokinesis through KIF13A-mediated recruitment of FYVE-CENT to the midbody. *Nat Cell Biol*, 12, 362-71.
- SAITO, S., LIU, X. F., KAMIJO, K., RAZIUDDIN, R., TATSUMOTO, T., OKAMOTO, I., CHEN, X., LEE, C. C., LORENZI, M. V., OHARA, N. & MIKI, T. 2004. Deregulation and mislocalization of the cytokinesis regulator ECT2 activate the Rho signaling pathways leading to malignant transformation. *J Biol Chem*, 279, 7169-79.
- SALIC, A., WATERS, J. C. & MITCHISON, T. J. 2004. Vertebrate shugoshin links sister centromere cohesion and kinetochore microtubule stability in mitosis. *Cell*, 118, 567-78.
- SALMELA, A. L. & KALLIO, M. J. 2013. Mitosis as an anti-cancer drug target. *Chromosoma*, 122, 431-49.
- SANSREGRET, L. & PETRONCZKI, M. 2013. Born equal: dual safeguards for daughter cell size symmetry. *Cell*, 154, 269-71.
- SANTAGUIDA, S., VERNIERI, C., VILLA, F., CILIBERTO, A. & MUSACCHIO, A. 2011. Evidence that Aurora B is implicated in spindle checkpoint signalling independently of error correction. *EMBO J*, 30, 1508-19.
- SANTAMARIA, A., NEEF, R., EBERSPACHER, U., EIS, K., HUSEMANN, M., MUMBERG, D., PRECHTL, S., SCHULZE, V., SIEMEISTER, G., WORTMANN, L., BARR, F. A. & NIGG, E. A. 2007a. Use of the novel Plk1 inhibitor ZK-thiazolidinone to elucidate functions of Plk1 in early and late stages of mitosis. *Mol Biol Cell*, 18, 4024-36.
- SANTAMARIA, D., BARRIERE, C., CERQUEIRA, A., HUNT, S., TARDY, C., NEWTON, K., CACERES, J. F., DUBUS, P., MALUMBRES, M. & BARBACID, M. 2007b. Cdk1 is sufficient to drive the mammalian cell cycle. *Nature*, 448, 811-5.
- SANTI, S. A. & LEE, H. 2010. The Akt isoforms are present at distinct subcellular locations. *Am J Physiol Cell Physiol*, 298, C580-91.
- SATTERWHITE, L. L., LOHKA, M. J., WILSON, K. L., SCHERSON, T. Y., CISEK, L. J., CORDEN, J. L. & POLLARD, T. D. 1992. Phosphorylation of myosin-II regulatory light chain by cyclin-p34cdc2: a mechanism for the timing of cytokinesis. *J Cell Biol*, 118, 595-605.
- SATTERWHITE, L. L. & POLLARD, T. D. 1992. Cytokinesis. *Curr Opin Cell Biol*, 4, 43-52.
- SATYANARAYANA, A. & KALDIS, P. 2009. Mammalian cell-cycle regulation: several Cdks, numerous cyclins and diverse compensatory mechanisms. *Oncogene*, 28, 2925-39.
- SAURIN, A. T., DURGAN, J., CAMERON, A. J., FAISAL, A., MARBER, M. S. & PARKER, P. J. 2008. The regulated assembly of a PKCepsilon complex controls the completion of cytokinesis. *Nat Cell Biol*, 10, 891-901.
- SCHIEL, J. A., PARK, K., MORPHEW, M. K., REID, E., HOENGER, A. & PREKERIS, R. 2011. Endocytic membrane fusion and buckling-induced microtubule severing mediate cell abscission. *J Cell Sci*, 124, 1411-24.

- SCHIEL, J. A. & PREKERIS, R. 2013. Membrane dynamics during cytokinesis. *Curr Opin Cell Biol*, 25, 92-8.
- SCHIEL, J. A., SIMON, G. C., ZAHARRIS, C., WEISZ, J., CASTLE, D., WU, C. C. & PREKERIS, R. 2012. FIP3-endosome-dependent formation of the secondary ingression mediates ESCRT-III recruitment during cytokinesis. *Nat Cell Biol*, 14, 1068-78.
- SCHMITZ, M. H., HELD, M., JANSSENS, V., HUTCHINS, J. R., HUDECZ, O., IVANOVA, E., GORIS, J., TRINKLE-MULCAHY, L., LAMOND, A. I., POSER, I., HYMAN, A. A., MECHTLER, K., PETERS, J. M. & GERLICH, D. W. 2010. Live-cell imaging RNAi screen identifies PP2A-B55alpha and importin-beta1 as key mitotic exit regulators in human cells. *Nat Cell Biol*, 12, 886-93.
- SCHNEIDER, B. L., YANG, Q. H. & FUTCHER, A. B. 1996. Linkage of replication to start by the Cdk inhibitor Sic1. *Science*, 272, 560-2.
- SCHROEDER, T. E. 1972. The contractile ring. II. Determining its brief existence, volumetric changes, and vital role in cleaving *Arbacia* eggs. *J Cell Biol*, 53, 419-34.
- SCHUYLER, S. C., LIU, J. Y. & PELLMAN, D. 2003. The molecular function of Ase1p: evidence for a MAP-dependent midzone-specific spindle matrix. Microtubule-associated proteins. *J Cell Biol*, 160, 517-28.
- SCHWEITZER, J. K. & D'SOUZA-SCHOREY, C. 2002. Localization and activation of the ARF6 GTPase during cleavage furrow ingression and cytokinesis. *J Biol Chem*, 277, 27210-6.
- SEDZINSKI, J., BIRO, M., OSWALD, A., TINEVEZ, J. Y., SALBREUX, G. & PALUCH, E. 2011. Polar actomyosin contractility destabilizes the position of the cytokinetic furrow. *Nature*, 476, 462-6.
- SEGUIN, L., LIOT, C., MZALI, R., HARADA, R., SIRET, A., NEPVEU, A. & BERTOGLIO, J. 2009. CUX1 and E2F1 regulate coordinated expression of the mitotic complex genes Ect2, MgcRacGAP, and MKLP1 in S phase. *Mol Cell Biol*, 29, 570-81.
- SEKI, A., COPPINGER, J. A., JANG, C. Y., YATES, J. R. & FANG, G. 2008. Bora and the kinase Aurora a cooperatively activate the kinase Plk1 and control mitotic entry. *Science*, 320, 1655-8.
- SEVERSON, A. F., BAILLIE, D. L. & BOWERMAN, B. 2002. A Formin Homology protein and a profilin are required for cytokinesis and Arp2/3-independent assembly of cortical microfilaments in *C. elegans*. *Curr Biol*, 12, 2066-75.
- SHANNON, K. B., CANMAN, J. C., BEN MOREE, C., TIRNAUER, J. S. & SALMON, E. D. 2005. Taxol-stabilized microtubules can position the cytokinetic furrow in mammalian cells. *Mol Biol Cell*, 16, 4423-36.
- SHERR, C. J. & ROBERTS, J. M. 1999. CDK inhibitors: positive and negative regulators of G1-phase progression. *Genes Dev*, 13, 1501-12.
- SHUSTER, C. B. & BURGESS, D. R. 2002. Targeted new membrane addition in the cleavage furrow is a late, separate event in cytokinesis. *Proc Natl Acad Sci U S A*, 99, 3633-8.
- SIMON, G. C., SCHONTEICH, E., WU, C. C., PIEKNY, A., EKIERT, D., YU, X., GOULD, G. W., GLOTZER, M. & PREKERIS, R. 2008. Sequential Cyk-4 binding to ECT2 and FIP3 regulates cleavage furrow ingression and abscission during cytokinesis. *EMBO J*, 27, 1791-803.
- SIVAKUMAR, S. & GORBSKY, G. J. 2015. Spatiotemporal regulation of the anaphase-promoting complex in mitosis. *Nat Rev Mol Cell Biol*, 16, 82-94.
- SKOP, A. R., BERGMANN, D., MOHLER, W. A. & WHITE, J. G. 2001. Completion of cytokinesis in *C. elegans* requires a brefeldin A-sensitive membrane accumulation at the cleavage furrow apex. *Curr Biol*, 11, 735-46.

- SKOP, A. R., LIU, H., YATES, J., 3RD, MEYER, B. J. & HEALD, R. 2004. Dissection of the mammalian midbody proteome reveals conserved cytokinesis mechanisms. *Science*, 305, 61-6.
- SMUTNY, M., COX, H. L., LEERBERG, J. M., KOVACS, E. M., CONTI, M. A., FERGUSON, C., HAMILTON, N. A., PARTON, R. G., ADELSTEIN, R. S. & YAP, A. S. 2010. Myosin II isoforms identify distinct functional modules that support integrity of the epithelial zonula adherens. *Nat Cell Biol*, 12, 696-702.
- SOMERS, W. G. & SAINT, R. 2003. A RhoGEF and Rho family GTPase-activating protein complex links the contractile ring to cortical microtubules at the onset of cytokinesis. *Dev Cell*, 4, 29-39.
- STEIGEMANN, P., WURZENBERGER, C., SCHMITZ, M. H., HELD, M., GUIZETTI, J., MAAR, S. & GERLICH, D. W. 2009. Aurora B-mediated abscission checkpoint protects against tetraploidization. *Cell*, 136, 473-84.
- STEMMANN, O., ZOU, H., GERBER, S. A., GYGI, S. P. & KIRSCHNER, M. W. 2001. Dual inhibition of sister chromatid separation at metaphase. *Cell*, 107, 715-26.
- STEWART, S. & FANG, G. 2005. Destruction box-dependent degradation of aurora B is mediated by the anaphase-promoting complex/cyclosome and Cdh1. *Cancer Res*, 65, 8730-5.
- STRAIGHT, A. F., FIELD, C. M. & MITCHISON, T. J. 2005. Anillin binds nonmuscle myosin II and regulates the contractile ring. *Mol Biol Cell*, 16, 193-201.
- STRAUSFELD, U., FERNANDEZ, A., CAPONY, J. P., GIRARD, F., LAUTREDOU, N., DERANCOURT, J., LABBE, J. C. & LAMB, N. J. 1994. Activation of p34cdc2 protein kinase by microinjection of human cdc25C into mammalian cells. Requirement for prior phosphorylation of cdc25C by p34cdc2 on sites phosphorylated at mitosis. *J Biol Chem*, 269, 5989-6000.
- STREBHARDT, K. 2010. Multifaceted polo-like kinases: drug targets and antitargets for cancer therapy. *Nat Rev Drug Discov*, 9, 643-60.
- STRICKLAND, L. I., DONNELLY, E. J. & BURGESS, D. R. 2005. Induction of cytokinesis is independent of precisely regulated microtubule dynamics. *Mol Biol Cell*, 16, 4485-94.
- SU, K. C., BEMENT, W. M., PETRONCZKI, M. & VON DASSOW, G. 2014. An astral simulacrum of the central spindle accounts for normal, spindle-less, and anucleate cytokinesis in echinoderm embryos. *Mol Biol Cell*, 25, 4049-62.
- SU, K. C., TAKAKI, T. & PETRONCZKI, M. 2011. Targeting of the RhoGEF Ect2 to the equatorial membrane controls cleavage furrow formation during cytokinesis. *Dev Cell*, 21, 1104-15.
- SU, K. C. A. 2013. *Control of cleavage furrow formation during cytokinesis in human cells*. Thesis (Ph.D.), University College London (University of London).
- SU, L., AGATI, J. M. & PARSONS, S. J. 2003. p190RhoGAP is cell cycle regulated and affects cytokinesis. *J Cell Biol*, 163, 571-82.
- SU, L., PERTZ, O., MIKAWA, M., HAHN, K. & PARSONS, S. J. 2009. p190RhoGAP negatively regulates Rho activity at the cleavage furrow of mitotic cells. *Exp Cell Res*, 315, 1347-59.
- SUBRAMANIAN, R., WILSON-KUBALEK, E. M., ARTHUR, C. P., BICK, M. J., CAMPBELL, E. A., DARST, S. A., MILLIGAN, R. A. & KAPOOR, T. M. 2010. Insights into antiparallel microtubule crosslinking by PRC1, a conserved nonmotor microtubule binding protein. *Cell*, 142, 433-43.
- SUDAKIN, V., CHAN, G. K. & YEN, T. J. 2001. Checkpoint inhibition of the APC/C in HeLa cells is mediated by a complex of BUBR1, BUB3, CDC20, and MAD2. *J Cell Biol*, 154, 925-36.
- SUGIMOTO, K., URANO, T., ZUSHI, H., INOUE, K., TASAKA, H., TACHIBANA, M. & DOTSU, M. 2002. Molecular dynamics of Aurora-A kinase in living mitotic cells

- simultaneously visualized with histone H3 and nuclear membrane protein importin α . *Cell Struct Funct*, 27, 457-67.
- SULLIVAN, M. & MORGAN, D. O. 2007. Finishing mitosis, one step at a time. *Nat Rev Mol Cell Biol*, 8, 894-903.
- SUMARA, I., GIMENEZ-ABIAN, J. F., GERLICH, D., HIROTA, T., KRAFT, C., DE LA TORRE, C., ELLENBERG, J. & PETERS, J. M. 2004. Roles of polo-like kinase 1 in the assembly of functional mitotic spindles. *Curr Biol*, 14, 1712-22.
- SUMARA, I., VORLAUFER, E., STUKENBERG, P. T., KELM, O., REDEMANN, N., NIGG, E. A. & PETERS, J. M. 2002. The dissociation of cohesin from chromosomes in prophase is regulated by Polo-like kinase. *Mol Cell*, 9, 515-25.
- SUNKEL, C. E. & GLOVER, D. M. 1988. polo, a mitotic mutant of Drosophila displaying abnormal spindle poles. *J Cell Sci*, 89 (Pt 1), 25-38.
- SUZUKI, K., SAKO, K., AKIYAMA, K., ISODA, M., SENOO, C., NAKAJO, N. & SAGATA, N. 2015. Identification of non-Ser/Thr-Pro consensus motifs for Cdk1 and their roles in mitotic regulation of C2H2 zinc finger proteins and Ect2. *Sci Rep*, 5, 7929.
- TAN, S. Y. & BROWN, J. 2006. Rudolph Virchow (1821-1902): "pope of pathology". *Singapore Med J*, 47, 567-8.
- TANAKA, S. & ARAKI, H. 2010. Regulation of the initiation step of DNA replication by cyclin-dependent kinases. *Chromosoma*, 119, 565-74.
- TANAKA, T. U., RACHIDI, N., JANKE, C., PEREIRA, G., GALOVA, M., SCHIEBEL, E., STARK, M. J. & NASMYTH, K. 2002. Evidence that the Ipl1-Sli15 (Aurora kinase-INCENP) complex promotes chromosome bi-orientation by altering kinetochore-spindle pole connections. *Cell*, 108, 317-29.
- TANENBAUM, M. E. & MEDEMA, R. H. 2010. Mechanisms of centrosome separation and bipolar spindle assembly. *Dev Cell*, 19, 797-806.
- TANG, B. L. 2012. Membrane trafficking components in cytokinesis. *Cell Physiol Biochem*, 30, 1097-108.
- TANG, C. J., LIN, C. Y. & TANG, T. K. 2006a. Dynamic localization and functional implications of Aurora-C kinase during male mouse meiosis. *Dev Biol*, 290, 398-410.
- TANG, Z., SHU, H., QI, W., MAHMOOD, N. A., MUMBY, M. C. & YU, H. 2006b. PP2A is required for centromeric localization of Sgo1 and proper chromosome segregation. *Dev Cell*, 10, 575-85.
- TATSUMOTO, T., SAKATA, H., DASSO, M. & MIKI, T. 2003. Potential roles of the nucleotide exchange factor ECT2 and Cdc42 GTPase in spindle assembly in Xenopus egg cell-free extracts. *J Cell Biochem*, 90, 892-900.
- TATSUMOTO, T., XIE, X., BLUMENTHAL, R., OKAMOTO, I. & MIKI, T. 1999. Human ECT2 is an exchange factor for Rho GTPases, phosphorylated in G2/M phases, and involved in cytokinesis. *J Cell Biol*, 147, 921-8.
- THOMPSON, H. M., SKOP, A. R., EUTENEUER, U., MEYER, B. J. & MCNIVEN, M. A. 2002. The large GTPase dynamin associates with the spindle midzone and is required for cytokinesis. *Curr Biol*, 12, 2111-7.
- THORESEN, S. B., PEDERSEN, N. M., LIESTOL, K. & STENMARK, H. 2010. A phosphatidylinositol 3-kinase class III sub-complex containing VPS15, VPS34, Beclin 1, UVRAG and BIF-1 regulates cytokinesis and degradative endocytic traffic. *Exp Cell Res*, 316, 3368-78.
- THURIAUX, P., NURSE, P. & CARTER, B. 1978. Mutants altered in the control coordinating cell division with cell growth in the fission yeast *Schizosaccharomyces pombe*. *Mol Gen Genet*, 161, 215-20.
- TOURE, A., DORSEUIL, O., MORIN, L., TIMMONS, P., JEGOU, B., REIBEL, L. & GACON, G. 1998. MgcRacGAP, a new human GTPase-activating protein for

- Rac and Cdc42 similar to *Drosophila rotundRacGAP* gene product, is expressed in male germ cells. *J Biol Chem*, 273, 6019-23.
- TOURNEBIZE, R., POPOV, A., KINOSHITA, K., ASHFORD, A. J., RYBINA, S., POZNIAKOVSKY, A., MAYER, T. U., WALCZAK, C. E., KARSENTI, E. & HYMAN, A. A. 2000. Control of microtubule dynamics by the antagonistic activities of XMAP215 and XKCM1 in *Xenopus* egg extracts. *Nat Cell Biol*, 2, 13-9.
- TOYOSHIMA-MORIMOTO, F., TANIGUCHI, E., SHINYA, N., IWAMATSU, A. & NISHIDA, E. 2001. Polo-like kinase 1 phosphorylates cyclin B1 and targets it to the nucleus during prophase. *Nature*, 410, 215-20.
- TRUNNELL, N. B., POON, A. C., KIM, S. Y. & FERRELL, J. E., JR. 2011. Ultrasensitivity in the Regulation of Cdc25C by Cdk1. *Mol Cell*, 41, 263-74.
- TSAI, M. Y. & ZHENG, Y. 2005. Aurora A kinase-coated beads function as microtubule-organizing centers and enhance RanGTP-induced spindle assembly. *Curr Biol*, 15, 2156-63.
- TUCKER, J. B. 1971. Microtubules and a contractile ring of microfilaments associated with a cleavage furrow. *J Cell Sci*, 8, 557-71.
- UBERSAX, J. A., WOODBURY, E. L., QUANG, P. N., PARAZ, M., BLETHROW, J. D., SHAH, K., SHOKAT, K. M. & MORGAN, D. O. 2003. Targets of the cyclin-dependent kinase Cdk1. *Nature*, 425, 859-64.
- UEHARA, R. & GOSHIMA, G. 2010. Functional central spindle assembly requires de novo microtubule generation in the interchromosomal region during anaphase. *J Cell Biol*, 191, 259-67.
- UEHARA, R., GOSHIMA, G., MABUCHI, I., VALE, R. D., SPUDICH, J. A. & GRIFFIS, E. R. 2010. Determinants of myosin II cortical localization during cytokinesis. *Curr Biol*, 20, 1080-5.
- UEHARA, R., NOZAWA, R. S., TOMIOKA, A., PETRY, S., VALE, R. D., OBUSE, C. & GOSHIMA, G. 2009. The augmin complex plays a critical role in spindle microtubule generation for mitotic progression and cytokinesis in human cells. *Proc Natl Acad Sci U S A*, 106, 6998-7003.
- UEHARA, R., TSUKADA, Y., KAMASAKI, T., POSER, I., YODA, K., GERLICH, D. W. & GOSHIMA, G. 2013. Aurora B and Kif2A control microtubule length for assembly of a functional central spindle during anaphase. *J Cell Biol*, 202, 623-36.
- UHLMANN, F., LOTTSPREICH, F. & NASMYTH, K. 1999. Sister-chromatid separation at anaphase onset is promoted by cleavage of the cohesin subunit Scc1. *Nature*, 400, 37-42.
- UREN, A. G., WONG, L., PAKUSCH, M., FOWLER, K. J., BURROWS, F. J., VAUX, D. L. & CHOO, K. H. 2000. Survivin and the inner centromere protein INCENP show similar cell-cycle localization and gene knockout phenotype. *Curr Biol*, 10, 1319-28.
- VAGNARELLI, P., RIBEIRO, S., SENNELS, L., SANCHEZ-PULIDO, L., DE LIMA ALVES, F., VERHEYEN, T., KELLY, D. A., PONTING, C. P., RAPPSILBER, J. & EARNSHAW, W. C. 2011. Repo-Man coordinates chromosomal reorganization with nuclear envelope reassembly during mitotic exit. *Dev Cell*, 21, 328-42.
- VANDRE, D. D. & WILLS, V. L. 1992. Inhibition of mitosis by okadaic acid: possible involvement of a protein phosphatase 2A in the transition from metaphase to anaphase. *J Cell Sci*, 101 (Pt 1), 79-91.
- VARNAI, P. & BALLA, T. 1998. Visualization of phosphoinositides that bind pleckstrin homology domains: calcium- and agonist-induced dynamic changes and relationship to myo-[3H]inositol-labeled phosphoinositide pools. *J Cell Biol*, 143, 501-10.

- VAZQUEZ-NOVELLE, M. D. & PETRONCZKI, M. 2010. Relocation of the chromosomal passenger complex prevents mitotic checkpoint engagement at anaphase. *Curr Biol*, 20, 1402-7.
- VERBRUGGHE, K. J. & WHITE, J. G. 2007. Cortical centralspindlin and G alpha have parallel roles in furrow initiation in early *C. elegans* embryos. *J Cell Sci*, 120, 1772-8.
- VERMA, R., ANNAN, R. S., HUDDLESTON, M. J., CARR, S. A., REYNARD, G. & DESHAIES, R. J. 1997. Phosphorylation of Sic1p by G1 Cdk required for its degradation and entry into S phase. *Science*, 278, 455-60.
- VETTER, I. R. & WITTINGHOFER, A. 2001. The guanine nucleotide-binding switch in three dimensions. *Science*, 294, 1299-304.
- VLAHOS, C. J., MATTER, W. F., HUI, K. Y. & BROWN, R. F. 1994. A specific inhibitor of phosphatidylinositol 3-kinase, 2-(4-morpholinyl)-8-phenyl-4H-1-benzopyran-4-one (LY294002). *J Biol Chem*, 269, 5241-8.
- VOGEL, S. K., PETRASEK, Z., HEINEMANN, F. & SCHWILLE, P. 2013. Myosin motors fragment and compact membrane-bound actin filaments. *Elife*, 2, e00116.
- WACHTLER, V., RAJAGOPALAN, S. & BALASUBRAMANIAN, M. K. 2003. Sterol-rich plasma membrane domains in the fission yeast *Schizosaccharomyces pombe*. *J Cell Sci*, 116, 867-74.
- WALKER, D. H. & MALLER, J. L. 1991. Role for cyclin A in the dependence of mitosis on completion of DNA replication. *Nature*, 354, 314-7.
- WALTER, A. O., SEGHEZZI, W., KORVER, W., SHEUNG, J. & LEES, E. 2000. The mitotic serine/threonine kinase Aurora2/AIK is regulated by phosphorylation and degradation. *Oncogene*, 19, 4906-16.
- WANG, C., DU, X. N., JIA, Q. Z. & ZHANG, H. L. 2005. Binding of PLCdelta1PH-GFP to PtdIns(4,5)P2 prevents inhibition of phospholipase C-mediated hydrolysis of PtdIns(4,5)P2 by neomycin. *Acta Pharmacol Sin*, 26, 1485-91.
- WATANABE, N., BROOME, M. & HUNTER, T. 1995. Regulation of the human WEE1Hu CDK tyrosine 15-kinase during the cell cycle. *EMBO J*, 14, 1878-91.
- WATANABE, N., MADAULE, P., REID, T., ISHIZAKI, T., WATANABE, G., KAKIZUKA, A., SAITO, Y., NAKAO, K., JOCKUSCH, B. M. & NARUMIYA, S. 1997. p140mDia, a mammalian homolog of *Drosophila* diaphanous, is a target protein for Rho small GTPase and is a ligand for profilin. *EMBO J*, 16, 3044-56.
- WATANABE, S., ANDO, Y., YASUDA, S., HOSOYA, H., WATANABE, N., ISHIZAKI, T. & NARUMIYA, S. 2008. mDia2 induces the actin scaffold for the contractile ring and stabilizes its position during cytokinesis in NIH 3T3 cells. *Mol Biol Cell*, 19, 2328-38.
- WEINBERG, R. A. 1995. The retinoblastoma protein and cell cycle control. *Cell*, 81, 323-30.
- WELBURN, J. P., TUCKER, J. A., JOHNSON, T., LINDERT, L., MORGAN, M., WILLIS, A., NOBLE, M. E. & ENDICOTT, J. A. 2007. How tyrosine 15 phosphorylation inhibits the activity of cyclin-dependent kinase 2-cyclin A. *J Biol Chem*, 282, 3173-81.
- WERNER, M., MUNRO, E. & GLOTZER, M. 2007. Astral signals spatially bias cortical myosin recruitment to break symmetry and promote cytokinesis. *Curr Biol*, 17, 1286-97.
- WHITE, J. G. & BORISY, G. G. 1983. On the mechanisms of cytokinesis in animal cells. *J Theor Biol*, 101, 289-316.
- WIENKE, D. C., KNETSCH, M. L., NEUHAUS, E. M., REEDY, M. C. & MANSTEIN, D. J. 1999. Disruption of a dynamin homologue affects endocytosis, organelle morphology, and cytokinesis in *Dictyostelium discoideum*. *Mol Biol Cell*, 10, 225-43.

- WIESER, S. & PINES, J. 2015. The biochemistry of mitosis. *Cold Spring Harb Perspect Biol*, 7, a015776.
- WILSON, G. M., FIELDING, A. B., SIMON, G. C., YU, X., ANDREWS, P. D., HAMES, R. S., FREY, A. M., PEDEN, A. A., GOULD, G. W. & PREKERIS, R. 2005. The FIP3-Rab11 protein complex regulates recycling endosome targeting to the cleavage furrow during late cytokinesis. *Mol Biol Cell*, 16, 849-60.
- WOLFE, B. A., TAKAKI, T., PETRONCZKI, M. & GLOTZER, M. 2009. Polo-like kinase 1 directs assembly of the HsCyk-4 RhoGAP/Ect2 RhoGEF complex to initiate cleavage furrow formation. *PLoS Biol*, 7, e1000110.
- WOLPERT, L. 1960. The mechanics and mechanism of cleavage. *Int Rev Cytol*, 10.
- WOLTHUIS, R., CLAY-FARRACE, L., VAN ZON, W., YEKEZARE, M., KOOP, L., OGINK, J., MEDEMA, R. & PINES, J. 2008. Cdc20 and Cks direct the spindle checkpoint-independent destruction of cyclin A. *Mol Cell*, 30, 290-302.
- WONG, R., HADJIYANNI, I., WEI, H. C., POLEVOY, G., MCBRIDE, R., SEM, K. P. & BRILL, J. A. 2005. PIP2 hydrolysis and calcium release are required for cytokinesis in *Drosophila* spermatocytes. *Curr Biol*, 15, 1401-6.
- WOODARD, G. E., HUANG, N. N., CHO, H., MIKI, T., TALL, G. G. & KEHRL, J. H. 2010. Ric-8A and Gi alpha recruit LGN, NuMA, and dynein to the cell cortex to help orient the mitotic spindle. *Mol Cell Biol*, 30, 3519-30.
- WU, D., ASIEDU, M., ADELSTEIN, R. S. & WEI, Q. 2006. A novel guanine nucleotide exchange factor MyoGEF is required for cytokinesis. *Cell Cycle*, 5, 1234-9.
- WURZENBERGER, C. & GERLICH, D. W. 2011. Phosphatases: providing safe passage through mitotic exit. *Nat Rev Mol Cell Biol*, 12, 469-82.
- XU, H., BRILL, J. A., HSIEN, J., MCBRIDE, R., BOULIANNE, G. L. & TRIMBLE, W. S. 2002. Syntaxin 5 is required for cytokinesis and spermatid differentiation in *Drosophila*. *Dev Biol*, 251, 294-306.
- YAMASHIRO, S., TOTSUKAWA, G., YAMAKITA, Y., SASAKI, Y., MADAULE, P., ISHIZAKI, T., NARUMIYA, S. & MATSUMURA, F. 2003. Citron kinase, a Rho-dependent kinase, induces di-phosphorylation of regulatory light chain of myosin II. *Mol Biol Cell*, 14, 1745-56.
- YAMASHIRO, S., YAMAKITA, Y., TOTSUKAWA, G., GOTO, H., KAIBUCHI, K., ITO, M., HARTSHORNE, D. J. & MATSUMURA, F. 2008. Myosin phosphatase-targeting subunit 1 regulates mitosis by antagonizing polo-like kinase 1. *Dev Cell*, 14, 787-97.
- YANAI, A., ARAMA, E., KILFIN, G. & MOTRO, B. 1997. ayk1, a novel mammalian gene related to *Drosophila* aurora centrosome separation kinase, is specifically expressed during meiosis. *Oncogene*, 14, 2943-50.
- YANG, D., RISMANCHI, N., RENVOISE, B., LIPPINCOTT-SCHWARTZ, J., BLACKSTONE, C. & HURLEY, J. H. 2008. Structural basis for midbody targeting of spastin by the ESCRT-III protein CHMP1B. *Nat Struct Mol Biol*, 15, 1278-86.
- YEN, T. J., COMPTON, D. A., WISE, D., ZINKOWSKI, R. P., BRINKLEY, B. R., EARNSHAW, W. C. & CLEVELAND, D. W. 1991. CENP-E, a novel human centromere-associated protein required for progression from metaphase to anaphase. *EMBO J*, 10, 1245-54.
- YOSHIGAKI, T. 2003. Theoretical evidence that more microtubules reach the cortex at the pole than at the equator during anaphase in sea urchin eggs. *Acta Biotheor*, 51, 43-53.
- YOSHIZAKI, H., OHBA, Y., KUROKAWA, K., ITOH, R. E., NAKAMURA, T., MOCHIZUKI, N., NAGASHIMA, K. & MATSUDA, M. 2003. Activity of Rho-family GTPases during cell division as visualized with FRET-based probes. *J Cell Biol*, 162, 223-32.

- YUCE, O., PIEKNY, A. & GLOTZER, M. 2005. An ECT2-centralspindlin complex regulates the localization and function of RhoA. *J Cell Biol*, 170, 571-82.
- YUMURA, S., UEDA, M., SAKO, Y., KITANISHI-YUMURA, T. & YANAGIDA, T. 2008. Multiple mechanisms for accumulation of myosin II filaments at the equator during cytokinesis. *Traffic*, 9, 2089-99.
- ZACHARIAS, H. 2001. Key word: chromosome. *Chromosome Res*, 9, 345-55.
- ZANIN, E., DESAI, A., POSER, I., TOYODA, Y., ANDREE, C., MOEBIUS, C., BICKLE, M., CONRADT, B., PIEKNY, A. & OEGEMA, K. 2013. A conserved RhoGAP limits M phase contractility and coordinates with microtubule asters to confine RhoA during cytokinesis. *Dev Cell*, 26, 496-510.
- ZENG, K., BASTOS, R. N., BARR, F. A. & GRUNEBERG, U. 2010. Protein phosphatase 6 regulates mitotic spindle formation by controlling the T-loop phosphorylation state of Aurora A bound to its activator TPX2. *J Cell Biol*, 191, 1315-32.
- ZHANG, D. & GLOTZER, M. 2015. The RhoGAP activity of CYK-4/MgcRacGAP functions non-canonically by promoting RhoA activation during cytokinesis. *Elife*, 4.
- ZHANG, D. & NICKLAS, R. B. 1996. 'Anaphase' and cytokinesis in the absence of chromosomes. *Nature*, 382, 466-8.
- ZHANG, J., KONG, C., XIE, H., MCPHERSON, P. S., GRINSTEIN, S. & TRIMBLE, W. S. 1999. Phosphatidylinositol polyphosphate binding to the mammalian septin H5 is modulated by GTP. *Curr Biol*, 9, 1458-67.
- ZHANG, W. & ROBINSON, D. N. 2005. Balance of actively generated contractile and resistive forces controls cytokinesis dynamics. *Proc Natl Acad Sci U S A*, 102, 7186-91.
- ZHANG, X., EMS-MCCLUNG, S. C. & WALCZAK, C. E. 2008. Aurora A phosphorylates MCAK to control ran-dependent spindle bipolarity. *Mol Biol Cell*, 19, 2752-65.
- ZHAO, W. M. & FANG, G. 2005. MgcRacGAP controls the assembly of the contractile ring and the initiation of cytokinesis. *Proc Natl Acad Sci U S A*, 102, 13158-63.
- ZHOU, M. & WANG, Y. L. 2008. Distinct pathways for the early recruitment of myosin II and actin to the cytokinetic furrow. *Mol Biol Cell*, 19, 318-26.
- ZHU, C. & JIANG, W. 2005. Cell cycle-dependent translocation of PRC1 on the spindle by Kif4 is essential for midzone formation and cytokinesis. *Proc Natl Acad Sci U S A*, 102, 343-8.
- ZHU, C., LAU, E., SCHWARZENBACHER, R., BOSSY-WETZEL, E. & JIANG, W. 2006. Spatiotemporal control of spindle midzone formation by PRC1 in human cells. *Proc Natl Acad Sci U S A*, 103, 6196-201.
- ZOU, Y., SHAO, Z., PENG, J., LI, F., GONG, D., WANG, C., ZUO, X., ZHANG, Z., WU, J., SHI, Y. & GONG, Q. 2014. Crystal structure of triple-BRCT-domain of ECT2 and insights into the binding characteristics to CYK-4. *FEBS Lett*, 588, 2911-20.
- ZUMDIECK, A., KRUSE, K., BRINGMANN, H., HYMAN, A. A. & JULICHER, F. 2007. Stress generation and filament turnover during actin ring constriction. *PLoS One*, 2, e696.